Group 4 Metal Alkoxide Complexes as Initiators for the Ring Opening Polymerisation of Cyclic Esters

Chmura, Amanda

Award date:
2008

Awarding institution:
University of Bath

Group 4 Metal Alkoxide Complexes as Initiators for the Ring Opening Polymerisation of Cyclic Esters

Amanda J. Chmura

A thesis submitted for the degree of Doctor of Philosophy

Department of Chemistry
University of Bath
April 2008

Table of Contents

For my parents John and Becky Chmura,
my grandparents Norma and Gerald Wells and John and Anna Chmura,

and

for Paul

Acknowledgements

I wish to thank my supervisor Professor Matthew Davidson for giving me the opportunity to work on this project, for encouraging me to go out and talk about it and for his guidance over the past three years.

EPSRC, Johnson Matthey plc and DTI are also gratefully acknowledged for financial support of this project. Drs Arran Tulloch, Richard Ward and Matthew Lunn of Johnson Matthey plc are thanked for their contributions.

Drs Mary Mahon and Gabriele Kociok-Kohn, and Dr John Lowe are thanked for their assistance with X-ray crystal structure determination and NMR spectroscopic experiments, respectively.

I also wish to thank my labmates and friends for all their help and for making the last few years a time I will always look back on with happiness. Drs Matthew Jones and Luke Turner are particularly acknowledged for all their advice and assistance in the lab. Special thanks also to Dr Chris Chuck, Luisa Pachés Samblás, Dr Elizabeth Milsom, David Bandy, Dr Matthew Durbin and Cathy Frankis, whose friendship I cherish.

Finally, thank you Paul for being there with me, every step of the way.

Abstract

Ring-opening polymerisation (ROP) of cyclic esters can afford poly(ester)s which may be (bio)degradable and/or compostable. In addition, some cyclic ester monomers may be prepared from annually renewable resources. This thesis presents Group 4 metal complexes which have been prepared as potential initiators for ROP of cyclic esters and their activity towards ROP of ε-caprolactone (ε-CL) and L- and D,L-lactide (L- and D,L-LA).

Chapter 1 discusses the need for such polymers in light of increasing global demand for plastics, rising crude oil prices and environmental stewardship. Mechanisms by which the ROP of cyclic esters may proceed are introduced, with particular emphasis on the metal-mediated coordination-insertion mechanism. A brief review of the chemical literature on ROP of ε-CL and L-LA provides context for discussion of the novel complexes prepared in this work. Polymer microstructures available when the racemic mixture of D-LA and L-LA is used as monomer are discussed.

Chapter 2 concerns the preparation of ligands with a variety of N,O donor sets, particularly amine bis(phenolate) and amine tris(phenolate) ligands. The synthesis and characterisation of Group 4 metal complexes employing these ligands is reported.

ROP of ε-CL and L-LA initiated by the complexes introduced in Chapter 2 is the focus of Chapter 3. The activity of the complexes towards these polymerisations is discussed and reaction monitoring experiments are used to gain insight into the polymerisation.

Chapter 4 focuses on results obtained when the complexes described in Chapter 2 are used as initiators for the ROP of D,L-LA. Polymer microstructures are examined using ^{1}H homonuclear decoupled NMR spectroscopy. In some cases, a high degree of stereocontrol is achieved; the origin of this stereocontrol is considered.

Chapter 5 details the synthesis of the reported complexes and the analytical techniques used to characterise both the metal complexes and the polymers described herein.

Chapter 1
Introduction

1 Introduction

1.1 Plastics – Applications, Consumption and Market Growth

Plastics play a vital role in the everyday lives of people around the world. Natural and synthetic polymers are used in a wide variety of industries including packaging, transport, construction, electronics, clothing, agriculture, healthcare and cosmetics. Although the history of plastics manufacturing reaches back over a century to the development of Celluloid by Alexander Parkes in 1862,[1] plastics are still considered modern materials relative to other bulk materials such as wood, clay, steel and cement.

Although the thermoplastic Celluloid, derived from cellulose and patented in 1870, is widely considered the first plastic, the thermoset Bakelite was the first wholly synthetic plastic. Made from phenol and formaldehyde, Bakelite was introduced in 1907 and subsequently used in electrical insulators and in the production of door knobs and jewellery. Since the early 20th century plastics production and consumption has been increasing steadily. In 1950, worldwide production levels of all types of plastics was 1.3 million tonnes per annum (Figure 1.1).[1] Just over half a century later in 2002, annual production reached the 200 million tonne per annum level.

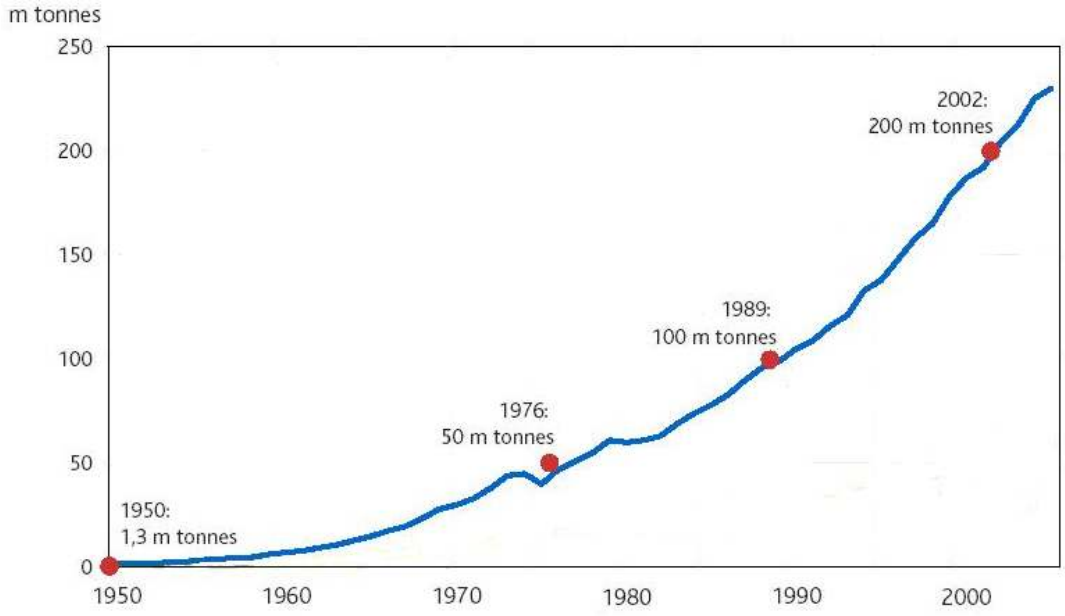

Figure 1.1 Growth in world plastics production, 1950-2005. Reproduced from reference [1].

Recent figures for worldwide production of all plastics indicate that in 2003 worldwide production capacity was 230 million tonnes per annum.[2] Indeed, in terms of bulk materials, the usage of plastics has been increasing and is set to continue rising relative to more traditional materials. A European Commission Joint Research Centre report[3] published in 2002 gave growth projections for bulk material production in Europe for the period 2000-2030, with low, base and high values (Table 1.1). In all three scenarios,

plastics production is expected to increase by the greatest amount relative to the other materials under consideration.

Table 1.1 Projections for bulk material production growth rates in the EU.[3]

Material	Growth Forecast for 2000-2030		
	Low growth/%	Base growth/%	High growth/%
Steel	-0.9	-0.2	0.4
Aluminium	1.0	1.2	2.4
Plastics	**1.3**	**2.3**	**3.3**
Paper and Board	0.8	1.7	2.4
Cement	-0.7	0	0.6
Glass	0.6	1.0	1.9

As noted, one of the factors behind these increases is that plastics are still at an early stage of their use, and in some cases at an early stage of their development. Another key factor in the rise in consumption of plastics is their extreme versatility. Plastics are in general less dense than many other materials and consequently more lightweight, making them easier and more economical to transport. In addition, they can be moulded to many different shapes and sizes depending on the application. Some plastics can be used for thermal and/or electrical insulation, and some are resistant to corrosion. Others can accept colouring and some can be made transparent. The variety of plastic types and the physical variations which can be induced by formulation and processing means that there is a plastic to fit almost any application. The wide-ranging applicability of plastics has resulted in markets for both low-value, high-volume plastics (described in the next section) and specialty, low-volume, high-value plastics for use in the healthcare and electronics industries, to name but a few.

High-volume Plastics and Their Manufacture

Plastic is a cover-all term which can be used to describe many different types of materials. There are hundreds of different types of plastics which, according to the British Plastics Federation,[4] can be classified into around twenty groups. The plastics which are produced in the highest volumes worldwide are linear low density poly(ethylene) (LLDPE), low density poly(ethylene) (LDPE) and high density poly(ethylene) (HDPE), poly(propylene) (PP), poly(vinyl chloride) (PVC), poly(styrene) (PS) and poly(ethylene terephthalate) (PET). These five groups of plastics account for over 95% of the plastics production capacity in Europe (EU25 + Norway and Switzerland) and nearly 74% of the market demand. These figures are consistent with recent plastics consumption in the United Kingdom (Figure 1.2).

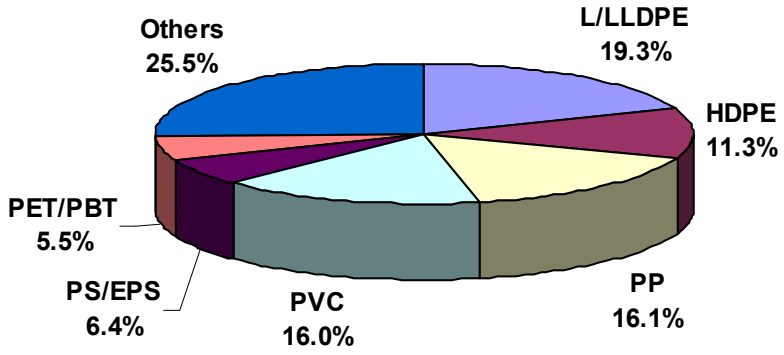

Figure 1.2 Consumption of plastics in the United Kingdom by type, 2005. Adapted from data obtained from the British Plastics Federation.[4]

Figure 1.3 illustrates the industrial methods used to produce poly(styrene).[5] Similar flow diagrams can be made for the other high-volume plastics, as the starting materials for the production of all five of the high-volume plastic groups are ethylene, benzene, or both. Ultimately, all these plastics are derived from petrochemicals.[6]

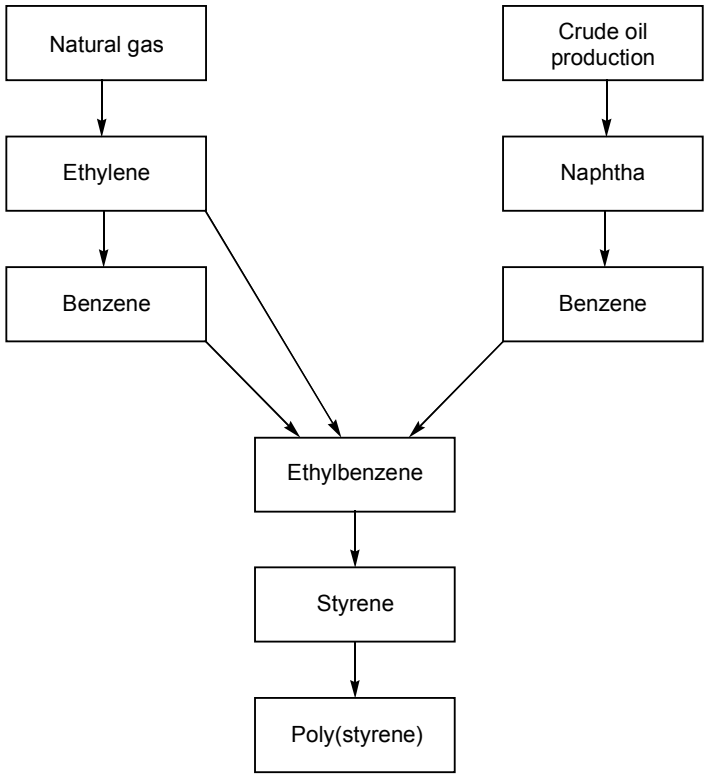

Figure 1.3 Industrial process for making polystyrene polymers. Adapted from reference [5].

Limitations and Drawbacks of Individual High-volume Plastics

All of the high-volume plastics described in the previous section are made from petrochemical feedstocks, which are derived from non-renewable, fossil fuels, finite in terms of human timescales. Although the manufacture of plastics makes up only about 4% of the annual worldwide consumption of crude oil and natural gas (with transportation and energy being the main consumers),[2] there is a drive and a need to reduce reliance on petrochemical feedstocks. In addition, the price of the crude oil 'starting material' is

increasing, leading to increased costs for all products made from this feedstock, including plastic. Figure 1.4 shows the price in United States dollars for a barrel of Brent Crude Oil, a benchmark oil type, through the period mid-1987 to 2007. The red line shows the absolute price while the blue line is the price in 2006 dollars (i.e. adjusted for inflation, constructed using data obtained from the U.S. Department of Energy).

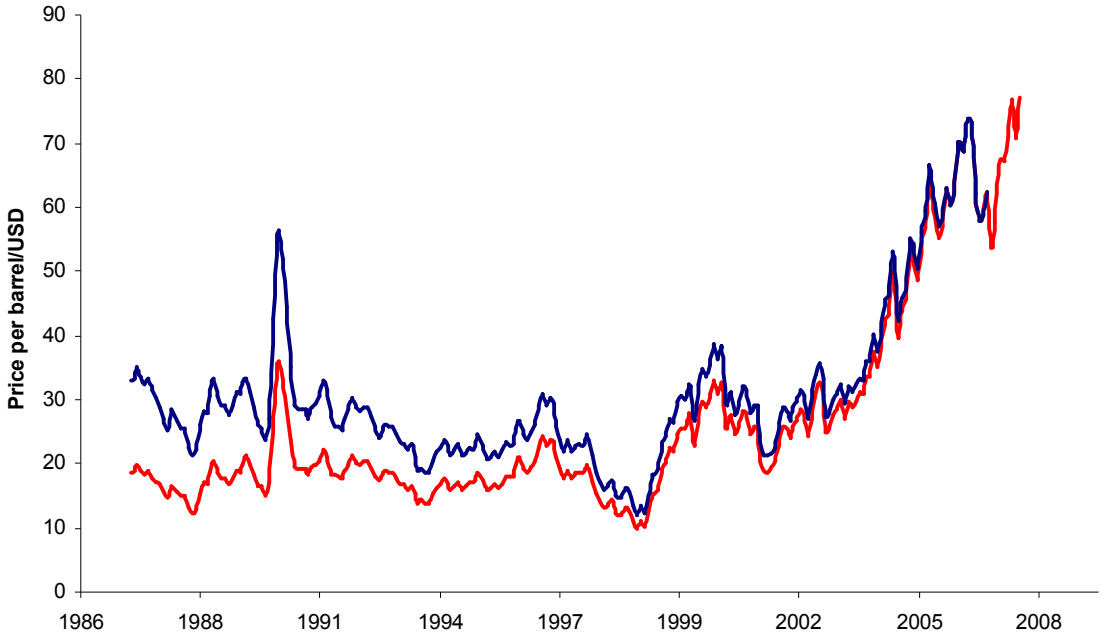

Figure 1.4 Price per barrel of Brent Crude in USD from May 1987. Chart created using data from the Energy Information Administration, Department of Energy, US Government.

As well as the use of finite resources and increasing starting material costs, waste treatment and the environmental fate of plastics are both important issues when dealing with the high volumes of plastics being produced around the world today. As worldwide production of plastics for use in disposable (both in the short and the long term) applications increases, the volume of plastics waste increases as well. Three of the main waste treatment options are incineration, landfill and physical recycling. Incineration releases carbon dioxide, a greenhouse gas implicated in climate change. Landfill requires appropriate facilities; in addition, the high-volume plastics under discussion persist in the landfill environment for many years. Some of these plastics have been shown to degrade when certain microbial agents are present in the soil but are generally considered to be inert.[7] From an environmental perspective, physical recycling is the most attractive option. However, in the United Kingdom, only around 19% of plastic consumed is recycled.[8]

Figure 1.5 Recycling codes for high-volume plastics.

In summary, the global demand and production of plastics has been increasing since their development began in the early 20th century and the demand is set to continue increasing in the coming decades. All of the main high-volume plastics are ultimately prepared from petrochemical starting materials. There is a drive to reduce fossil fuel (e.g. petrochemical) consumption and reducing the amount of plastics made from petrochemicals can help achieve this goal. Recycling of plastics is one way to reduce oil consumption from plastic production and environmentally, recycling is the most attractive plastic waste treatment option. However, the percentage of recycled plastic is low, even in developed nations such as the United Kingdom. Also, the high-volume plastics described above persist in the environment and create environmental problems. One way to address these issues is to increase recycling, but another is to create plastics from renewable resources which have similar properties to traditional, petrochemical-derived plastics and which can meet the demands of the wide range of application areas currently served by traditional plastics. The ideal plastics would be readily prepared from renewable resources, have desirable physical properties and degrade in a controllable manner to environmentally benign products under specific conditions.

1.2 Degradable Plastics

As industrial interest and public consciousness about degradable plastics made from renewable resources has increased in recent years, many new products claiming to be environmentally friendly, degradable or compostable have been introduced to the market, particularly in the packaging sector. Standards have therefore been developed to provide purchasers and consumers with a clearer idea of what they are buying. The American Society for Testing and Materials (ASTM) defines biodegradable, compostable and photodegradable plastics as follows (ASTM standard D 883):

Biodegradable Plastic – a degradable plastic in which the degradation results from the action of naturally-occurring micro-organisms such as bacteria, fungi and algae.

Compostable Plastic – a plastic that undergoes biological degradation during composting to yield carbon dioxide, water, inorganic compounds, and biomass at a rate consistent with other known compostable materials and leaves no visually distinguishable or toxic residues.

Photodegradable Plastic – a degradable plastic in which the degradation results from the action of natural daylight.

European standard EN 13432 gives a similar definition of compostable material, also stipulating that a biodegradation level of 90% should be reached within a time period of six months. One plastic which has seen increased use in recent years is poly(ethylene) incorporating additives which induce photo-degradation; these plastics are labelled as oxo-biodegradable.[9] Although oxo-biodegradable poly(ethylene) does physically break down, it cannot be composted and is prepared from petrochemical starting materials. Although these materials do have their benefits over non-degradable poly(ethylene), further discussion will be limited to plastics which degrade to water and carbon dioxide. Logos have been developed (Figure 1.6) to identify compostable products which meet the US and European standards, which are conferred by third-party organisations.

Figure 1.6 Labels used for compostable materials in the United States, conferred by the Biodegradable Products Institute (left) and Europe, conferred by European Bioplastics (right).

The growing interest in degradable plastics from renewable resources, has been manifested in the growing production and consumption of these materials. In 2003, the worldwide production capacity of so-called 'bioplastics' or 'biopolymers' was estimated at 222,000 tonnes (<0.1% of global plastic production capacity) and this figure is estimated to rise seven-fold by 2010.[2] It has been estimated that plastics from renewable resources could eventually claim up to 33% of the market share of their petrochemical-based counterparts. Currently, there are several types of 'bioplastic' on the market. Polymers which are present in plants and directly obtainable, such as cellulose and starch may be used unmodified or modified as plastics and these make up a major portion of the

'bioplastics' market. Others include poly(hydroxyl alkanoates) produced by bacteria, and polyurethanes in which the polyol component is derived from renewable resources. One group of materials which have generated a great deal of interest in recent years are poly(ester)s prepared via the ring-opening polymerisation (ROP) of cyclic esters, which will be discussed in the next section.

Aliphatic Polyesters

Cyclic esters such as those shown in Figure 1.7 are monomers which can be used to prepare high molecular weight poly(ester)s via ring-opening polymerisation processes, producing plastics which can in some cases have similar physical properties to their traditional, petrochemical-based counterparts. The cyclic ester starting materials may be derived from either petrochemical or renewable resources, and the resultant polymers can be degradable, biodegradable or compostable.

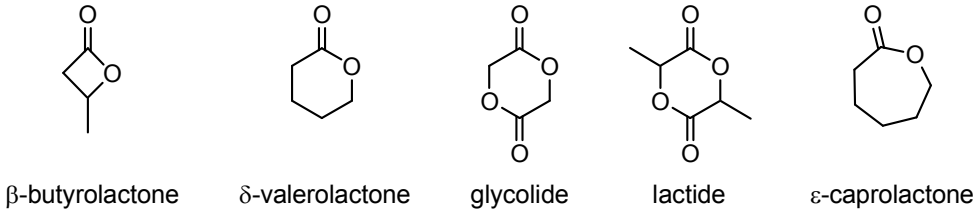

Figure 1.7 Common cyclic esters, which may undergo ring-opening polymerisation.

Although ROP of all these monomers is known,[10-12] this review will focus solely on the ROP of ε-caprolactone (ε-CL) and L- and D,L-lactide (L- and D,L-LA). As the ROP of cyclic esters is driven by the relief of ring strain, the depolymerisation reaction can be a problem at higher temperatures.[13] The polymerisation reactions will be discussed in terms of reaction conditions, conversion and the time needed to reach reported conversions, molecular weights and molecular weight distributions as described by the polymer's polydispersity index, PDI. The *number average molecular weight* of a polymer (M_n) is the average of the molecular weights of the individual polymer molecules (i.e. the sum of the molecular weights of each polymer molecule divided by the number of polymer molecules), which may be obtained by Gel Permeation Chromatography (GPC) measurement (details of this technique are given in chapter 5). The *weight average molecular weight* (M_w) reflects the fact that the larger polymer molecules in the polymer sample (with a greater number of repeat units) contain a greater proportion of the sample mass than do the smaller polymer molecules. M_w may be accurately determined by light scattering techniques, amongst others. The PDI of a polymer sample is the ratio between the weight average molecular weight and the number average molecular weight, M_w/M_n, and so is a measure of the distribution of the molecular weights of individual polymer molecules in a sample. For ROP of cyclic esters, which in many cases can be considered

to be a living polymerisation, the PDI values of the resultant polymers may be close to 1.0, the value at which all polymer chain lengths (and the molecular weights of all polymer molecules) in the sample are the same.

Both the ε-caprolactone and lactide monomers have been known since the 1930s, when initial work on their preparation was carried out by Carothers.[14] Polymers of lactic acid units were prepared by a polycondensation route, however it was difficult to achieve desired high molecular weight polymers or controlled polymerisations. Recently, progress has been made in this area and Mitsui Chemicals have developed process to produce higher molecular weight poly(L-lactic acid) without the use of solvent.[15] Ring-opening polymerisation of cyclic esters was developed to circumvent problems such as the continuous removal of reaction by-products (namely water) associated with polycondensation routes and is widely used today. Although both are abbreviated as PLA, polymer resulting from the polycondensation route is often called poly(lactic acid) and polymer resulting from ROP is often called poly(lactide). Unless explicitly stated that the polymer is from a polycondensation route, PLA described in this thesis is poly(lactide).

ε-Caprolactone monomer is prepared via a Baeyer-Villager oxidation reaction of cyclohexanone and *m*-chloroperbenzoic acid. In this way, the monomer is still obtained from petrochemical sources, although new syntheses are being developed which use hydrogen peroxide as the oxidant resulting in water as the only by-product which reduces the environmental impacts of the process.[16] ROP of ε-caprolactone gives poly(caprolactone) (PCL) polymers which are highly desirable for use in drug delivery systems, due to their slow degradation rate and permeability to active pharmaceutical species.[17, 18] PCL is also used as a plasticiser for PVC (instead of phthalates),[19] to produce polyols used for polyurethane production,[20, 21] as an adhesive[22] and for biodegradable films used as wound dressings.[23] Co-polymerisation with other monomers, including other cyclic esters, and blending can be used to achieve a range of properties, again particularly desirable for drug delivery applications.[24, 25] Currently, PCL is produced commercially by companies including Solvay (under the brand name CAPA), Union Carbide (Tone) and Daicel (Celgreen).

Today, one of the major producers of poly(lactide) is Natureworks LLC, which began as a joint venture between Cargill Inc. and The Dow Chemical Company in 1995, although Dow subsequently pulled out of the partnership and today Natureworks LLC is a partnership between Cargill Inc. and Teijin Ltd. of Japan.[26] In the industrial process used by Natureworks,[15] lactide is prepared by the oligomerisation of lactic acid to low

molecular weight prepolymers, which are then depolymerised to afford the cyclic lactide monomer. The lactic acid itself is obtained through a fermentation process, using high starch content biomass such as maize, potatoes or sugar beet. Dextrose obtained via enzymatic hydrolysis of starch is then fermented, giving 99.5% L-lactic acid and 0.5% D-lactic acid.

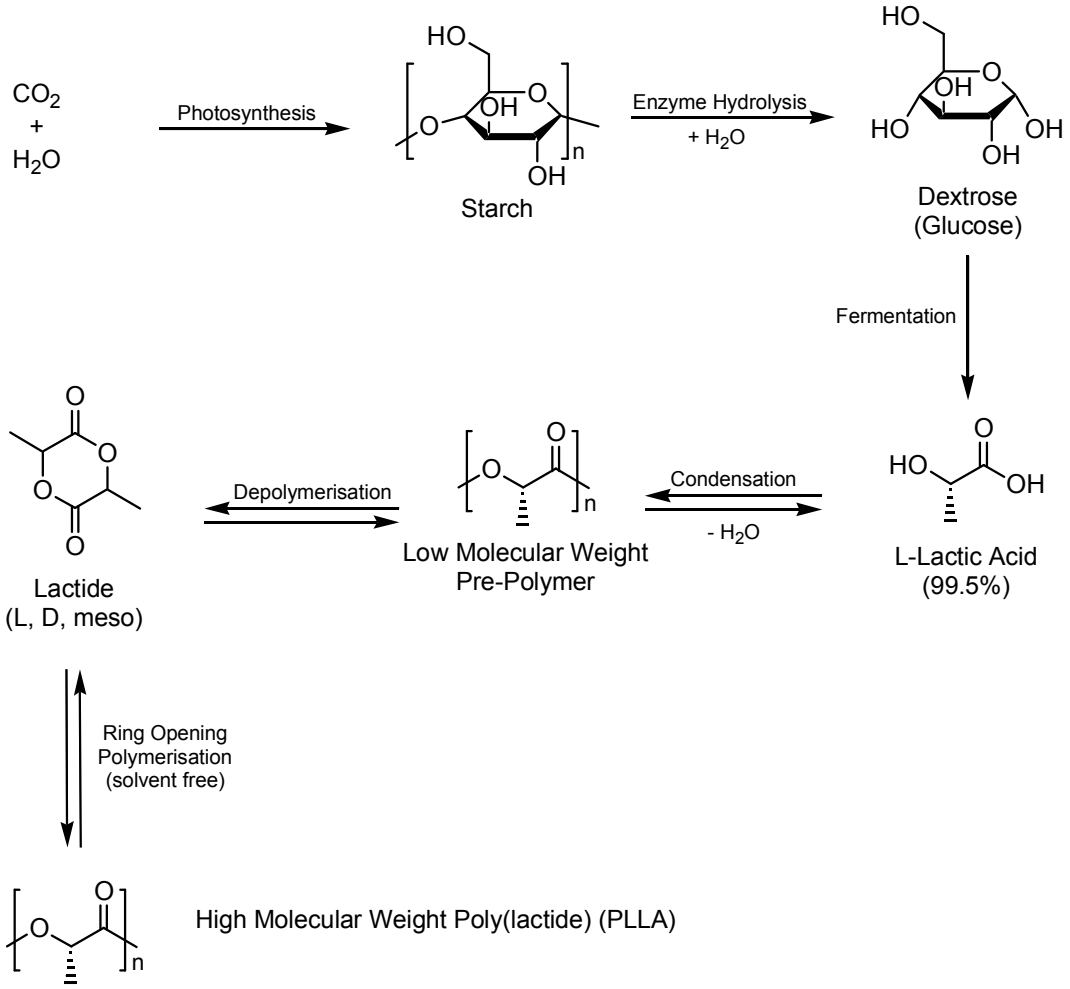

Figure 1.8 Current industrial process used for production of PLLA from starch.[15]

The presence of the small amount of the D-lactic acid enantiomer means that three forms of lactide are produced in the oligomerisation/depolymerisation process: L-lactide (L-LA) with both stereocentres in the *S* configuration, D-lactide (D-LA) with both stereocentres in the *R* configuration and *meso*-lactide (*meso*-LA), with one stereocentre in the *S* configuration and one in the *R*. The D-LA and *meso*-LA are removed by distillation prior to polymerisation of L-LA, although D-LA is sometimes added if a more amorphous polymer is required, as pure poly(L-lactide) (PLLA) is highly crystalline. The plant flow diagram is shown in Figure 1.9.

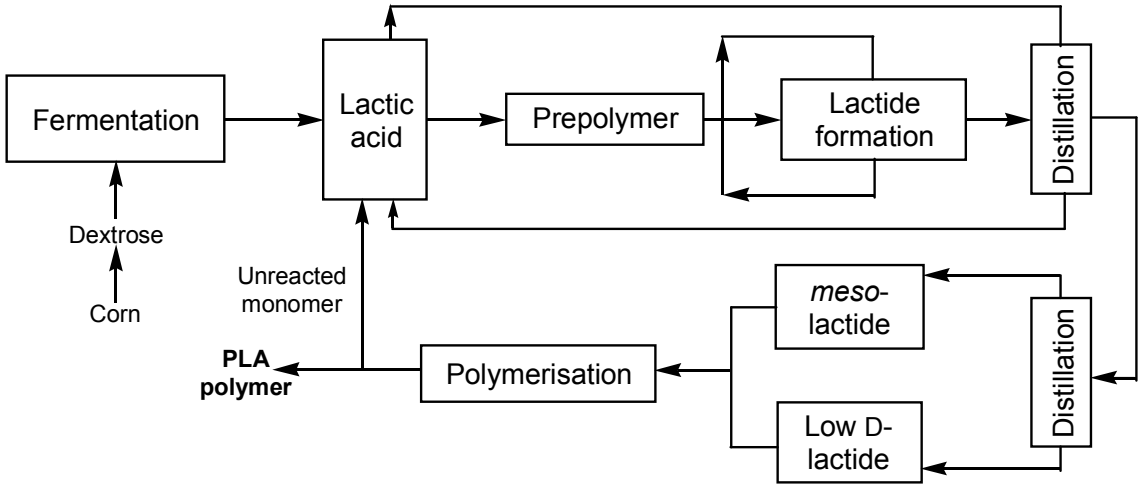

Figure 1.9 Natureworks PLA plant flow diagram. Adapted from reference [27].

Other commercial producers of PLLA include Hycail (under the brand name Hycail PLA), Shimadzu (Lacty) and Toyota (Eco-Plastic). The worldwide PLLA production capacity as of 2003 was 143,500 tonnes and it is estimated that production will increase to between 530,000-1,150,000 tonnes per annum by 2010.[2] Natureworks LLC reports that their Blair, Nebraska PLLA plant is currently running at its capacity of 140,000 tonnes per annum.[26]

Ring-Opening Polymerisation - Mechanisms

ROP of cyclic esters may occur via one of several potential mechanisms including cationic, anionic, coordination-insertion or enzymatic.[13] The mechanism for cationic ROP of cyclic esters postulated by the research groups of Kricheldorf[27] and Dittrich[28] centres on the protonation or alkylation of the exocyclic carbonyl oxygen atom. This activates the O-CH bond which is cleaved by nucleophilic attack of another equivalent of monomer, propagating the polymer. This process continues until a monofunctional nucleophile (e.g. water) is available to cause a termination step. Strong acids have been shown to initate ROP of ε-CL, but control of molecular weight in these cases is difficult to achieve.[10] However, controlled cationic ROP of D,L-LA has recently been achieved using triflic acid/alcohol initiator systems by Bourissou *et al*, yielding linear polymers with polydispersity index values in the range of 1.13-1.48.[29] One of the major issues regarding the use of cationic initiator systems for ROP of a cyclic ester monomer such as lactide, with a chiral carbon centre, is that the mechanism involves nucleophilic substitution at the chiral carbon, opening up the possibility of epimerisation. Controlled polymerisation with retention of configuration at the stereocentre occurs quite slowly at temperatures of <50 ºC. For example, using the triflic acid/isopropanol initiator system at

25 ºC in dichloromethane solution, the ROP of D,L-LA proceeded to >96% conversion after 28 hours. The polymerisation rate may be enhanced by increasing the temperature of the reaction, but the use of higher reaction temperatures has been shown to induce undesirable racemisation.[30]

The mechanism for ROP of cyclic esters initiated by an anionic group, R^-, is shown in Figure 1.10.[10] Typical anionic initiators are alkali metal alkoxides.[31] The ring-opening event may occur at one of two separate sites. With the so-called 'O-acyl scission', if the nucleophilic group attacks at the carbonyl carbon, a linear polyester with an active alkoxide chain end results. If the nucleophile attacks at the carbon atom adjacent to the endocyclic oxygen atom, 'O-alkyl scission', again a linear polyester results, with a carboxylate active chain end. In each case the other end group of the polymer is determined by the nature of R.

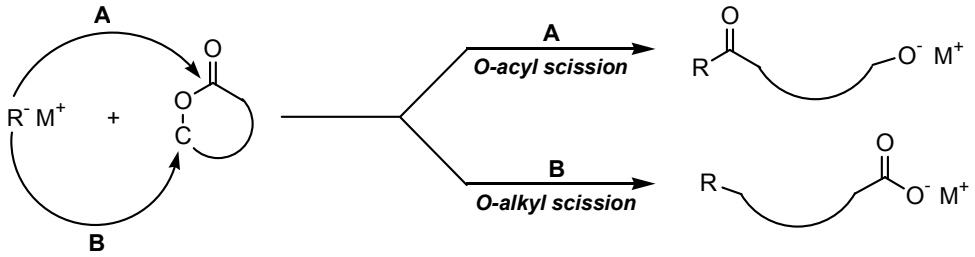

Figure 1.10 Anionic ROP of cyclic esters may occur through two routes.

ROP of smaller cyclic esters such as the four-membered propiolactone is known to occur via both O-acyl and O-alkyl scission.[32] However, for the larger rings such as ε-caprolactone and lactide, ROP only occurs via the O-acyl scission route.[33]

By far the most widely studied initiators are the (transition) metal complexes which effect ROP of cyclic esters via a coordination-insertion mechanism. The mechanism proceeds in a similar manner as anionic ROP and indeed, the distinction between these mechanisms is not always clear.[34] This mechanism was first postulated in 1971 by Dittrich and Schulz, subsequent experimental and theoretical evidence has lent support to the mechanism.[28] The metal d orbitals allow coordination of the monomer to the metal centre through the carbonyl oxygen atom. A nucleophilic labile ligand or co-initiator then attacks the activated carbonyl group, leading to O-acyl scission. This mechanism is illustrated in Figure 1.11, with the initiator shown as a metal alkoxide supported by one or more additional ligands $\mathbf{L_n}$, one of the most common types of initiator system. Subsequent monomer molecules proceed to coordinate to the metal centre and insert in to the metal-alkoxide bond, resulting in the formation of the polymer. Finally, termination

is achieved by quenching the polymerisation with a suitable proton source. This results in a poly(ester) with one hydroxyl and one ester end group.

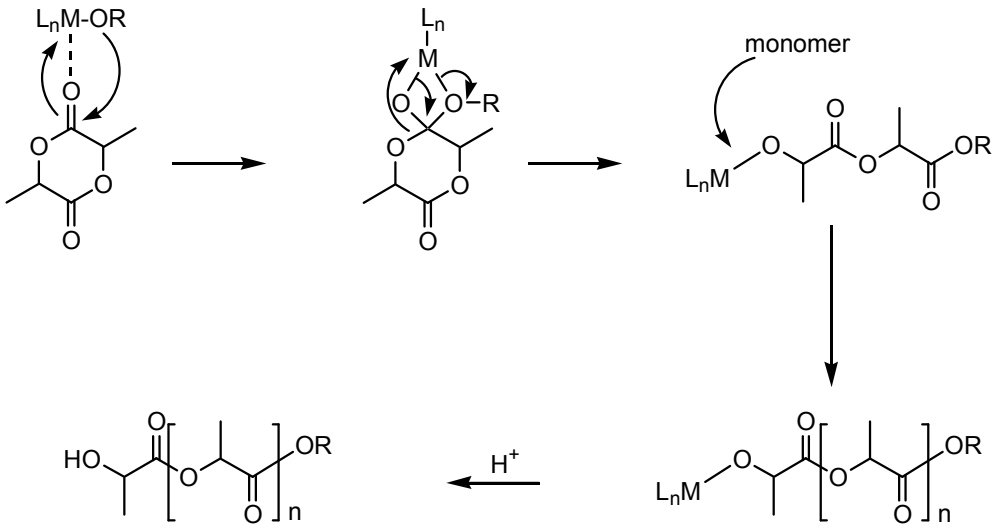

Figure 1.11 Ring-opening polymerisation of LA by a metal-mediated coordination-insertion mechanism.

Enzyme catalysed ROP of D,L-LA was first achieved by Uyama and Kobayashi using lipase *Pseudomonas fluorescens* (lipase PS) at temperatures between 80 ºC and 130 ºC; [35] subsequently a wide variety of enzymes have been demonstrated to be active initiators for the process and one of the most extensively used lipases is immobilised *Candida antarctica*.[36] While in some cases remarkable selectivities (in terms of polymer stereochemistry, which will be further discussed in subsequent sections) have been achieved, enzyme catalysed ROP of D,L-LA is known to suffer from major issues relating to rates of reaction, low conversions and yields.[13]

Recently, purely organic *N*-heterocyclic carbenes have shown utility in ROP of lactide, through a postulated activated monomer mechanism.[37] These initiator systems are relatively less well-developed than many of those described previously, but they do show great promise in the field of metal-free ROP of cyclic esters.

Many complexes which are active initiators for the ROP of cyclic esters may also catalyse transesterification reactions. Transesterification is an undesirable side reaction to the ring-opening polymerisation reaction and can occur both intermolecularly and intramolecularly (Figure 1.12).

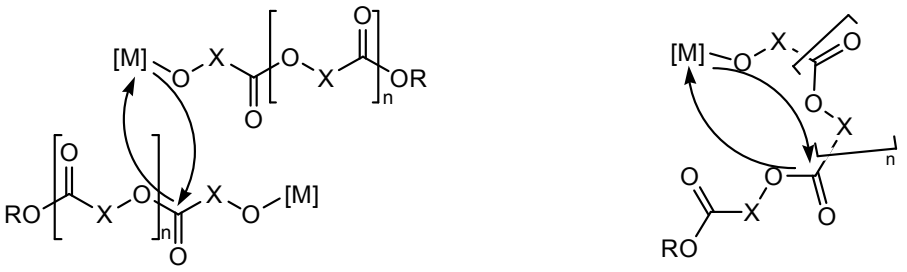

Figure 1.12 Transesterification in ROP reactions, X = $(CH_2)_5$ for ε-CL.

Both types of transesterification reactions can lead to broadening of the molecular weight distribution.

1.3 Coordination-Insertion ROP of ε-caprolactone and L-lactide

The ROP of ε-CL and L-LA via a coordination-insertion mechanism has previously been extensively reviewed.[10, 13, 30, 38, 39] This discussion aims to present an overview of important aspects of the field by reviewing key examples, but is by no means an exhaustive review.

Due to the high level of interest in poly(caprolactone) and poly(lactide), a wide variety of (transition) metal initiators have been studied over the past decade. ROP via the coordination-insertion mechanism is often referred to as 'living' and is characterised by (i) the rate of initiation being faster than the rate of propagation, (ii) an absence of termination or chain transfer steps and (iii) a linear dependence of molecular weight on conversion leading to narrow molecular weight distributions.[13] Metal alkoxides such as tin(II) *tert*-butoxide and aluminium(III) isopropoxide are effective initiators for the ROP of cyclic esters, however, their solution behaviour is complex with equilibria existing between mononuclear and aggregated species. The development of 'single-site' initiators has therefore been a key goal for understanding the ROP mechanism and producing polymers with controllable molecular weights and polydispersities. Industrially, the initiator used to prepare commercial grade PCL and PLLA is tin(II) 2-ethylhexanoate, also known as stannous octoate, often abbreviated $Sn(oct)_2$ (Figure 1.13).[38] This initiator is commercially available, soluble in both common organic solvents and in melt monomers. It may be used for the preparation of polymers with molecular weights of up to 10^6 g mol^{-1} when used with an alcohol co-initiator.

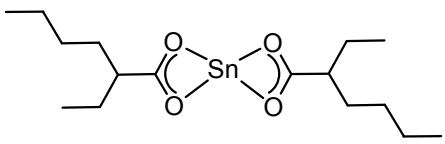

Figure 1.13 Tin(II) 2-ethylhexanoate, an initiator used industrially to prepare PCL and PLLA.

Tin(II) 2-ethylhexanoate is an initiator with reaction times from a few hours to a few days. The initiating species when tin(II) 2-ethylhexanoate is used in the absence of a co-initiator is thought to include protic impurities including free lactic acid or water; in this case the polymerisation proceeds relatively slowly. However, the ROP reaction has been found to be accelerated and with enhanced control when an alcohol was added. The mechanism of the ROP initiated by tin(II) 2-ethylhexanoate has been the subject of extensive experimental and theoretical studies and has been determined to proceed via a coordination-insertion mechanism.[40, 41]

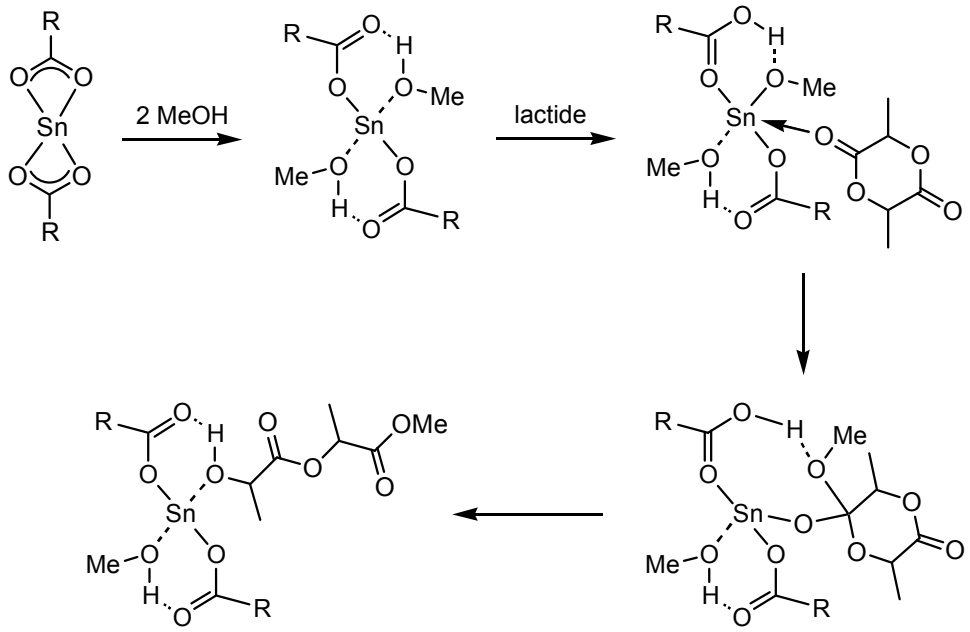

Figure 1.14 Theoretical mechanism for ROP of LA by tin(II) 2-ethylhexanoate (R = Me).[42]

Density Functional Theory (DFT) calculations carried out by Albertsson and co-workers suggest that the coordination of the two molecules of methanol to the metal centre through the oxygen atoms is favoured by 59-60 kJ mol^{-1} with the carboxylate ligand retained, i.e. an associative step (Figure 1.14).[42] This is followed by coordination of lactide, which is considered favourable but weak at 16 kJ mol^{-1} and induces proton transfer to the carboxylate ligand, resulting in the formation of an alkoxide. The authors favour this mechanism but concede that due to entropic factors and high ROP reaction temperatures, dissociation of the carboxylate ligand from the metal centre may occur. This dissociation of the carboxylate ligand and association of the alcohol would lead to a tin(II) bis(alkoxide) complex which is a known initiator for the ROP of cyclic esters, as noted previously (Figure 1.15).

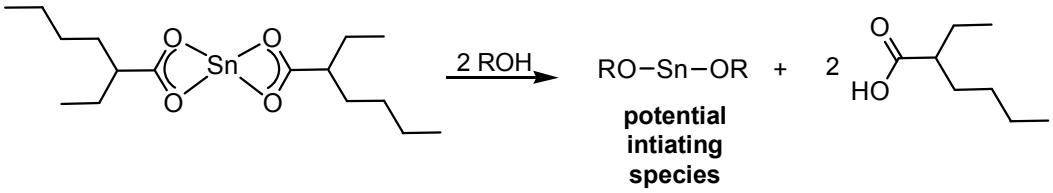

Figure 1.15 Reaction scheme for generation of the potential initiating species when an alcohol co-initiator is used with tin(II) 2-ethylhexanoate.

Several other groups have made similiar observations, i.e. an increased polymerisation rate is observed as the concentration of alcohol is increased. For example, tin(II) alkoxide complexes of bulky, bidentate benzamidinate ligands prepared by Hillmyer, Tolman and co-workers also showed increased control and reactivity in the ROP of L-LA in toluene solution at 80 ºC when benzyl alcohol was added as a co-initiator.[43] As the presence of alcohol is necessary for both mechanisms, at the moment they seem equally possible, although the theoretical studies do lend support to the 'coordinated alcohol' mechanism described in Figure 1.14.

In addition to its utility in the ROP of ε-CL and L-LA, tin(II) 2-ethylhexanoate has also been approved as a food additive by the United States Food and Drug Administration. However, there are toxicity issues related to organo-tin compounds and the United States Occupational Safety and Health Administration (OSHA) has set a workplace limit for tin(II) 2-ethylhexanoate and other similar compounds of 0.1 milligrams per cubic meter air. This has led to significant efforts to develop initiator systems based on less controversial, more environmentally acceptable metals.

As noted previously, simple aluminium(III) alkoxides are also active initiators for the ROP of cyclic esters and their first reported use for this reaction was by Teyssie and co-workers.[44] Particularly in the case of aluminium(III) isopropoxide, which was used to help discern the coordination-insertion mechanism, an induction period is seen for the polymerisation, due to aggregation effects. As for the tin(II) alkoxides mentioned previously, aggregation also leads to broad molecular weight distributions due to a lack of control over the active site, and in some cases to a total inhibition of ROP activity. For instance, several groups including Duda and Penczek,[45] and Albertsson[46] have shown that aluminium(III) isopropoxide tetramer (Figure 1.16 A_4) is unreactive towards ROP of ε-CL, but that the trimeric analogue produces polymer with M_n values of around 3 x 10^5 g mol^{-1}.

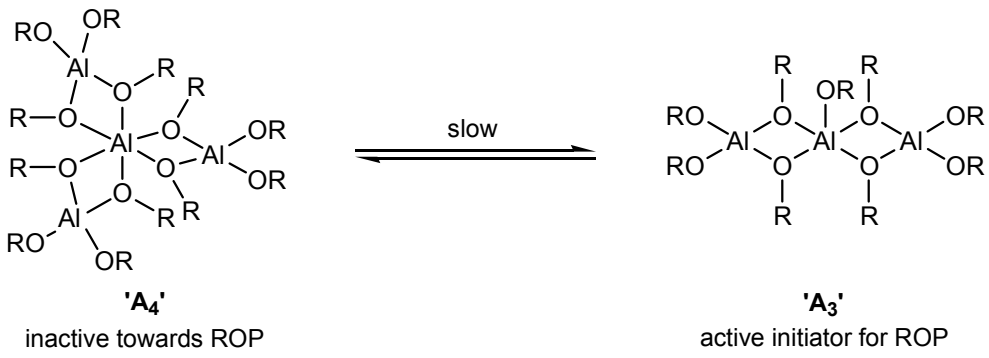

Figure 1.16 Aluminium(III) isopropoxide (R = $CH(CH_3)_2$) initiators which have been tested for ROP.

Recently, Duda and Penczek have highlighted the importance of the aluminium-alkoxide bond for ROP activity.[47] The ROP of ε-CL and L-LA initiated by aluminium(III) acetylacetonate at 80 ºC in tetrahydrofuran solution proceeds very slowly (taking over 100 h to reach 50% conversion). However, when isopropoanol is added as a co-initiator the rate of polymerisation of ε-CL and L-LA increases; the authors attribute this increase to the formation of an aluminium(III) alkoxide/carboxylate complex. The polymerisation rate increases as alcohol is added up to a point where complete exchange of acetylacetonate for alkoxide takes place (Figure 1.17).

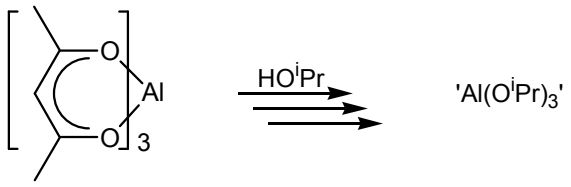

Figure 1.17 Generation of the active aluminium(III) isopropoxide initiator.

As with the tin(II) based initiators discussed previously, aggregation is considered to have detrimental effects on the control of the polymerisation and consequently there has been a search for 'single-site' aluminium initiators for the ROP of cyclic esters. One class of such initiators have been prepared by Okuda and co-workers who synthesised aluminium(III) complexes of tetradentate ligands bearing bisphenolato groups bridged by dithioethers (Figure 1.18).[48] The solid-state structures of these complexes were obtained via X-ray crystallography and ^{1}H NMR spectroscopic studies indicated the structures were maintained in solution.

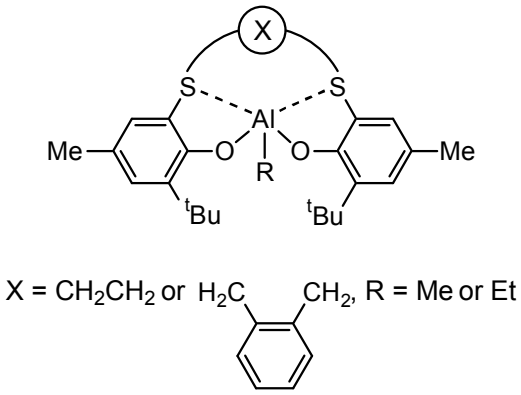

Figure 1.18 Aluminium(III) initiators prepared by Okuda and co-workers.[48]

As with many L_nMR aluminium(III) initiators, the alkoxide is generated in situ upon addition of alcohol. When the bridging group X is ethyl, the polymerisation of D,L-LA carried out in toluene solution at 70 ºC reaches 92% conversion in ten hours, producing a polymer with a polydispersity index of 1.04, suggesting few undesirable side reactions occur. When the bridging group is $CH_2(C_6H_4)CH_2$, 92% conversion is reached in 118 hours. Although the polymerisation occurs much more slowly, the resultant polymer has a similarly narrow molecular weight distribution, with a PDI value of 1.07. Aluminium(III) initiators have been very important in the development of stereoselective ROP of D,L-LA and will be discussed in more detail later in this chapter.

In addition to initiation by aluminium(III) alkoxides, the ROP of ε-CL may also be initiated by aluminium(III) thiolates. In one case, Lin and co-workers prepared aluminium(III) alkyl or chloride complexes of 2-methoxy benzenethiol, which were active initiators for ROP of ε-CL in toluene at 25 ºC, producing polymer to 100% conversion in less than two hours, with moderate PDI values of 1.19 – 2.21.[49] The presence of the carboxylic acid *S*-methyl ester end group was confirmed by ^{1}H NMR spectroscopy. When X = Cl (Figure 1.19(a)), an increase in PDI values was observed relative to when X = Me and although the authors note this unexpected result no explanation is put forth. The monomeric aluminium(III) complex where X = Me is also active for the ROP of L-LA in toluene solution at 110 ºC, producing PLLA with a PDI value of 1.16 to 92% conversion after 24 hours. Dimeric aluminium(III) alkyl complexes of (2,4,6-trimethylphenyl)-methanethiol (Figure 1.19(b)) were also found to be active for the ROP of ε-CL, under the same conditions. Polymerisations initiated with these complexes proceeded more slowly than those initiated by the monomeric complexes, reaching full conversion in five hours (R = Et) and twenty hours (R = ^{i}Bu) and producing polymers with PDI values in the range 1.21 – 1.37. The authors attribute the apparent

decrease in polymerisation rate for the complex where R = ^{i}Bu to the increased steric bulk at the aluminium(III) centres.

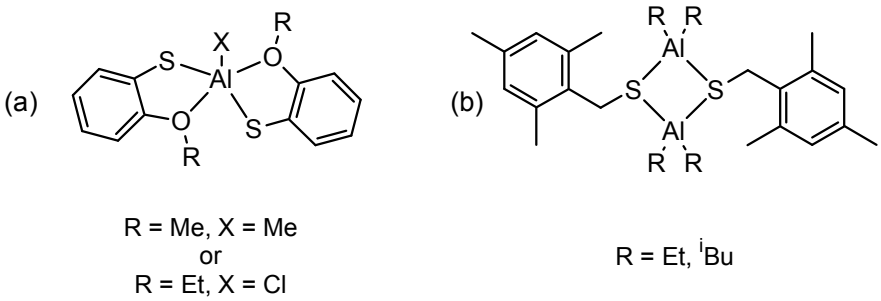

Figure 1.19 Aluminium(III) thiolate initiators prepared by Lin and co-workers.[49]

Although aluminium(III) complexes have been shown to be active for the controlled, living ROP of cyclic esters, the polymerisation rates are several orders of magnitude smaller than for their tin(II) analogues. In addition, cerebral aluminium has been linked with the formation of β-amyloids and neurofibrillary tangles in the brains of humans suffering from Alzheimer's disease. β-amyloids are the main constituents of amyloid plaques in the brains Alzheimer's disease sufferers, while neurofibillary tangles are the pathological protein aggregates found in the neurons of Alzheimer's disease sufferers. These connections have led some researchers to investigate the possibility that aluminium exposure could have some link to the cause of Alzheimer's disease in those individuals who are susceptible to it.[50]

Zinc(II) complexes have also been the subject of investigation as initiators for ROP of cyclic esters, particularly due to their low toxicity. Indeed, zinc metal is an active heterogeneous catalyst for the ROP of L-LA but lacks control over the polymerisation process.[13] However, zinc(II) bis(lactate) is a much more active initiator for the polymerisation when combined with an alcohol co-initiator.[51]

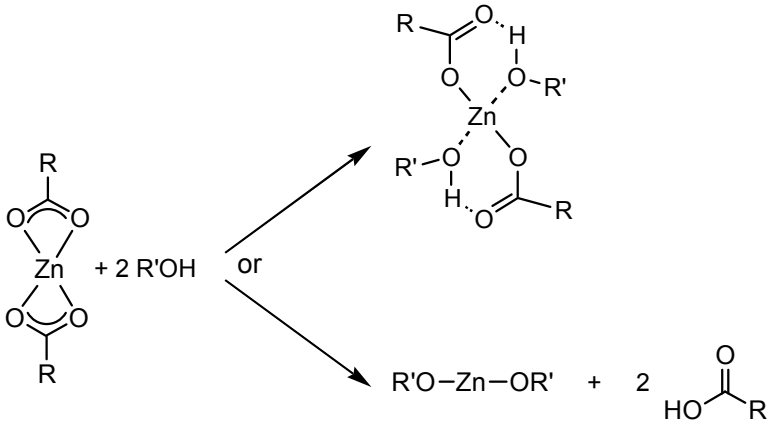

Figure 1.20 Postulated initiating species for the ROP of cyclic esters co-initiated by zinc(II) carboxylates and alcohol.

The debate over the mechanism for ROP initiated by zinc(II) carboxylates is echoes that over ROP initiated by tin(II) carboxylates (Figure 1.20).[13] Some researchers suggest the mechanism is similar to that described for the polymerisation initiated with tin(II) 2-ethylhexanoate, where alcohol coordinates to the carboxylate and the coordinated alcohol oxygen atom's lone pairs attack the activated cyclic ester carbonyl carbon atom. This increase in reactivity on addition of alcohol was also seen for ROP initiated with zinc(II) 2-ethylhexanoate carried out by Duda, Penczek and co-workers;[47] however, the authors feel that the polymerisation proceeds by insertion of the monomer into the zinc-alkoxide bond, which has itself been formed by the complete exchange of carboxylate for alkoxide ligands. The authors support their case by citing kinetic data which show that the rate of polymerisation increases as alcohol concentration increases up to a point where complete exchange for alkoxide ligands takes place.

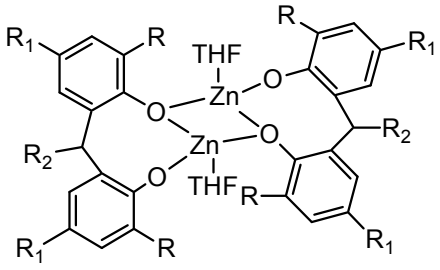

R = R_1 = ^{t}Bu, R_2 = Me
R = ^{t}Bu, R_1 = Me, R_2 = *o*-(OMe)C_6H_4
R = R_1 = $C(CH_3)_2Ph$, R_2 = *o*-(OMe)C_6H_4

Figure 1.21 Zinc(II) aryloxide complexes which are active for the ROP of ε-CL and L-LA prepared by Lin and co-workers.[52]

Zinc(II) complexes of more complex ligands have also been utilised for ROP of ε-CL and L-LA. Kricheldorf and co-workers have utilised zinc(II) complexes of amino acids as effective initiators, although these were found to be less active than zinc(II) bis(lactate).[53] Lin and co-workers prepared dimeric zinc(II) complexes of bidentate aryloxides as shown in Figure 1.21.[52] With the addition of an alcohol co-initiator, these complexes initiated the ROP of ε-CL in toluene solution at 50 ºC. Polymerisations carried out under these conditions generally reached >95% conversion within four hours. The PCL polymer produced from these experiments had narrow molecular weight distributions with PDI values of between 1.05 and 1.17. These initiators were also active for the ROP of L-LA under the same solution and temperature conditions again producing polymers with PDI values in the range 1.08 – 1.20. Based on calculations performed by the same authors on a similar magnesium(II) system, the mechanism which has been postulated for the ROP initiated by these complexes is illustrated in Figure 1.22.

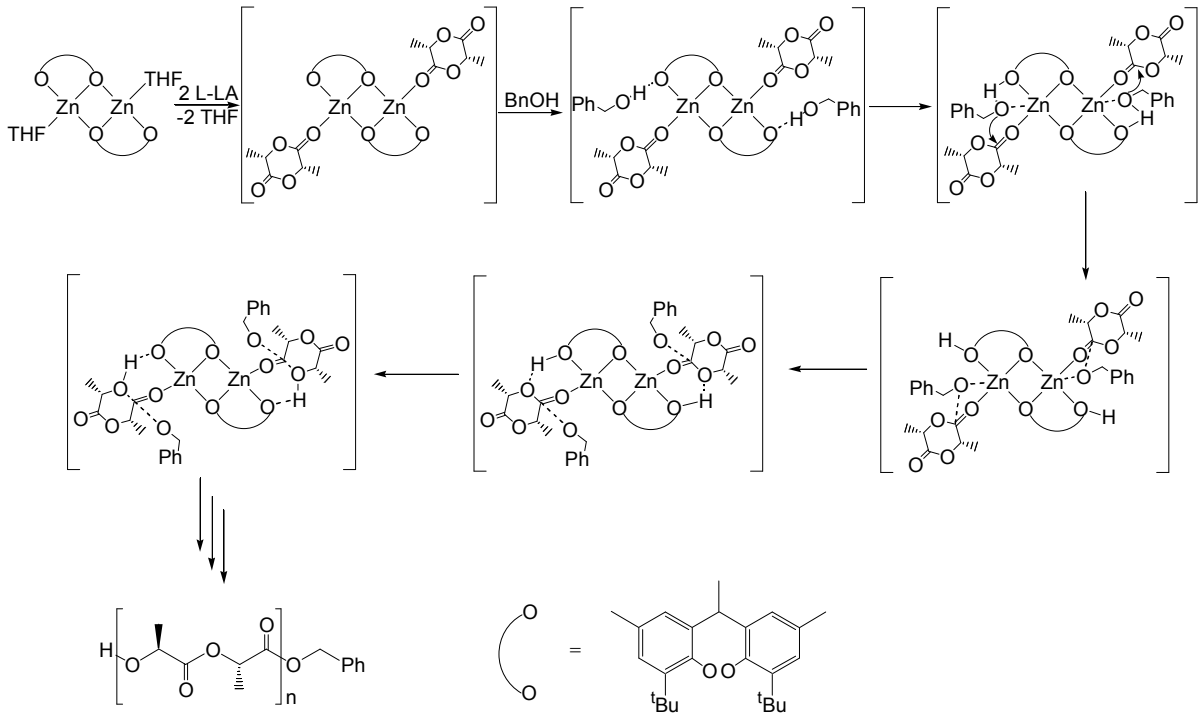

Figure 1.22 Proposed mechanism of ROP of LA by the initiators prepared by Lin and co-workers.

The mechanism involves dissociation of the THF in the presence of excess monomer.[54] This is followed by activation of the alcohol, in this case benzyl alcohol, by the formation of a hydrogen bond with one arm of the bidentate aryloxide ligand. The formation of a similar hydrogen bond between benzyl alcohol and the same ligand has been observed in the solid-state structure of a lithium complex of the aryloxide ligand.[55] The activation of benzyl alcohol results in the formation of the corresponding alkoxide, which attacks the carbonyl carbon and is followed by insertion of the cyclic ester into the zinc-alkoxide bond.

Another class of initiator which has shown utility in the ROP of cyclic esters and has low biological toxicity are iron(III) alkoxides. Iron(III) complexes employing carboxylate ligands such as lactate have been studied by several groups, but slow polymerisation rates and the need for high temperatures were considered prohibitive to their success.[56-58] More recently, several groups have found iron(III) alkoxides to be useful in the ROP of cyclic esters. Liao and co-workers utilised $Fe(OR)_3$ complexes where R = Et, ^{n}Pr, ^{i}Pr, and ^{n}Bu, which they found to be active initiators for ROP of L-LA in bulk at temperatures >130 ºC although the initiators were not structurally characterised.[59] The narrowest polydispersity index values were achieved when iron(III) ethoxide was used as the initiator; initiators with bulkier R groups produced polymers with higher PDI values. Tolman and co-workers sought to compare mono- and dinuclear iron(III) complexes and prepared both with an $-OCHPh_2$ group as the alkoxide, in order to compare the effect of

the ancillary ligand L and of initiator aggregation (Figure 1.23).[60] Both complexes were active for the ROP of ε-CL, proceeding to complete conversion in toluene at room temperature, however, there were some notable differences in polymerisation activity. Polymerisations initiated with the mononuclear complex $L_2Fe(OCHPh_2)$ took longer to reach complete conversion (for a monomer to initiator ratio of 200:1, the polymerisation initiated by $Fe_2(OCHPh_2)_6$ was complete in 26 minutes, when $L_2Fe(OCHPh_2)$ was used the polymerisation was complete in 255 minutes). In addition, the polymers produced with the mononuclear $L_2FeOCHPh_2$ had broader molecular weight distributions (PDI values of 1.8 – 2.0) than those produced using $Fe_2(OCHPh_2)_6$ as the initiator (PDI values of ≤ 1.2).

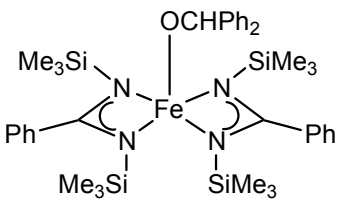

$L_2FeOCHPh_2$

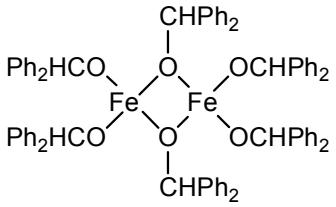

$Fe_2(OCHPh_2)_6$

Figure 1.23 Iron(III) alkoxide initiators for ROP of ε-CL and L-LA.[60]

ROP of L-LA in toluene solution at 80 ºC using these complexes also proceeded readily, with conversions of 95% and 88% being reached after 37 minutes and 77 minutes using the dinuclear and mononuclear complexes, respectively. As for the ROP of ε-CL, PDI values were higher for polymers produced using $L_2Fe(OCHPh_2)$ as the initiator. However, in contrast to the ROP of ε-CL, PDI values for polymers produced with either initiator increased dramatically (1.09 to 1.60 for $Fe_2(OCHPh_2)_6$, 1.34 to 1.88 for $L_2Fe(OCHPh_2)$ at higher conversions indicating transesterification was occurring. The kinetic data for polymerisations initiated by the mononuclear species were more complicated than for the dinuclear species. In both the ROP of ε-CL and L-LA, narrower molecular weight distributions were observed for the dinuclear species, which was unexpected, as well defined single site initiators are considered to offer more control compared to their aggregated analogues. The authors note this interesting conundrum, but present no potential explanation. As initiators for the ROP of L-LA, both complexes are inferior to an iron(III) cluster complex prepared by the same authors (Figure 1.24).

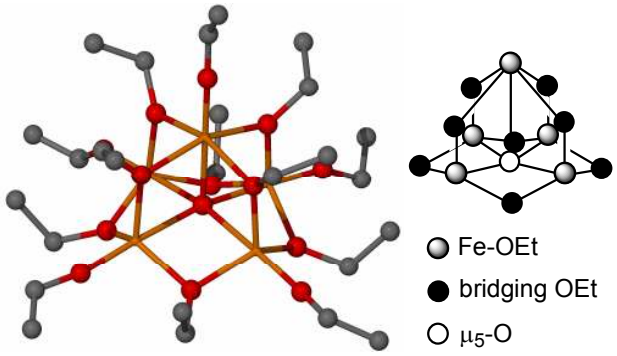

Figure 1.24 Iron(III) ethoxide cluster prepared by Tolman and co-workers.[61]

This complex was an active initiator for the ROP of L-LA in toluene solution at 70 ºC, producing PLA at 97% conversion in a controlled fashion over a range of monomer to initiator ratios with narrow PDI value of 1.17.[61]

As well as iron(III) clusters, similar clusters of lanthanide(III) atoms have also been prepared as potential cyclic ester ROP initiators. These initiators were prepared by Spassky and co-workers[62] after early work by the group of Stevels,[63, 64] which found that commercially available yttrium oxo-isopropoxide was active for the ROP of L-lactide. Stevels also prepared yttrium(III) alkoxides via an exchange reaction between yttrium(III) 2,6-di-*tert*-butylphenoxide and various alcohols including isopropanol, *n*-butanol, 1-methoxyethanol and *N,N*-dimethylaminoethanol using a similar method to that described for aluminium(III) complexes previously. These initiators were found to give a rate of polymerisation for ROP of ε-CL and L-LA at room temperature in dichloromethane solution several orders of magnitude higher than the commercial yttrium oxo-isopropoxide initiator, with the polymerisations proceeding to near complete conversion in five minutes or less and the resulting polymers having molecular weight distributions of between 1.04 and 1.28.[64, 65] The lanthanide clusters Ln(μ_5-O)(O^iPr)$_{13}$ (Figure 1.25, Ln = Y, La, Sm, Yb) prepared by Spassky adopt a similar structure to the iron(III) ethoxide cluster discussed previously, although the isopropoxide groups which bridge to the apical lanthanide(III) atom bridge between three metal(III) atoms rather than two as seen for the iron(III) complex.

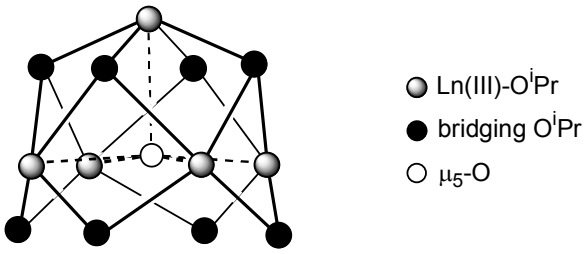

Figure 1.25 Lanthanide clusters prepared by Stevels and co-workers, Ln = Y, La, Sm, Yb.[62]

Of these clusters, the lanthanum(III) initiator displayed the highest reactivity for the polymerisation of D,L-LA proceeding to 50% conversion in 45 seconds. The trend in reactivity La>>Sm>>Yb was attributed by the authors to the increase in size of the lanthanide(III) centre. Although the lanthanum(III) complex was most active for the ROP of D,L-LA, the molecular weight distribution increased readily with conversion, suggesting undesirable side reactions were taking place. In contrast, when the yttrium(III), samarium(III) or ytterbium(III) complexes were used to initiate the ROP, the PDI values remained relatively constant over a range of conversions, suggesting a much better controlled polymerisation process.

In the search for monomeric lanthanide(III) alkoxide initiators, Arnold and co-workers prepared the four-coordinate lanthanum(III) diketiminate complex shown in Figure 1.26.[66] When this complex was used as an initiator for the ROP of L-LA in dichloromethane solution at 25 ºC good control over molecular weight was achieved and relatively narrow PDI values were maintained until high conversion was reached, when the PDI values increased.

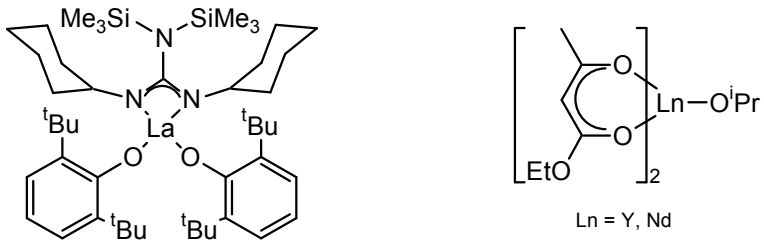

Figure 1.26 Monomeric lanthanide(III) complexes which are active initiators for the ROP of cyclic esters.[66, 67]

The yttrium(III) and neodymium(III) isopropoxide complexes employing two substituted acetylacetonate ligands (Figure 1.26) were also active initiators for the ROP of ε-CL at 25 ºC in tetrahydrofuran solution.[67] Although the complexes were not structurally characterised, the polymerisation data suggests the five-coordinate structure is accurate; these complexes effected controlled polymerisation yielding PCL polymers with PDI < 1.10 and linear M_n versus conversion plots.

Homoleptic titanium(IV) alkoxide are another group of active initiators for the ROP of ε-CL and L-LA, but their use leads to poorly controlled polymerisation and the formation of polymers with broad molecular weight distributions.[13] Single-site titanium(IV) alkoxide initiators were first investigated by Verkade and co-workers in 2002 and work on this class of initiators has progressed significantly in recent years.[68] As this thesis details the synthesis of novel Group 4 initiators for the ROP of ε-CL, L-LA and D,L-LA, discussion of other Group 4 initiators is confined to chapters 3 and 4.

1.4 Stereospecific Ring-Opening Polymerisation of D,L-LA

Due to the presence of two chiral carbon atoms in the lactide molecule, three possible stereoisomers exist (Figure 1.27). These are D-LA, where both stereocentres are in the *R* configuration, L-LA, where both are in the *S* configuration, and *meso*-lactide, in which one stereocentre is in the *S* configuration and one in the *R*. Thus, when these monomers undergo ROP, polymers of differing tacticities may be formed.

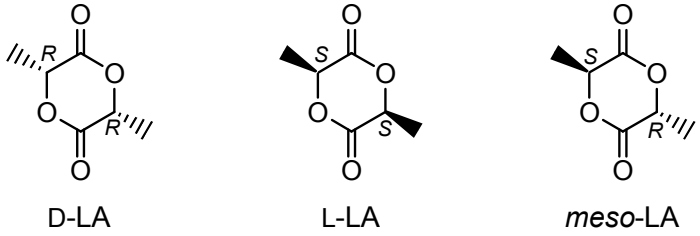

Figure 1.27 Stereoisomers of lactide.

When either pure D- or pure L-LA undergoes ROP via a coordination-insertion process, isotactic PDLA or PLLA is formed, respectively, as the coordination-insertion mechanism does not involve epimerisation (Figure 1.28). In this type of polymer all the stereocentres along the chain are in the same configuration.

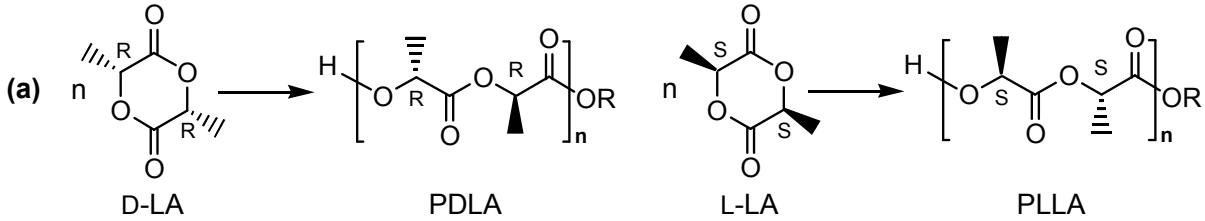

Figure 1.28 The ROP of D-LA and L-LA to give isotactic PDLA and PLLA, respectively.

However, when a mixture of D- and L-LA is used as the monomer, the formation of other stereopolymers becomes possible. For a 1:1 mixture of D- and L-lactide (called D,L-lactide or *rac*-lactide, Figure 1.29) the polymers (poly-D,L-lactide or PDLLA) produced may be (i) atactic, with the stereocentres distributed in a random fashion along the polyester backbone, (ii) stereoblock isotactic, which is a result of all the monomer of one

stereochemistry being polymerised first, followed by the monomer of opposite stereochemistry, or (iii) heterotactic (also called disyndiotactic), in which one enantiomer is ring opened followed by the other enantiomer. These limiting cases, especially for stereoblock isotactic (ii) rely on the assumption that all monomer has been converted to polymer. However, it is possible that an initiator could be selective for a single enantiomer of lactide, resulting in the formation of pure isotactic PLLA or PDLA, while the other enantiomer remained in the reaction medium as unreacted monomer.

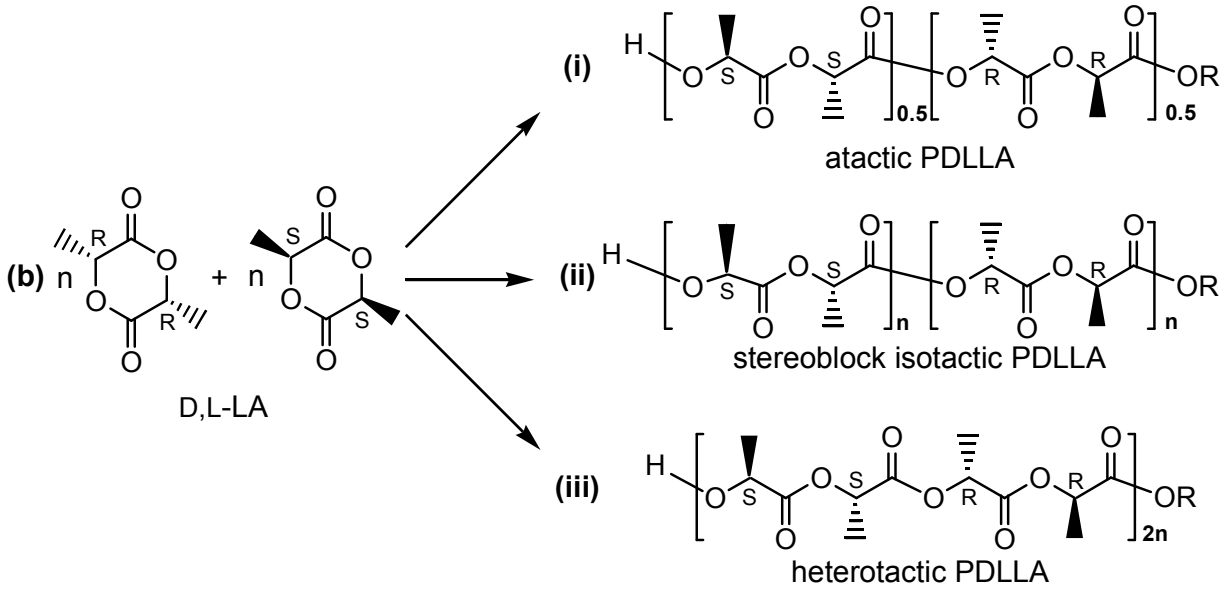

Figure 1.29 The ROP of D,L-LA may produce several types of PDLLA polymer.

In the case of *meso*-lactide, two possible polymer types exist (Figure 1.30). Syndiotactic PDLLA (i) is formed if each subsequent monomer is ring opened at the same site, resulting in a polymer with alternating stereocentres. Heterotactic PDLLA (ii) may also be formed by using *meso*-lactide, in this case each subsequent monomer would be ring opened at alternating sites, resulting in a polymer with an $(RRSS)_n$ distribution along its backbone.

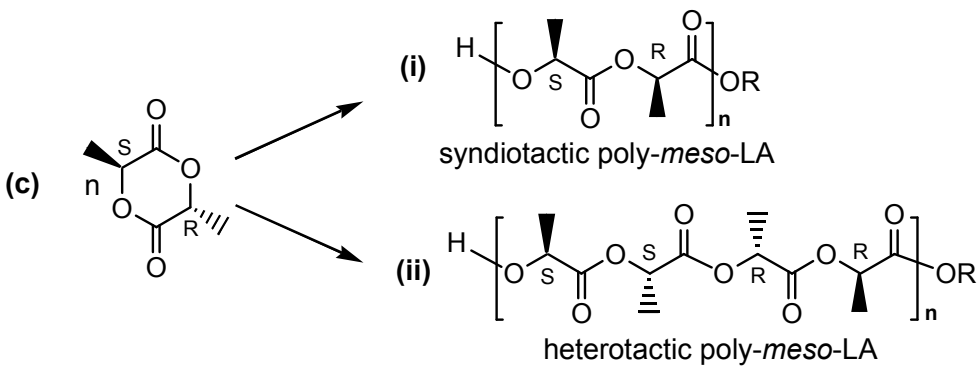

Figure 1.30 Possible stereopolymers which may be formed from the ROP of *meso*-LA.

Each type of PDLLA stereopolymer, with differing tacticity, has differing physical properties and potential applications. Isotactic PLLA and PDLA and syndiotactic PDLLA are crystalline, whereas atactic and heterotactic PDLLA are amorphous. Table 1.2 gives values for some common physical parameters for the various types of poly(lactide) stereopolymers. Unfortunately, sufficient data for heterotactic PDLLA is not currently available. The melting temperature, T_m, is the temperature at which the ordered regions of crystalline polymers begin to melt and determines the temperature at which the plastic can be processed. At the glass transition temperature, T_g, the glassy polymer becomes viscous or rubbery as amorphous regions of the polymer chain gain thermal energy and slide past one another. The tensile strength σ_B is a measure of the force required to pull oriented fibres or non-oriented films (see table) to breaking point. The Young's modulus, E, is a measure of the material's stiffness and is the rate of change of stress with strain.[69] The percentage elongation at break is given as ε_B. Controllable synthesis of each stereopolymer is an important goal both industrially and in academic terms.

Table 1.2 Physical properties of PLA stereopolymers.[70] [a]Density; [b]tensile strength; [c]Young's modulus; [d]elongation at break; [e]oriented fibre; [f]non-oriented film.

Tacticity	T_m / °C	T_g / °C	d^a / g cm^{-3}	$\sigma_B{}^b$ / GPa	E^c / GPa	$\varepsilon_B{}^d$ / %
Atactic	-	50-60	1.27	0.04-0.05[f]	1.5-1.9[f]	5-10[f]
Heterotactic	-	-	-	–	-	-
Syndiotactic	152	45	-	–	-	-
Isotactic	170-190	50-65	1.25-1.29	0.12-2.3[e]	7-10[e]	12-26[e]
PDLA-PLLA Stereocomplex	220-240	65-72	-	0.88[e]	8.6[e]	30[e]

In addition to the various stereopolymers, the formation of a stereocomplex between isotactic PLLA and isotactic PDLA via van der Waals interactions of the enantiomeric polymer chains is also possible (Figure 1.31).[70] While the glass transition temperatures (T_g) of the various forms of poly(lactide) are quite similar, the melting temperatures (T_m)

of the stereopolymers are quite different. In particular, the T_m of isotactic PLLA, which is the commercially produced polymer, is between 170-180 ºC which obviously limits its use above these temperatures. For example, processing of PLLA fibres at ≥120 ºC (common fabric processing temperatures) damages the fibre. However, the PLLA-PDLA stereocomplex has a melting temperature of between 220-230 ºC, making it particularly desirable. Fibres of stereocomplex PLLA-PDLA are stable at temperatures of 160 ºC or above. The production of this stereocomplex polymer is currently limited by the lack of commercial-scale production of D-lactic acid, but recent research has shown fermentation of sugar cane by bacteria which produce the D-LA enantiomer in high enantiomeric purity,[71] suggesting commercial interest in its production may grow in the future.

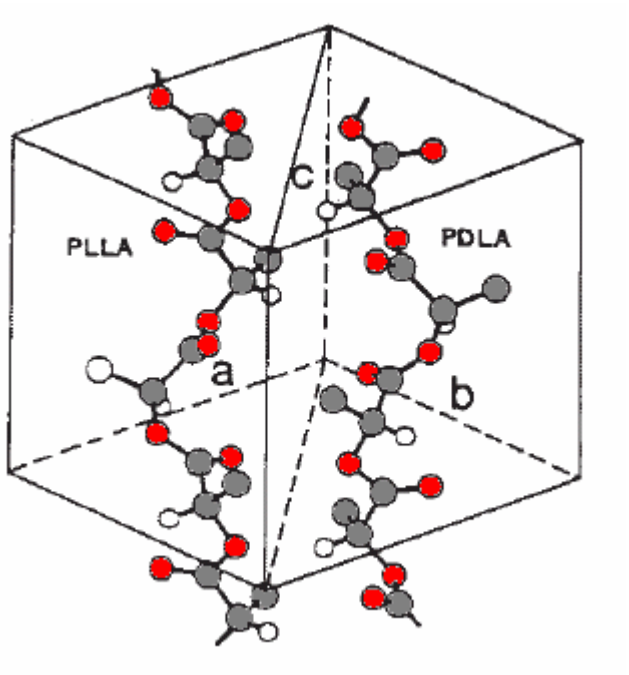

Figure 1.31 PLLA/PDLA stereocomplex.[70]

PDLLA Microstructure Analysis via NMR Spectroscopy

As discussed previously, due to the presence of a chiral carbon centre in the lactide molecule, ring-opening polymerisation of this monomer can lead to polymers with differing stereosequences along the polymer backbone. Significant efforts have been made to control the polymer microstructure in order to produce polymers with particularly desired physical properties. Therefore, the ability to characterise these macromolecules on a very detailed level is paramount. NMR spectroscopy has been shown to be an extremely useful tool for aiding in the determination of polymer stereochemistry and in particular, homonuclear decoupled ^{1}H NMR and ^{13}C NMR spectroscopy.

The homonuclear decoupled ^{1}H NMR spectroscopic experiment determines through-bond connectivities.[72] Radiofrequency irradiation at the frequency of a particular resonant line gives information about coupled proton signals. The signal at the chosen irradiation frequency is saturated and any coupling between the signal at the irradiation frequency and signals in the rest of the spectrum will be lost. So, loss of coupling in this experiment is indicative of coupled nuclei.

In the determination of the stereochemical microstructure along the backbone of a PDLLA polymer, ^{1}H homonuclear decoupled NMR spectroscopy is used in the following way. The ^{1}H NMR spectrum of the lactide monomer in $CDCl_3$ solution at 400.13 MHz exhibits a doublet of integral 3 at ~1.2 ppm due to the three $\mathbf{H_b}$ nuclei from the lactide methyl group coupling to the adjacent $\mathbf{H_a}$ and a quartet of integral 1 at ~3.8 ppm due to $\mathbf{H_a}$ coupling to the three methyl $\mathbf{H_b}$ nuclei (Figure 1.32). In isotactic PLLA or PDLA, the NMR pattern is the same (albeit shifted in ppm) because all $\mathbf{H_a}$ and $\mathbf{H_b}$ nuclei in the polymer are in the same environment, respectively. That is, each adjacent stereocentre is in the same stereochemical configuration, either *R* (for PDLA) or *S* (for PLLA). In these cases, if the doublet due to the three $\mathbf{H_b}$ nuclei was selected for decoupling a loss of coupling to the adjacent $\mathbf{H_a}$ would result and a singlet would be observed for $\mathbf{H_a}$, instead of the quartet observed in the non-decoupled spectrum.

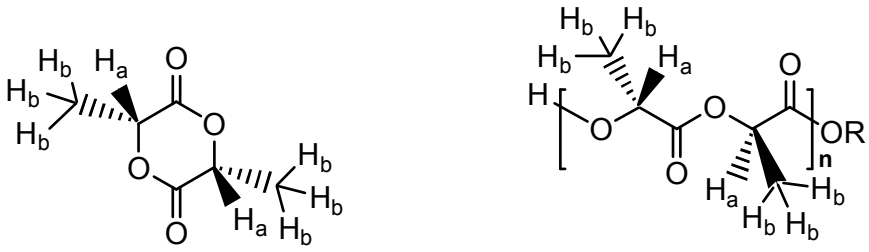

Figure 1.32 Protons at the methine carbon in D-LA and isotactic PDLA**.**

However, when a PDLLA polymer is atactic, stereoblock isotactic, heterotactic or in any way enriched in a certain stereosequence, the ^{1}H NMR spectrum becomes more complicated. Adjacent chiral centres influence one another, particularly with regard to the chemical shift of $\mathbf{H_a}$. Whereas in isotactic PLLA or PDLA a simple quartet is observed due to the shift of all $\mathbf{H_a}$ nuclei in the polymer being coincident (Figure 1.33(a)), the differing chemical environments adjacent to each $\mathbf{H_a}$ in a non-isotactic polymer results in the resonances for each of the respective $\mathbf{H_a}$ nuclei being shifted slightly, depending on the arrangement of adjacent stereocentres. As a result, the quartets due to $\mathbf{H_a}$, rather than being coincident, are shifted slightly from one another. In effect the observed signal is a multitude of quartets overlaid on one another. Figure 1.33(b) shows

three quartets overlaid on one another, resulting in a complicated pattern. In reality, as there are methine protons many in differing chemical and magnetic environments the actual pattern is hugely complicated.

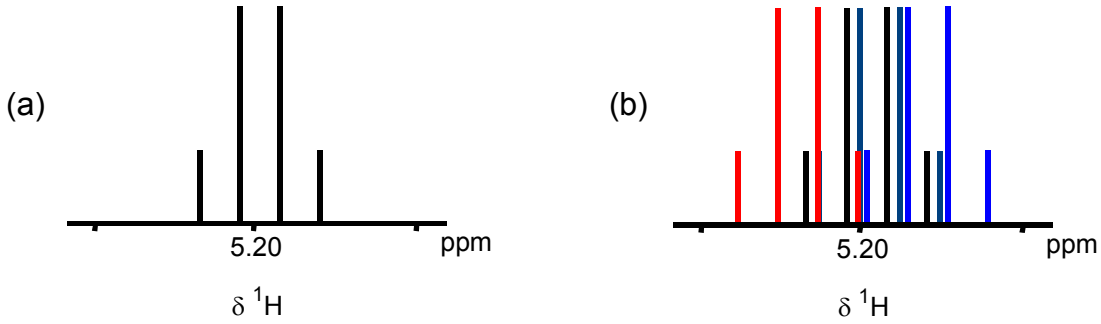

Figure 1.33 Diagram of the pattern in the methine region of the ^{1}H NMR spectrum expected from (a) isotactic PLLA or PDLA and (b) atactic, heterotactic or stereoblock isotactic (i.e. non-isotactic) PDLLA.

Homonuclear decoupling of the ^{1}H NMR spectrum can deconvolute this array of peaks into signals which can be interpreted to give meaningful information about the microstructure of the polymer. The arrangements of stereocentres are labelled based on whether the linkage between adjacent stereocentres is isotactic or syndiotactic. An isotactic connection (*i*) is one in which the two adjacent stereocentres are of the same stereochemistry while a syndiotactic connection (*s*) exists where two stereocentres of opposite stereochemistry are adjacent to one another. It should be noted that some researchers use an *r*/*m* notation for the stereocentres, with *r* indicating a syndiotactic connection and *m* an isotactic connection. However, the *i*/*s* notation has been dominant in the recent past. In the PDLLA polymer segment shown in Figure 1.34 the sequence of stereocentres is *RSSRSS*. This translates into a linkage sequence of *sissi*.

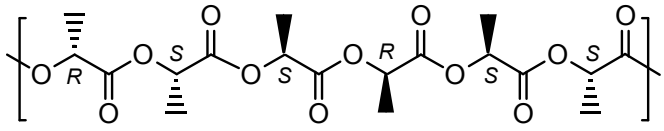

Stereocentre sequence: . . . **R S S R S S** . . .

Linkage sequence: . . . *s i s s i* . . .

Figure 1.34 A PDLLA polymer segment, stereocentre sequence, linkage sequence.

The homonuclear decoupled ^{1}H NMR spectrosocopic experiment has been shown to be sensitive to up to four adjacent stereocentres, three linkages or *tetrads* using high resolution NMR spectrometers. At the tetrad level, five linkages may arise from the ROP of D,L-LA. These are *sis*, *isi*, *sii*, *sis*, and *iii* (Figure 1.35). Because D,L-LA is a mixture of pure D (*R,R*)-LA and pure L (*S,S*)-LA, only 'paired' stereosequences should be present in PDLLA polymers.

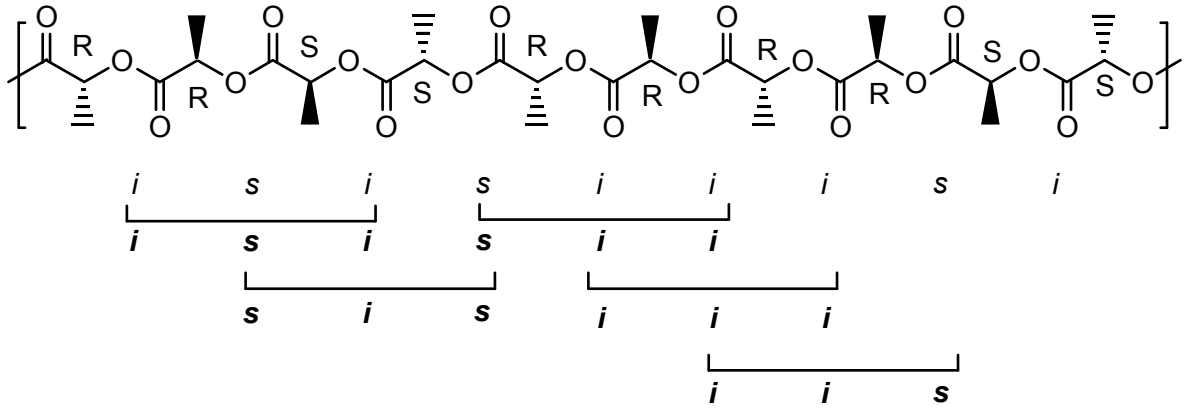

Figure 1.35 A PDLLA polymer sequence and the resulting tetrad linkages.

The tetrad sequences which may arise from the ROP of *meso*-lactide are *sis, ssi, iss, isi* and *sss* (Figure 1.36).

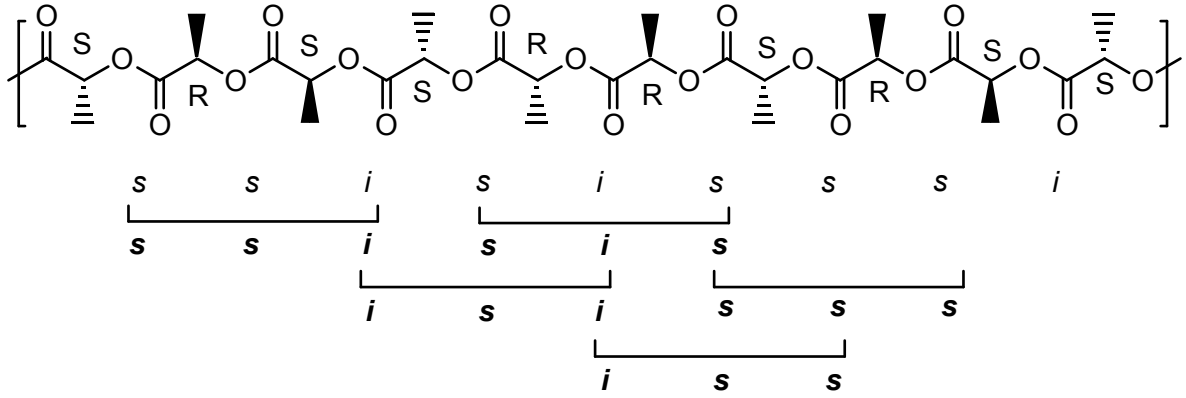

Figure 1.36 A poly-*meso*-LA sequence and the resulting tetrad linkages.

It has been calculated using Bernoullian statistics that for atactic PDLLA, the distribution of tetrad stereosequences should obey the pattern shown in Figure 1.37. That is, the peaks due to the *sis*, *sii*, *iis*, *iii* and *isi* tetrads should be in a ratio of 1:1:1:3:2, respectively.[73]

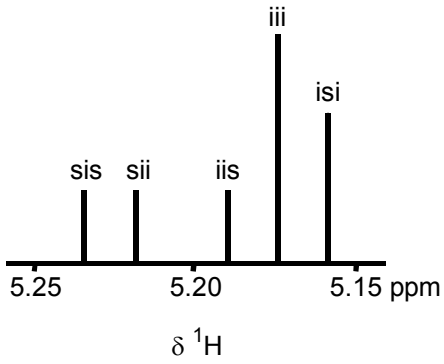

Figure 1.37 Methine region of the ^{1}H homonuclear decoupled NMR spectrum expected for an atactic PDLLA polymer.[73]

These spectroscopic assignments were made after extensive ^{1}H-^{13}C heteronuclear correlation NMR experiments were carried out on PDLLA polymers with various

stereosequence distributions.[73-77] These assignments also take into account the directionality of PLA with the convention being that the C terminus of the polymer (with the ester end group) is on the left and the O terminus (with the hydroxyl end group) to the right. As the intensity/integration ratios between the peaks shown in Figure 1.37 are representative of atactic PDLLA, deviation from these ratios gives an indication of isotactic or heterotactic stereoenrichment (Figure 1.38) of the polymer.[77]

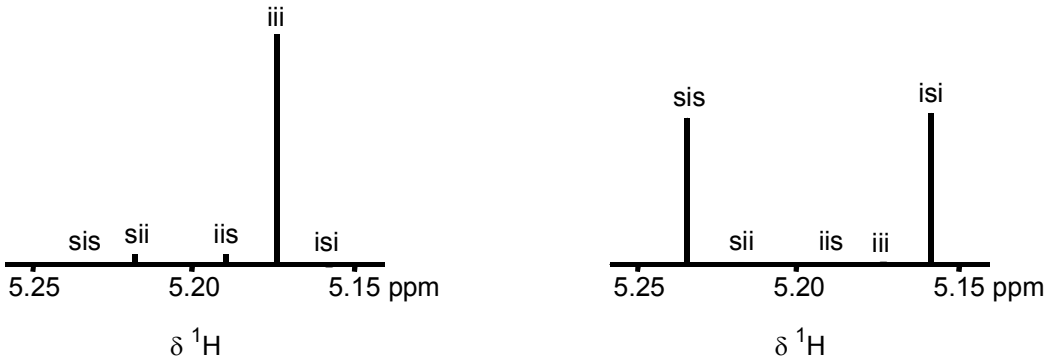

Figure 1.38 Predicted methine region of the ^{1}H homonuclear decoupled NMR spectrum for a stereoblock isotactic (left) or heterotactic (right) PDLLA polymer.

Using the intensities and/or the integrations of these peaks in the ^{1}H homonuclear decoupled NMR spectrum, it is possible to calculate the probabilities of racemic enchainment in P_r or isotactic enchainment P_m in the polymer using the equations given in Table 1.3.[78]

Table 1.3 Equations for the determination of P_r and P_m from the examination of the methine region of the ^{1}H homonuclear decoupled NMR spectrum of a sample of PDLLA or poly-*meso*-LA.[78]

	probability	
tetrad	**D,L-lactide**	***meso*-lactide**
[*iii*]	$P_m^2 + P_rP_m/2$	0
[*iis*]	$P_rP_m/2$	0
[*sii*]	$P_rP_m/2$	0
[*sis*]	$P_r^2/2$	$(P_m^2 + P_rP_m)/2$
[*sss*]	0	$P_r^2 + P_rP_m/2$
[*ssi*]	0	$P_rP_m/2$
[*iss*]	0	$P_rP_m/2$
[*isi*]	$(P_r^2 + P_rP_m)/2$	$P_m^2/2$

A P_r value of 1 indicates a high probability of racemic enchainment and results from a heterotactic PDLLA polymer. A P_r value of 0 indicates negligible racemic enchainment, resulting from an isotactic (or stereoblock isotactic) PDLLA polymer. Atactic PDLLA has a P_r value of 0.5.

^{13}C NMR spectroscopy can also give information about the polymer microstructure and is generally used to support conclusions made from examination of the methine region of the homonuclear decoupled ^{1}H NMR spectrum of the polymer.

Stereoselective ROP of D,L-LA by discrete metal complexes

Stereoselectivity in the ROP of cyclic esters initiated by metal complexes is usually attributed to one of two mechanisms, or a combination of these.[79] The first is *chain-end control* (CEC) in which the chirality of the growing polymer chain controls the next insertion of monomer. When there is chirality associated with the metal initiator complexes, *enantiomorphic site control* (ESC) is also possible (Figure 1.39). In this case, the chirality of the ligand(s), the complex or both determines the stereoselectivity of the polymerisation.

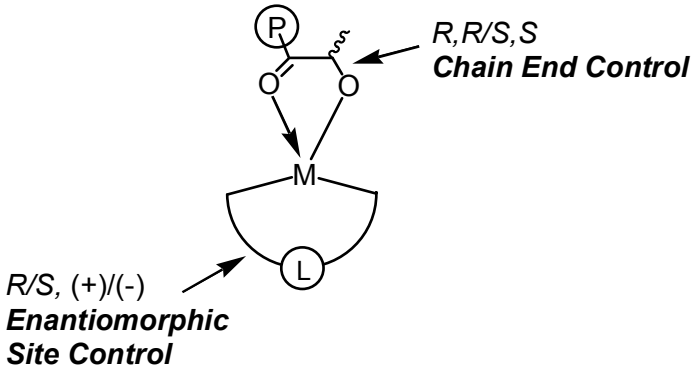

Figure 1.39 Chain end control and enantiomorphic site control, two mechanisms by which the stereochemistry of a PDLLA polymer may be achieved when discrete metal initiators are used.

One of the earliest reports of the stereoselective ROP of D,L-LA was provided by Kasperczyk who was able to produce PDLLA with heterotactic enrichment using lithium *tert*-butoxide.[80, 81] This enrichment was inferred by deriving equations for calculation of the probabilities for adding two of the same monomers versus two different monomers. The author discovered through observation of the carbonyl region of the ^{13}C NMR spectrum of the resulting polymer that the intensities and pattern of the signals deviated from those expected for a totally random, atactic polymer.

A range of aluminium(III) alkoxide complexes based on Schiff base or salen ligands have been shown to exert stereocontrol over the ROP of D,L-LA. Spassky and co-workers reported the first use of the *R*-salbinap aluminium(III) methoxide complex (Figure 1.40) for ROP D,L-LA;[82] they reported formation of PDLLA with a high degree of isotactic enrichment low conversions while at higher conversion, the istotactic enrichment decreased. The authors reasoned that the decrease in isotactic enrichment observed at high conversion was due to an increase in concentration of the unfavoured enantiomer of the monomer in the reaction mixture. They also found that the *R* initiator was selective for ROP of D-LA over L-LA and a 'gradient' stereoblock polymer was postulated, with a PDLA block followed by an atactic PDLLA block and a PLLA block.

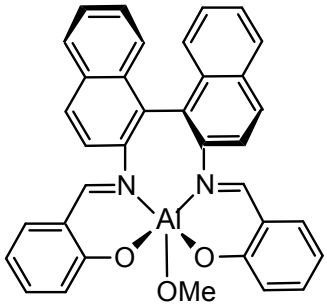

Figure 1.40 An aluminium(III) complex synthesised by Spassky and co-workers which produced PDLLA with a high degree of isotactic enrichment.[82]

Ovitt and Coates prepared an analogous complex where X = ^{i}Pr and achieved synthesis of a polymer with an exceptional degree of syndiotactic enrichment from *meso*-lactide.[83] The degree of syndiotactic enrichment was calculated at 96% from examination of the methine region of the homonuclear decoupled ^{1}H NMR spectrum of the polymer. In contrast to the conditions in Spassky's study, the concentration of *R* and *S* stereocentres in the reaction mixture remains constant relative to one another as both are present in equal proportions in the monomer molecule. It is interesting to note that Coates *et al* also prepared an yttrium(III) 2-dimethylamino ethoxide complex of the *R*-salbinap ligand; this initiator failed to exert any stereocontrol over the polymerisation of *meso*-lactide.

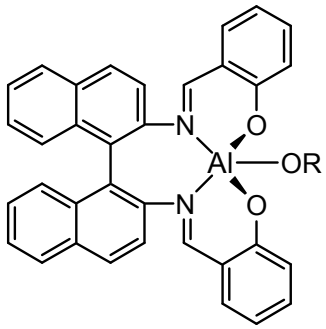

Ligand chirality	R	monomer	polymer	reference
R	Me	D,L-LA	gradient isotactic	[82]
R	^{i}Pr	*meso*-LA	highly syndiotactic	[83]
rac	^{i}Pr	D,L-LA	highly isotactic	[84]
rac	^{i}Pr	*meso*-LA	highly heterotactic	[85]

Figure 1.41 Aluminium(III) salbinap initiators prepared by Spassky, Radano and Coates.

In light of Spassky's work, Radano and co-workers prepared the racemic aluminium(III) initiator and employed it in the ROP of D,L-LA, producing highly isotactic PDLLA which formed the PLLA/PDLA stereocomplex.[84] Knowing the enantiopure complex forms highly isotactic PLA at low conversions from D,L-LA, formation of the respective isotactic polymers in high enantiopurity was expected as Spassky had shown one enantiomer of the initiator shows a kinetic preference for ROP of one enantiomer of the monomer and vice versa. Unlike in Spassky's work, as both enantiomers are present in equal concentration, a decrease in isotactic enrichment with time was not observed.

At the same time Coates and co-workers showed that the *R*-initiator preferred ring-opening *meso*-LA at the B site of the monomer (Figure 1.42).[85] This was achieved by

reaction of the enantiopure *R*-initiator with one equivalent of *meso*-LA, followed by hydrolysis and reaction of the hydrolysed product with (*S*)-(+)-α-ethoxy-α(trifluoromethyl)phenyl acetyl chloride [(*S*)-MTPA(Cl)] forming the Mosher ester. After purification the diastereomeric mixture was analysed by ^{1}H NMR spectroscopy; analysis via integration showed the concentration of the ester derived from lactide which had been ring-opened at one site was much greater than that which had been opened at the other site, in a ratio of 96:4. The solid-state structure of the major product revealed it to be the derivative of the product of ring-opening at the B site.

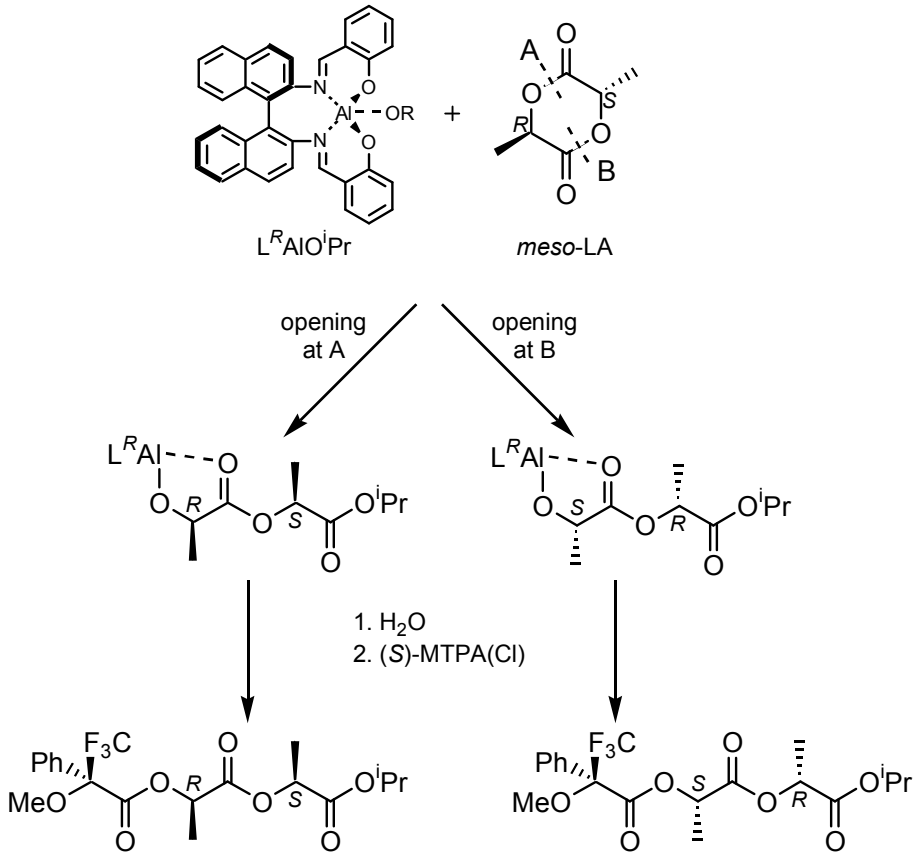

Figure 1.42 Determination of enantiomeric preference for ROP of D,L-LA by the aluminium(III) *R*-salbinap initiator prepared by Spassky and Coates.[85]

The authors subsequently determined that the *S*-initiator showed a similarly marked preference for ring-opening *meso*-LA at the A site. When a racemic mixture of the two initiator complexes was used, highly heterotactic PDLLA was formed, with a P_r value of 0.80. This result was unexpected as the enantiomerically pure initiators both produced syndiotactic PDLLA under the same conditions. Although for the polymerisations initiated by the enantiomerically pure aluminium(III) complexes were considered to proceed via and enantiomorphic site control mechanism, a polymer exchange process was proposed by Coates for the formation of highly heterotactic PDLLA using the racemic initiator (Figure 1.43). In this mechanism individual polymer chains are exchanged between the two enantiomeric forms of the initiator complex after each subsequent

monomer insertion. The authors suggest that this polymer transfer could be achieved through a μ-alkoxide or ionic $[L_nAl]^+[OPolymer]^-$species.

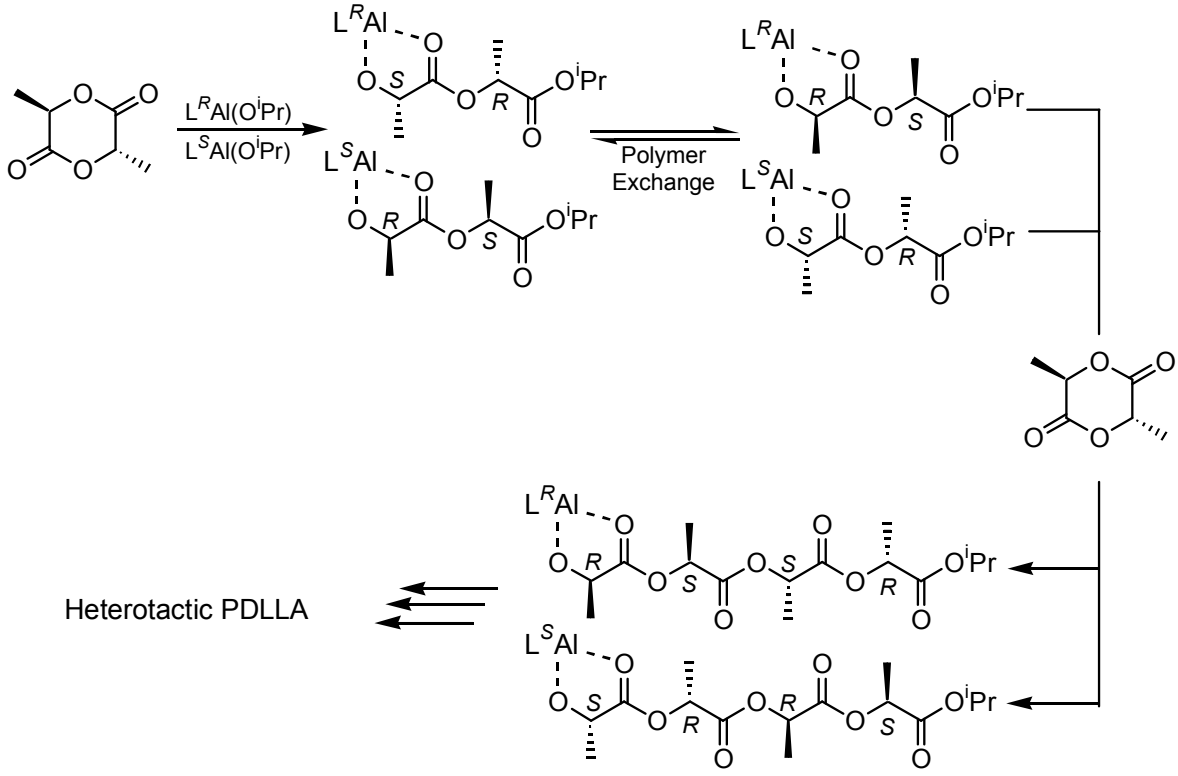

Figure 1.43 Polymer exchange mechanism postulated by Coates and Ovitt.[85]

Since the promising early results reported with aluminium(III) complexes of salbinap ligands, a great deal of interest and activity has centred on varying the N-N linker as well as the phenol substituents to optimise the stereoselectivity of the initiator. Alkyl backbones, $(CH_2)_n$ where n = 2, 3 with and without substituents have been used, as illustrated in Figure 1.44.

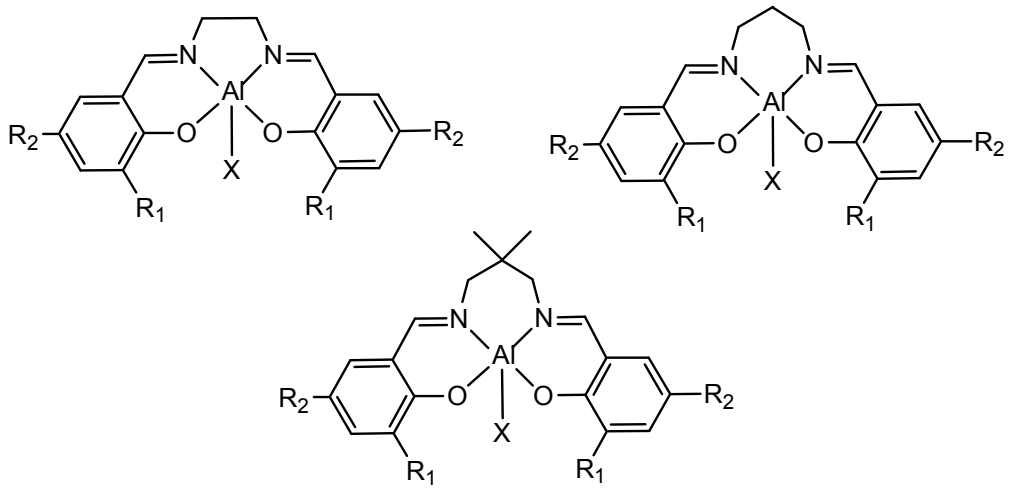

Figure 1.44 Aluminium(III) salen initiators for the stereoselective ROP of D,L-LA prepared by Gibson[86] and Nomura.[87] Longer N-N linkers of the form $(CH_2)_n$ where n=2,3,4 have also been used.

Nomura and co-workers found strong correlation between tacticity and T_m values for the group of aluminium(III) complexes X=Et illustrated in Figure 1.44.[87, 88] In these cases (Table 1.4) the corresponding alkoxide complexes were generated in solution by the addition of benzyl alcohol. Polymerisations of D,L-LA initiated by these types of complexes with bulkier substituents in the phenol *ortho* and *para* positions led to an increase in isotactic enrichment. The introduction of triphenyl-, triisopropyl- or *tert*-butyldiphenylsilyl groups into the *ortho* position completely prevented the polymerisation from occurring. In addition, changes along the N-N backbone were also manifested in changes in the value of P_m. Increasing the alkyl chain length from n=2 to 3 led to a marked increase in isotactic enrichment for otherwise analogous initiators. The stereocontrol could be further enhanced by introducing two methyl groups on one of the backbone carbon atoms. The combination of this N-N linker with bulky *tert*-butyl dimethylsilyl groups in the phenol *ortho* position gave the highest value of P_m (0.97). Preparation and isolation of the active alkoxide complex and its use in the initiation of the ROP of D,L-LA resulted in a polymer with a similarly high P_m value of 0.98. The authors attributed the origin of the stereocontrol to the pseudo trigonal bipyramidal geometry of the complex, which was thought to amplify the chirality of the monomer molecule.

Table 1.4 Aluminium(III) salen complexes prepared by Nomura and co-workers, and the analysis of PDLLA polymers produced using these complexes as initiators. [M]:[I] = 100, toluene solution, 70 ºC.[87, 88]

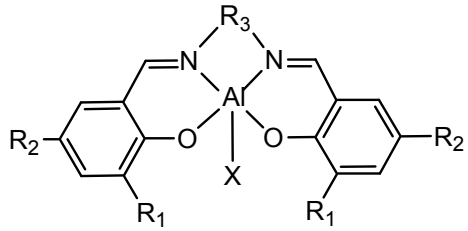

R_1	R_2	R_3	X	time/h	conversion/%	M_n/g mol^{-1}	PDI	P_m
Me	Me	$(CH_2)_2$	Et	40	72	10200	1.24	0.69
^{t}Bu	^{t}Bu	$(CH_2)_2$	Et	72	19	5300	1.07	0.79
Me	Me	$(CH_2)_3$	Et	1.8	95	23000	1.36	0.78
Me_3Si	Ph	$(CH_2)_3$	Et	12	75	12500	1.06	0.92
^{t}BuMe$_2$Si	H	$CH_2CMe_2CH_2$	Et	19	93	20000	1.09	0.97
^{t}Bu	^{t}Bu	$CH_2CMe_2CH_2$	OBz	14	96	22000	1.07	0.98

Gibson and co-workers prepared a wide range of similar complexes, introducing linked and fused aryl groups as well as alkyl chains along the N-N backbone (Figure 1.45).[86] The corresponding alkoxide complexes were generated in solution by the addition of benzyl alcohol; these were active initiators for the ROP of D,L-LA in toluene solution at 70 ºC, in some cases producing highly isotactically enriched PDLLA.

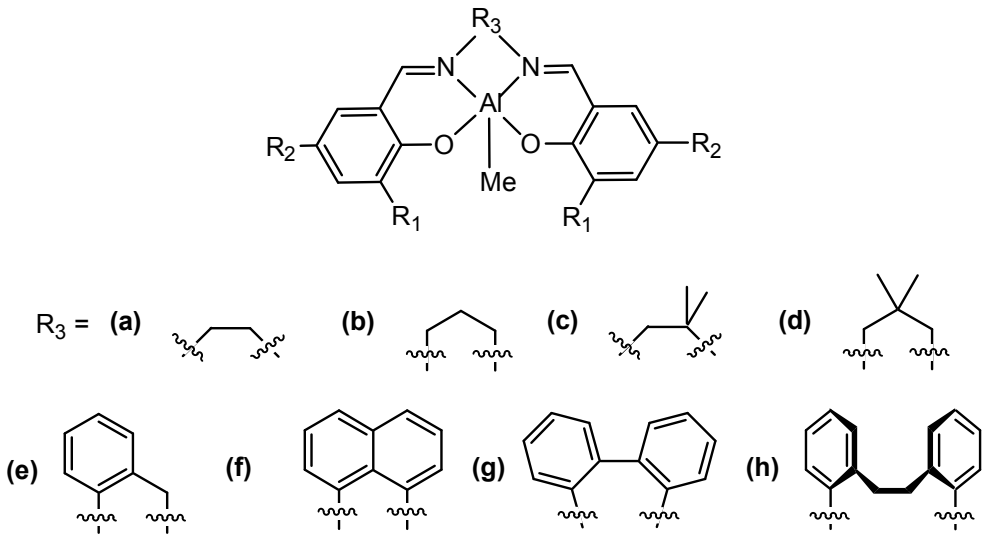

Figure 1.45 Aluminium(III) initiators prepared by Gibson and co-workers.[86]

One of the major findings from this work was that subtle variations to the initiator ligand substituents have a significant effect on the tacticity of the resulting polymer. In particular, changing the phenol *ortho* and *para* substituents from ^{t}Bu (which gave the highest isotactic selectivities) to Cl resulted in a decrease in the isotactic enrichment of the polymer produced by these initiators (Table 1.5).

Table 1.5 Aluminium(III) salen initiators for the ROP of D,L-LA prepared by Gibson and co-workers and some properties of the resultant polymers. [M]:[I] = 50, toluene solution, T = 70 ºC, reaction times and conversions not given.[86]

R_1	R_2	R_3	M_n/g mol^{-1}	PDI	P_m
^{t}Bu	^{t}Bu	$(CH_2)_2$	5900	1.27	0.83
Cl	Cl	$(CH_2)_2$	7100	1.58	0.56
^{t}Bu	^{t}Bu	$CH_2CMe_2CH_2$	7400	1.20	0.85
Cl	Cl	$CH_2CMe_2CH_2$	7500	1.37	0.59
^{t}Bu	^{t}Bu	C_6H_5Me	7900	1.08	0.86
Cl	Cl	C_6H_5Me	9300	1.13	0.63
^{t}Bu	^{t}Bu	1,1'-biphenyl	6600	1.26	0.63
Cl	Cl	1,1'-biphenyl	3500	1.33	0.37

The authors found that complexes with N-N linkers ((a)-(e)) produced PDLLA with a greater degree of isotactic enrichment than those containing diaryl linkers ((f)-(h)) and suggest that the factors governing the stereocontrol imparted by these initiators are complex, but that the relative lack of stereocontrol may be related to the increased rigidity of the N-N backbone. They also suggest that the origin of stereocontrol is related to the minimisation of steric repulsion between the growing polymer chain, the incoming monomer and the salen ligand substituents, and that more flexible ligand systems are better equipped to minimise these unfavourable interactions.

Other successful initiators of this type (in terms of stereoselective polymerisation) are the aluminium(III) complexes of racemic and enantiopure Jacobsen's ligand employed by Feijen and co-workers (Figure 1.46).[89]

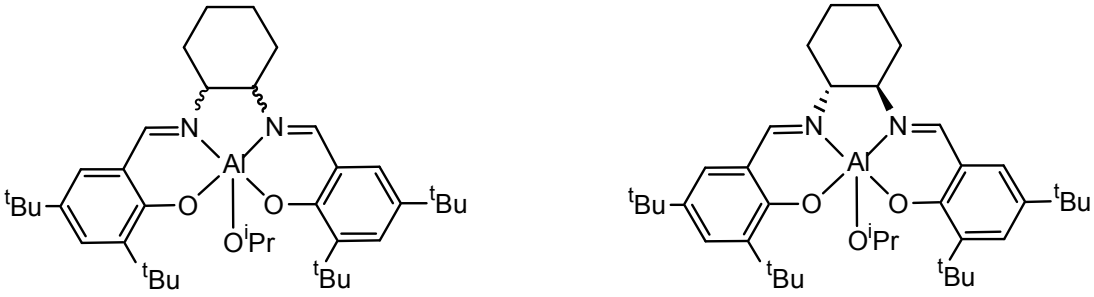

Figure 1.46 Aluminium(III) complexes of Jacobsen's ligand, prepared by Feijen and co-workers.[89]

Using the enantiopure (*R,R*) complex a gradient isotactic PDLLA could be formed. Similar to the results obtained by Spassky and co-workers discussed previously, a high degree of isotactic enrichment was observed at low conversions, with that enrichment decreasing as conversion increased and a greater concentration of the unfavoured monomer remained in the reaction mixture. It was found that this initiator favoured the polymerisation of L-LA, while the (*S,S*) analogue selectively polymerised D-LA. When the racemic initiator was used, highly isotactic PDLLA could be formed, even at high conversions. This isotacticity was maintained (though slightly decreased) in the bulk polymerisation at 130 ºC; this report constituted the first example of high stereoenrichment under bulk ROP conditions.

Table 1.6 Analysis of PDLLA polymers produced by Feijen and co-workers using the initiators described in Figure 1.45. [M]:[I] = 62, toluene solution, T = 70 ºC.[89]

Initiator stereochemistry	T/ºC	time/h	conversion/%	M_n/g mol^{-1}	PDI	P_i
R,R	70	48	21.1	3300	1.04	0.92
rac	70	288	85.3	7700	1.06	0.93

Feijen and co-workers used P_i to describe the stereochemical microstructure of their polymers, which, like P_m, denotes the probability of isotactic enchainment, sometimes denoted as based on enantiomorphic site control statistics. However, it is calculated slightly differently, using [*iii*] = $[P_i^2 + (1\text{-}P_i)^2 + P_i^3 + (1\text{-}P_i)^3]/2$. For the same value of [iii], using P_i results in a higher apparent degree of isotactic enchainment (i.e. $P_i > P_m$).

In an attempt to distinguish between enantiomorphic site control and chain end control mechanisms as the origin of stereoselectivity in polymerisations of D,L-LA initiated by the complexes described by Feijen and Gibson, Chisholm and co-workers identified several factors which could influence the stereoselectivity.[90] These factors are (i) the chirality of the salen ligand, namely the N-N linker; (ii) the helicity of the chiral salen

ligand, upon coordination of the lactide monomer, the complex would become six coordinate and the λ and Δ enantiomers become possible; (iii) the chirality of the alkoxide ligand, i.e. the chirality of the growing polymer chain, particularly the last inserted monomer. Using aluminium(III) complexs of (*R,R*)-, (*S,S*)- and (*rac*)-salen Jacobsen's ligand with both chiral (*S*-OCHMeCl) non-chiral (OEt) alkoxides, the authors sought to discover if either the chirality of the salen ligand or of the alkoxide ligand emerged as a dominant factor. However, no clear trend emerged and the authors concluded that the factors governing stereoselectivity in this polymerisation process were too complex to be discerned.

Salen ligands have been used with other metals in addition to aluminium(III). Coates and co-workers reported an yttrium(III) amide complex of the salbinap ligand discussed earlier.[83] Gibson *et al*[91] reported titanium(IV) alkoxide complexes employing salen ligands containing ethyl or cylcohexyl groups in the R_3 position and in one case, phenols with ethynyl ferrocene substituents in the *ortho*-positions.[92] These complexes were found to be active as initiators for the ROP of D,L-LA but consistently produced atactic PDLLA.

Another class of ligands which are easily prepared and whose complexes have been shown as stereoselective initiators for the ROP of D,L-LA are the aminophenols, also called aminophenolates or amine bis(phenolates). These ligands can be prepared from the reaction of a diamine with a phenol in the presence of formaldehyde or by the reduction of the corresponding Schiff base. Moreover there is a wide scope for variation at the phenol and nitrogen substituents and along the N-N backbone.

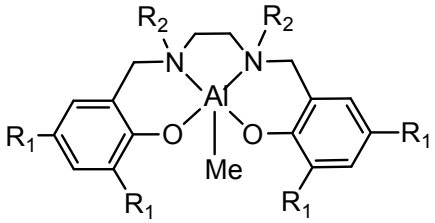

Figure 1.47 Amine bis(phenolate) complexes of the type utilised by Gibson *et al*.[93, 94]

Gibson and co-workers prepared aluminium(III) complexes of the type shown in Figure 1.47 (X = Me) as initiators for the ROP of D,L-LA.[93, 94] The active aryloxide complex was generated in situ on the addition of an equivalent of benzyl alcohol and the stereoselectivity of the initiator was highly sensitive to the choice of R_1 and R_2, displaying dramatic shifts from isotactic preference to heterotactic preference on variation (Table 1.7). For complexes where R_2 = Bz changing the R_1 substituent from H to Me resulted in

a change in the value of P_r from 0.21 (*isotactic* enrichment) to 0.88 (*heterotactic* enrichment).

Table 1.7 Analysis of PDLLA polymers prepared using initiators synthesised by Gibson and co-workers (Figure 1.46). [M]:[I] = 100, toluene solution. [a][M]:[I] = 50.[93, 94]

R_1	R_2	time/h	conversion/%	M_n/g mol^{-1}	PDI	P_r/P_m
H	Me	23	97	18900	1.07	0.32/0.68
Me	Me	24	87	12700	1.09	0.80/0.20
^{t}Bu	Me	1464	66	4700	1.08	0.42/0.58
Cl	Me	24	94	12500	1.11	0.88/0.12
H	Bz	21	98	21200	1.08	0.21/0.79
Me	Bz	24	75	13400	1.06	0.83/0.17
^{t}Bu	Bz	120	77	11300	1.05	0.61/0.39
Cl	Bz	21	94	17700	1.06	0.96/0.04

Coates *et al* reported the formation of highly heterotactic PDLLA using zinc(II) complexes of bulky β-diiminate (BDI) ligands as initiators in dichloromethane solution at 20 ºC (Figure 1.48).[78] The same initiators could also be used to form highly syndiotactic PDLLA from *meso*-lactide. The highest value of P_r was achieved when a dimeric zinc(II) complex with bulky isopropyl substituents on the BDI phenyl groups was used as the initiator. The P_r value could be increased slightly by lowering the temperature at which the reaction was carried out. At 20 ºC PDLLA with P_r = 0.90 (Table 1.7) was produced while the polymer produced at 0 ºC exhibited P_r = 0.94. The authors concluded that a chain end control mechanism was in operation as the zinc(II) initiator was achiral. An analogous magnesium(II) complex afforded no stereocontrol over the ROP of D,L-LA under the same conditions (Table 1.8).

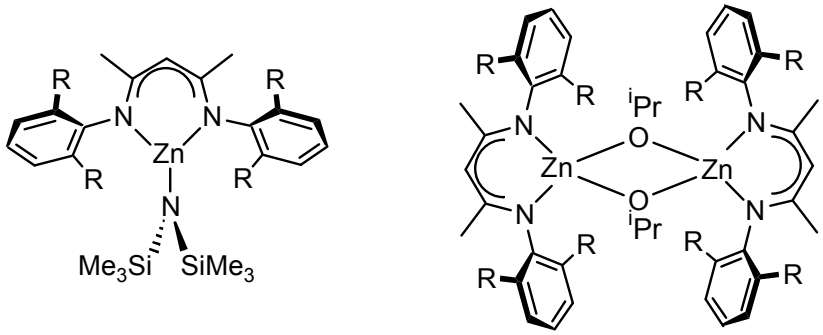

Figure 1.48 Zinc(II) complexes of β-diiminate ligands prepared by Coates *et al*.[78]

Gibson and co-workers reported an iron(II) complex bearing a BDI ligand which produced atactic PDLLA in toluene solution at 25 ºC.[95] Similar monomeric tin(II) complexes were also reported by the same authors (Table 1.8);[96] these produced PDLLA with a much decreased yet still heterotactic enrichment at 60 ºC in toluene solution.

Table 1.8 Results for the ROP of D,L-LA initiated by complexes prepared by Coates *et al*[78] and Gibson *et al*[95, 96]. [a]Ref. 77, [M]:[I] = 200, CH_2Cl_2 solution; [b]Ref. 94, [M]:[I] = 100, toluene solution; [c]Ref. 95, [M]:[I] = 100, toluene solution; [d]reported atactic.

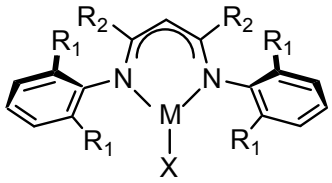

M	R_1	R_2	X	T/ºC	time /h	conversion/ %	PDI	P_r
Zn[a]	^{i}Pr	CH_3	$N(SiMe_3)_2$	20	10	97	2.95	-
Zn[a]	^{i}Pr	CH_3	OAc	20	20	97	1.83	-
Zn[a]	^{i}Pr	CH_3	O^{i}Pr[b]	20	0.33	95	1.10	0.90
Zn[a]	Et	CH_3	O^{i}Pr[b]	20	8	97	1.09	0.79
Zn[a]	^{n}Pr	CH_3	O^{i}Pr[b]	20	19	97	1.18	0.76
Zn[a]	^{i}Pr	CH_3	O^{i}Pr[b]	0	2	97	1.09	0.94
Mg[a]	^{i}Pr	CH_3	O^{i}Pr[b]	20	0.03	97	1.29	0.50[d]
Sn[b]	^{i}Pr	CH_3	O^{i}Pr	60	4	94	1.06	0.64
Sn[b]	^{i}Pr	CH_3	NMe_2	60	7	92	1.18	0.64
Sn[b]	^{i}Pr	^{t}Bu	O^{i}Pr	60	8	96	1.16	0.63
Sn[b]	Me	Me	O^{i}Pr	60	3	92	1.12	0.65
Sn[b]	H	Me	O^{i}Pr	60	2	93	1.13	0.67
Sn[b]	Cl	Me	NMe_2	60	1.75	92	1.23	0.64
Fe[c]	^{i}Pr	^{t}Bu	O^{i}Pr	25	0.33	94	1.12	0.50[d]

The authors concluded that the lack of varying stereoselectivity (particularly in comparison to related zinc(II) complexes) must be due to the influence of the stereochemically active lone pair on the tin(II) centre, and also reasoned this to be the explanation for the observation of a similar level of heterotactic enrichment when other tin(II) initiators were used. Indeed, computational studies revealed that the minimisation of repulsive forces between the lone pairs on the tin(II) centre and carbonyl oxygen atom in either the monomer or the ring-opened lactide unit was important for the insertion process.[97]

Hillmyer, Tolman and co-workers have also prepared the dimeric zinc(II) *N*-heterocyclic carbene complex shown in Figure 1.49 (R = 2,4,6-trimethylphenyl), which was active for the ROP of D,L-LA in dichloromethane solution at room temperature.[98] This initiator produced PDLLA with a slight heterotactic bias (P_r = 0.60), attributed to a chain end control mechanism by the authors. *N*-heterocyclic carbenes have themselves been shown to initiate the ROP of lactide (when an alcohol co-initiator is used) and so the authors also tested the free *N*-heterocyclic carbene ligand under the same conditions.[99]

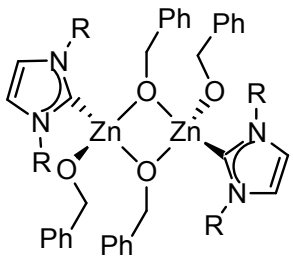

Figure 1.49 Zinc(II) *N*-heterocyclic carbene initiator prepared by Hillmyer, Tolman and co-workers.[98]

The rate of the polymerisation initiated by the free *N*-heterocyclic carbene was slightly larger than that of the polymeriation initiated by the dimeric zinc(II) *N*-heterocyclic carbene complex, leading to the conclusion that ROP may be occurring via both initiators. However, the tacticity of the polymer obtained when a free *N*-heterocyclic carbene/benzyl alcohol initiating system was used as the initiator was quite surprising. At a temperature of -20 ºC a PDLLA polymer with a significant degree of isotactic enrichment (P_r = 0.25) was obtained.

Chisholm and co-workers also sought to prepare monomeric zinc(II), calcium(II) and magnesium(II) complexes for stereoselective ROP of D,L-LA.[100] In order to minimise aggregation, they employed a strategy to encapsulate the metal centre in a sterically bulky multidentate nitrogen donor framework (Figure 1.50) specifically using tris(pyrazolyl) borate ligands. The resulting complexes were considered to be monomeric in the solid state and in solution based on X-ray crystallographic and NMR spectroscopic studies, respectively.

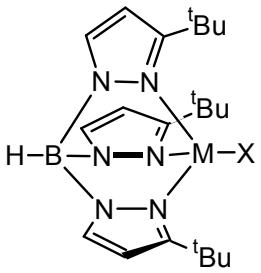

Figure 1.50 Initiators for the ROP of D,L-LA prepared by Chisholm and co-workers (M = Mg, Ca, Zn).[100]

The calcium(II) complexes where X = $N(SiMe_3)_2$ and O-2,6-$^{i}Pr_2C_6H_4$ showed a significant degree of stereocontrol over the ROP of D,L-LA, producing PDLLA with a high degree of heterotactic enrichment in tetrahydrofuran solution (P_r = 0.90 in each case) to 90% conversion in less than five minutes at room temperature. Of the three metal amide complexes, the calcium(II) complex was by far the most active for the ROP of D,L-LA and the order Ca>Mg>Zn was established, attributed to the increasing polarity of the M-OR bond on going from zinc(II) to magnesium(II) to calcium(II) as the carbonyl carbon was presumed to be most effectively activated by the more electropositive metal.

Lanthanide(III) complexes of amine bis(phenolate) ligands linked by a single nitrogen atom of the type shown in Figure 1.51 have also been shown to be active, stereoselective initiators for the ROP of D,L-LA in tetrahydrofuran or toluene solution at 20 ºC.[101, 102]

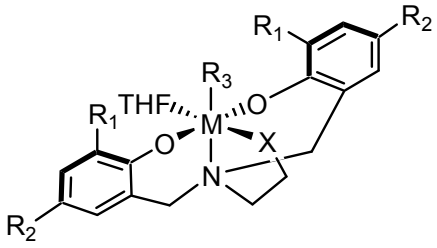

Figure 1.51

Carpentier and co-workers prepared a range of complexes, varying the metal atom, the phenol *ortho* and *para* substituents, and the donor group X, generating initiators which were active for the ROP of D,L-LA in tetrahydrofuran solution.[101] Complexes of lanthanum(III) and neodymium(III) produced PDLLA polymers to 100% conversion within 20 minutes which were either atactic or had a small amount of heterotactic enrichment (Table 1.9). In contrast, yttrium(III) complexes in general produced polymers with a high degree of heterotactic enrichment, manifested in P_r values of between 0.80 and 0.90. The only exception was the complex in which the phenol *ortho* and *para* substituents were methyl groups. The authors reasoned that formation of aggregates in solution was responsible for the low degree of heterotactic enrichment. In addition, they suggested that the increase in size of the metal centre from yttrium(III) to neodymium(III) accounted for the observed decrease in stereoselectivity. The authors reasoned that, as the yttrium(III) centre is smaller, the steric effects of the amine bis(phenolate ligands) are more pronounced, better controlling the approach of the lactide monomer in this chain-end controlled ROP.

Table 1.9 Results for the ROP of D,L-LA initiated by the lanthanide complexes prepared by Carpentier and co-workers.[101] All polymerisations proceeded to complete conversion at 20 ºC in tetrahydrofuran solution.

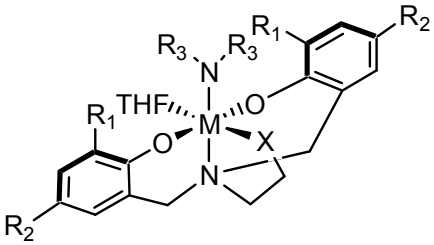

M	R_1	R_2	R_3	X	[M]:[I]	time/min	PDI	P_r
Y	Me	Me	$SiMe_3$	OMe	200	10	1.25	0.56
Y	^{t}Bu	^{t}Bu	$SiHMe_2$	OMe	100	5	1.33	0.80
La	^{t}Bu	^{t}Bu	$SiHMe_2$	OMe	100	5	1.34	0.65
Nd	^{t}Bu	^{t}Bu	$SiMe_3$	OMe	200	10	1.28	0.49
Y	^{t}Bu	^{t}Bu	$SiHMe_2$	NMe_2	100	5	1.17	0.60
Y	Adamantyl	Me	$SiHMe_2$	OMe	200	10	1.22	0.80
La	Adamantyl	Me	$SiHMe_2$	OMe	200	10	1.29	0.55
Nd	Adamantyl	Me	$SiMe_3$	OMe	100	5	1.18	0.62
Y	Adamantyl	^{t}Bu	$SiHMe_2$	OMe	200	10	1.22	0.80
Y	CMe_2Ph	CMe_2Ph	$SiHMe_2$	NMe_2	100	20	1.19	0.90

Work by Cui and co-workers concentrated on complexes of yttrium(III) and lutetium(III) employing amine bis(phenolate) ligands in which the fourth donor group was a tertiary amine (Table 1.10 and figure therein).[102] ROP of D,L-LA initiated by either yttrium(III) complex at 20 ºC in tetrahydrofuran solution proceeded to complete conversion in one hour, in each case producing PDLLA with a relatively narrow molecular weight distribution and very high degree of heterotactic enrichment.

Table 1.10 Results for the ROP of D,L-LA initiated by complexes prepared by Cui and co-workers.[102] [M]:[I] = 300, tetrahydrofuran solution, 20 ºC, 1h.

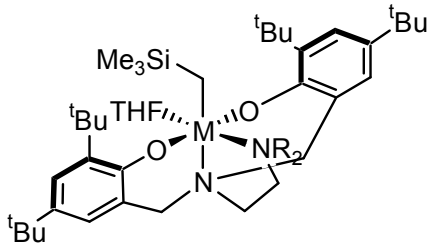

M	R	conversion/%	M_n/g mol^{-1}	PDI	P_r
Y[b]	Me	100	56600	1.32	0.96
Y[b]	Et	100	39600	1.43	0.97
Lu[b]	Et	70	38600	1.59	0.94

Variation of the R groups on the pendant amine donor from methyl to ethyl had little effect, increasing the P_r value from 0.96 to 0.97. The ROP initiated by the lutetium(III) complex in toluene solution required a reaction temperature of 70 ºC to reach 70% conversion in one hour. Although the PDI value for the polymer produced using this initiator is significantly higher than those of the polymer produced using the yttrium(III)

initiators, this initiator displays a similar, if somewhat reduced, degree of stereocontrol over the polymerisation, producing a polymer with $P_r = 0.94$.

1.5 Summary

In summary, the production and consumption of plastics has been increasing steadily since their discovery at the beginning of the 20th century, and are set to continue increasing in years to come. Many plastics, including the five highest volume plastics, are prepared directly or indirectly from fossil fuel starting materials, particularly natural gas and crude oil. In order to balance the continued demand for plastics with increasing crude oil prices and an ultimately finite resource supply, new plastics prepared from renewable resources are required. In addition, the development of plastics which retain the physical stability and robustness of traditional, petrochemical-based plastics but do non persist in the environment is also vital. The ROP of cyclic esters to produce poly(ester)s offers a solution to both issues. The cyclic esters, in particular lactide, may be produced from high starch content renewable resources and the resulting polymers may be biodegradable and compostable.

The ROP of cyclic esters such as ε-CL and L- and D,L-LA can be achieved through a variety of mechanisms including cationic, enzymatic and anionic. However, the coordination-insertion mechanism mediated by discrete metal complexes is a particularly attractive route to polymers with specific molecular weights and narrow molecular weight distributions, and in many cases is considered to be a living polymerisation. In the case of chiral monomers such as lactide, the polymerisation occurs with retention of configuration with respect to the chiral carbon centre. This area of research has generated enormous interest in recent years; researchers have sought to prepare novel initiators, identify trends of reactivity and discern mechanistic details, but with varying degrees of success. Particularly regarding activity trends, properties such as the coordinative ability of the metal centre and the degree of nuclearity in a complex have been shown to be important, but not absolute. Perhaps the overarching conclusion that can be drawn from the multitude of polymerisation studies is that the ROP reaction is far too complex to be dependent on a single variable. Each initiator complex is unique and a combination of several factors (i.e. steric, electronic, aggregation etc.) determines the overall polymerisation activity and the control of the initiator over molecular weight and molecular weight distribution.

In addition to achieving controlled polymerisations and high conversions in reaction times on the hours to days timescale, researchers have also sought to develop initiators which

exert stereocontrol over the ROP of D,L-LA. This control can be the result of the chirality of either the growing polymer chain, particularly the last inserted monomer, or the result of the influence of chirality of the ligand or of the complex itself. In practice, however, it has often been observed that the origin of stereocontrol is a combination of several factors.

Despite the advances which have been made in the field of ROP of cyclic esters, there still exists a need for the development of novel initiators. However, despite the continuing search for new metal initiators, the focus of research in this field has shifted slightly in recent years towards the development of initiators which are based on environmentally benign metals and effect controlled polymerisations, in terms of molecular weight, molecular weight distributions and polymer stereochemistry. Research efforts have also been aimed at understanding the origins and nature of stereocontrol in the ROP of D,L-LA and retaining stereocontrol at high reaction temperatures. This thesis details research efforts in this area, particularly the synthesis and characterisation of Group 4 metal complexes of aminophenolate ligands and investigations into their utility for the ROP of ε-CL, L-LA and D,L-LA.

References

[1] Association of Plastics Manufacturers in Europe, *Compelling Facts about Plastics*, **2005**,

[2] O. Wolf, M. Crank, M. Patel, F. Marscheider-Weidemann, J. Schleich, B. Husig and G. Angerer, *Techno-economic Feasability of Large-Scale Production of Bio-Based Polymers in Europe*, **2005**, EUR 22103 EN.

[3] Institute for Prospective Technological Studies, D. Phylipsen, K. Merssemeeckers, K. Blok, M. Patel, J. de Beer, P. Eder and O. Wolf, *Assessing the Environmental Potential of Clean Material Technologies*, **2002**, EUR 20515.

[4] British Plastics Federation, accessed *17 January 2008*, http://www.bpf.co.uk/bpfissues/Business_Conditions.cfm.

[5] Association of Plastic Manufacturers in Europe, accessed *January 15 2008*, http://www.plasticseurope.org/Content/Default.asp?PageID=1265.

[6] D. J. Walton and J. P. Lorimer, *Polymers*, Oxford University Press, Oxford, **2000**.

[7] H. Kaczmarek, *Polimery* **1997,** 42, (9), 521-531.

[8] WRAP, accessed *05 January 2008*, http://www.wrap.org.uk/manufacturing/info_by_material/plastic/index.html.

[9] E. Chiellini, A. Corti and S. D'Antone, *Polym. Degrad. Stab.* **2007,** 92, (7), 1378-1383.

[10] A. C. Albertsson and I. K. Varma, *Biomacromolecules* **2003,** 4, (6), 1466-1486.

[11] N. V. Toncheva and R. P. Mateva, *Adv. Polym. Technol.* **2007,** 26, (2), 121-131.

[12] L. R. Rieth, D. R. Moore, E. B. Lobkovsky and G. W. Coates, *J. Am. Chem. Soc.* **2002,** 124, (51), 15239-15248.

[13] O. Dechy-Cabaret, B. Martin-Vaca and D. Bourissou, *Chem. Rev.* **2004,** 104, (12), 6147-6176.

[14] W. H. Carothers, G. L. Dorough and F. J. Van Natta, *J. Am. Chem. Soc.* **1932,** 54, 761.

[15] E. T. H. Vink, K. R. Rabago, D. A. Glassner and P. R. Gruber, *Polym. Degrad. Stab.* **2003,** 80, (3), 403-419.

[16] R. Llamas, C. Jimenez-Sanchidrian and J. R. Ruiz, *Appl. Catal., B* **2007,** 72, (1-2), 18-25.
[17] V. R. Sinha, K. Bansal, R. Kaushik, R. Kumria and A. Trehan, *Int. J. Pharm.* **2004,** 278, (1), 1-23.
[18] F. L. Jin and S. J. Park, *J. Ind. Eng. Chem.* **2007,** 13, (4), 608-613.
[19] J. Choi and S. Y. Kwak, *Environ. Sci. Technol.* **2007,** 41, (10), 3763-3768.
[20] T. Dikic, W. Ming, P. C. Thune, R. Van Benthem and G. De With, *J. Polym. Sci., Part A: Polym. Chem.* **2008,** 46, (1), 218-227.
[21] L. Tatai, T. G. Moore, R. Adhikari, F. Malherbe, R. Jayasekara, I. Griffiths and P. A. Gunatillake, *Biomaterials* **2007,** 28, (36), 5407-5417.
[22] W. Y. Choi, C. M. Lee and H. J. Park, *Food. Sci. Tech.* **2006,** 39, (6), 591-597.
[23] K. W. Ng, H. N. Achuth, S. Moochhala, T. C. Lim and D. W. Hutmacher, *J. Biomater. Sci., Polym. Ed.* **2007,** 18, (7), 925-938.
[24] Y. C. Wang, L. Y. Tang, T. M. Sun, C. H. Li, M. H. Xiong and J. Wang, *Biomacromolecules* **2008,** 9, (1), 388-395.
[25] A. R. Simioni, C. Vaccari, M. I. Re and A. C. Tedesco, *J. Mater. Sci.* **2008,** 43, (2), 580-584.
[26] Natureworks LLC, accessed *14 January 2008*, http://www.natureworksllc.com/.
[27] H. R. Kricheldorf and R. Dunsing, *Makromol. Chem.-Macromol. Symp.* **1986,** 187, (7), 1611-1625.
[28] W. Dittrich and R. C. Schulz, *Angew. Makromol. Chem.* **1971,** 15, 109-&.
[29] D. Bourissou, B. Martin-Vaca, A. Dumitrescu, M. Graullier and F. Lacombe, *Macromolecules* **2005,** 38, (24), 9993-9998.
[30] H. R. Kricheldorf, *Chemosphere* **2001,** 43, (1), 49-54.
[31] L. Sipos, M. Zsuga and T. Kelen, *Polymer Bulletin* **1992,** 27, (5), 495-502.
[32] A. Hofman, S. Slomkowski and S. Penczek, *Makromol. Chem.-Macromol. Symp.* **1984,** 185, (1), 91-101.
[33] Z. Jedlinski, W. Walach, P. Kurcok and G. Adamus, *Makromol. Chem.-Macromol. Symp.* **1991,** 192, (9), 2051-2057.
[34] O. Coulembier, P. Degee, J. L. Hedrick and P. Dubois, *Prog. Polym. Sci.* **2006,** 31, (8), 723-747.
[35] H. Uyama and S. Kobayashi, *Chem. Lett.* **1993**, (7), 1149-1150.
[36] I. K. Varma, A. C. Albertsson, R. Rajkhowa and R. K. Srivastava, *Prog. Polym. Sci.* **2005,** 30, (10), 949-981.
[37] O. Coulembier, B. G. G. Lohmeijer, A. P. Dove, R. C. Pratt, L. Mespouille, D. A. Culkin, S. J. Benight, P. Dubois, R. M. Waymouth and J. L. Hedrick, *Macromolecules* **2006,** 39, (17), 5617-5628.
[38] M. H. Chisholm and Z. P. Zhou, *J. Mater. Chem.* **2004,** 14, (21), 3081-3092.
[39] G. W. Coates, *J. Chem. Soc.-Dalton Trans.* **2002**, (4), 467-475.
[40] A. Kowalski, A. Duda and S. Penczek, *Macromolecules* **2000,** 33, (20), 7359-7370.
[41] A. Kowalski, A. Duda and S. Penczek, *Macromolecules* **2000,** 33, (3), 689-695.
[42] M. Ryner, K. Stridsberg, A. C. Albertsson, H. von Schenck and M. Svensson, *Macromolecules* **2001,** 34, (12), 3877-3881.
[43] K. B. Aubrecht, M. A. Hillmyer and W. B. Tolman, *Macromolecules* **2002,** 35, (3), 644-650.
[44] P. Dubois, C. Jacobs, R. Jerome and P. Teyssie, *Macromolecules* **1991,** 24, (9), 2266-2270.
[45] T. Biela, A. Kowalski, J. Libiszowski, A. Duda and S. Penczek, *Macromol. Symp.* **2006,** 240, 47-55.
[46] H. von Schenck, M. Ryner, A. C. Albertsson and M. Svensson, *Macromolecules* **2002,** 35, (5), 1556-1562.
[47] A. Kowalski, J. Libiszowski, K. Majerska, A. Duda and S. Penczek, *Polymer* **2007,** 48, (14), 3952-3960.

[48] H. Y. Ma, G. Melillo, L. Oliva, T. P. Spaniol, U. Englert and J. Okuda, *Dalton Trans.* **2005**, (4), 721-727.
[49] C. H. Huang, F. C. Wang, B. T. Ko, T. L. Yu and C. C. Lin, *Macromolecules* **2001,** 34, (3), 356-361.
[50] J. R. Walton, *Neurosci. Lett.* **2007,** 412, (1), 29-33.
[51] H. R. Kricheldorf, I. Kreiser-Saunders and D. O. Damrau, *Macromol. Symp.* **2000,** 159, 247-257.
[52] B. H. Huang, C. N. Lin, M. L. Hsueh, T. Athar and C. C. Lin, *Polymer* **2006,** 47, (19), 6622-6629.
[53] H. R. Kricheldorf and D. O. Damrau, *Macromol. Chem. Phys.* **1998,** 199, (8), 1747-1752.
[54] M. L. Shueh, Y. S. Wang, B. H. Huang, C. Y. Kuo and C. C. Lin, *Macromolecules* **2004,** 37, (14), 5155-5162.
[55] T. L. Yu, C. C. Wu, C. C. Chen, B. H. Huang, J. C. Wu and C. C. Lin, *Polymer* **2005,** 46, (16), 5909-5917.
[56] P. Dobrzynski, J. Kasperczyk, H. Janeczek and M. Bero, *Polymer* **2002,** 43, (9), 2595-2601.
[57] A. Sodergard and M. Stolt, *Macromol. Symp.* **1998,** 130, 393-402.
[58] M. Stolt and A. Sodergard, *Macromolecules* **1999,** 32, (20), 6412-6417.
[59] X. Y. Wang, K. R. Liao, D. P. Quan and Q. Wu, *Macromolecules* **2005,** 38, (11), 4611-4617.
[60] B. J. O'Keefe, L. E. Breyfogle, M. A. Hillmyer and W. B. Tolman, *J. Am. Chem. Soc.* **2002,** 124, (16), 4384-4393.
[61] B. J. O'Keefe, S. M. Monnier, M. A. Hillmyer and W. B. Tolman, *J. Am. Chem. Soc.* **2001,** 123, (2), 339-340.
[62] N. Spassky, V. Simic, M. S. Montaudo and L. G. Hubert-Pfalzgraf, *Macromol. Chem. Phys.* **2000,** 201, (17), 2432-2440.
[63] W. M. Stevels, P. J. Dijkstra and J. Feijen, *Trends Pol. Sci.* **1997,** 5, (9), 300-305.
[64] W. M. Stevels, M. J. K. Ankone, P. J. Dijkstra and J. Feijen, *Macromolecules* **1996,** 29, (9), 3332-3333.
[65] W. M. Stevels, M. J. K. Ankone, P. J. Dijkstra and J. Feijen, *Macromolecules* **1996,** 29, (19), 6132-6138.
[66] I. Westmoreland and J. Arnold, *Dalton Trans.* **2006**, (34), 4155-4163.
[67] Y. Q. Shen, Z. Q. Shen, Y. F. Zhang and K. M. Yao, *Macromolecules* **1996,** 29, (26), 8289-8295.
[68] Y. Kim and J. G. Verkade, *Organometallics* **2002,** 21, (12), 2395-2399.
[69] J. M. G. Cowie, *Polymers: Chemistry and Physics of Modern Materials*, Intertext, Aylesbury, **1973**.
[70] K. Fukushima and Y. Kimura, *Polym. Int.* **2006,** 55, (6), 626-642.
[71] B. P. Calabia and Y. Tokiwa, *Biotechnol. Lett.* **2007,** 29, (9), 1329-1332.
[72] J. W. Akitt and B. E. Mann, *NMR and chemistry: an introduction to modern NMR spectroscopy*, 4th ed., Stanley Thornes, Cheltenham, **2000**.
[73] K. A. M. Thakur, R. T. Kean, E. S. Hall, J. J. Kolstad, T. A. Lindgren, M. A. Doscotch, J. I. Siepmann and E. J. Munson, *Macromolecules* **1997,** 30, (8), 2422-2428.
[74] M. H. Chisholm, S. S. Iyer, M. E. Matison, D. G. McCollum and M. Pagel, *Chem. Commun.* **1997**, (20), 1999-2000.
[75] M. H. Chisholm, S. S. Iyer, D. G. McCollum, M. Pagel and U. Werner-Zwanziger, *Macromolecules* **1999,** 32, (4), 963-973.
[76] K. A. M. Thakur, R. T. Kean, E. S. Hall, J. J. Kolstad and E. J. Munson, *Macromolecules* **1998,** 31, (5), 1487-1494.
[77] M. T. Zell, B. E. Padden, A. J. Paterick, K. A. M. Thakur, R. T. Kean, M. A. Hillmyer and E. J. Munson, *Macromolecules* **2002,** 35, (20), 7700-7707.

[78] B. M. Chamberlain, M. Cheng, D. R. Moore, T. M. Ovitt, E. B. Lobkovsky and G. W. Coates, *J. Am. Chem. Soc.* **2001,** 123, (14), 3229-3238.
[79] B. J. O'Keefe, M. A. Hillmyer and W. B. Tolman, *J. Chem. Soc.-Dalton Trans.* **2001**, (15), 2215-2224.
[80] J. Kasperczyk and M. Bero, *Polymer* **2000,** 41, (1), 391-395.
[81] J. E. Kasperczyk, *Macromolecules* **1995,** 28, (11), 3937-3939.
[82] N. Spassky, M. Wisniewski, C. Pluta and A. LeBorgne, *Macromol. Chem. Phys.* **1996,** 197, (9), 2627-2637.
[83] T. M. Ovitt and G. W. Coates, *J. Polym. Sci., Part A: Polym. Chem.* **2000,** 38, 4686-4692.
[84] C. P. Radano, G. L. Baker and M. R. Smith, *J. Am. Chem. Soc.* **2000,** 122, (7), 1552-1553.
[85] T. M. Ovitt and G. W. Coates, *J. Am. Chem. Soc.* **2002,** 124, (7), 1316-1326.
[86] P. Hormnirun, E. L. Marshall, V. C. Gibson, R. I. Pugh and A. J. P. White, *Proc. Natl. Acad. Sci. U. S. A.* **2006,** 103, (42), 15343-15348.
[87] N. Nomura, R. Ishii, Y. Yamamoto and T. Kondo, *Chem. Eur. J.* **2007,** 13, (16), 4433-4451.
[88] N. Nomura, R. Ishii, M. Akakura and K. Aoi, *J. Am. Chem. Soc.* **2002,** 124, (21), 5938-5939.
[89] Z. Y. Zhong, P. J. Dijkstra and J. Feijen, *Angew. Chem., Int. Ed. Engl.* **2002,** 41, (23), 4510-+.
[90] M. H. Chisholm, N. J. Patmore and Z. P. Zhou, *Chem. Commun.* **2005**, (1), 127-129.
[91] C. K. A. Gregson, I. J. Blackmore, V. C. Gibson, N. J. Long, E. L. Marshall and A. J. P. White, *Dalton Trans.* **2006**, (25), 3134-3140.
[92] R. C. J. Atkinson, K. Gerry, V. C. Gibson, N. J. Long, E. L. Marshall and L. J. West, *Organometallics* **2007,** 26, (2), 316-320.
[93] P. Hormnirun, E. L. Marshall, V. C. Gibson, A. J. P. White and D. J. Williams, *J. Am. Chem. Soc.* **2004,** 126, (9), 2688-2689.
[94] Z. H. Tang and V. C. Gibson, *Eur. Polym. J.* **2007,** 43, (1), 150-155.
[95] V. C. Gibson, E. L. Marshall, D. Navarro-Llobet, A. J. P. White and D. J. Williams, *J. Chem. Soc.-Dalton Trans.* **2002**, (23), 4321-4322.
[96] A. P. Dove, V. C. Gibson, E. L. Marshall, A. J. P. White and D. J. Williams, *Chem. Commun.* **2001**, (03), 283-284.
[97] A. P. Dove, V. C. Gibson, E. L. Marshall, H. S. Rzepa, A. J. P. White and D. J. Williams, *J. Am. Chem. Soc.* **2006,** 128, (30), 9834-9843.
[98] T. R. Jensen, C. P. Schaller, M. A. Hillmyer and W. B. Tolman, *J. Organomet. Chem.* **2005,** 690, (24-25), 5881-5891.
[99] T. R. Jensen, L. E. Breyfogle, M. A. Hillmyer and W. B. Tolman, *Chem. Commun.* **2004**, (21), 2504-2505.
[100] M. H. Chisholm, J. Gallucci and K. Phomphrai, *Chem. Commun.* **2003**, (1), 48-49.
[101] A. Amgoune, C. M. Thomas, T. Roisnel and J. F. Carpentier, *Chem. Eur. J.* **2005,** 12, (1), 169-179.
[102] X. L. Liu, X. M. Shang, T. Tang, N. H. Hu, F. K. Pei, D. M. Cui, X. S. Chen and X. B. Jing, *Organometallics* **2007,** 26, (10), 2747-2757.

Chapter 2

Synthesis and Characterisation of Novel Group 4 Initiators

2 Synthesis and Characterisation of Novel Group 4 Initiators

2.1 Introduction

As discussed in the previous chapter, a need exists to develop environmentally friendly processes for the production of both high- and low-volume plastics for use in both general and very specific applications. Specifically, attention has been focussed on poly(oxygenate)s derived from various cyclic ester monomers as alternatives to petrochemical-based polymers. Central to this need are initiators for the ring opening polymerisation (ROP) of these monomers.

The amine bis(phenolate) class of ligands (Figure 2.1) are a versatile group which may be synthesised in a relatively straightforward manner. Simple alterations to the starting materials may afford potential ligands with diverse steric and electronic attributes. In the majority of metal complexes of this ligand type, the phenolate arms are bound to the metal centre through the oxygen atoms. The 'third' arm of the ligand, R'', which may be alkyl or aryl and possibly incorporate a heteroatom is often referred to as the 'pendant' arm. Variation of the pendant group in this manner may mediate the availability of free coordination sites available to a catalytic process involving the metal centre. Transition metal complexes of this ligand class have shown utility in a wide range of areas; iron(III) and molybdenum(VI) complexes have been useful in modelling biological systems such as catechol dioxygenases[1] and galactose oxidases[2, 3], respectively, while some Group 4 metal chloride complexes have been reported as active catalysts for the polymerisation of 1-hexene.[4]

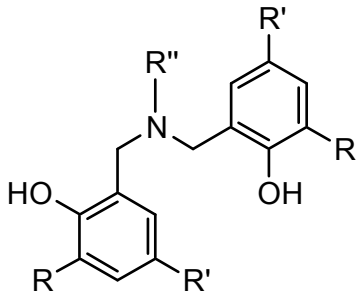

Figure 2.1 A generic amine bis(phenolate).

The utility of metal alkoxides as initiators for the ROP of cyclic esters was also discussed in the preceding chapter. Polymerisation may proceed via a coordination-insertion mechanism with the cyclic ester monomer inserting into a metal alkoxide or aryloxide bond. Although homoleptic metal alkoxides are active initiators for the ROP of cyclic esters,[5] substitution of a number of the alkoxide ligands with other supporting ligands may afford greater control over the polymerisation resulting in increased conversions and polymers with more narrow molecular weight distributions for the polymers.[6] As noted

previously, toxicity issues surrounding the industrially favoured tin(II) 2-ethylhexanoate initiator has led to a search for more environmentally and biologically friendly alternatives, both from an economical and a regulatory perspective. Dangers to the environment and to the health of those handling the initiator complex pre-polymerisation are important issues, as well as removal of residual initiator and/or initiator decomposition products. Indeed, studies have shown complete removal of tin material from poly(lactide) to be very difficult.[7] This issue is particularly important in the context of biomedical applications of polyesters.

Complexes of lanthanides and Group 1 and Group 2 metals have been proposed as possible alternatives, but aluminium(III) alkoxide complexes with supporting ligands are by far the most widely studied class of potential substitute.[8, 9] Many are highly active initiators which deliver controlled polymerisation of cyclic esters. However, the desire for information about correlation between initiator structure and polymer properties (molecular weights, PDI and tacticity) drives the need for new initiator, and some doubt about the suitability of aluminium(III) complexes as initiators exists due to the possible implication of aluminium ions in Alzheimer's disease.[9] However, if aluminium(III) alkoxide complexes are not the most suitable alternative to current tin(II)-based initiators, much useful information can be gleaned from the extensive research carried out using these initiators. In particular, aluminium(III) alkoxide complexes with supporting ligands based on a mixed donor atom motif are very active and well-documented in the literature.[10-12] The N,O donor set has been used in the so-called salen[13] and salan[10] ligand classes, as well as the Schiff bases,[14] to great effect. Aluminium(III) alkoxide complexes of another type of ligand with an N,O donor set, amine bis(phenolate) ligands, have been described in the literature as well.[15]

One group of transition metals which are compatible with ligands bearing an N,O donor set and which, prior to the commencement of this work were relatively unexplored for ROP of cyclic esters are the Group 4 metals. Complexes of titanium(IV) alkoxides with various ancillary ligands have been reported as active initiators for these types of polymerisations.[9] Our intent was to use amine phenolate ligands, easily synthesised and varied, as supporting ligands for titanium(IV), zirconium(IV) and hafnium(IV) alkoxide complexes. These complexes would then be tested for activity towards the ROP of cyclic esters. In addition, comparisons of the solid-state and solution structures and the activity towards ROP for the complexes would be made, where possible.

2.2 Ligand Synthesis

Di-anionic Amine Bis(Phenolate)s

The substituted amine bis(phenolate) ligands employing a pyridine moiety, **L1**H_2 and **L2**H_2 (Figure 2.2), were synthesised by a modified Mannich reaction of the corresponding *ortho*, *para*- disubstituted phenol, paraformaldehyde and 2-aminomethylpyridine according to a published literature method.[4] Refluxing a methanol solution of the reactants for 16 hours, followed by removal of volatiles, afforded viscous oils which were triturated with methanol, giving products **L1**H_2 and **L2**H_2**,** in high (>90%) yield.

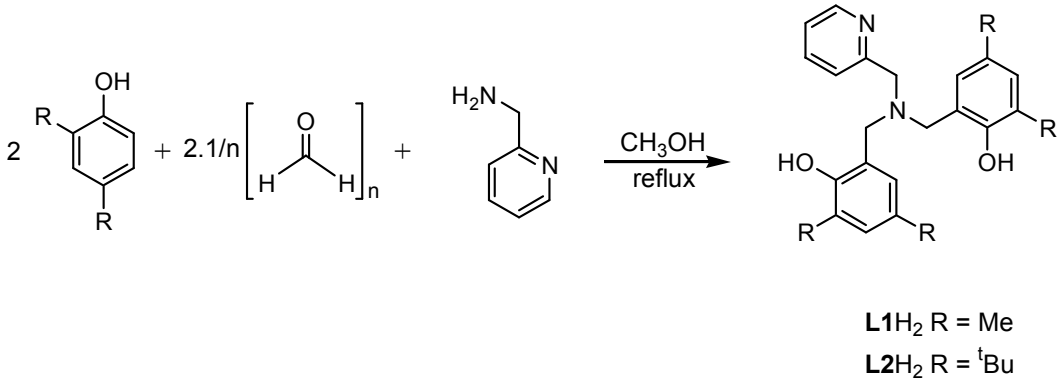

Figure 2.2 Synthetic route to **L1**H_2 and **L2**H_2.[4]

The synthesis of **L3**H_2, with *para*-nitro substituents on the phenol rings, was again carried out according to a literature procedure.[3] Two equivalents of 2-chloromethyl-4-nitro phenol were reacted at room temperature with 2-aminomethyl pyridine in THF (Figure 2.3). Triethylamine was also added to the reaction mixture, in order to remove the hydrochloric acid formed during the reaction. Filtration followed by removal of volatiles to give a crude solid product, and crystallisation from chloroform yielded the desired product in 92% yield.

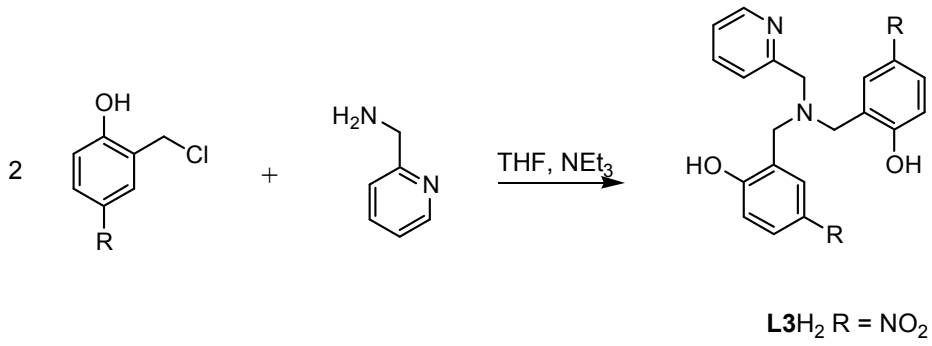

Figure 2.3 Synthetic route to **L3**H_2.[3]

N-alkyl substituted amine bis(phenolate) ligands such as those shown in Figure 2.4 are known in the literature and have been prepared in an analogous manner to **L1**H_2 and

L2H_2**,** replacing the pyridyl amine used in those reactions with methyl or propyl amine.[16, 17] However, our attempts to extend this work towards the synthesis of novel aryl-substituted derivatives [–CH_2R_{Ar} (R_{Ar} = phenyl, naphthalene)] via this method proved unsuccessful.

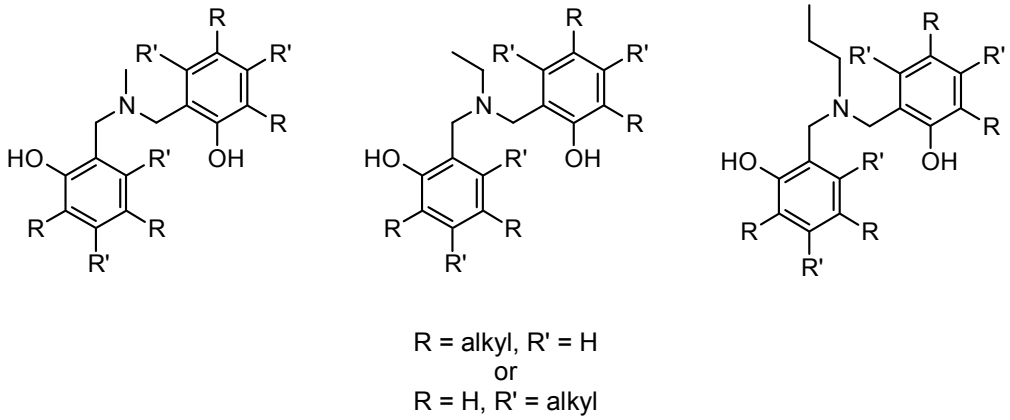

Figure 2.4 Known amine bis(phenolate) ligands with alkyl pendant groups.[16, 17]

A previous literature report indicated that the use of amine bis(phenolate) ligands lacking both a fourth coordinating moiety and steric bulk in the phenol *ortho* position would lead to the formation of homoleptic, $\mathbf{L_2}$M complexes when reacted with Group 4 metal alkoxides (Figure 2.5).[17] In order to avoid this, 2,4-di-*tert*-butylphenol was used for these reactions.

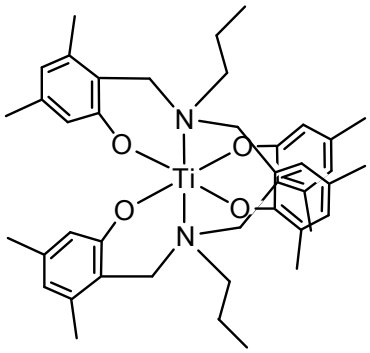

Figure 2.5 $\mathbf{L_2}$M complex formed when an amine bis(phenolate) ligand lacking both steric bulk in the phenolate *ortho* position and a coordinating group on the pendant arm. [17]

Reaction of the appropriate primary amine [for **L4**: benzylamine, for **L5**: 1-naphthalenemethylamine] with paraformaldehyde and 2,4-di-*tert*-butylphenol resulted in a mixture of products, which could be separated by column chromatography. The major product in these reactions was a substituted benzoxazine (Figure 2.6), confirmed by ^{1}H NMR spectroscopy.

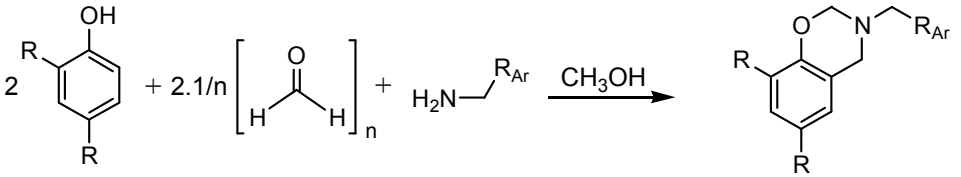

L4 R = ^{t}Bu, R_{Ar} = Ph

L5 R = ^{t}Bu, R_{Ar} = 1-Napth

Figure 2.6 Synthetic route to substituted benzoxazines **L4** and **L5**.

In the case of **L4**, the integration ratio of C*H*$_3$ peaks due to *tert*-butyl group protons to C*H*$_2$ peaks due to methylene protons was 9:9:6 (Figure 2.7, 2.10a). This contrasted with the expected ratio of 18:18:6. In addition, three 2H C*H*$_2$ signals were apparent around 4-5 ppm instead of the two (one 4H and one 2H) expected for the amine bis(phenolate) molecule (Figure 2.7). A similar ^{1}H NMR spectrum was observed for **L5**.

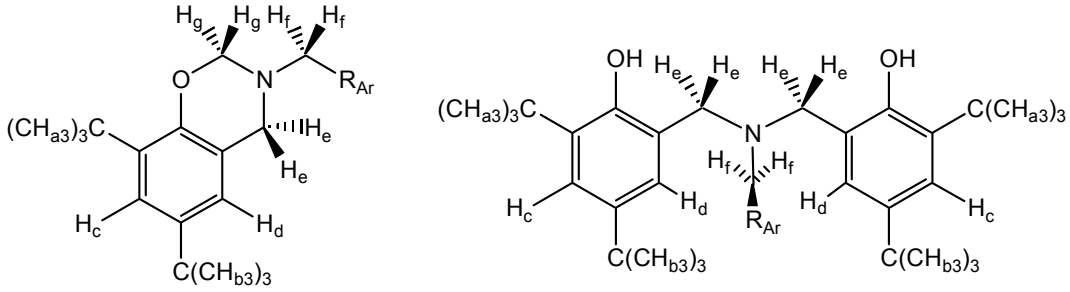

H_a : H_b : H_c : H_d : H_e : H_f : H_g	H_a : H_b : H_c : H_d : H_e : H_f
9 : 9 : 1 : 1 : 2 : 2 : 2	18 : 18 : 2 : 2 : 4 : 2

Figure 2.7 (Predicted) ^{1}H NMR spectral signal intensities for a benzoxazine and an amine bis(phenolate) bearing an R_{Ar} group.

Earlier literature reports suggested benzoxazine formation as a common problem in these types of syntheses.[18] The initial step in the Mannich reaction is the formation of an iminium ion from the amine and formaldehyde with loss of water, which is then followed by carbon-carbon bond formation via electrophilic aromatic substitution of the iminium ion at the *ortho*-proton on one phenol molecule. Subsequently, a second iminium ion is formed from the second equivalent of formaldehyde and the now secondary amine. At this point, benzoxazine formation may occur because instead of the iminium ion reacting with the second equivalent of phenol as in the first stage of the reaction, a competing intramolecular ring closure reaction may occur between the phenol oxygen and the iminium ion (Figure 2.8).

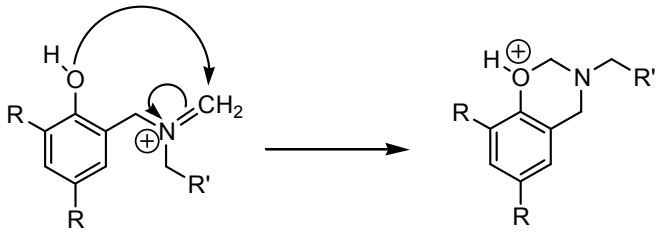

Figure 2.8 Intramolecular cyclisation to form a substituted benzoxazine.

In order to overcome this problem a new synthetic method was required. A study of the polymerisation of benzoxazines revealed a synthetic method which could be applied to reaction products **L4** and **L5**. In each case, the benzoxazine isolated from the initial reaction (Figure 2.6) was combined with a further equivalent of 2,4-di-*tert*-butylphenol and heated to 155 ºC in a solvent free environment. On heating, the iminium ion 'lost' by the intermolecular cyclisation reaction is regenerated allowing reaction with the second equivalent of phenol. The products of these reactions were purified by column chromatography yielding the desired bis(phenolate) products. Subsequently, syntheses of the benzoxazine intermediates were carried out with a phenol:paraformaldehyde:amine ratio of 1:2.1:1 to achieve the most efficient synthetic route (Figure 2.9). Both ligands **L6**H_2 and **L7**H_2 were synthesised by this route and characterised by ^{1}H and ^{13}C NMR spectroscopy, mass spectrometry and elemental analysis.

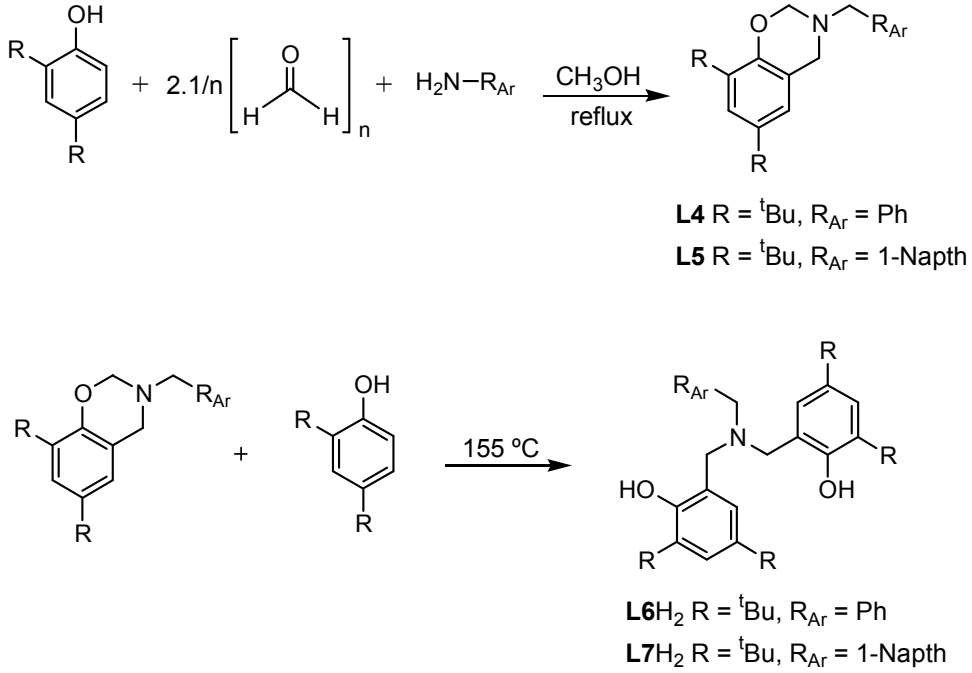

Figure 2.9 Full synthetic route to **L6**H_2 and **L7**H_2.

The ^{1}H NMR spectrum of **L6**H_2 is shown in Figure 2.10 and contrasted with that of the benzoxazine **L4**. Here the expected 2H and 4H singlets for the two types of CH_2 – aryl and phenoxy - are observed.

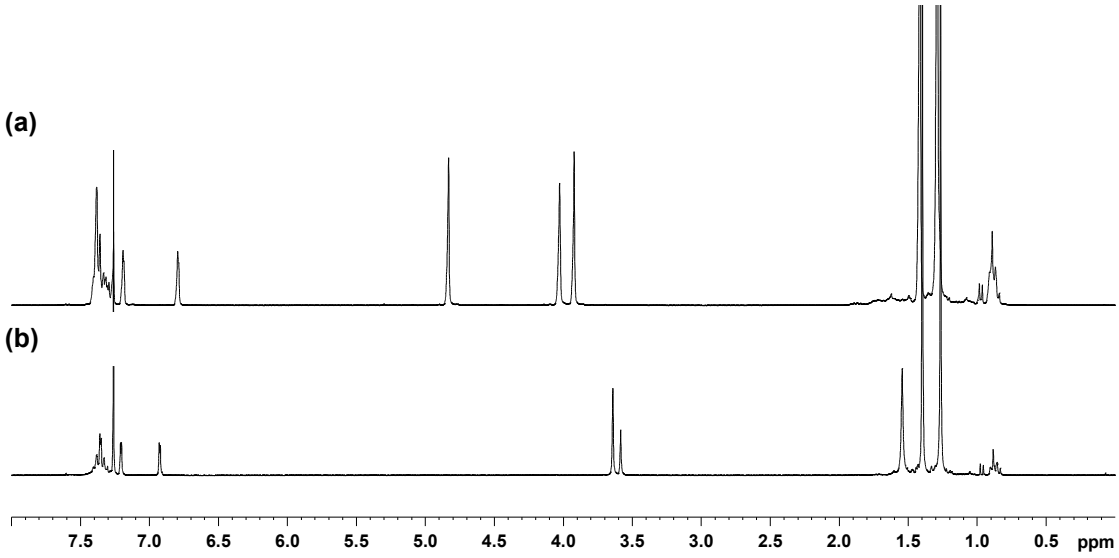

Figure 2.10 ^{1}H NMR spectra of (a) benzoxazine **L4** and (b) amine bis(phenolate) **L6**H_2.

Variation of the steric bulk of the ligand in metal complexes which act as cyclic ester ROP initiators has been shown to be important, both in terms of activity and stereoselectivity (when the racemic mixture of D- and L-LA is used). When using aluminium(III) complexes of amine bis(phenolate) ligands derived from ethylenediamine as initiators for the ROP of D,L-LA, Gibson and co-workers found a large variation in activity and stereoselectivity by changing the phenolate substituents from methyl to *tert*-butyl.[10] With this in mind, ligand **L8**H_2, incorporating bulky dimethylbenzyl groups on one side of the molecule and an unsubstituted second phenolate arm, was prepared. The difference in steric bulk on the two phenolate arms of the ligand may have implications in the ROP of D,L-LA initiated by any potential metal complexes of this ligand, by affording asymmetry to the complexes. Preparation of this ligand was achieved by reaction of 2-(2-hydroxybenzylaminomethyl)pyridine,[3] paraformaldehyde and 2,4-bis(α,α-dimethylbenzyl)phenol under solvent-free conditions at 110 ºC. The resulting crude orange oil was triturated with methanol, affording the desired product as a white solid in 69% yield (Figure 2.11).

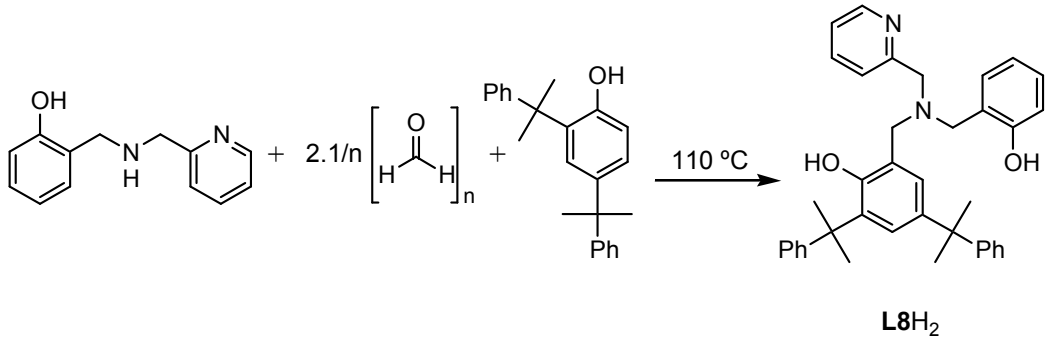

L8H_2

Figure 2.11 Synthesis of **L8**H_2.

In addition to variation of steric bulk, variation of the pendant arm of the ligand in Group 4 complexes of amine bis(phenolate) ligands has also been shown to influence reactivity. For example, Kol and co-workers prepared titanium(IV) dibenzyl complexes of amine bis(phenolate) ligands incorporating either furan or tetrahydrofuran groups on the pendant arm of the ligand.[19] A ten-fold difference in activity towards the polymerisation of 1-hexene was observed, with the furan complex being more active. The authors reasoned that this was due to the strength of binding between the heterocyclic oxygen and the metal centre, with the more weakly bound furan group leaving the metal centre more open for catalysis. In order to investigate the possibility of a similar effect in the ROP of LA, thiophene-substituted ligands **L9**H_2 and **L10**H_2 were prepared for comparison with **L1**H_2 and **L2**H_2 (which contain a pyridine moiety).

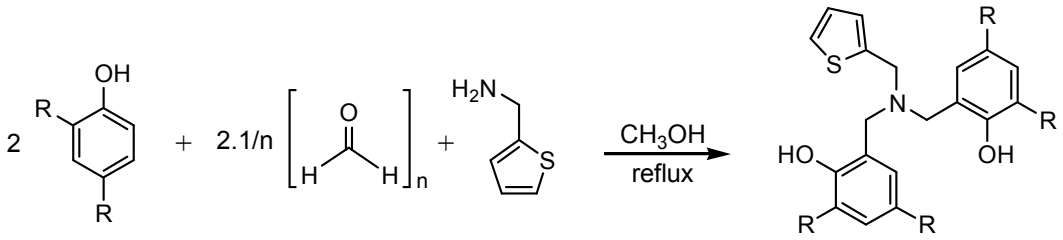

L9H$_2$ R = Me
L10H$_2$ R = ^{t}Bu

Figure 2.12 Synthetic route to **L9**H_2 and **L10**H_2.

These ligands were prepared in a similar manner to their pyridyl analogues (Figure 2.12), by reaction of the disubstituted phenol with paraformaldehyde and 2-aminomethyl thiophene. Refluxing a methanol solution of the reactants overnight and column chromatography following work-up afforded the desired ligands in low yields (22% and 30% yield, respectively).

Tri-anionic [O_3N] ligands

Tripodal amine tris(phenolate) ligands (Figure 2.13) also offer the possibility of tetradentate coordination to a Group 4 metal centre, but are tri-anionic in their deprotonated forms as opposed to the di-anionic amine bis(phenolate) ligands.

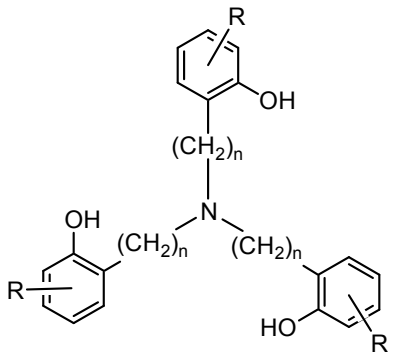

Figure 2.13 A generic amine tris(phenolate).

Indeed, these types of ligands have attracted a great deal of interest due to their ability to coordinate and stabilise a wide range of metals, generally as monomeric complexes.[20-22] In addition, the C_3 symmetry of the ligands can result in the formation of racemic metal complexes, as the ligand wraps itself around the metal centre in a helical fashion.

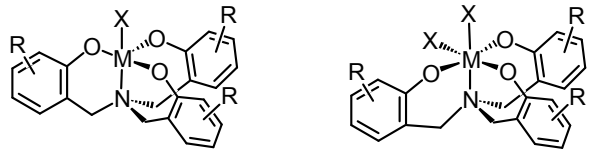

pseudo trigonal bipyramidal *pseudo* octahedral

Figure 2.14 Binding modes for amine trisphenolate ligands.

Depending on the nature of the metal centre and the number of other ligands, these ligands may coordinate a metal centre in one of two modes. The resulting metal complexes may have a five-coordinate *pseudo* trigonal bipyramidal coordination geometry (when one X ligand is present), or a six-coordinate, *pseudo* octahedral geometry (when there are two X ligands). The six-coordinate geometry may persist even when sterically bulky amine tris(phenolate) ligands are used (Figure 2.14).[23] Ligands **L11**H_3 and **L12**H_3 generally coordinate Group 4 metals in the trigonal mode, but examples of six coordinate titanium(IV) complexes have been described by Brown and co-workers.[24] Indeed, for both titanium(IV) and vanadium(V)[20] the amine tris(phenolate) ligand may bind in a different mode for the same metal having the same oxidation state. Titanium(IV) isopropoxide complexes of these types of ligands have recently been shown to be active initiators for the ROP of cyclic esters.[25] **L12**H_3 is readily synthesised by the reaction of 2,4-di-*tert*-butyl phenol and hexamethylenetetramine under solvent-free melt conditions (Figure 2.15), which gives the desired ligand in moderate yield.[26]

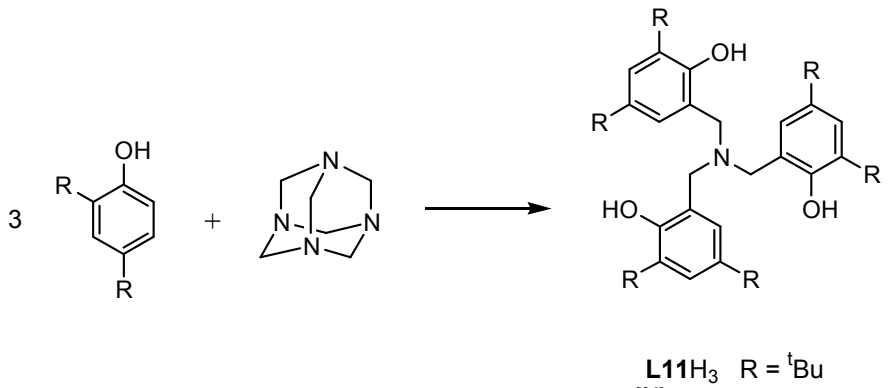

L11H_3 R = ^{t}Bu

Figure 2.15 Synthetic route to **L11**H_3.[26]

In addition to the tri-anionic amine tris(phenolate) ligand, we also sought a similar, tetradentate, tri-anionic ligand which lacked the C_3 symmetry of the tris(phenolate) molecule. With this in mind, **L12**H_3 was prepared, incorporating a hydroxyl-alkyl arm. This ligand was prepared by reaction of 2,4-di-*tert*-butyl phenol, paraformaldehyde and ethanolamine in a methanol solution. The solution was refluxed for 16 hours, resulting in formation of an yellow oil which crystallised on standing and which, after washing with hexane, afforded the product as a white solid in 24% yield (Figure 2.16).

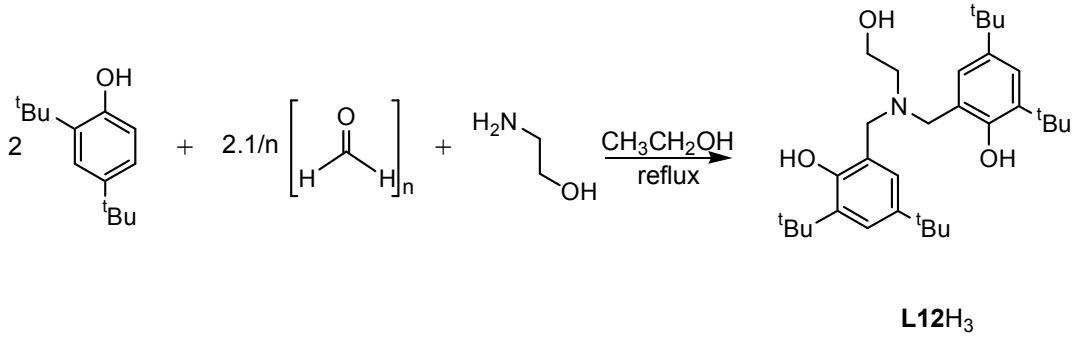

L12H_3

Figure 2.16 Synthetic route to **L12**H_3.

The complete library of ligands synthesised is shown in Figure 2.17. Between compounds **L1**H_2 and **L2**H_2 the size of the group at the positions *ortho* and *para* to the phenolic OH is increased from methyl to *tert*-butyl in an attempt induce a change in steric bulk around the metal centre of any potential complex. Furthermore, in compound **L3**H_2 electron withdrawing NO_2 groups *para* to the phenolic OH are introduced. The potentially coordinating pyridyl group of **L1**H_2 is replaced with a more innocent in **L6**H_2. The size of the aryl arm of the ligand is increased on going from **L6**H_2 (derived from benzylamine) to **L7**H_2 (derived from 1-naphthalenemethylamine). Asymmetry and variation of substituent size between the phenolate arms of the ligand have been introduced with **L8**H_2. A potential sulfur donor is introduced in **L9**H_2 and **L10**H_2; between these ligands, the size of the *ortho* and *para* substituents is again varied from methyl to *tert*-butyl. Amine tris(phenolate) ligand **L11**H_3 is introduced as a further tripodal, tetradentate ligand but as one which is highly symmetric and tri-anionic in its

deprotonated form. **L12**H_3 is again tri-anionic in its deprotonated form but lacks the C_3 symmetry of **L11**H_3.

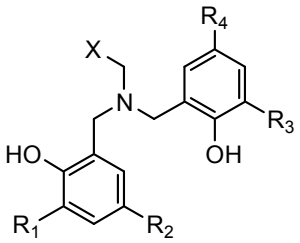

Ligand	R_1	R_2	R_3	R_4	X
L1H_2	Me	Me	Me	Me	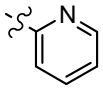
L2H_2	^{t}Bu	^{t}Bu	^{t}Bu	^{t}Bu	
L3H_2	H	NO_2	H	NO_2	
L6H_2	^{t}Bu	^{t}Bu	^{t}Bu	^{t}Bu	
L7H_2	^{t}Bu	^{t}Bu	^{t}Bu	^{t}Bu	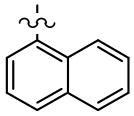
L8H_2	H	H	$C(CH_3)_2Ph$	$C(CH_3)_2Ph$	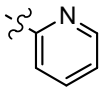
L9H_2	Me	Me	Me	Me	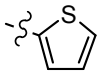
L10H_2	^{t}Bu	^{t}Bu	^{t}Bu	^{t}Bu	
L11H_2	^{t}Bu	^{t}Bu	^{t}Bu	^{t}Bu	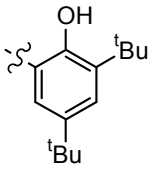
L12H_2	^{t}Bu	^{t}Bu	^{t}Bu	^{t}Bu	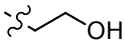

Figure 2.17 Ligands synthesised and described herein.

2.3 Synthesis and Characterisation of Group 4 Metal Complexes

All metal complexes were prepared by the alcoholysis reaction of the ligands described herein with the appropriate metal alkoxide precursors (Figure 2.18), which is an entropically favourable process. Detailed synthetic procedures and characterisation data are given in chapter 5.

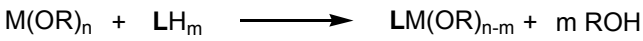

Figure 2.18 General synthetic route to Group 4 metal alkoxide complexes of ligands described herein.

Titanium(IV) Complexes of L1-L3H_2

The synthesis of a titanium(IV) complex of the potentially di-anionic ligand **L1**H_2 (and **L2**H_2) was achieved by adding a solution of the ligand in dichloromethane to a solution of the metal tetra-isopropoxide in the same solvent, in equimolar quantities, under inert atmosphere conditions. Removal of the solvent and crystallisation from hexane yielded a single product (by ^{1}H NMR spectroscopy) in near quantitative yield. The ^{1}H NMR spectrum showed two 6H doublets at 1.18 and 1.46 ppm, along with two 1H septets at 4.82 and 5.31 ppm, corresponding to isopropyl methyl (CH(CH_3)$_2$) protons and methine (CH(CH$_3$)$_2$) protons, respectively. These signals indicate the presence of two non-equivalent isopropoxide groups, which is expected as no likely conformation of ligand **L1**H_2 could result in equivalent isopropoxide groups. A pair of sharp doublets for the diastereotopic methylene protons of **L1** within an AX spin system indicates the ligand to be coordinated in a tetradentate fashion, through the two phenolic oxygen, amine nitrogen and pyridyl nitrogen atoms. Six geometric isomers are possible for the complex; three involving a mutually *cis* conformation of the two isopropoxide groups and three with the isopropoxide groups in a mutually *trans* orientation (Figure 2.19).

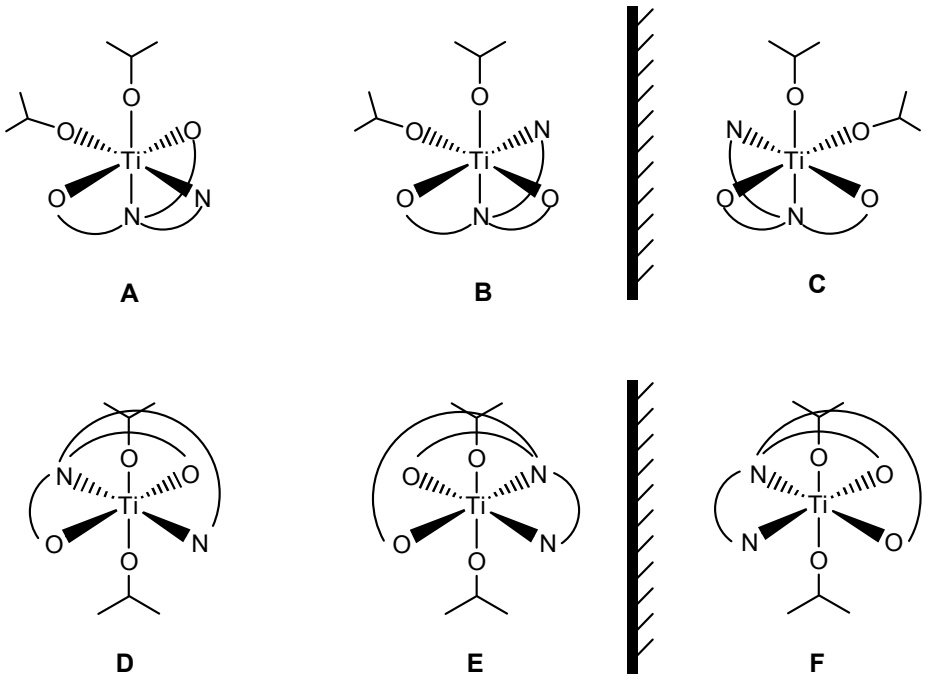

Figure 2.19 Possible conformations of titanium(IV) bis(isopropxide) complexes of tetradentate ligands such as **L1** and **L2**.

If the ligand is coordinated in a tetradentate fashion, the non-equivalent isopropoxide groups are likely to adopt a mutually *cis* configuration (Figure 2.19 **A-C**). The isopropoxide groups adopting a mutually *trans* orientation (Figure 2.19 **D-F**) would force the amine bis(phenolate) ligand to undertake a highly strained conformation in order to remain bound through all four coordinating atoms. Thus, assuming a mutually *cis*

orientation of isopropoxide groups in a monomeric complex, then there can only be three isomeric configurations for the tetradentate ligand to adopt, namely configurations **A-C** shown in Figure 2.19. Configuration **A** has phenolate arms of the ligand mutually *trans* and bisected by the pyridyl arm, while enantiomers **B** and **C** have the ligand's phenolate arms in mutually *cis* positions with the pyridyl moiety *cis* to one phenolate arm and *trans* to the other.

The ^{1}H NMR spectrum of the reaction product of **L1**H_2 with Ti(O^{i}Pr)$_4$ supports the conclusion that the ligand is bound in a tetradentate fashion, with two septet-doublet pairs due to the two isopropoxide ligands. On coordination to the metal centre, the diastereotopic phenolic methylene protons shift from a 4H singlet at 3.76 ppm to two 2H doublets with ^{3}J(H-H) 12 Hz at 3.29 and 4.64 ppm. The signal for the methylene protons on the pyridyl arm of the ligand, a 2H singlet at 3.78 ppm, remains unchanged in multiplicity and is shifted only slightly upfield to 3.75 ppm. The only signal in the aromatic region which shifts significantly is that for the proton *ortho* to the pyridyl nitrogen atom, which shifts from 7.05 ppm to 6.43 ppm in the reaction product, presumably due to coordination to the metal centre which brings it closer to the electron density of the metal, shielding the nucleus and causing an upfield shift.

These observations indicate that the ligand has adopted conformation **A** (Figure 2.19) in the complex. In this *pseudo* C_s symmetric conformation the pyridyl methylene protons are equivalent and therefore would be observed as a singlet, whereas in enantiomeric conformations **B** and **C**, the methylene protons are inequivalent and therefore would appear as a pair of 1H doublets. Also, if conformation **B** and/or **C** were adopted, the phenolic methylene protons would all be inequivalent and appear as four 1H doublets. The presence of merely two 2H doublets implies two pairs of symmetry related protons, facing either towards the pendant –CH_2pyridyl group or towards the equatorial isopropoxide. With evidence from the ^{1}H NMR spectrum in mind, the structure which has been assigned to this reaction product is that shown in Figure 2.19, **A**. NMR data for the reaction of ligand **L2**H_2 with Ti(O^{i}Pr)$_4$ are also consistent with this structure and show no indication of the presence of isomers **B** or **C**. The reaction scheme for the synthesis of complexes **L1**Ti(O^{i}Pr)$_2$ and **L2**Ti(O^{i}Pr)$_2$ is shown in Figure 2.20. These complexes were also characterised by ^{13}C NMR spectroscopy and elemental analysis.

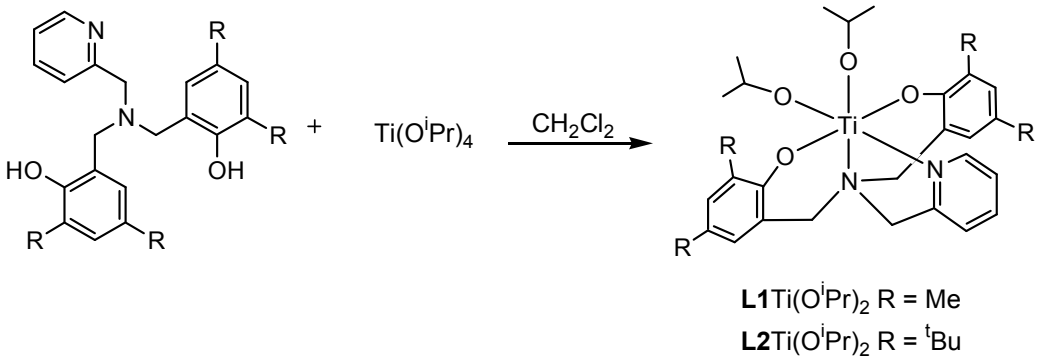

Figure 2.20 Reaction scheme for the formation of complexes **L1**Ti(O^iPr)$_2$ and **L2**Ti(O^iPr)$_2$.

Crystals of **L1**Ti(O^iPr)$_2$ and **L2**Ti(O^iPr)$_2$ suitable for X-ray diffraction analysis were grown from hexane solutions. In the solid state, **L1**Ti(O^iPr)$_2$ and **L2**Ti(O^iPr)$_2$ are isostructural and their solid-state structures agree with those predicted in solution using ^{1}H NMR spectroscopy analysis (Figures 2.21 and 2.22). The amine bis(phenolate) ligands chelate in a tetradentate fashion with the phenoxide ligands in a mutually *trans* orientation and the isopropoxide groups are in a mutually *cis* conformation.

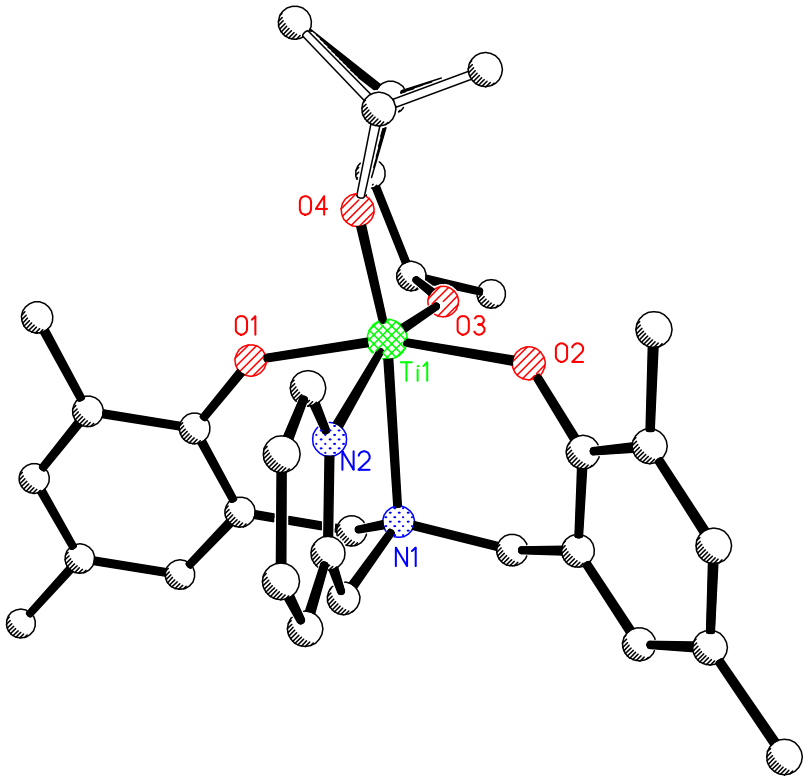

Figure 2.21 Molecular structure of **L1**Ti(O^iPr)$_2$ determined by X-ray crystallography. Hydrogen atoms omitted for clarity. A minor component of disorder in the O^iPr ligand is shown with open bonds.

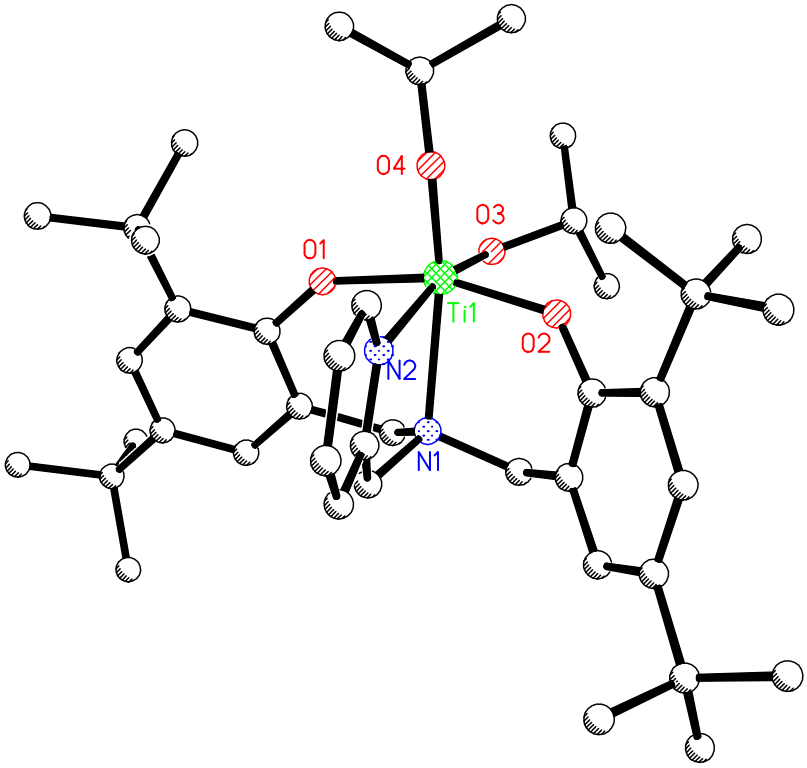

Figure 2.22 Molecular structure of **L2**Ti(O^{i}Pr)$_2$ determined by X-ray crystallography. Hydrogen atoms omitted for clarity.

No appreciable difference in structural parameters such as bond lengths and bond angles between the principal atoms (i.e. Ti, four O and two N) was observed for the two complexes. The phenoxide oxygen-titanium-phenoxide oxygen bond angles of 162.56(6)º for **L1**Ti(O^{i}Pr)$_2$ and 162.11(10)º for **L2**Ti(O^{i}Pr)$_2$ indicate that the phenoxide donors are somewhat 'bent back' towards the pyridyl donor and moreover away from the isopropoxide ligand that is *trans* to the pyridyl donor.

In 2005, Mountford and co-workers reported the synthesis and characterisation of similar titanium(IV) compounds **L1**Ti(X)$_2$ and **L2**Ti(X)$_2$ where X = Cl, NMe$_2$.[27] The solid-state structures of **L1**TiCl$_2$ and **L2**TiCl$_2$ revealed that the ligand adopted a conformation in which the two phenoxide groups were mutually *cis*, complexes with C_1 symmetry as opposed to the complexes of C_s symmetry observed when X = O^{i}Pr, i.e. **L1**Ti(O^{i}Pr)$_2$ and **L2**Ti(O^{i}Pr)$_2$, described herein. A small amount of the C_s isomer **L1**TiCl$_2$ and **L2**TiCl$_2$ was observed in solution, though in both cases this was less than 10% and no interconversion between the two isomers was observed up to 90 ºC. However, when **L1**Ti(NMe$_2$)$_2$ and **L2**Ti(NMe$_2$)$_2$ were prepared, the C_s form was solely observed, as was the case for the titanium isopropoxide complexes reported herein.

Table 2.1 Selected bond lengths for **L2**Ti(X)$_2$ where X = O^{i}Pr (reported herein) and NMe$_2$.[27]

	X = O^{i}Pr	NMe$_2$[27]
Ti-X$_1$	1.8114(16)	1.927(3)
Ti-X$_2$	1.8049(14)	1.940(3)
Ti-N$_1$	2.3679(16)	2.342(3)
Ti-N$_2$	2.2856(17)	2.338(3)
Ti-O$_1$	1.8752(17)	1.927(3)
Ti-O$_2$	1.9175(15)	1.909(2)

Reaction of equimolar amounts of the *para*-nitro substituted **L3**H$_2$ and titanium(IV) isopropoxide in dichloromethane yielded the titanium(IV) complex **L3**Ti(O^{i}Pr)$_2$. The ^{1}H NMR spectrum of the complex again showed an AX spin system for the diastereotopic methylene protons, indicating the ligand to be tightly bound to the metal centre and that the phenoxide groups to be in a mutually *trans* configuration. No evidence for C_s/C_i isomerism of the complex in solution is apparent. The solid-state structure of **L3**Ti(O^{i}Pr)$_2$ shown in Figure 2.23 confirms the above.

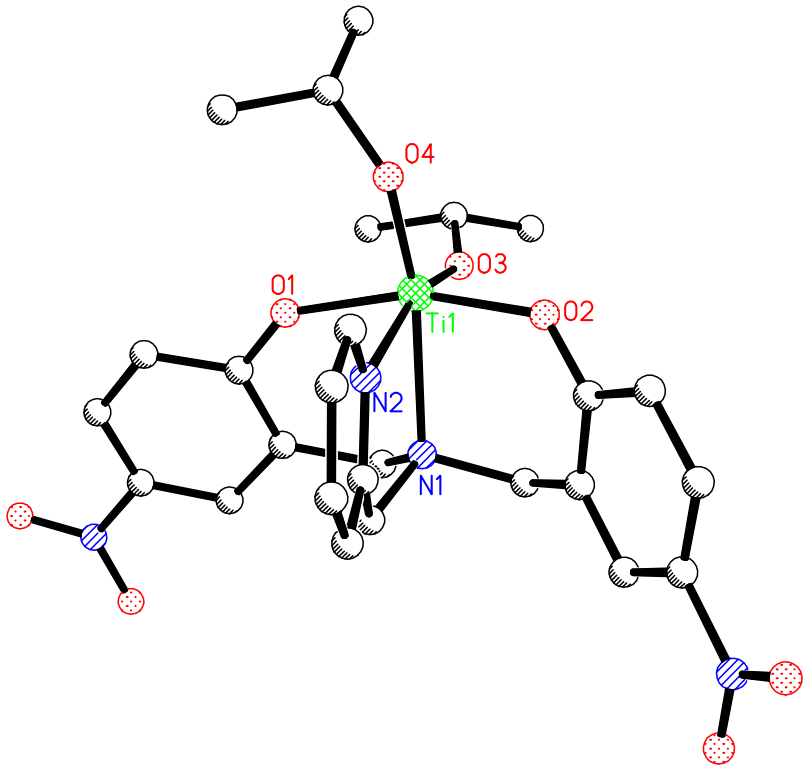

Figure 2.23 Molecular structure of **L3**Ti(O^{i}Pr)$_2$ determined by X-ray crystallography. Hydrogen atoms omitted for clarity.

The main difference between this complex and the 2,4-dimethyl substituted analogue, **L1**Ti(O^{i}Pr)$_2$, is in the metal-phenolic oxygen bond distances, which are significantly shorter in **L3**Ti(O^{i}Pr)$_2$ (Table 2.2). In addition, the phenolic oxygen to *ipso* carbon (O-C$_{ipso}$) bond distances are 1.303(5) and 1.329(5) Å in the *para*-nitro substituted **L3**Ti(O^{i}Pr)$_2$ and 1.332(3) and 1.332(2) Å in the 2,4-dimethyl substituted **L1**Ti(O^{i}Pr)$_2$.

Table 2.2 Comparison of bond lengths for **L3**(O^iPr)$_2$ and **L1**(O^iPr)$_2$.

ortho, para =	H, NO_2	Me, Me
Ti-O_1	1.939(3)	1.8752(17)
Ti-O_2	1.955(3)	1.9175(15)
Ti-O_3	1.782(3)	1.8114(16)
Ti-O_4	1.776(3)	1.8049(14)
Ti-N_1	2.317(3)	2.3679(16)
Ti-N_2	2.271(3)	2.2856(17)

The highlighted differences in bond lengths for **L3**Ti(O^iPr)$_2$ are likely to be due to the presence of the NO_2 groups. These groups withdraw π-electron density from the aryl rings resulting in a shortening of the C_{ipso}-O bond lengths and concomitant elongation of the O-Ti bond lengths.

Zirconium(IV) and Hafnium(IV) Complexes of L1H_2 and L2H_2

Zirconium(IV) and hafnium(IV) complexes of ligands **L1**H_2 and **L2**H_2 were prepared in a similar manner to that described for complexes **L1-L3**Ti(O^iPr)$_2$ (Figure 2.24). In these cases, the metal(IV) isopropoxide mono-isopropanol complex, [M(O^iPr)$_4$HO^iPr] (M = Zr, Hf), was used as the starting material, yielding complexes **L1**Zr(O^iPr)$_2$, **L2**Zr(O^iPr)$_2$, **L1**Hf(O^iPr)$_2$ and **L2**Hf(O^iPr)$_2$, respectively.

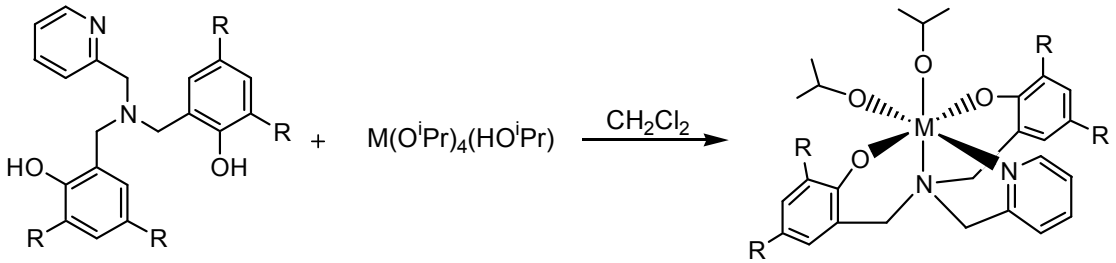

Figure 2.24 Synthetic route to complexes **L1**Zr(O^iPr)$_2$, **L2**Zr(O^iPr)$_2$, **L1**Hf(O^iPr)$_2$ and **L2**Hf(O^iPr)$_2$.

^{1}H NMR spectra of these complexes imply solution structures similar to those of their titanium analogues. Sharp AX spin system doublets for the diastereotopic methylene protons of ligands **L1** and **L2** indicate that in each case the multidentate ligand is tightly bound to the metal centre in each case and that the ligand adopts a conformation in which the phenoxide groups are mutually *trans*.

Full structural characterisation, including X-ray crystallographic analysis was possible for complexes **L1**Zr(O^iPr)$_2$, **L2**Zr(O^iPr)$_2$ and **L2**Hf(O^iPr)$_2$, (Figures 2.25 and 2.27) and the solid-state structures so obtained agreed with the predictions made from examination of

the solution ^{1}H NMR spectroscopic data for the complexes. Suitably sized single crystals of **L1**Hf(O^{i}Pr)$_2$ were not obtained and so its solid-state structure was not determined.

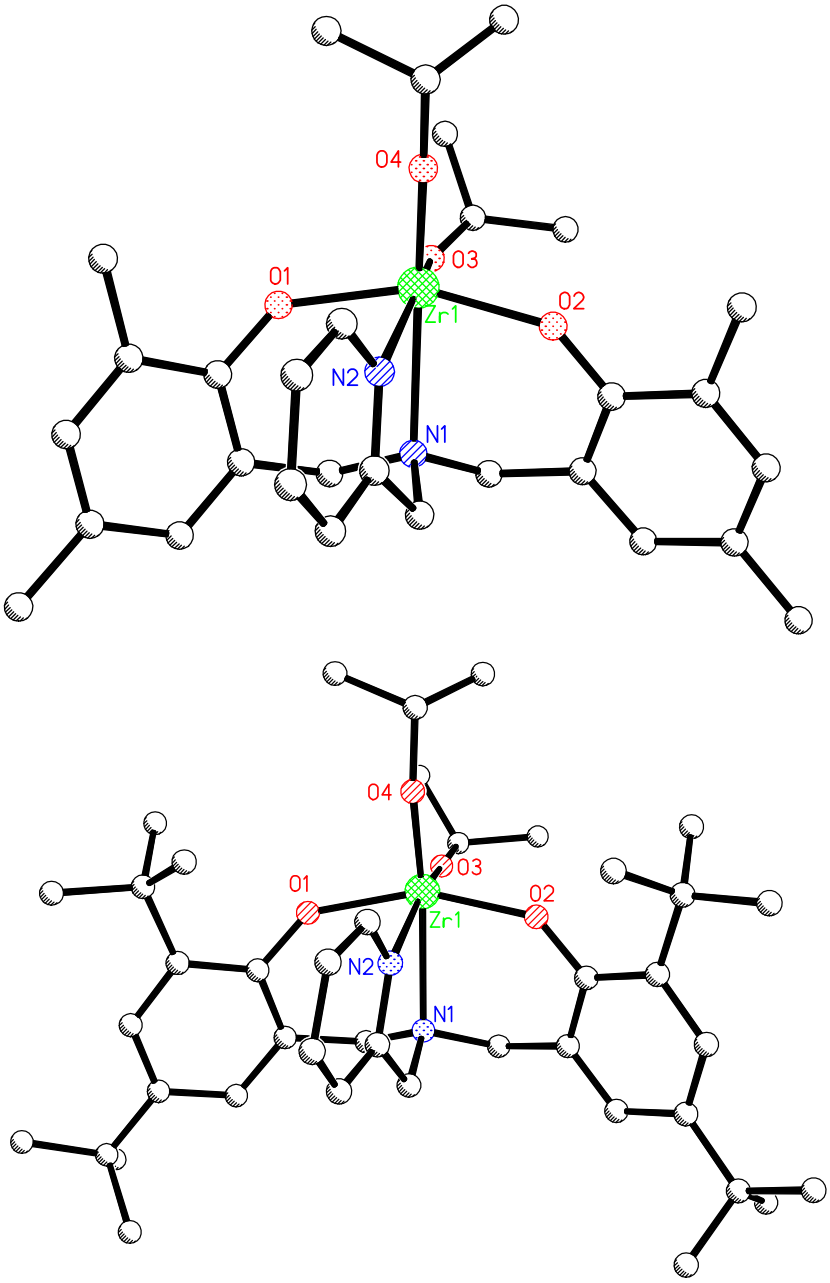

Figure 2.25 Molecular structures of **L1**Zr(O^{i}Pr)$_2$ and **L2**Zr(O^{i}Pr)$_2$ as determined by X-ray crystallography. Hydrogen atoms omitted for clarity.

Mountford and co-workers recently reported analogous zirconium complexes **L1**Zr(X)$_2$ and **L2**Zr(X)$_2$ where X = NMe$_2$, Me, η^3-C$_3$H$_5$, CH$_2$SiMe$_3$, CH$_2$CMe$_3$ and CH$_2$Ph.[28] In the case of **L1**ZrCl$_2$ and **L2**ZrCl$_2$, room temperature the ^{1}H NMR spectra of both complexes showed broad resonances for all signals. On cooling to -60 ºC a sharpening of the resonances occurred and the presence of two distinct sets of resonances corresponding to two distinct compounds was observed. As with the titanium(IV) complexes **L1**TiCl$_2$ and **L2**TiCl$_2$[27] described earlier, the sets of resonances were attributed to the presence of

two isomers, one in which the phenoxide groups are mutually *cis*, with C_1 symmetry, and one in which they are mutually *trans* with approximate C_s symmetry (Figure 2.26).

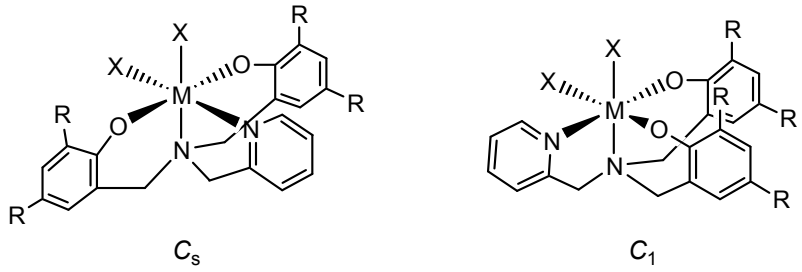

Figure 2.26 Isomeric forms of complexes of **L1**M(X)$_2$ and **L2**M(X)$_2$.

For the 2,4-dimethyl substituted complex **L1**ZrCl$_2$, these isomers are observed in solution in a 95:5 C_1:C_s ratio; the solid-state structure obtained for this complex was indeed that of the C_1 isomer. In the case of 2,4-di-*tert*-butyl substituted complex **L1**ZrCl$_2$, the reported ratio of isomers was 65:35 C_1:C_s and the solid-state structure obtained was that of the minor C_s isomer. These isomers were determined to be in dynamic interconversional exchange by ^{1}H NMR spectroscopy. Interestingly, when the homoleptic 2,4-dimethyl substituted zirconium(IV) complex (of the form **L**$_2$Zr) was prepared only the isomer with the phenoxide groups in mutually *cis* positions was observed, both by ^{1}H NMR spectroscopy and by X-ray crystallography of a crystalline sample. In contrast, for complexes X = NMe$_2$, Me, η^3-C$_3$H$_5$, CH$_2$SiMe$_3$, CH$_2$CMe$_3$ and CH$_2$Ph, no interconversion was apparent in the ^{1}H NMR spectra of the complexes.

For both complexes **L1**Zr(O^{i}Pr)$_2$ and **L2**Zr(O^{i}Pr)$_2$, X-ray crystallographic analysis of crystalline samples indicated a *pseudo* C_s geometry and sharp signals for all protons in the complexes were observed in their ^{1}H NMR spectra. Thus, no indication of the presence of a C_1 isomer with mutually *cis* phenoxide groups was evident in the ^{1}H NMR spectra. In these complexes, the phenoxide groups orient so as to be mutually *trans* and in doing so, avoid adopting a conformation in which they are *trans* to the highly *trans* influencing and π-donating isopropoxide groups. Metal-heteroatom bond lengths for **L1**Zr(O^{i}Pr)$_2$ and **L1**Zr(O^{i}Pr)$_2$ are given in Tables 2.3 and 2.4, respectively, along with comparisons with similar complexes prepared by Mountford *et al*. In both cases, only complexes with solid-state structures of C_s symmetry are compared.

Table 2.3 Selected bond lengths for complexes **L1**Zr(X)$_2$ where X = O^{i}Pr (this work), Me and CH$_2$Ph.[27]

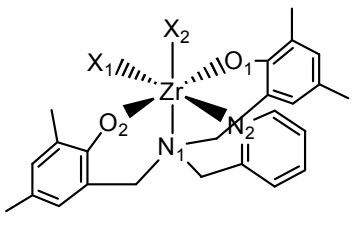

X =	O^{i}Pr	Me[27]	CH$_2$Ph[27]
Zr-X$_1$	1.966(3)	2.278(4)	2.312(3)
Zr-X$_2$	1.927(3)	2.241(4)	2.300(3)
Zr-N$_1$	2.458(3)	2.504(3)	2.447(2)
Zr-N$_2$	2.425(3)	2.452(3)	2.476(2)
Zr-O$_1$	2.049(3)	1.988(3)	2.022(2)
Zr-O$_2$	2.029(3)	2.003(3)	1.990(2)

For **L1**Zr(O^iPr)$_2$, the metal-ligand bond lengths are within the range reported for similar complexes as shown in comparison to those for the zirconium(IV) dimethyl and dibenzyl complexes previously reported (Table 2.3).[27] One significant difference observed in the Zr-$X_{1,2}$ bond lengths is that these are shorter when X = O^iPr.

Table 2.4 Selected bond lengths for complexes **L2**Zr(X)$_2$ where X = O^iPr (this work), Cl, NMe_2 and Me.[27]

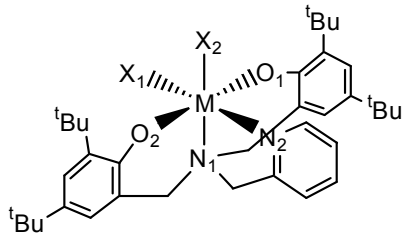

X =	O^iPr	Cl[27]	NMe_2[27]	Me[27]
Zr-X_1	1.939(2)	2.4205(6)	2.0706(14)	2.343(2)
Zr-X_2	1.937(2)	2.4309(6)	2.0832(14)	2.267(2)
Zr-N_1	2.446(2)	2.397(2)	2.4670(13)	2.446(2)
Zr-N_2	2.431(3)	2.377(2)	2.4597(14)	2.497(2)
Zr-O_1	2.036(2)	1.966(2)	2.0245(11)	2.009(2)
Zr-O_2	2.033(2)	1.997(2)	2.0380(11)	2.002(2)

For the zirconium(IV) di(isopropoxide) complex of the 2,4-*tert*-butyl substituted ligand, **L2**, the metal-ligand bond lengths are comparable with those observed in other complexes employing ligand **L2**. The metal-nitrogen bond lengths are significantly longer in **L2**Zr(O^iPr)$_2$ than in **L2**$ZrCl_2$. As both nitrogen donors are *trans* to an X group (Table 2.4), this elongation reflects the better π-donor ability of the isopropoxide ligand as compared to chloride. The metal-amine bis(phenolate) bond lengths for **L2**Zr(O^iPr)$_2$ are closer in value to those obtained for the solid-state structures of the zirconium(IV) bis(dimethylamino) and dimethyl complexes. The metal-phenolic oxygen distances are very similar to those observed for the complex where X = NMe_2, and are longer than those observed for the complexes where X = Cl and Me.

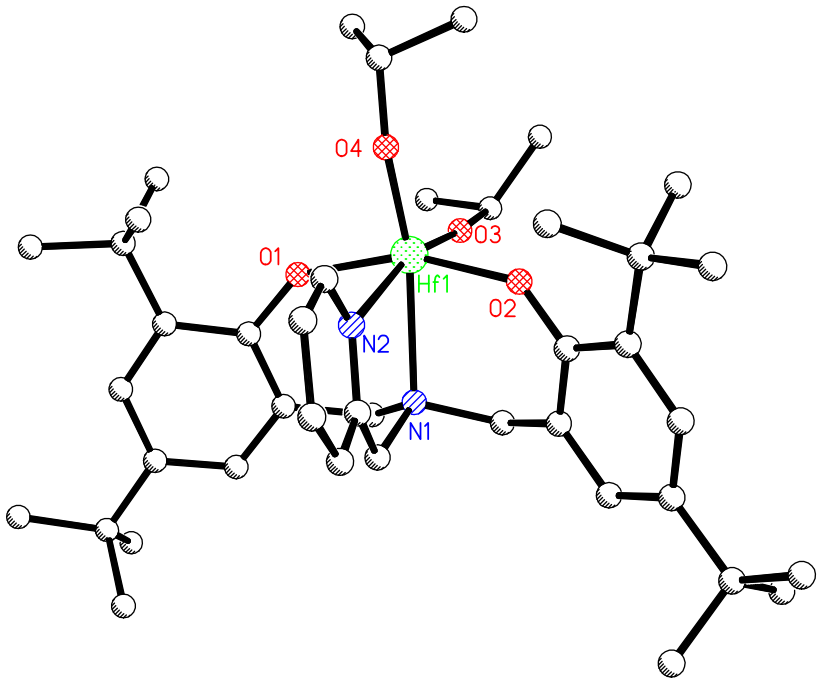

Figure 2.27 Molecular structure of **L2**Hf(O^iPr)$_2$ as determined by X-ray crystallography. Hydrogen atoms omitted for clarity.

The synthesis of the series of complexes **L1**-**L2**M(O^iPr)$_2$ M = Ti, Zr, Hf allows for a direct comparison of complexes of all three metals in the Group 4 triad. The atom numbering scheme adopted for these complexes is shown in Figure 2.28.

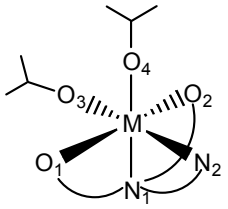

Figure 2.28 Atom numbering scheme for structural parameter comparison.

For the zirconium(IV) complexes **L1**Zr(O^iPr)$_2$ and **L2**Zr(O^iPr)$_2$, no significant differences in bond angles and bond lengths is evident on moving from the methyl substituted to the *tert*-butyl substituted complex (Table 2.5). Also, *in general*, metric parameters for **L1**Zr(O^iPr)$_2$, **L2**Zr(O^iPr)$_2$ and **L2**Hf(O^iPr)$_2$ are very similar; an observation often evident for the second and third row transition metals in a triad which is due to the lanthanide contraction, which renders the atomic radii of zirconium and hafnium to be similar.

Table 2.5 Solid state structural parameters for the named complexes determined by X-ray crystallographic analysis. Bond lengths M-X (Å) and bond angles Y-M-Z (º).

	L1Ti(O^iPr)$_2$	**L2**Ti(O^iPr)$_2$	**L1**Zr(O^iPr)$_2$	**L2**Zr(O^iPr)$_2$	**L2**Hf(O^iPr)$_2$
M-O$_1$	1.876(2)	1.923(2)	2.029(3)	2.036(2)	2.025(2)
M-O$_2$	1.918(2)	1.896(2)	2.049(3)	2.033(2)	2.025(2)
M-O$_3$	1.811(2)	1.817(2)	1.966(3)	1.939(2)	1.925(2)
M-O$_4$	1.809(1)	1.805(2)	1.927(3)	1.937(2)	1.928(2)
M-N$_1$	2.368(2)	2.340(3)	2.458(3)	2.446(2)	2.418(2)
M-N$_2$	2.286(2)	2.280(3)	2.425(3)	2.431(3)	2.394(2)
O$_1$-M-O$_2$	162.56(6)	162.11(10)	156.49(12)	156.72(8)	158.03(7)
O$_3$-M-O$_4$	104.46(7)	103.95(12)	106.66(15)	106.29(10)	106.07(8)
O$_4$-M-N$_1$	162.66(7)	162.31(11)	157.97(13)	157.73(9)	158.24(7)
N$_1$-M-N$_2$	72.20(6)	72.93(9)	69.57(11)	69.33(8)	70.17(6)

However, it is interesting to note that the bond lengths between the metal centre and the principal atoms in its coordination sphere (4 x oxygen, 2 x nitrogen) decrease from M=Zr to M=Hf, with a particularly marked decrease in the metal-nitrogen bond lengths. A recent review noted that hafnium has long been considered a 'twin' to zirconium in terms of complex structures and reactivity, but highlighted that recently, significant differences between zirconium and hafnium complexes have been reported, particularly with regard to C-H and N_2 activation.[29] Considering the titanium(IV) complexes relative to the zirconium(IV) and hafnium(IV) analogues, some structural differences are apparent. The bond lengths between the metal centre and the principal atoms in its coordination sphere increase slightly from M=Ti to M=Zr, Hf. The O_1-M-O_2 bond angle decreases for **L1**Zr(O^iPr)$_2$, **L2**Zr(O^iPr)$_2$ and **L2**Hf(O^iPr)$_2$ with respect to the analogous titanium(IV)

complexes, while the angle between the *cis* oriented isopropoxide groups (O_3-M-O_4) increases. Finally, the pyridyl nitrogen-metal-amine nitrogen bond angle and the isopropoxide-metal-amine nitrogen bond angle (O_4-M-N_1) decreases from M=Ti to M=Zr, Hf. This difference observed in the complexes of the second and third row Group 4 metals is most likely due to the larger size of these metal centres as compared to titanium(IV).

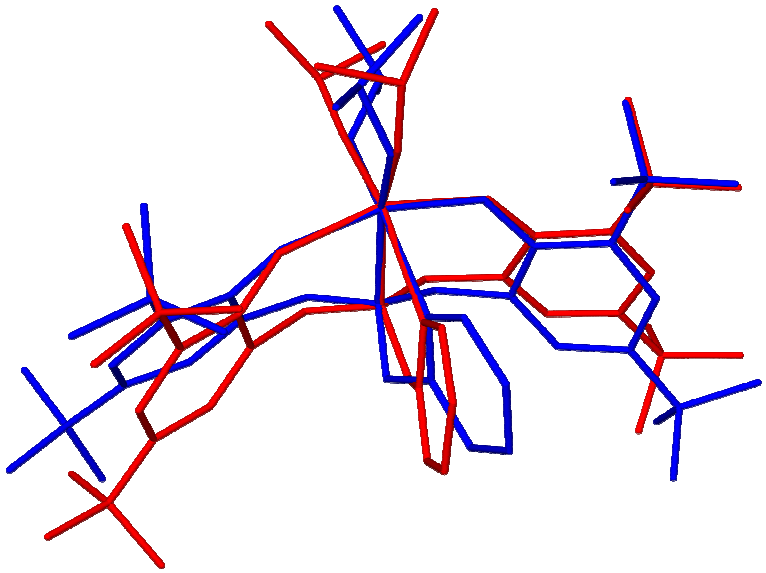

Figure 2.29 An overlay of the solid-state structures of **L2**Hf(O^iPr)$_2$ (blue) and **L2**Ti(O^iPr)$_2$ (red) illustrating their structural similarities, as well as subtle differences.

Titanium(IV) Complexes of L6-L7H_2 and L9-L10H_2

Previous reports in the literature detail the synthesis of amine bis(phenolate) ligands with tridentate coordination ability, of the type shown in Figure 2.29 above.[1, 30] In the coordination chemistry of titanium(IV) complexes of these ligands a common problem is the formation of homoleptic complexes **L**$_2$M, with two equivalents of the ligand each bound in a *meridional* fashion to the titanium centre (Figure 2.30).[17, 31] These types of complexes are considered to be undesirable for ROP of cyclic esters as they lack a metal-alkoxide bond into which the cyclic ester monomer may be inserted.[9]

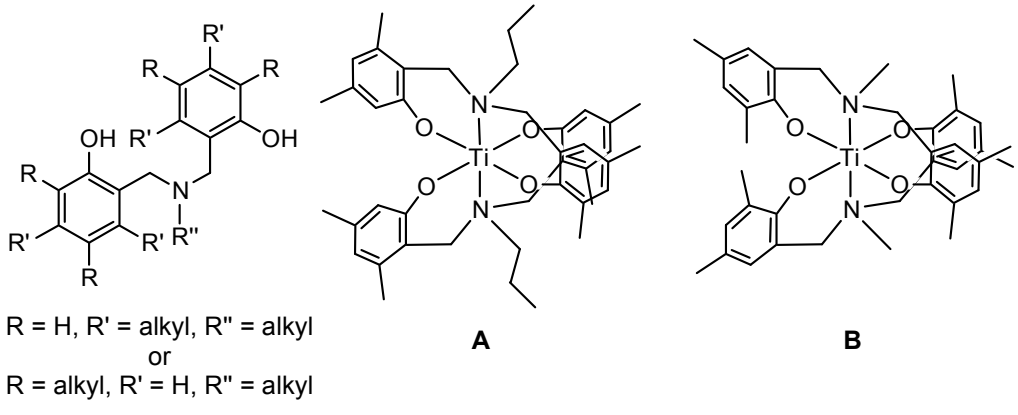

Figure 2.30 Titanium(IV) complexes of amine bis(phenolate) ligands with alkyl pendant arms.[17, 31]

One explanation for the formation of these complexes is the lack of bulk within the ligand structure. Increasing the size of the *ortho* substituents on the phenolic arms has been considered as a method of avoiding the disubstituted complex, but in some cases this strategy proved unsuccessful. For instance, when an amine bis(phenolate) ligand incorporating 3,5-dimethyl substituted phenolic groups and a propyl pendant arm was reacted with titanium(IV) isopropoxide, the homoleptic $\mathbf{L}_2$Ti complex formed (Figure 2.30 A), regardless of reaction stoichiometry.[17] A later example in which the pattern of substitution on the phenyl ring was changed, most notably with a bulkier methyl group replacing the proton in the *ortho* position of the phenolic rings, did not prevent $\mathbf{L}_2$Ti complex formation (Figure 2.30 B).[31] As such, the tetradentate ligands with a fourth donor atom on the pendant arm have been developed to overcome this problem.[2, 3, 28, 32, 33]

In an attempt to retain an O,N,O type ligand motif and avoid the formation of the homoleptic $\mathbf{L}_2$M-type complex, we proposed to increase the size of both the *ortho* and *para* phenolic substituents as well as increase the size of the amine substituent, moving from aliphatic derivatives, which had been synthesised previously, to the novel benzyl and naphthalenemethyl derivatives.

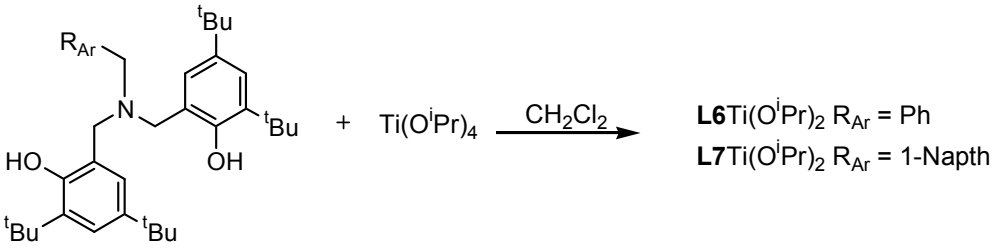

Figure 2.31 Synthetic route to complexes **L6**Ti(O^iPr)$_2$ and **L7**Ti(O^iPr)$_2$.

Titanium(IV) complexes of **L6**H_2 and **L7**H_2 were prepared by reaction of titanium(IV) isopropoxide with the appropriate ligand in a dichloromethane solution (Figure 2.31). For both reaction products, the presence of two septet-doublet pairs in the ^{1}H NMR spectrum indicates that the complexes contain two non-equivalent isopropoxide groups and that formation of the homoleptic $\mathbf{L}_2$M complex had been avoided. The three possible arrangements of the ligands in a complex of this type are shown in Figure 2.32.

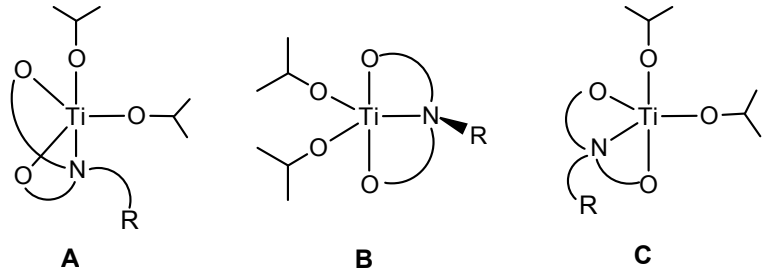

Figure 2.32 Possible conformations for titanium complexes of **L6-7**H_2, assuming two non-equivalent isopropoxide groups.

The amine bis(phenolate) ligand may be bound in a *pseudo meridional* arrangement with the isopropoxide groups mutually *trans* to one another (Figure 2.32B), in a *pseudo facial* arrangement with the two isopropoxide groups mutually *cis* and the phenolate oxygen atoms in the equatorial plane (Figure 2.32A) or with two mutually *cis* isopropoxide groups and a phenolate oxygen atom and the amine nitrogen in the equatorial plane (Figure 2.32C). In each of these possible structures, the unbound pendant arm of the nitrogen donor is free to rotate, thus rendering the isopropoxide groups inequivalent.

Single crystals suitable for X-ray diffraction analysis were obtained for both **L6**Ti(O^iPr)$_2$ and **L7**Ti(O^iPr)$_2$ and are shown in Figure 2.33 and 2.34, respectively. These reveal that in the solid-state both complexes adopt a five-coordinate pseudo trigonal bipyramidal geometry conformation in which the amine bis(phenolate) ligand is bound in a tridentate fashion. The phenolic oxygen atoms of the amine bis(phenolate) ligand and the oxygen atom of one isopropoxide group occupy the equatorial positions, while the apical nitrogen atom and the oxygen atom of the other isopropoxide group occupy the axial positions.

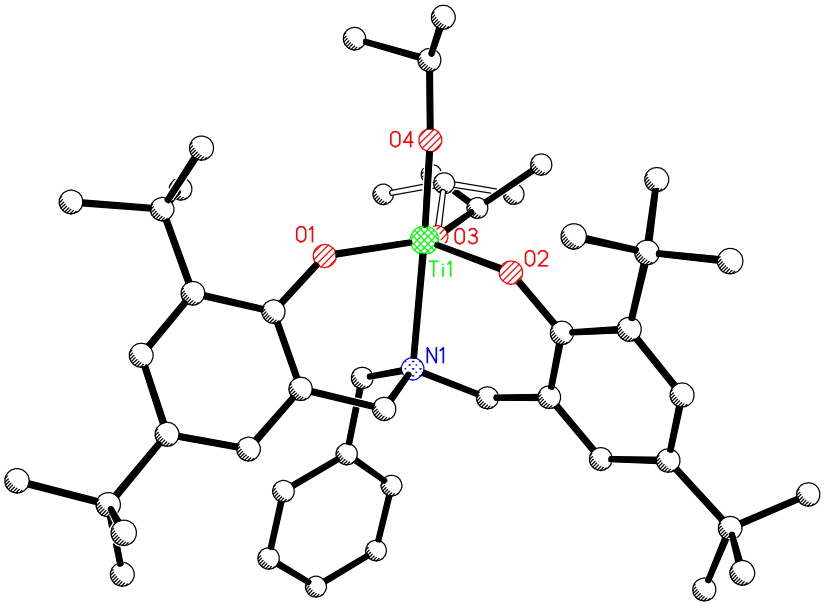

Figure 2.33 Molecular structure of **L6**Ti(O^iPr)$_2$ as determined by X-ray crystallography. Hydrogen atoms omitted for clarity. A minor component of disorder in one O^iPr group is shown with open bonds.

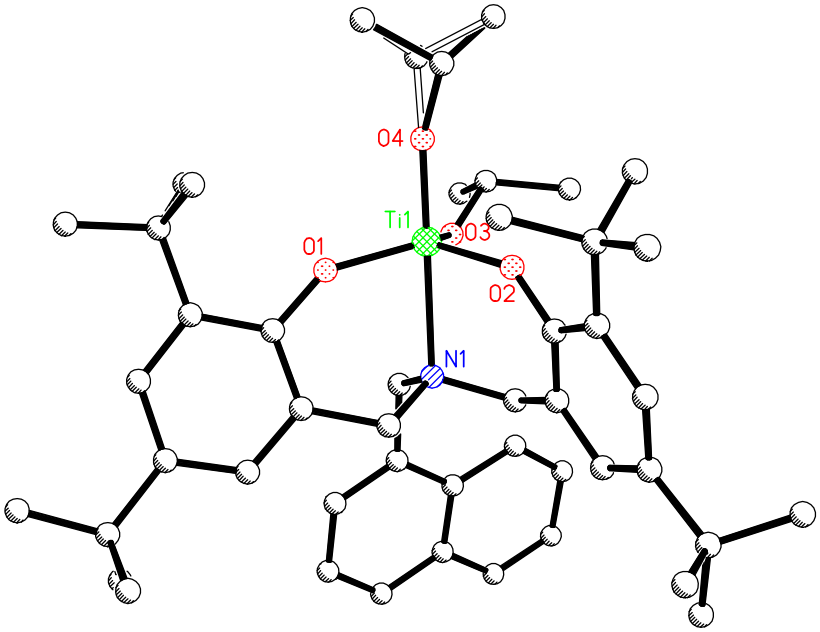

Figure 2.34 Molecular structure of **L7**Ti(O^{i}Pr)$_2$ as determined by X-ray crystallography. Hydrogen atoms omitted for clarity. A minor component of disorder in one O^{i}Pr group is shown with open bonds.

On examination of these structures, their conformation seems favourable, as it minimises steric interaction between the bulky *tert*-butyl groups. The bond lengths within the metal-ligand coordination sphere are similar between the two complexes and with the six-coordinate titanium complexes **L1**Ti(O^{i}Pr)$_2$ and **L2**Ti(O^{i}Pr)$_2$ described previously. Comparing the solid-state structures of **L2**Ti(O^{i}Pr)$_2$ and **L6**Ti(O^{i}Pr)$_2$, where the only significant difference in the molecular formulae of the complexes is the substitution of N for C-H, all of the bond distances in the metal-ligand coordination sphere are significantly shorter for the five coordinate complex **L6**Ti(O^{i}Pr)$_2$ (Table 2.6). This observation is in line with the findings of See and co-workers[34] who, after studying the factors influencing metal-ligand bond lengths in complexes of the first row transition metals concluded that such bond distances increase with increasing metal coordination number such that the metal centre may reach a particular bond order sum which depends on the oxidation state of the metal centre and the nature of the ligands. Comparing the solid-state structures of **L6**Ti(O^{i}Pr)$_2$ and **L7**Ti(O^{i}Pr)$_2$, in which the aryl substituent on the pendant arm changes from benzene to naphthalene, the titanium-nitrogen bond distance increases from 2.330(1) Å to 2.830(2) Å, presumably due to the increasing steric demands of the larger aryl group. This increase in titanium-nitrogen bond length is accompanied by a decrease in the bond lengths from the metal to the phenolic oxygen donor atoms and an increase in the equatorial isopropoxide oxygen-metal bond length (Table 2.6).

Table 2.6 Solid state structural parameters for the named complexes determined by X-ray crystallographic analysis. Bond lengths M-X (Å) and bond angles Y-M-Z (º).

	L6Ti(O^{i}Pr)$_2$	**L7**Ti(O^{i}Pr)$_2$	**L2**Ti(O^{i}Pr)$_2$
M-O$_1$	1.850(1)	1.837(1)	1.923(2)
M-O$_2$	1.860(2)	1.851(1)	1.896(2)
M-O$_3$	1.800(2)	1.831(1)	1.817(2)
M-O$_4$	1.781(1)	1.782(1)	1.805(2)
M-N$_1$	2.330(1)	2.380(2)	2.340(3)
O$_1$-M-O$_2$	121.15(5)	118.66(16)	
O$_3$-M-O$_4$	99.70(6)	98.99(6)	
O$_4$-M-N$_1$	176.28(5)	178.20(6)	
O$_2$-M-N$_1$	80.13(4)	80.60(6)	
O$_1$-M-N$_1$	81.97(4)	81.98(6)	
N$_1$-C$_3$-C$_{31}$	117.25(11)	117.92(2)	

In addition, while for **L6**Ti(O^{i}Pr)$_2$ the angle subtended by the phenolic oxygens, O$_1$-M-O$_2$ is, at 121.15(5)º, slightly larger than the 120º expected for the equatorial substituents of a true trigonal bipyramidal metal complex, the corresponding angle in **L7**Ti(O^{i}Pr)$_2$ is reduced to 118.66(16)º. This reduction could be due to any number of factors, but is unlikely to be due to the increased steric bulk of the pendant arm.

The room temperature ^{1}H NMR spectrum of **L6**Ti(O^{i}Pr)$_2$ is shown in Figure 2.35 and appears quite complicated, but may be explained by considering the solid-state structure of the complex. This structure shows that the conformation of the complex affords six differentiable methylene protons arising due to the 'buckled' methylene bridges within the amine bis(phenolate) ligand. A similar spectrum is observed for **L7**Ti(O^{i}Pr)$_2$ and the spectra of these two complexes contrast with that of **L2**Ti(O^{i}Pr)$_2$, in which a sharp singlet and two pairs of sharp doublets were observed in the methylene region.

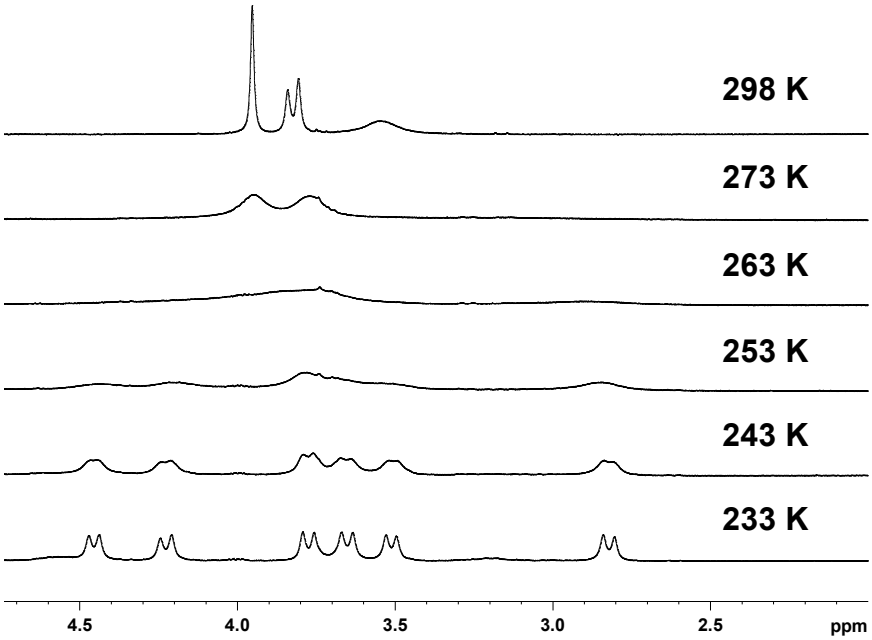

Figure 2.35 ^{1}H NMR spectra of **L6**Ti(O^{i}Pr)$_2$ at 298 K (top), 273 K, 263 K, 253 K, 243 K and 233 K.

The ^{1}H NMR spectrum of **L6**Ti(O^iPr)$_2$ was acquired at a range of temperatures (298 K – 233 K) in an attempt to resolve the behaviour of the methylene protons (Figure 2.35); this series of experiments showed that at as the sample's temperature is reduced, six 1H doublets become apparent. This indicates that all methylene protons due to the ligand **L6** are inequivalent at this temperature, i.e the conformation of the complex in solution possesses no symmetry, at this temperature. Unfortunately, these experiments shed no further light on the solution conformation of **L6**Ti(O^iPr)$_2$ at 233 K. However, it is important to note that only one set of signals is observed at 233 K. This indicates that only one isomer of the complex is present at this temperature.

Ligands **L1**H_2 and **L2**H_2 feature a pyridine ring on the pendant arm of the ligand, which was shown, by X-ray crystallography and ^{1}H NMR spectroscopy, to be coordinated to the metal centre through the nitrogen atom both in the solid-state and in solution for complexes **L1**M(O^iPr)$_2$ and **L2**M(O^iPr)$_2$ where M = Ti, Zr, Hf. In order to investigate the effect of a different heterocycle, thiophene, on the coordinative ability of the ligand to Group 4 metal centres and the reactivity of such a metal complex, the synthesis of a titanium(IV) complex of **L9** was attempted. An equimolar amount of **L9**H_2 was added to titanium(IV) isopropoxide in dichloromethane solution under an argon atmosphere. After stirring for several hours the volatiles were removed and the bright orange-red solid formed was washed with hexane. ^{1}H NMR of the crude reaction product indicated that no isopropoxide groups were present in the molecule, as no corresponding resonances were observed. In fact, a well-resolved but very complicated spectrum was observed which indicated each proton in the ligand was magnetically inequivalent. The sharp resonances, particularly in the aromatic region, implied that the thiophene moiety was perhaps bound to the metal centre. However, thiophene is considered to be a very poor donor to metal centres and few metal complexes featuring a sulfur-bound thiophene are known.[35] In addition, the absence of any isopropoxide groups indicated the complex was likely to be the undesired homoleptic, of the form **L9**$_2$Ti (Figure 2.36).

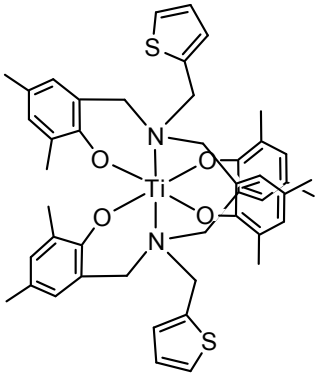

Figure 2.36 Possible conformation for the reaction product of **L9**H_2 with Ti(O^iPr)$_2$ in which the thiophene group is not bound to the metal centre.

If the complex is homoleptic (Figure 2.36), the thiophene groups are unlikely to be bound, as this would require an eight-coordinate titanium(IV) centre, which is uncommon for titanium(IV). A complex of this form, **L9**$_2$Ti, with a six-coordinate titanium(IV) centre and non-coordinated thiophene groups is not entirely unexpected. A similar complex, with *non-bulky* methyl groups in the phenoxide *ortho* positions, was discussed earlier (Figure 2.30 B). However, if this were the case, significant broadening of the signals due to the methylene protons of the ligand **L9** would be expected due to the free rotation of the thiophene group in solution.

^{1}H NMR experiments were carried out at variable temperatures up to 55 ºC and no broadening of any of the peaks was observed (Figure 2.37), indicating that no fluxional processes were underway in the system.

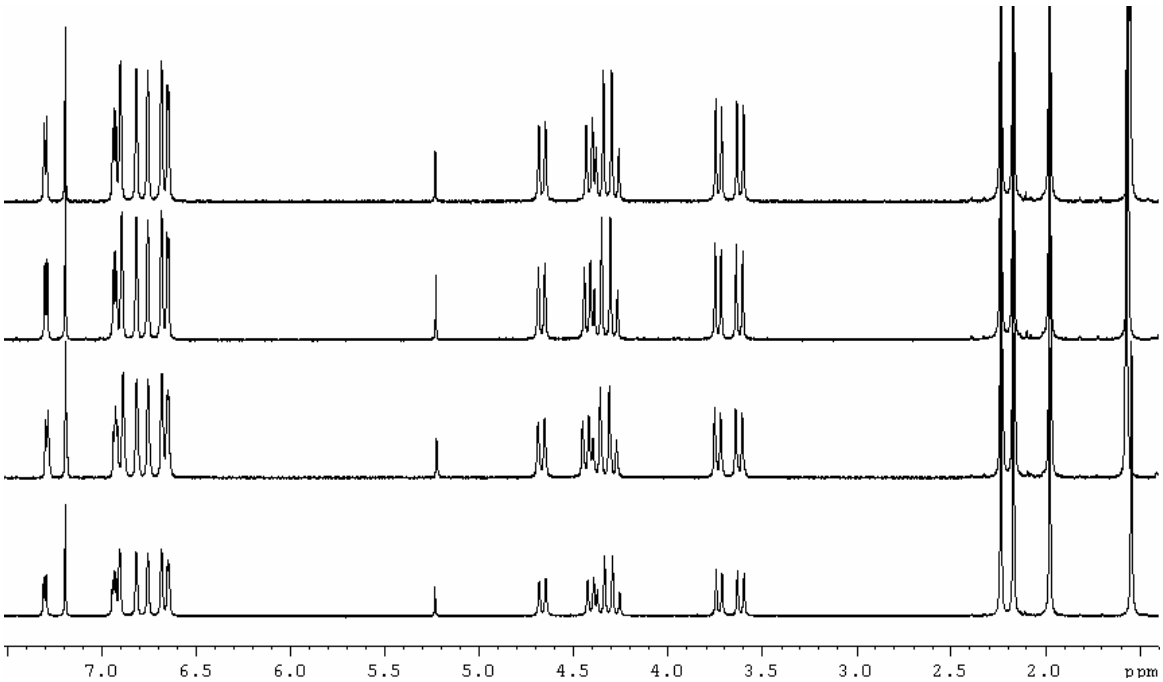

Figure 2.37 ^{1}H NMR spectra of the reaction product of **L9**H_2 and Ti(O^iPr)$_4$ at 298 K (bottom), 308 K, 318 K and 328 K (top).

The bright red solid isolated from the reaction of **L9**H_2 and Ti(O^iPr)$_4$ was analysed by fast atom bombardment mass spectrometry which revealed MH^+ at an m/z of ~807. The mass of the complex illustrated in Figure 2.36 is 806.09 g mol^{-1}. It was therefore concluded that the solution structure of the reaction product of **L9**H_2 and Ti(O^iPr)$_4$ corresponded to that shown in Figure 2.36. The reaction scheme for this complex is shown in Figure 2.38.

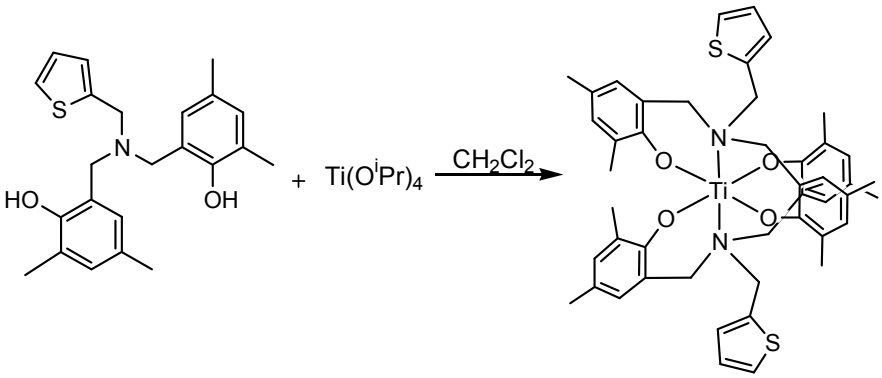

L9$_2$Ti

Figure 2.38 Synthetic route to **L9**$_2$Ti.

Subsequently, single crystals suitable for X-ray diffraction analysis were grown and the solid-state structure was found to be that predicted by ^{1}H NMR spectroscopy and mass spectrometry (Figure 2.39). The titanium(IV) centre is approximately octahedral in geometry and the two ligands **L9** are coordinated to the metal centre through both phenolic oxygen atoms and the amine nitrogen atom. Each ligand is coordinated in a *meridional* fashion, with the phenolate arms in mutually *trans* positions.

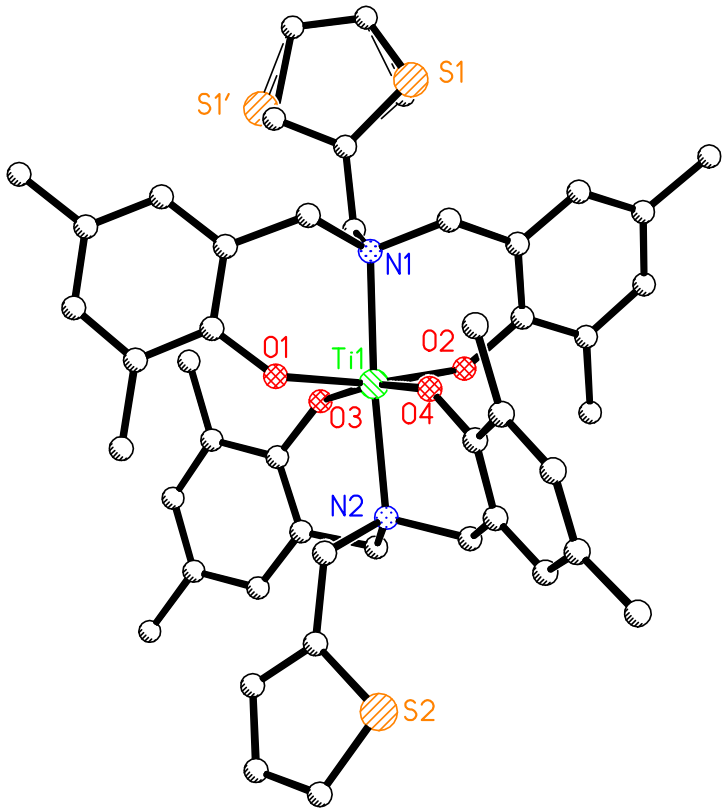

Figure 2.39 Molecular structure of $\mathbf{L9}_2$Ti as determined by X-ray crystallography. Hydrogen atoms omitted for clarity. The disorder of the thiophene group (including S1) is modelled 50:50.

The bond lengths within the metal-ligand coordination sphere are similar to those of complexes reported herein. However, unusually for such homoleptic complexes the two ligands display distinct coordination geometries. Defining $\mathbf{L9}_a$ as the ligand on the 'top' of the complex as shown in Figure 2.39, with the disordered thiophene system, we see that when compared to $\mathbf{L9}_b$ the metal-oxygen bond lengths are longer and the metal-nitrogen bond length is shorter. The molecular structure obtained sheds light on the solution ^{1}H NMR spectrum of the complex shown earlier in Figure 2.37. The solid-state structure implies the complex has a *pseudo* C_2 axis which would seem likely to persist in solution. This supports the chemical and magnetic inequivalence of the backbone methylene protons as observed in the solution ^{1}H NMR spectrum of the complex (Figure 2.37).

Comparison of the principal bond lengths in the metal-ligand coordination sphere for $\mathbf{L9}_2$Ti and $\mathbf{L1}$Ti(O^iPr)$_2$, where the only difference between the ligands is the identity of the pendant heterocycle (thiophene and pyridine, respectively), the metal-phenolic oxygen bond lengths are similar, although the Ti-O_1 distance is slightly longer in $\mathbf{L1}$Ti(O^iPr)$_2$ and the Ti-O_2 distance slightly shorter. A large change in these bond lengths would not be expected as in both cases, the ligand phenolate groups are mutually *trans* and so the degree of *trans* influence on each phenolate arm should be similar. The metal-nitrogen

bond length in **L9**$_2$Ti, where the two amine nitrogen atoms are *trans* to one another, is >0.1 Å shorter than in **L1**Ti(O^{i}Pr)$_2$, where the nitrogen atom is *trans* to an isopropoxide group. Comparing the solid-state structure of **L9**$_2$Ti with that of **L6**Ti(O^{i}Pr)$_2$, another complex in which the ligand is chelated in a tridentate fashion, the metal-phenolic oxygen bond distances are somewhat shorter in the five-coordinate **L6**Ti(O^{i}Pr)$_2$.

Table 2.7 Solid-state structural parameters for **L9**$_2$Ti in comparison to those for **L1**Ti(O^{i}Pr)$_2$ and **L6**Ti(O^{i}Pr)$_2$.

	L9$_2$Ti	**L1**Ti(O^{i}Pr)$_2$	**L6**Ti(O^{i}Pr)$_2$
Ti-O$_1$	1.892(2)	1.918(2)	1.850(1)
Ti-O$_2$	1.881(2)	1.876(2)	1.860(2)
Ti-N$_1$	2.262(2)	2.368(2)	2.330(1)
Ti-O$_3$	1.873(2)	-	-
Ti-O$_4$	1.857(2)	-	-
Ti-N$_2$	2.278(2)	-	-

In the hope of preventing formation of a homoleptic **L**$_2$M-type titanium(IV) complex, a the more sterically bulky ligand **L10**H$_2$ was reacted with titanium(IV) isopropoxide in dichloromethane, and the reaction mixture was stirred for several hours (Figure 2.40). After removal of the volatiles, the ^{1}H NMR spectrum of the crude, solid reaction product indicated the presence of two isopropoxide groups. In addition, peaks due to the methylene protons on the phenoxy and thiophene arms of the ligand were observed, in a pattern identical to those seen for **L6**Ti(O^{i}Pr)$_2$ and **L7**Ti(O^{i}Pr)$_2$, described earlier. These were broad, indicating the thiophene moiety was unbound and free to rotate in solution. Single crystals suitable for X-ray diffraction analysis were grown from hexane solution and their analysis revealed the solid state structure to be as predicted, a monomeric, five-coordinate titanium(IV) complex.

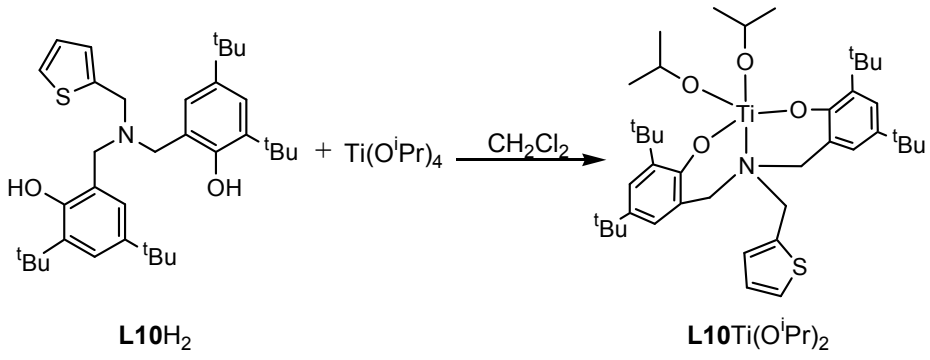

L10H$_2$ **L10**Ti(O^{i}Pr)$_2$

Figure 2.40 Synthetic route to **L10**Ti(O^{i}Pr)$_2$.

The coordination environment around the titanium(IV) centre is approximately trigonal bipyramidal, with the phenolic oxygen atoms of the amine bis(phenolate) ligand sitting in the equatorial plane, along with one isopropoxide group. The second isopropoxide group occupies an axial position, as does the amine nitrogen of **L10** (Figure 2.41).

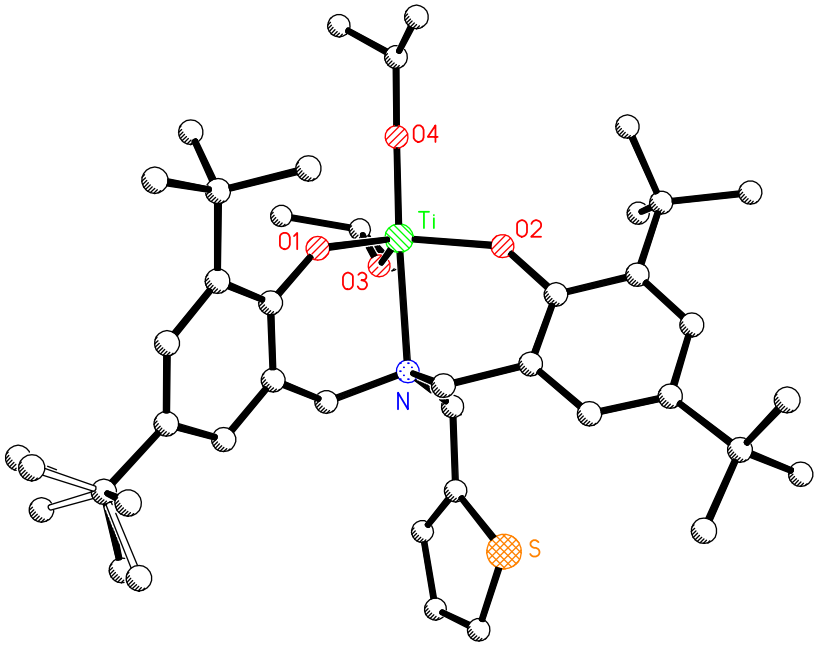

Figure 2.41 Molecular structure of **L10**Ti(O^{i}Pr)$_2$ as determined by X-ray crystallography. Hydrogen atoms omitted for clarity. A minor component of disorder in one *tert*-butyl group is shown with open bonds.

Comparisons may be made between the solid state structures of **L10**Ti(O^{i}Pr)$_2$, in which the pendant aromatic group is thiophene, and the previously described complexes **L6**Ti(O^{i}Pr)$_2$ and **L7**Ti(O^{i}Pr)$_2$, in which the pendant aromatic groups are benzene and naphthalene, respectively. The principle bond lengths in the metal-ligand coordination sphere are relatively consistent between the three complexes (Table 2.8). Indeed, the metal-phenolic oxygen bond lengths are most similar between **L10**Ti(O^{i}Pr)$_2$ and **L6**Ti(O^{i}Pr)$_2$; these complexes also have the most similar O_1-Ti-O_2 bond angles (121.23(18)º and 121.15(5)º, respectively). The metal-nitrogen bond length of 2.344(4) Å for **L10**Ti(O^{i}Pr)$_2$ is between that for **L6**Ti(O^{i}Pr)$_2$ (2.330(1) Å) and **L7**Ti(O^{i}Pr)$_2$ (2.380(2) Å).

Table 2.8 Selected bond lengths and angles for **L10**Ti(O^{i}Pr)$_2$ and comparative complexes.

	L10 Ti(O^{i}Pr)$_2$	**L6**Ti(O^{i}Pr)$_2$	**L7**Ti(O^{i}Pr)$_2$
Ti-O$_1$	1.860(4)	1.850(1)	1.837(1)
Ti-O$_2$	1.853(4)	1.860(2)	1.851(1)
Ti-N	2.344(4)	2.330(1)	2.380(2)
Ti-O$_3$	1.803(4)	1.800(2)	1.831(1)
Ti-O$_4$	1.783(4)	1.781(1)	1.782(1)
O$_1$-Ti-O$_2$	121.23(18)	121.15(5)	118.66(16)

The synthesis of a zirconium(IV) complex of **L10** was attempted by a similar route, resulting in the formation of a mixture of products, which was determined from ^{1}H NMR spectroscopic analysis to contain the homoleptic **L10**$_2$Zr complex as a major component. Isolation and further characterisation of this complex was not achieved.

Group 4 Complexes of $L11H_2$ and $L12H_2$

The coordination chemistry of tri-anionic amine tris(phenolate) ligands such as **L11**H_3 and **L12**H_3 was introduced previously in this chapter. The titanium(IV) isopropoxide complex of 2,4-dimethyl substituted amine tris(phenolate) ligand is known in the literature,[26] as well as the titanium and zirconium isopropoxide complexes of the 2,4-*tert*-butyl substituted **L11**H_3 (Figure 2.42).[26, 36] Davidson and co-workers[36] have shown that the 2,4-dimethyl substituted ligand forms a homoleptic, zwitterionic complex of the form $([\mathbf{L}H]^-)_2[M]^{2-}$ when M = Zr.

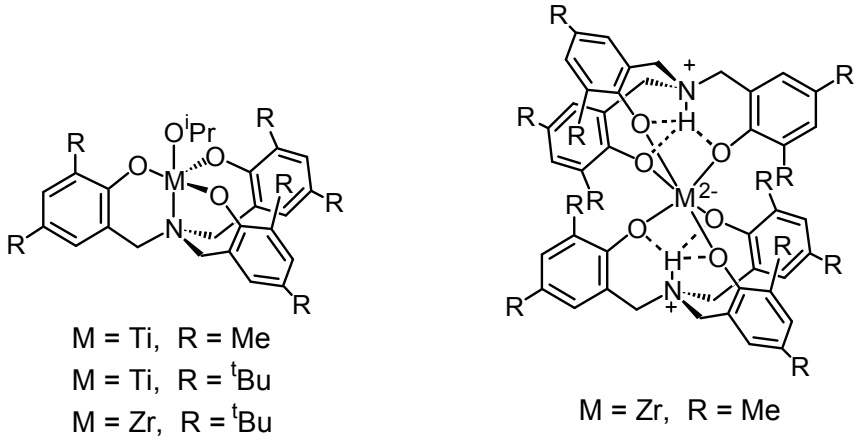

Figure 2.42 Known Group 4 complexes of **L11**H_3 and its 2,4-dimethyl substituted analogue.[26, 36]

Complexes **L11**M(O^iPr) where M = Ti, Zr, Hf have been prepared by reaction of the ligand with the appropriate Group 4 metal tetra-isopropoxide starting material in toluene as shown in Figure 2.43.

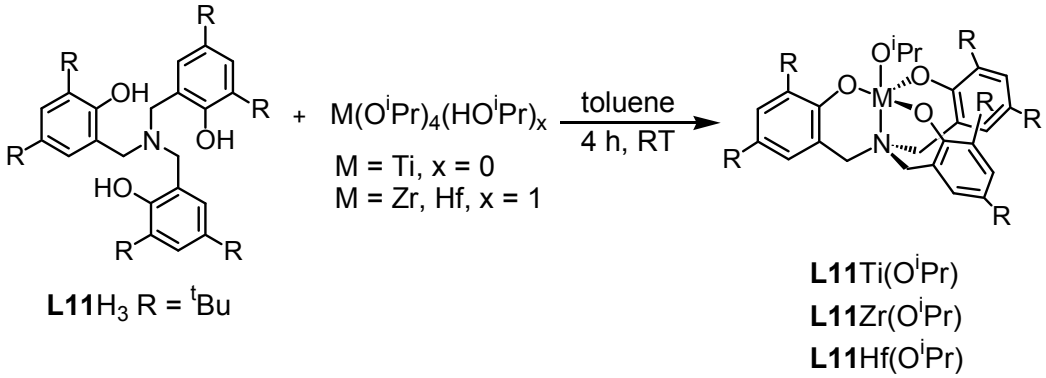

Figure 2.43 Synthetic route to complexes **L11**Ti(O^iPr), **L11**Zr(O^iPr) and **L11**Hf(O^iPr).

The hafnium(IV) isopropoxide complex of **L11** was prepared in a similar manner, by reaction of **L11**H_3 with hafnium(IV) isopropoxide mono-isopropanol in toluene solution. After stirring for several hours, the volatiles were removed and the ^1H NMR spectrum of the crude, solid reaction product indicated that the desired complex had formed, evidenced by a clear septet-doublet pair for the isopropoxide group. The product was purified by crystallisation from toluene and the room temperature ^1H NMR spectrum of the purified product showed broad singlets for the signals due to the methylene protons of

the ligand **L11** (Figure 2.45), which indicate that the ligand is fluxional on the ^{1}H NMR timescale.

Due to the C_3 symmetry of the ligand **L11**, it can wrap itself around the metal centre in a helical fashion, resulting in the formation of two enantiomers, *P* (or plus) and *M* (or minus) (Figure 2.44).[37] For both enantiomers the methylene protons on the ligand **L11** should appear as doublets within an AX spin system when the complex is rigid in solution. Indeed, Kol and co-workers report a room temperature ^{1}H NMR spectrum for **L11**Ti(O^{i}Pr) with a sharp pair of doublets in the methylene region, which broaden and coalesce at higher temperatures.[26] The coalescence is attributed to facile conversion between enantiomers at elevated temperature.

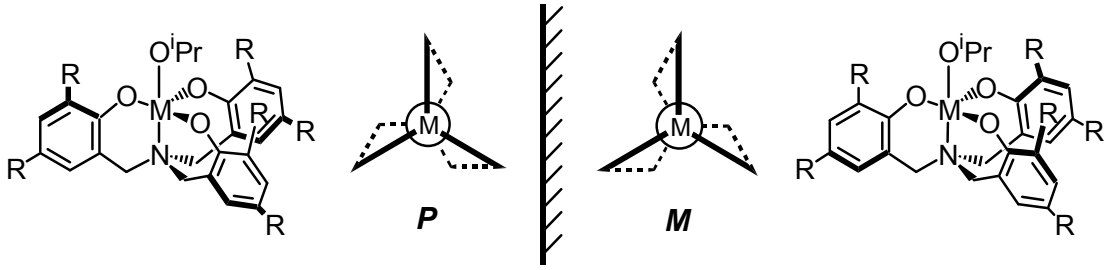

Figure 2.44 Enantiomers of Group 4 metal isopropoxide complexes of **L11** (R = ^{t}Bu).[37]

A similar scenario can be envisaged for the solution behaviour of **L11**Hf(O^{i}Pr), however, it is likely that the ligand **L11** is less tightly bound in the hafnium(IV) complex than in the analogous titanium(IV) complex, due the increased metallic radius of hafnium(IV) versus titanium(IV). All other things being equal, the complex with the more 'loosely' bound ligand would be more likely to begin to interconvert at a lower temperature; less energy would be required to 'flip' between enantiomers. Indeed, broad ^{1}H NMR spectral signals for the methylene protons of ligand **L11** are seen for both **L11**Zr(O^{i}Pr)[36] and **L11**Hf(O^{i}Pr), as previously noted. With regard to **L11**Hf(O^{i}Pr), doublets due to the diastereotopic methlylene protons of the ligand resolved at 213 K (Figure 2.45).

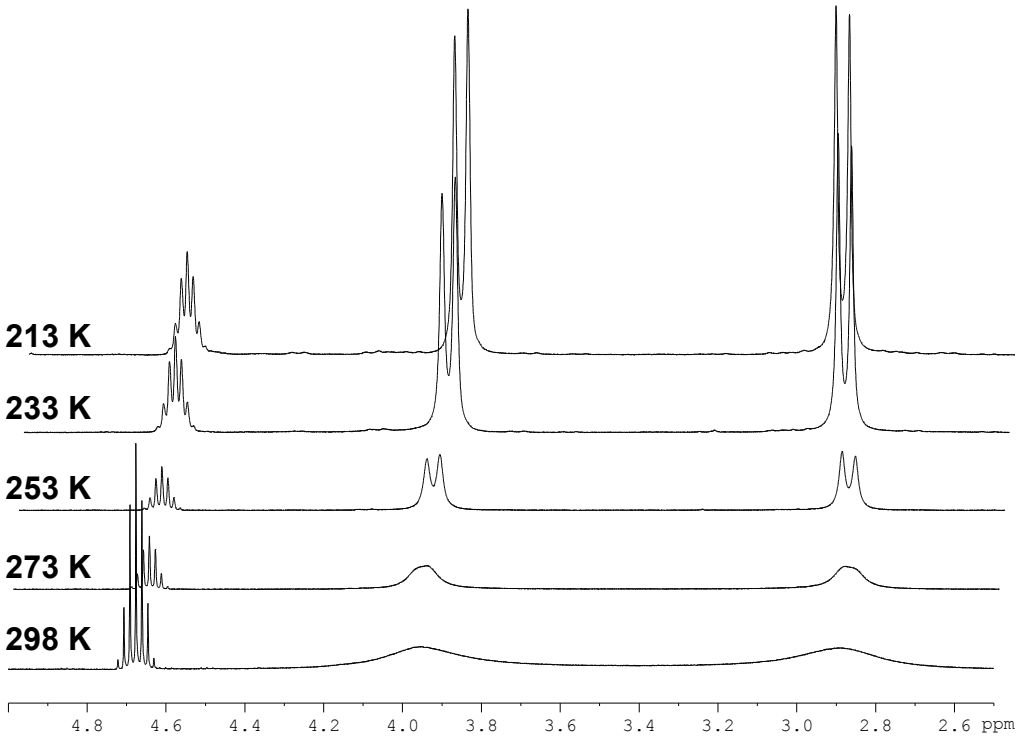

Figure 2.45 Variable temperature ^{1}H NMR spectra of **L11**Hf(O^{i}Pr) ($CDCl_3$, 400.13 MHz): (bottom) 298 K, 273 K, 253 K, 233 K and (top) 213 K.

Single crystals of **L11**Hf(O^{i}Pr) suitable for X-ray diffraction were grown from toluene solution and their analysis revealed that in the solid-state structure the **L11** ligand is disordered between both the *M* and *P* enantiomers (Figure 2.46). Each enantiomer comprises a central five-coordinate hafnium(IV) centre in an approximate trigonal bipyramidal geometry, with the phenolic oxygen atoms of **L11** occupying equatorial positions and the amine nitrogen atom and isopropoxide oxygen occupying the two axial positions, respectively. The ligand backbone (excluding *tert*-butyl groups and three of the aromatic ring carbon atoms) is disordered over two sites in an approximately 3:1 ratio, while the methyl groups of the isopropoxide ligand are disordered over two sites in an approximately 1:1 ratio.

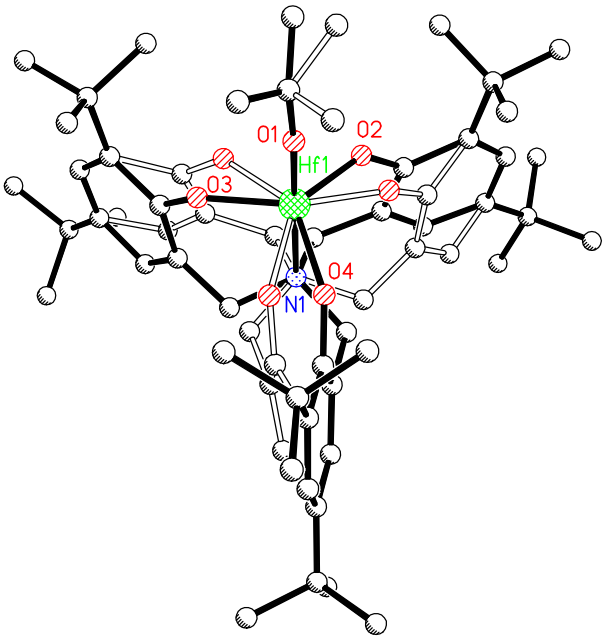

Figure 2.46 Molecular structure of **L11**Hf(O^{i}Pr) as determined by X-ray crystallography. Hydrogen atoms omitted for clarity. The disorder of the ligand backbone is modelled over two sites in an approximate 3:1 ratio while the disorder in the methyl groups of the O^{i}Pr ligand is modelled over two sites in an approximate 1:1 ratio.

In the solid state, **L11**Ti(O^{i}Pr) is racemic and the *P* and *M* enantiomers are related by inversion.[26] **L11**Hf(O^{i}Pr) is also racemic in the solid state, but the *P* and *M* enantiomers are located at the same crystallographic site. The principal bond lengths in the metal-ligand coordination sphere of **L11**Hf(O^{i}Pr) are similar to those in **L2**Hf(O^{i}Pr)$_2$ reported earlier. Comparing the solid-state structural parameters for the three complexes (Table 2.9), we see that the principal bond lengths in the metal-ligand coordination sphere increase on going from M = Ti to M = Zr, but are more similar between M =Zr and M = Hf. The only significant difference between the selected structural parameters of **L11**Zr(O^{i}Pr) and **L11**Hf(O^{i}Pr) is a shortening of the metal-nitrogen bond length in the hafnium(IV) complex.

Table 2.9 Solid state structural parameters for **L11**Hf(O^{i}Pr) and comparative parameters for **L11**Ti(O^{i}Pr)[26] and **L11**Zr(O^{i}Pr).[36]

	L11 Ti(O^{i}Pr)	**L11**Zr(O^{i}Pr)	**L11**Hf(O^{i}Pr)
M-O$_1$	1.778(4)	1.916(2)	1.922(2)
M-O$_2$	1.825(6)	1.967(2)	1.950(3)
M-O$_3$	1.833(6)	1.949(2)	1.946(3)
M-O$_4$	1.866(6)	1.993(2)	1.996(3)
M-N	2.233(5)	2.442(2)	2.409(2)

The potentially tetradentate ligand **L12**H$_3$ was prepared in order to obtain a ligand which was tri-anionic in its deprotonated form, but lacking the C_3 symmetry of **L11**H$_3$. The titanium complex of **L12**H$_3$ was prepared by reaction of the ligand with an equimolar amount of titanium(IV) isopropoxide. After several hours stirring, the volatiles were

removed and the yellow solid was crystallised from a toluene/hexane solution, yielding **L12**Ti(O^{i}Pr) as a pale yellow microcrystalline solid. The room temperature ^{1}H NMR spectrum of the reaction product showed a single septet (1H)-doublet (6H) pair implying the **L12** ligand in its tri-anionic form. The signals due to the phenolate and ethanolate methylene protons appear as broad resonances, suggesting some fluxional processes are occurring in the system.

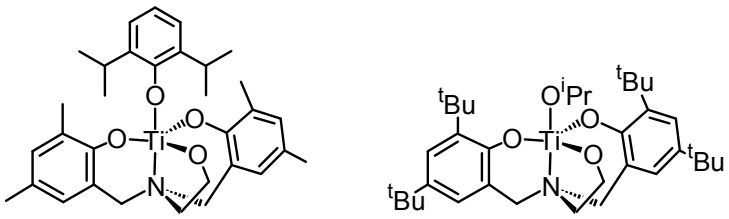

Figure 2.47 Representations of the solid-state structures of the titanium(IV) complex prepared by Verkade and co-workers[25](left) and **L12**Ti(O^{i}Pr), described herein and by Nomura and co-workers.[38]

Verkade and co-workers reported a similar ligand with 2,4-dimethyl-substituted phenolate groups.[25] The solid-state structure of the titanium(IV) 2,6-diisopropylphenoxide complex of the 2,4-dimethyl-substituted ligand showed the ligand was bound in a tetradentate fashion, with the phenolate groups in mutually *trans* positions. In 2007, Nomura and co-workers prepared **L12**Ti(O^{i}Pr) for use as a pre-catalyst for ethylene polymerisation (Figure 2.47).[38] The authors reported the solid-state structure as consistent with the conformation shown in Figure 2.48. The ^{1}H NMR spectrum for the reaction product of **L12**H$_2$ and zirconium(IV) isopropoxide mono-isopropoxide was very similar to that of **L12**Ti(O^{i}Pr); the reaction scheme for these two products is shown in Figure 2.48.

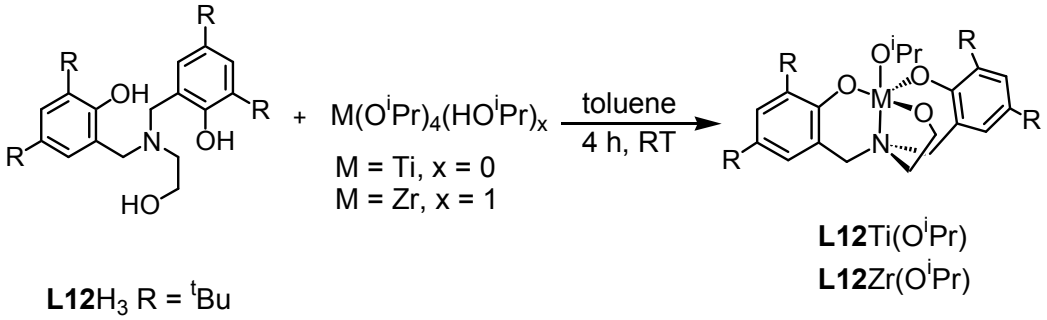

Figure 2.48 Synthetic route to **L12**Ti(O^{i}Pr) and **L12**Zr(O^{i}Pr).

As mentioned previously, the room temperature ^{1}H NMR spectra of these complexes exhibit broad signals for the phenolate and ethanolate methylene protons. This is likely due to fluxionality within the system. The phenolate methylene protons are in a similar pattern to those for **L6**Ti(O^{i}Pr)$_2$, **L7**Ti(O^{i}Pr)$_2$ and **L10**Ti(O^{i}Pr)$_2$.

2.4 Summary

In summary, a series of di- and tri-anionic amine bis(phenolate) and amine tris(phenolate) ligands have been synthesised with the potential for tridentate and tetradentate coordination to a Group 4 metal centre. The steric bulk of the potential ligands was varied both at the *ortho* and *para* positions of the phenolate rings (**L1**H_2, **L2**H_2 and **L9**H_2, **L10**H_2), and in one case (**L8**H_2) between the two rings by the preparation of a ligand with bulky groups on one phenolate and a lack of steric bulk on the other. Electron withdrawing groups in the *para* position on the phenolate rings were incorporated (**L3**H_2). For the ligands with tetradentate coordinative ability, the fourth donor atom was varied between nitrogen (pyridine, **L1**H_2, **L2**H_2, **L8**H_2), sulfur (thiophene, **L9**H_2, **L10**H_2) and oxygen (**L11**H_3 and **L12**H_3). For the ligands with tridentate coordinative ability, the steric bulk of the aryl group on the pendant arm was varied (**L6**H_2, **L7**H_2).

Group 4 metal complexes of these ligands were prepared by reaction of the ligands with the appropriate Group 4 metal isopropoxide starting material. Titanium(IV), zirconium(IV) and hafnium(IV) complexes of the ligands incorporating a pyridyl moiety, **L1** and **L2**, were prepared, characterised and their solid-state and solution structures compared both to similar complexes reported herein and in the literature. The solid-state structures of **L1**M(O^iPr)$_2$ (M = Ti, Zr), **L2**M(O^iPr)$_2$ (M = Ti, Zr, Hf) and **L3**Ti(O^iPr)$_2$ determined by X-ray crystallography indicated the amine bis(phenolate) ligand to be bound through all four heteroatoms, with the phenolic oxygen atoms in mutually *trans* positions and a complex with *pseudo* C_s symmetry. The ^{1}H NMR spectra of these complexes and of **L1**Hf(O^iPr)$_2$ and **L8**Zr(O^iPr)$_2$indicated the same structure was present in solution.

Ligands **L6**H_2 and **L7**H_2 were prepared with the aim of avoiding the formation of homoleptic **L**$_2$M-type complexes. Indeed, when their titanium(IV) complexes were prepared, the solid-state structures determined through X-ray crystallographic analysis showed that the desired complexes **L6**Ti(O^iPr)$_2$ and **L7**Ti(O^iPr)$_2$, had formed. The amine bis(phenolate) ligands in these complexes were coordinated, as expected, in a tridentate fashion and the ^{1}H NMR spectra of these complexes indicated fluxionality on the ^{1}H NMR spectroscopic timescale. Titanium(IV) complexes of ligands **L9**H_2 and **L10**H_2, incorporating a thiophene moiety, were also found to have the ligand coordinated in a tridentate fashion through both phenolic oxygen atoms and the nitrogen atom. Reaction of **L9**H_2 with titanium(IV) isopropoxide resulted in the formation of a homoleptic complex **L9**$_2$Ti in which both ligand were bound in a *mer* conformation, determined by X-ray crystallographic analysis. The solid-state structure of the titanium(IV) complex of

L10 incorporating bulkier *tert*-butyl groups was determined to be structurally very similar to that of **L6**Ti(O^iPr)$_2$ and **L7**Ti(O^iPr)$_2$.

Reaction of the C_3 symmetric ligand **L11**H_3 with hafnium(IV) isopropoxide mono-isopropanol resulted in the formation of a racemic mixture of the *P* and *M* enantiomers of **L11**Hf(O^iPr), due to the helical chirality of the complex, which agreed with the precedent established in the literature for the analogous titanium(IV) and zirconium(IV) complexes. The structure of this complex was determined by X-ray crystallography and solution ^{1}H NMR spectroscopic analysis indicated the structure was maintained in solution.

Finally, titanium(IV) and zirconium(IV) complexes of the potentially tri-anionic ligand **L12**H_2 were prepared. Although solid-state structural characterisation was not possible for these complexes, solution ^{1}H NMR spectroscopy and a recent structural report in the literature led to the conclusion that in each case the ligand was bound in a tetradentate fashion, with the phenolic arms of the ligand in a mutually *trans* conformation.

With the variation in ligands described earlier a variety of coordination geometries in the Group 4 metal complexes synthesised was achieved. Five- and six-coordinate titanium(IV) complexes were prepared and the use of ligands which are di- and tri-anionic in their deprotonated forms resulted in complexes with either one or two remaining isopropoxide ligands. This variety of structural types will be further considered when the complexes are tested for activity towards the ROP of cyclic esters, discussed in the following chapter.

References

[1] T. Weyhermuller, T. K. Paine, E. Bothe, E. Bill and P. Chaudhuri, *Inorg. Chim. Acta* **2002,** 337, 344-356.
[2] A. Lehtonen and R. Sillanpaa, *Polyhedron* **2005,** 24, (2), 257-265.
[3] Y. L. Tong, Y. Yan, E. S. H. Chan, Q. C. Yang, T. C. W. Mak and D. K. P. Ng, *J. Chem. Soc., Dalton Trans.* **1998**, (18), 3057-3064.
[4] E. Y. Tshuva, I. Goldberg, M. Kol and Z. Goldschmidt, *Organometallics* **2001,** 20, (14), 3017-3028.
[5] M. H. Chisholm and Z. P. Zhou, *J. Mater. Chem.* **2004,** 14, (21), 3081-3092.
[6] M. H. Chisholm, N. W. Eilerts, J. C. Huffman, S. S. Iyer, M. Pacold and K. Phomphrai, *J. Am. Chem. Soc.* **2000,** 122, (48), 11845-11854.
[7] A. C. Albertsson and I. K. Varma, *Biomacromolecules* **2003,** 4, (6), 1466-1486.
[8] J. Yang, Y. H. Yu, Q. B. Li, Y. Li and A. I. Cao, *J. Polym. Sci., Part A: Polym. Chem.* **2005,** 43, (2), 373-384.
[9] O. Dechy-Cabaret, B. Martin-Vaca and D. Bourissou, *Chem. Rev.* **2004,** 104, (12), 6147-6176.
[10] P. Hormnirun, E. L. Marshall, V. C. Gibson, A. J. P. White and D. J. Williams, *J. Am. Chem. Soc.* **2004,** 126, (9), 2688-2689.
[11] L. M. Alcazar-Roman, B. J. O'Keefe, M. A. Hillmyer and W. B. Tolman, *Dalton Trans.* **2003**, (15), 3082-3087.

[12] A. Kowalski, A. Duda and S. Penczek, *Macromolecules* **1998,** 31, (7), 2114-2122.
[13] Z. Y. Zhong, P. J. Dijkstra and J. Feijen, *Angew. Chem., Int. Ed. Engl.* **2002,** 41, (23), 4510-4513.
[14] Z. H. Tang, X. S. Chen, Y. K. Yang, X. Pang, J. R. Sun, X. F. Zhang and X. B. Jing, *J. Polym. Sci., Part A: Polym. Chem.* **2004,** 42, (23), 5974-5982.
[15] C. X. Cai, A. Amgoune, C. W. Lehmann and J. F. Carpentier, *Chem. Commun.* **2004**, (3), 330-331.
[16] T. K. Paine, T. Weyhermuller, E. Bill, E. Bothe and P. Chaudhuri, *Eur. J. Inorg. Chem.* **2003**, (24), 4299-4307.
[17] E. Y. Tshuva, M. Versano, I. Goldberg, M. Kol, H. Weitman and Z. Goldschmidt, *Inorg. Chem. Commun.* **1999,** 2, (8), 371-373.
[18] J. Dunkers and H. Ishida, *Spectrochim. Acta, Part A* **1995,** 51, (5), 855-867.
[19] S. Groysman, I. Goldberg, M. Kol, E. Genizi and Z. Goldschmidt, *Organometallics* **2003,** 22, (15), 3013-3015.
[20] S. Groysman, I. Goldberg, Z. Goldschmidt and M. Kol, *Inorg. Chem.* **2005,** 44, (14), 5073-5080.
[21] S. Groysman, I. Goldberg, M. Kol, E. Genizi and Z. Goldschmidt, *Adv. Synth. Catal.* **2005,** 347, (2-3), 409-415.
[22] L. E. Turner, M. G. Davidson, M. D. Jones, H. Ott, V. S. Schulz and P. J. Wilson, *Inorg. Chem.* **2006,** 45, (16), 6123-6125.
[23] S. Groysman, S. Segal, I. Goldberg, M. Kol and Z. Goldschmidt, *Inorg. Chem. Commun.* **2004,** 7, (8), 938-941.
[24] K. C. Fortner, J. P. Bigi and S. N. Brown, *Inorg. Chem.* **2005,** 44, (8), 2803-2814.
[25] Y. Kim and J. G. Verkade, *Organometallics* **2002,** 21, (12), 2395-2399.
[26] M. Kol, M. Shamis, I. Goldberg, Z. Goldschmidt, S. Alfi and E. Hayut-Salant, *Inorg. Chem. Commun.* **2001,** 4, (4), 177-179.
[27] C. L. Boyd, T. Toupance, B. R. Tyrrell, B. D. Ward, C. R. Wilson, A. R. Cowley and P. Mountford, *Organometallics* **2005,** 24, (2), 309-330.
[28] T. Toupance, S. R. Dubberley, N. H. Rees, B. R. Tyrrell and P. Mountford, *Organometallics* **2002,** 21, (7), 1367-1382.
[29] C. Marschner, *Angew. Chem., Int. Ed. Engl.* **2007,** 46, (36), 6770-6771.
[30] A. Lehtonen and R. Sillanpaa, *Inorg. Chem.* **2004,** 43, (20), 6501-6506.
[31] E. Y. Tshuva, I. Goldberg, M. Kol and Z. Goldschmidt, *Inorg. Chem.* **2001,** 40, (17), 4263-4270.
[32] S. Groysman, E. Y. Tshuva, I. Goldberg, M. Kol, Z. Goldschmidt and M. Shuster, *Organometallics* **2004,** 23, (22), 5291-5299.
[33] E. Y. Tshuva, I. Goldberg and M. Kol, *J. Am. Chem. Soc.* **2000,** 122, (43), 10706-10707.
[34] R. F. See, R. A. Kruse and W. M. Strub, *Inorg. Chem.* **1998,** 37, (20), 5369-5375.
[35] L. R. Hanton, C. Richardson, W. T. Robinson and J. M. Turnbull, *Chem. Commun.* **2000**, (24), 2465-2466.
[36] M. G. Davidson, C. L. Doherty, A. L. Johnson and M. F. Mahon, *Chem. Commun.* **2003**, (15), 1832-1833.
[37] IUPAC Compendium of Chemical Terminology, 2nd Edition, **1997**.
[38] S. Padmanabhan, S. Katao and K. Nomura, *Organometallics* **2007,** 26, (7), 1616-1626.

Chapter 3

Ring-Opening Polymerisation of ε-Caprolactone and L-Lactide

3 Ring-Opening Polymerisation of ε-Caprolactone and L-Lactide

3.1 Introduction

ROP of ε-CL Using Well-Defined Group 4 Metal Initiators

As discussed in chapter 1, ROP of ε-caprolactone via a coordination-insertion mechanism has generated much interest over the past decades.[1] PCL is a useful homopolymer, and co-polymerisation may also occur with other cyclic esters; recent examples show derivatives of ε-CL as convenient entries into chemically modifiable polyesters, with potential uses in biomedical applications.[2, 3] The ROP process for this monomer is easily examined using conventional analytical methods. The monomer itself exists as a viscous liquid at room temperature, whereas the polymer is a white solid.

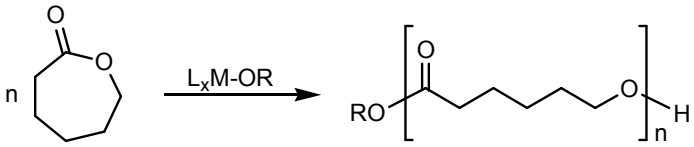

Figure 3.1 Ring-opening polymerisation of ε-caprolactone to give poly(caprolactone).

Prior to commencement of this work, there were few examples of the controlled ROP of ε-CL using single-site titanium(IV) initiators in the literature. Titanium(IV) isopropoxide, titanium(IV) n-propoxide and titanium(IV) phenoxide are known to initiate the polymerisation reaction, giving PCL with broad molecular weight distributions.[4] Aida and co-workers prepared titanium(IV) complexes of the 1,1'-methylene bis(phenolate) ligands shown in Figure 3.2.[5]

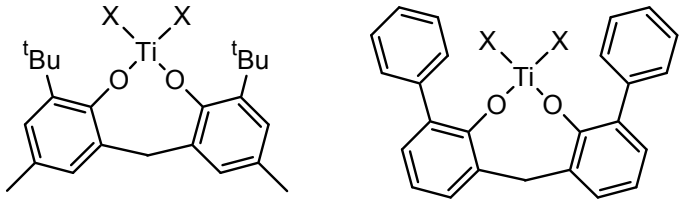

X = Cl or O^{i}Pr

Figure 3.2 Titanium(IV) complexes of 1,1'-methylene bis(phenolate) ligands prepared by Aida and co-workers.[5]

Complexes where X = O^{i}Pr were found to be active initiators for the ROP of ε-CL in dichloromethane solution at room temperature, although the rate of polymerisation was faster when the complex bearing the 2-*tert*-butyl-4-methyl substituted ligand was used as the initiator. Although complexes where X = Cl were inactive for the polymerisation, they were active for the ROP of propylene oxide. A ring-opened propylene oxide adduct

of the titanium(IV) complex bearing the 2-phenyl substituted ligand (i.e. an alkoxide) was an active initiator for the ROP of ε-CL.

With regard to the heavier Group 4 metals, zirconium(IV) alkoxides,[6] zirconocene[7] and zirconium(IV) acetylacetonate[8] complexes were known to be active for the ROP of ε-CL prior to the beginning of this work. No hafnium(IV) complexes have previously been reported as initiators.

Fajardo and co-workers prepared titanium(IV) complexes of various alcohols, including protected sugars (Figure 3.3), and although these complexes were not structurally characterised, the authors postulated two structural types: dimeric complexes with bridging isopropoxide groups ((i)-(v)) and monomeric complexes ((vi)-(viii)).[9]

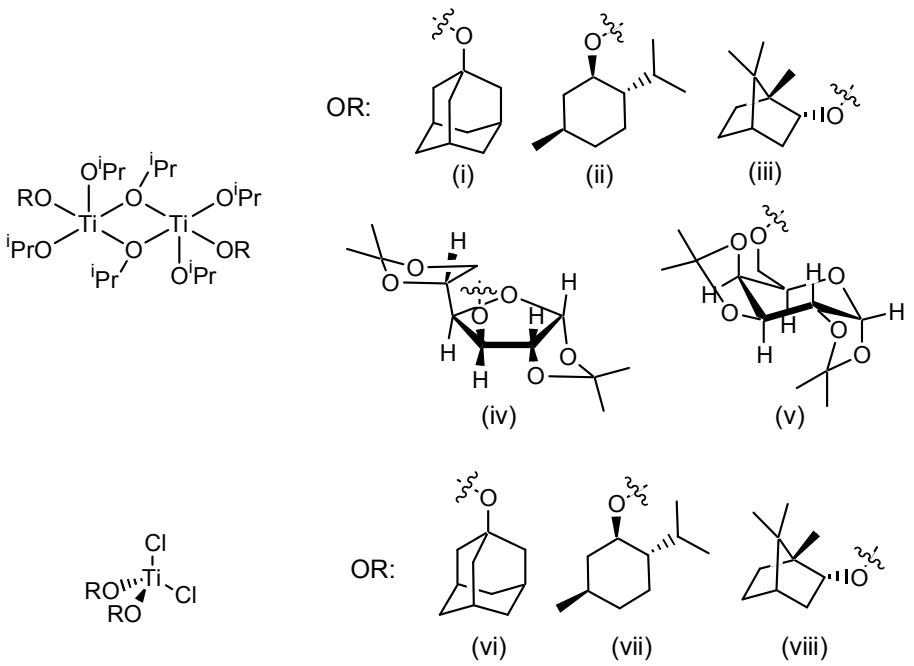

Figure 3.3 Titanium(IV) initiators prepared by Fajardo and co-workers.[9]

Polymerisations initiated by these complexes were not, in general, very well controlled, as evidenced by the broad molecular weight distributions for the polymers produced with PDI values in the range of 1.45-2.30. However, the PCL polymer produced using (vii) as the initiator was an exception, with a PDI value of 1.05. ^{1}H NMR spectroscopic analysis of this polymer revealed the partial incorporation of the menthol ester end group, leading the authors to conclude that the ROP may be initiated by both the chloride and the alkoxide ligands. No information was given with regard to the correlation between molecular weight and conversion of monomer to polymer for any of the polymers produced.

ROP of L-LA Using Well-Defined Group 4 Metal Initiators

Along with ε-CL, lactide in its various forms is one of the most commonly studied cyclic esters with regard to ROP. Its polymerisation may also proceed via a coordination-insertion mechanism mediated by a metal centre.

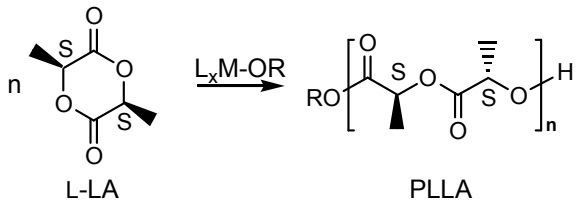

Figure 3.4 Ring-opening polymerisation of L-lactide to give poly(L-lactide).

Prior to the commencement of this work there were few examples of the ROP of L-LA by titanium(IV) complexes in the literature. Titanium(IV) isopropoxide is known to effect the ROP of L-LA in bulk[10] and solution,[11] leading to PLLA polymers with broad molecular weight distributions (PDI ≥ 2). Verkade and co-workers have prepared several titanium(IV) complexes based on N,O-donor ligands (Figure 3.5).[12]

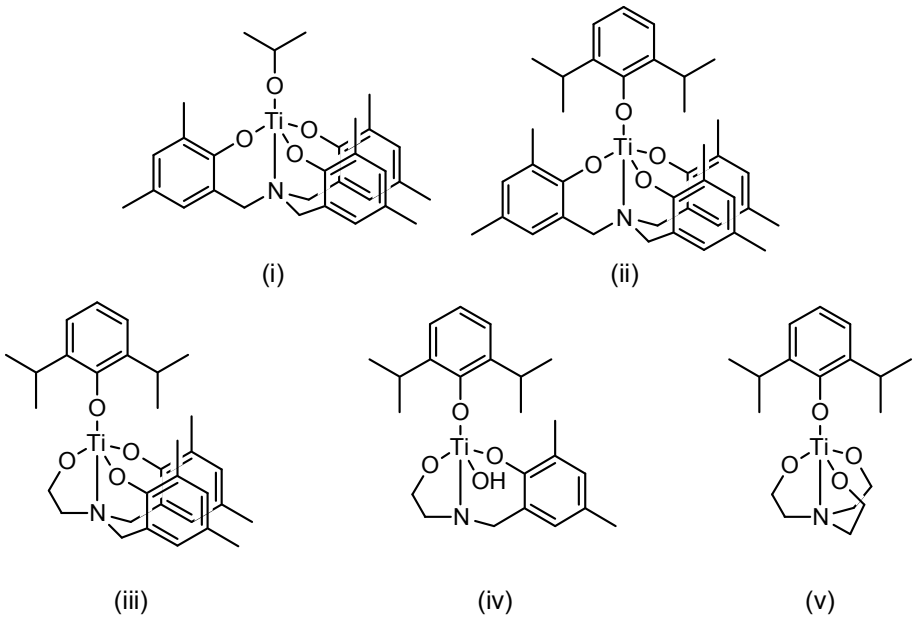

Figure 3.5 Titanium(IV) complexes prepared by Verkade *et al*.[12]

Complexes (i)-(v) all initiate the ROP of L-LA at 130 ºC under solvent-free conditions. After 4 hours, (i) produced PLLA in 55% yield, with a PDI value of 1.46. Polymerisations using (ii)-(v) were carried out for 24 hours and the yield of polymer obtained after this time ranged from 69% for (ii) to 99% for (v). The yield of polymer, as well as the polymers' molecular weight values, increased as the number aryl groups on the ligand decreased. PDI values were relatively consistent, in the range of 1.51-1.75.

The only examples of the application of zirconium(IV) complexes to the ROP of L-LA prior to this work were reported by Kricheldorf and co-workers[13] who found that

zirconium(IV) n-propoxide initiated the ROP of L-LA at 100 ºC under solvent-free conditions and Kasperczyk *et al*,[8, 14] who found that zirconium(IV) acetylacetonate was also able to initiate the polymerisation. The authors proposed the mechanism proceeded by deprotonation of the L-LA monomer, generating free acetylacetone.[15] No hafnium(IV) initiators have previously been reported.

3.2 Polymerisation Results and Discussion

ROP of ε-CL

Polymerisation Reactions

All attempted polymerisations of ε-CL were carried out in an argon-filled glove box. In all cases 0.1 mmol of initiator was dissolved in dry toluene in a round-bottomed flask, and 10 mmol of ε-caprolactone was injected via syringe. The reaction mixture was stirred for 24 hours at room temperature and then removed from the glove box. The polymerisation was quenched by adding a solution of 30% acetic acid in water. Hexanes were added and polymer which formed at the hexanes-water interface as the solution stirred was collected by filtration, washed with hexanes and dried under reduced pressure.

Analysis of Polymerisation Reaction Products

Gel Permeation Chromatography (GPC) and ^{1}H NMR spectroscopy were used to analyse the polymers produced using the Group 4 initiators described in chapter 2. An ^{1}H NMR spectrum of a PCL polymer is shown in Figure 3.6. Further details on the GPC instrumentation are given in chapter 5.

The multiplet due to the protons adjacent to the ester oxygen, H_a, shifts from around 3.6 ppm (in the ^{1}H NMR spectrum of the monomer) to near 4.0 ppm in the polymer. The peak due to H_e, protons adjacent to the carbonyl group, also shift slightly downfield on going from monomer to polymer. A downfield shift for the two multiplets due to H_b, H_c and H_d is observed in the spectrum for the polymer.

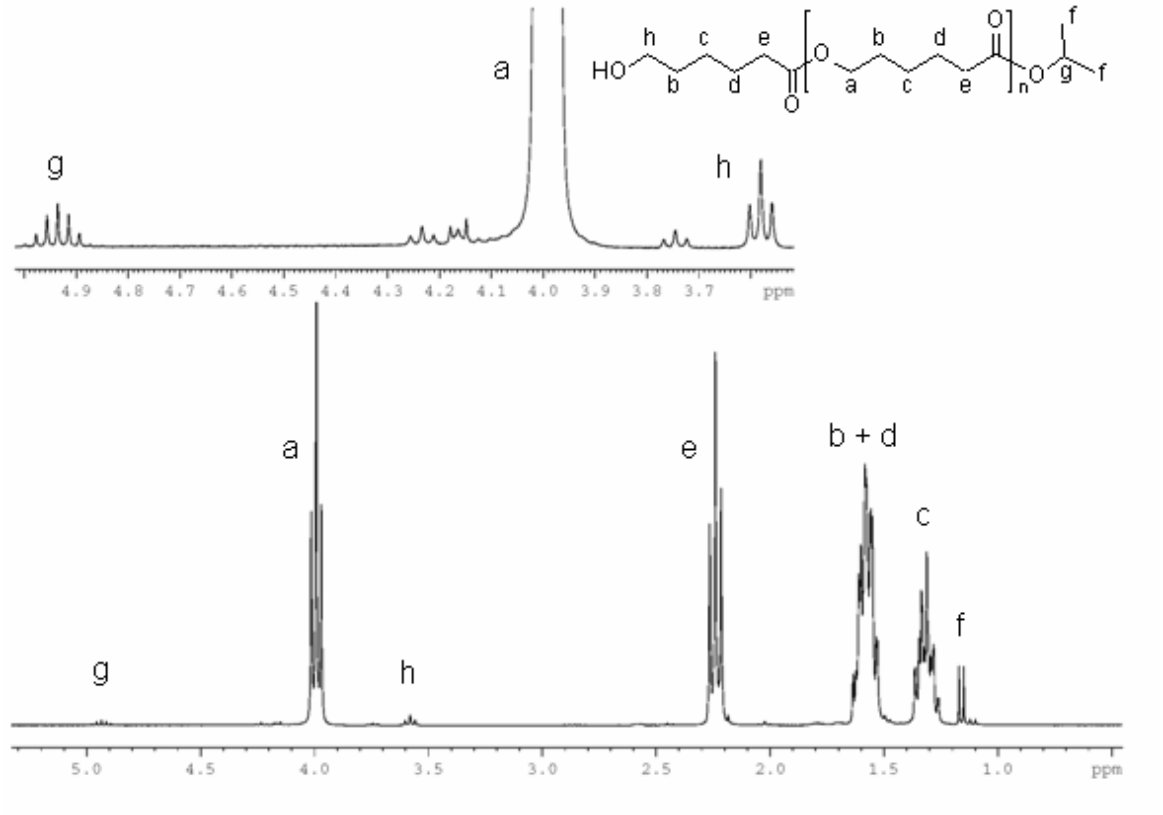

Figure 3.6 ^{1}H NMR spectrum (300 MHz, $CDCl_3$) of low molecular weight poly(caprolactone).

As well as signals due to the protons along the polymer backbone, signals due to the polymers' end groups may also be observed. For polymerisation reactions where the ring-opened monomer is inserted into a metal-isopropoxide bond, a septet due to the isopropoxide methine ($CH(CH_3)_2$) and a doublet due to the isopropoxide methyl ($CH(CH_3)_2$) protons may be observed. These are indicated in Figure 3.6 as H_g at ~4.9 ppm and H_f at ~1.15 ppm, respectively. The protons at the opposite end of the chain, on the carbon adjacent to the terminal hydroxyl group, H_h, may also be observed, as a triplet at ~3.6 ppm. ^{1}H NMR spectroscopy was also used to monitor the polymerisation reactions in situ, as detailed in a subsequent section.

ROP of ε-CL Using Six-Coordinate Group 4 Complexes

Of the six coordinate Group 4 metal complexes introduced in chapter 2, **L1**M(O^iPr)$_2$ M=Ti, Zr, Hf, **L2**M(O^iPr)$_2$ M=Ti, Zr, Hf, and **L3**Ti(O^iPr)$_2$ were tested for activity towards the ROP of ε-CL, under the conditions described previously. The positive results are summarised in Table 3.1.

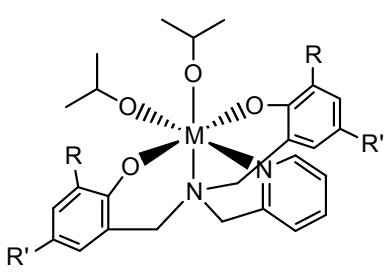

L1Ti(O^iPr)$_2$ M = Ti, R = R' = Me
L2Ti(O^iPr)$_2$ M = Ti, R = R' = ^{t}Bu
L3Ti(O^iPr)$_2$ M = Ti, R = H, R' = NO_2
L1Zr(O^iPr)$_2$ M = Zr, R = R' = Me
L2Zr(O^iPr)$_2$ M = Zr, R = R' = ^{t}Bu
L1Hf(O^iPr)$_2$ M = Hf, R = R' = Me
L2Hf(O^iPr)$_2$ M = Hf, R = R' = ^{t}Bu

Figure 3.7 Six-coordinate Group 4 complexes tested for activity towards the ROP of ε-CL.

Of the range of six-coordinate metal complexes with ligands **L1-L3** chelated in a tetradentate fashion, only the zirconium(IV) and hafnium(IV) complexes **L1**Zr(O^iPr)$_2$ and **L1**Hf(O^iPr)$_2$ (Figure 3.8), with *ortho* and *para* methyl substituents on the phenolate arms of the amine bis(phenolate) ligand, initiated the ROP of ε-CL.

Table 3.1 Results for the ROP of ε-caprolactone. Conditions [ε-CL]:[I] = 100:1, 10 mL toluene, time 24 hours, 20 °C. [a] isolated yield, [b] determined from GPC using poly(styrene) standards as the reference.

Initiator	Yield[a]/%	M_w[b]/g mol^{-1}	M_n[b]/g mol^{-1}	PDI[b]
L1Zr(O^iPr)$_2$	99	18600	13800	1.35
L1Hf(O^iPr)$_2$	99	16500	12400	1.17

Where polymerisation did occur, near quantitative yield of polymer was obtained. As the molecular weight of ε-CL is 114.14 g mol^{-1}, using a monomer to initiator ratio of 100:1 a polymer M_n of around 11,400 g mol^{-1} should be expected from a polymerisation reaction which reached near complete conversion, initiated by only one of the isopropoxide groups. The molecular weights of the polymers which were obtained from these reactions, determined by GPC, are close to the theoretical value for this system. However, as a refractive index detector was used and the molecular weight calibration curve was obtained using poly(styrene) standards a true comparison may not be made (see chapter 5 for further details). ^{1}H NMR spectroscopic analysis of the polymer revealed a septet at ~4.9 ppm, indicating the polymerisation had proceeded via a coordination-insertion mechanism as expected.

Considering the accepted coordination-insertion mechanism, it is unsurprising that the coordinatively saturated six coordinate titanium(IV) complexes failed to initiate the polymerisation of ε-CL. Although there does exist the possibility of hemilability of the pyridine nitrogen atom, solid-state structures of these complexes, as discussed in chapter 2, indicate that the pyridyl arm is tightly bound to the metal centre through the nitrogen atom. In addition, the room temperature ^{1}H NMR spectra of these complexes indicate the structures are maintained in solution. For polymerisation to take place via a coordination-insertion mechanism, initial coordination of an ε-CL molecule would have to occur,

forming a seven-coordinate titanium(IV) complex, which is unlikely. Seven-coordinate titanium(IV) complexes are known, but examples are rare. In 2000, a study of X-ray crystal structures of titanium(IV) complexes deposited in the Cambridge Structure Database by Sadler and co-workers showed that, of the 1000 structures analysed, only 2.5% were of titanium(IV) complexes in a seven-coordinate geometry.[16] In studies of titanium(IV) d^0 and iron(III) high-spin d^5 complexes, Fackler and Shepherd have postulated that a spherically symmetric charge distribution (as in the case of the titanium(IV) ion) prefers a pentagonal bipyramidal geometry over a monocapped trigonal prismatic geometry when the metal ion will accommodate more than six ligands or when the splitting of the ligand field does not force an octahedral coordination environment.[17] A pentagonal bipyramidal geometry for **L1**Ti(O^iPr)$_2$ with a coordinated ε-CL and subsequently, a growing PCL chain either in an axial or equatorial position seems highly unlikely as this would force the angle between the equatorial ligands close to an average of 72º, which is highly unfavourable.

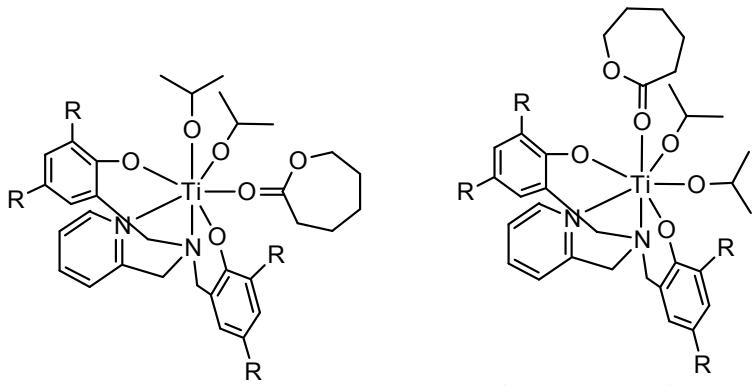

Figure 3.8 Coordination of ε-caprolactone monomer to **L1**Ti(O^iPr)$_2$ or **L2**Ti(O^iPr)$_2$ would force a seven-coordinate titanium(IV) centre.

However, the zirconium(IV) metal centre is larger than the titanium(IV) centre. The larger coordination sphere of zirconium(IV) can tolerate the additional ligand as the ε-CL monomer coordinates to the metal centre and indeed, **L1**Zr(O^iPr)$_2$ and **L1**Hf(O^iPr)$_2$ are active initiators for the ROP.

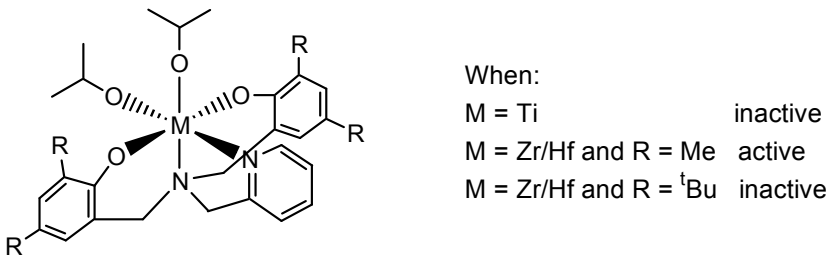

Figure 3.9 Activity of six-coordinate Group 4 initiators towards the ROP of ε-CL.

However, this balance seems to be delicate as the complexes **L2**M(O^iPr)$_2$ where M = Zr, Hf with the larger *tert*-butyl groups in the *ortho* and *para* positions on the phenolate arms

of the ligand are inactive towards initiation of the ROP of ε-CL (Figure 3.9). Perhaps the coordination sphere is just large enough to accommodate the ε-CL monomer when only methyl groups are present and the more sterically crowded derivative will simply not allow approach of the monomer to the metal centre. These results are supported by a subsequent study by Bochmann and co-workers who, in 2006, prepared titanium(IV) complexes of similar amine bis(phenolate) ligands, utilising *N,N*-dimethylethyleneamine as the pendant arm (Figure 3.10).[18] They also observed a complete lack of activity towards the ROP of ε-CL at 60 ºC in toluene solution using a monomer to initiator ratio of 200:1.

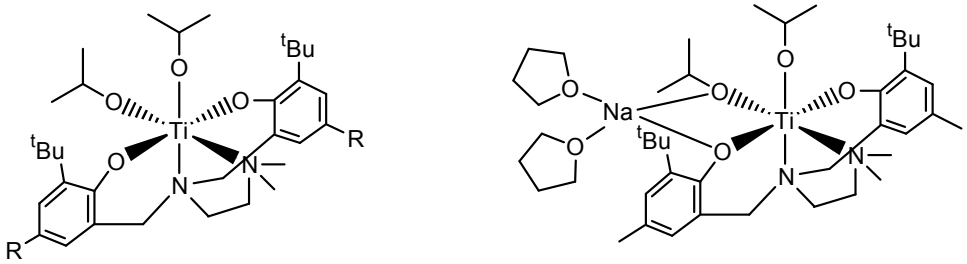

(i) R = ^{t}Bu
(ii) R = Me

(iii)

Figure 3.10 Titanium(IV) complexes prepared by Bochmann and co-workers.[18]

However, the bimetallic sodium/titanium complex was active for the polymerisation, producing PCL up to 94% conversion in 4 hours. The polymerisation was not well controlled, resulting in polymer with a PDI value of 2.5 and no correlation between molecular weight and conversion.

The only example of zirconium(IV) and hafnium(IV) alkoxide complexes applied to the ROP of ε-CL are those synthesised and structurally characterised by Huang and co-workers in 2006 (Figure 3.11).[19] These complexes produced PCL but with rather broad molecular weight distributions.

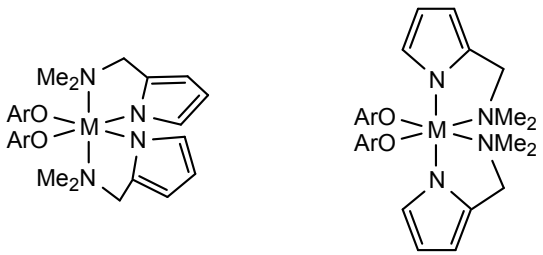

(i) M = Zr, Ar = 2,6-Me_2Ph
(ii) M = Hf, Ar = 2,6-Me_2Ph
(iii) M = Zr, Ar = 2,6-$^{i}Pr_2$Ph
(iv) M = Hf, Ar = 2,6-$^{i}Pr_2$Ph

Figure 3.11 Zirconium(IV) and hafnium(IV) arlyoxide initiators prepared by Huang *et al*.[19]

The aryloxide complexes (i)-(iv) initiated the ROP at 50 ºC in toluene solution and produced polymers with PDI values in the range of 1.23-1.55 (no reaction times were given). Under the conditions used, polymerisations initiated by (i) and (ii) proceeded to

lower conversions (76% and 75%, respectively) than those initiated by (iii) and (iv) (93% and 94%, respectively).

ROP of ε-CL Using Five-Coordinate Group 4 Complexes

In contrast to their six-coordinate counterparts, all three five-coordinate titanium(IV) complexes (**L6**Ti(O^iPr)$_2$, **L7**Ti(O^iPr)$_2$ and **L10**Ti(O^iPr)$_2$) ligated by tridentate amine bis(phenolate) ligands were active towards initiation of the ROP of ε-CL in toluene solution at room temperature, with the polymerisation proceeding to ≥94% conversion after 24 hours in each case (Table 3.2, Figure 3.12).

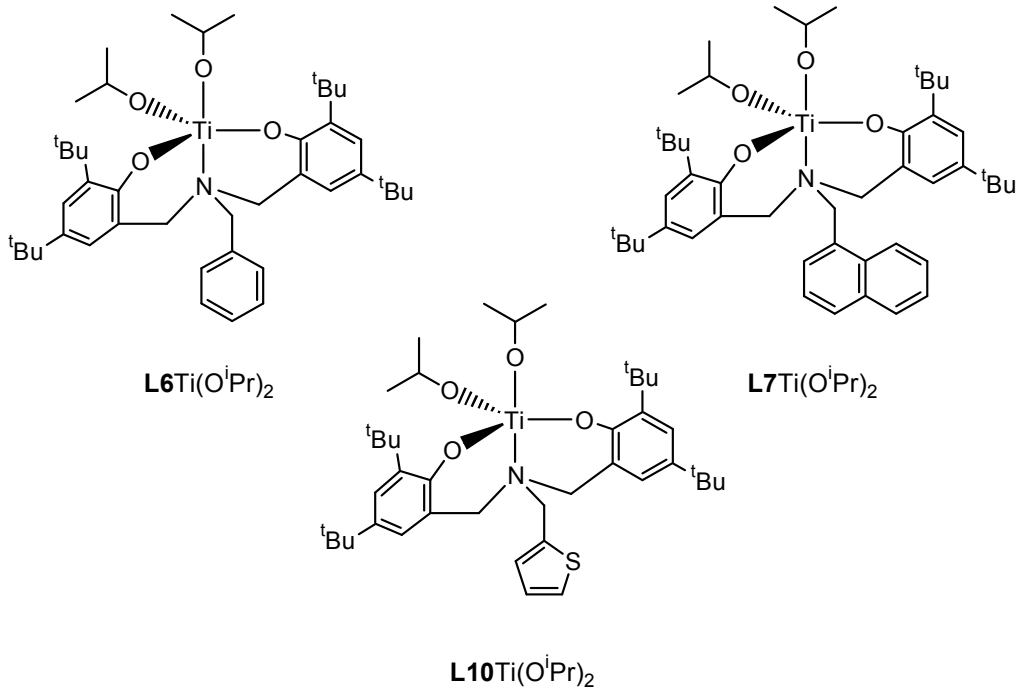

Figure 3.12 Five-coordinate Group 4 metal initiators complexes which were found to be active initiators for the ROP of ε-CL.

In addition, the ROP reaction yielded polymers with molecular weights in the expected range and narrow polydispersity indices. The PDI values for PCL produced using **L6**Ti(O^iPr)$_2$, **L7**Ti(O^iPr)$_2$ and **L10**Ti(O^iPr)$_2$ are noticeably smaller than that for PCL produced using **L1**Zr(O^iPr)$_2$, (which had a PDI value of 1.35). As noted in chapter 1, transesterification can have an impact on PDI in the ROP of cyclic esters, particularly at high (>95%) conversion. This is particularly prevalent with some aluminium(III) initiators, but has been observed when other metal alkoxide initiators are used as well.[20] Perhaps some transesterification is occurring in the case of the ROP initiated by **L1**Zr(O^iPr)$_2$, to a greater degree than in the polymerisation initiated by either of the five coordinate titanium complexes. ^{1}H NMR spectra of these polymers again indicated the presence of the expected –CH_2OH and isopropyl ester end groups.

Table 3.2 Results for the ROP of ε-caprolactone. Conditions [ε-CL]:[I] = 100:1, 10 mL toluene, time 24 hours, 20 °C. [a]isolated yield, [b]determined from GPC using polystyrene as the reference.

Initiator	Yield[a]/%	M_w[b]/gmol^{-1}	M_n[b]/gmol^{-1}	PDI[b]
L6Ti(O^{i}Pr)$_2$	99	15900	14300	1.11
L7Ti(O^{i}Pr)$_2$	99	12300	11400	1.08
L10 Ti(O^{i}Pr)$_2$	94	13200	12100	1.09

The high activity of the five-coordinate titanium(IV) complexes as compared to their inactive, six-coordinate counterparts **L1-L3**Ti(O^{i}Pr)$_2$ is most likely due to the reduction in coordination number. In the case of **L6**Ti(O^{i}Pr)$_2$ and **L7**Ti(O^{i}Pr)$_2$, the pendant arm of the amine bis(phenolate) ligand does not contain a functionality which may coordinate the metal centre and, in the case of **L10**Ti(O^{i}Pr)$_2$ there was no evidence from either the solid-state structure of the molecule or its solution ^{1}H NMR spectrum to indicate a sulfur-bound thiophene moiety, as noted in chapter 2. Thus, coordination of the ε-CL monomer to these coordinatively unsaturated complexes is more facile in comparison to the six-coordinate titanium(IV) complexes **L1-L3**Ti(O^{i}Pr)$_2$. On coordination of the lactide monomer, the coordination number of the titanium(IV) centre increases from five to six, which is not unfavourable. In addition, the PCL polymers produced using **L6**Ti(O^{i}Pr)$_2$, **L7**Ti(O^{i}Pr)$_2$ and **L10**Ti(O^{i}Pr)$_2$ as the initiators are very similar in terms of molecular weight and molecular weight distribution values, leading to the conclusion that the nature of the pendant group in these types of complexes is not of paramount importance.

Although there was a clear activity difference between the five- and six-coordinate titanium(IV) complexes reported herein, five-coordinate titanium(IV) alkoxide complexes are not always active initiators for the ROP of ε-CL. Titanium(IV) bis(isopropoxide) complexes were reported by Harada *et al* utilising bis(phenolate) ligands bridged by chalcogen atoms (Figure 3.14).[21, 22] Sulfur-bridged complex **23** was inactive for the ROP of ε-CL, even at temperatures of 100 ºC under solvent-free conditions. The tellurium-bridged analogue (iv) did initiate the ROP, but only under solvent-free conditions (no reaction occurred at 100 ºC in toluene solution), producing PCL in 85% yield after 12 hours with a PDI value of 1.43. The corresponding bis(chloride) complexes (i) and (iii) were both active at 100 ºC in toluene solution and under solvent-free conditions, although the polymerisation initiated by (i) produced PCL with particularly broad molecular weight distributions (PDI 2.07–2.28). The authors posited that coordination of the ε-CL monomer disrupted the dimeric structure, leading to a initiator-monomer complex which would in theory be similar to that envisioned for the five-coordinate titanium(IV) species discussed in this section. This example serves to

illustrate that coordination number of the metal centre is certainly not the only factor which governs the activity towards ROP of a potential initiator.

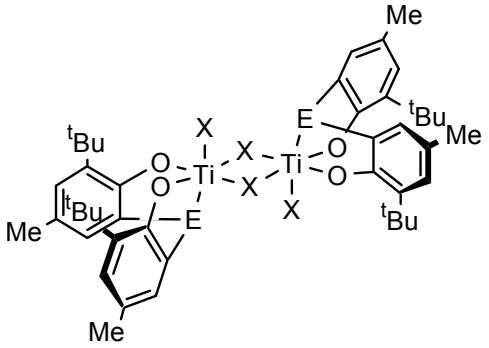

(i) E = S, X = Cl
(ii) E = S, X = O^{i}Pr
(iii) E = Te, X = Cl
(iv) E = Te, X =O^{i}Pr

Figure 3.13 Titanium(IV) complexes prepared by Harada and co-workers.[21, 22]

Further Investigations into the ROP of ε-CL

As described in the previous sections, in all cases where polymerisation occurred, ≥94% of the theoretical yield of polymer was isolated after the 24 hour reaction time. In order to study the conversion of monomer to polymer with time and elucidate the length of time needed to reach high (>90 %) conversion, ^{1}H NMR spectroscopic analysis of the polymerisation process was employed. Analysis of this polymerisation process via ^{1}H NMR spectroscopy was possible because the reaction proceeded readily in solution at room temperature. The ROP reaction was again carried out using a monomer to initiator ratio of 100:1. In an argon filled glove box, both monomer and initiator were dissolved in dry benzene-d_6, and the reaction mixture was combined in an NMR tube fitted with a Young's valve and sealed inside the glove box. The sample was immediately placed in an NMR spectrometer and ^{1}H NMR spectra were recorded at 30 minute intervals for 13 hours at room temperature. Conversion was measured by comparing the integrations of peaks due to methylene backbone protons of monomer and polymer at each time interval (Figure 3.14).

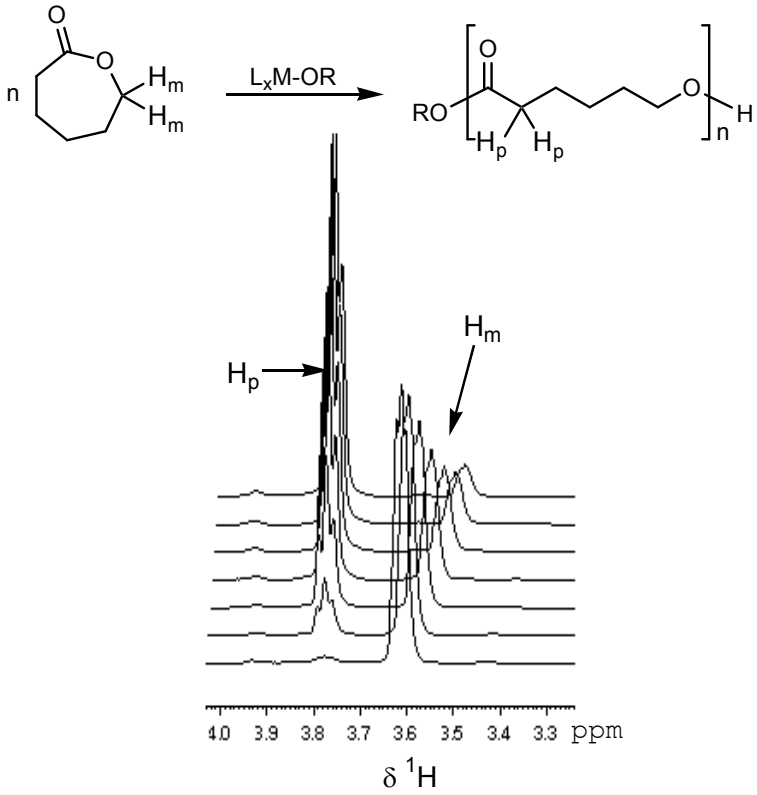

Figure 3.14 Peaks in the ^{1}H NMR spectrum of the polymerisation reaction mixture monitored for the study of conversion of monomer to polymer with time.

Conversion versus time plots for polymerisations initiated by the six-coordinate complexes **L1**Zr(O^{i}Pr)$_2$ and **L1**Hf(O^{i}Pr)$_2$ are shown in Figure 3.15. While the polymerisation initiated by **L1**Zr(O^{i}Pr)$_2$ reached full conversion after seven hours, the polymerisation initiated by the hafnium(IV) analogue **L1**Hf(O^{i}Pr)$_2$ proceeded somewhat slower, and reached 99% conversion after thirteen hours, a similar result as obtained from the 24 hour polymerisation experiment (Table 3.1). The reason for this difference in activity is not readily apparent, although differences in the reactivity of complexes of these two metals are increasingly recognised, as noted in chapter 1.[23] Bond angles and distances are very similar betweens the two complexes. Previous work suggested that comparable zirconium(IV) and hafnium(IV) initiators exhibited very similar activities towards the ROP of ε-CL (Figure 3.13).

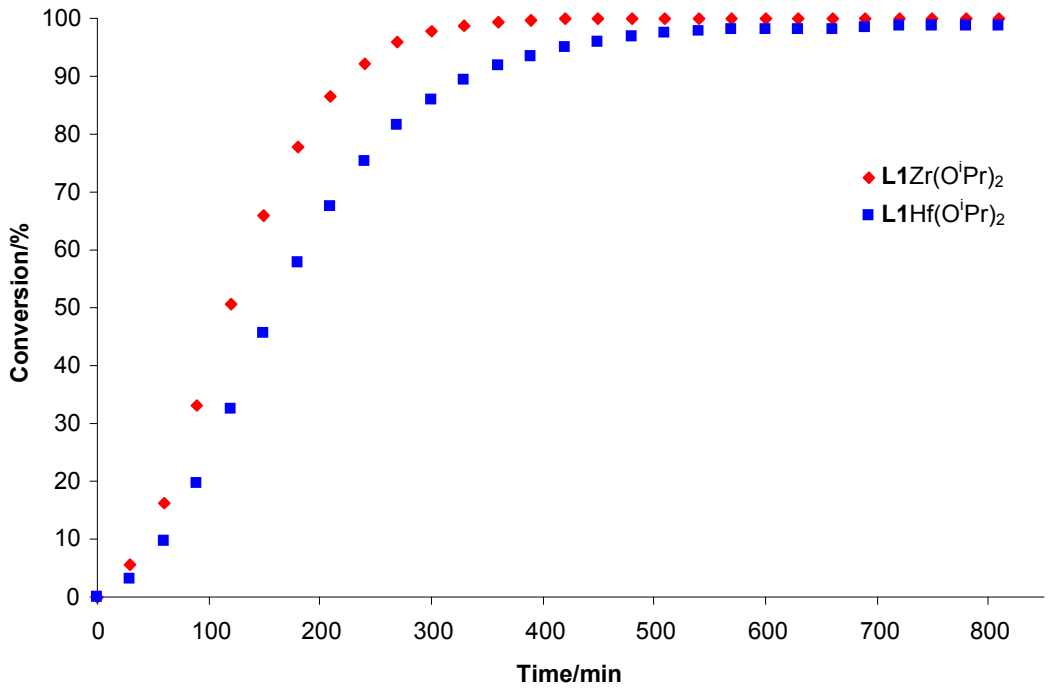

Figure 3.15 Plot of conversion versus time for the ROP of ε-CL initiated by **L1**Zr(O^iPr)$_2$ and **L1**Hf(O^iPr)$_2$.

^{1}H NMR spectroscopic analyses of the ROP of ε-CL initiated by the five-coordinate titanium(IV) complexes **L6**Ti(O^iPr)$_2$, **L7**Ti(O^iPr)$_2$ and **L10**Ti(O^iPr)$_2$ were also carried out and the results are shown in Figure 3.16. The complexes with aryl substituents, **L6**Ti(O^iPr)$_2$ and **L7**Ti(O^iPr)$_2$, were very similar in their activity and reached higher percent conversion of monomer to polymer more quickly than the thiophene-substituted analogue, **L10**Ti(O^iPr)$_2$. The comparison of the solid-state structures of the three complexes presented in chapter 2 described the structural similarities between **L6**Ti(O^iPr)$_2$ and **L10**Ti(O^iPr)$_2$, principally with regard to titanium-nitrogen bond lengths and phenolate oxygen-titanium-phenolate oxygen bond angles. These structural similarities and differences do not, however, seem to correspond to differences in activity for the ROP of ε-CL. This is not particularly unexpected, as the observed differences are small, but this result does lead to the suggestion that differences in activity with regard to ROP may be due to electronic differences between the complexes. The substitution of the heterocyclic thiophene moiety on the pendant arm of the ligand results in a decrease in ROP activity as compared to the benzene and naphthalene analogues. However, polymerisations initiated by each of the complexes reached ≥97% conversion within the thirteen hour reaction monitoring time frame.

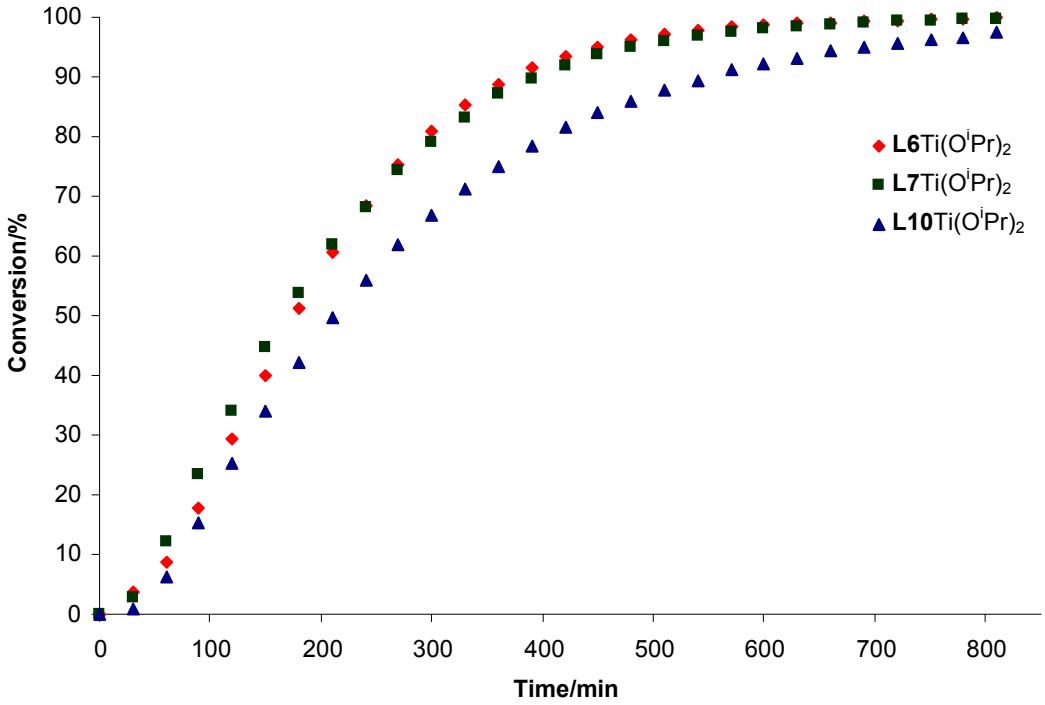

Figure 3.16 Plot of conversion versus time for the ROP of ε-CL initiated by **L6**Ti(O^{i}Pr)$_2$, **L7**Ti(O^{i}Pr)$_2$ and **L10**Ti(O^{i}Pr)$_2$.

Although the results of the ^{1}H NMR spectroscopic monitoring experiments indicate that the ring-opening polymerisation of ε-CL proceeded most quickly when initiated by complex **L1**Zr(O^{i}Pr)$_2$, as noted previously the polydispersity index of the polymer produced corresponded to the highest such value obtained in this series. However, all polymerisation reactions were carried out for 24 hours (results given in Tables 3.1 and 3.2), and the reaction initiated by **L1**Zr(O^{i}Pr)$_2$ reached >99% conversion earliest and therefore the polymer chains in this sample could have been subject to side reactions such as transesterification for the longest period of time. Waymouth and co-workers have found that with some aluminium(III) alkoxide initiators, the extent of transesterification increases greatly as high or near complete (≥95%) conversion is approached.[24] It was considered that a similar phenomenon could occurr when **L1**Zr(O^{i}Pr)$_2$ was used to initiate the ROP of ε-CL. As the polymerisation initiated by the six-coordinate zirconium(IV) complex **L1**Zr(O^{i}Pr)$_2$ proceeded to complete conversion most quickly, the initiator would have more time to catalyse the transesterification reactions which would result in the broader molecular weight distribution observed. However, if this was the case, it would be expected that the PCL produced with the analogous hafnium(IV) complex **L1**Hf(O^{i}Pr)$_2$, which proceeds to high conversion more slowly, would have a PDI value closer to that of the PCLs produced with **L6**Ti(O^{i}Pr)$_2$, **L7**Ti(O^{i}Pr)$_2$ and **L10**Ti(O^{i}Pr)$_2$. The PDI value for the PCL produced using **L1**Hf(O^{i}Pr)$_2$ as the initiator is lower than that for the polymer produced using **L1**Zr(O^{i}Pr)$_2$ (1.17 versus 1.35, respectively).

In order to test whether the PDI increases with conversion for the ROP initiated by **L1**Zr(O^iPr)$_2$, the polymerisation was carried out under identical conditions for a period of three hours, after which time the polymerisation is known (from the ^{1}H NMR spectroscopic studies discussed previously) to have reached around 78% conversion of monomer to polymer. In this way, the PDI values for the two polymers could be compared and a significant increase in the PDI value for the polymer obtained from the twenty four hour experiment relative to that from the three hour experiment would lend support to the hypothesis that transesterification at high conversion was responsible for the higher PDI value.

Table 3.3 Results for the ROP of ε-caprolactone. Conditions [ε-CL]:[I] = 100:1, 10 mL toluene, time as noted, 20 °C. [a]isolated yield, [b]determined from GPC using polystyrene as the reference.

Initiator	Time/h	Yield[a]/%	M_w[b]/g mol^{-1}	M_n[b]/g mol^{-1}	PDI[b]
L1Zr(O^iPr)$_2$	3	74	14000	10500	1.36
L1Zr(O^iPr)$_2$	24	99	18600	13800	1.35

After three hours a 74% yield of polymer was isolated, with an M_n value of 15800 and a PDI value similar to that obtained for the polymer isolated after a reaction time of 24 hours (Table 3.3). This suggests that the higher PDI value for the PCL obtained from the polymerisation initiated by **L1**Zr(O^iPr)$_2$ as compared to those PDI values for the polymers obtained from polymerisation reactions initiated by **L1**Hf(O^iPr)$_2$, **L6**Ti(O^iPr)$_2$, **L7**Ti(O^iPr)$_2$ and **L10**Ti(O^iPr)$_2$ is not a result of transesterification increasing at high conversion as a function of reaction time, but is more likely due to differences in the metal initiators. Indeed, the extent of transesterification has shown a dependence on the metal in metal-initiated ROP of cyclic esters.[20]

As shown previously in Figures 3.15 and 3.16, monitoring the ROP processes and conversion showed a steady increase in conversion with time. The corresponding plot of ln([ε-CL]$_0$/[ε-CL]$_t$) versus time for **L1**Zr(O^iPr)$_2$ (Figure 3.17) shows a linear increase with time after an initial induction period, thus indicating a first order dependence on monomer concentration.

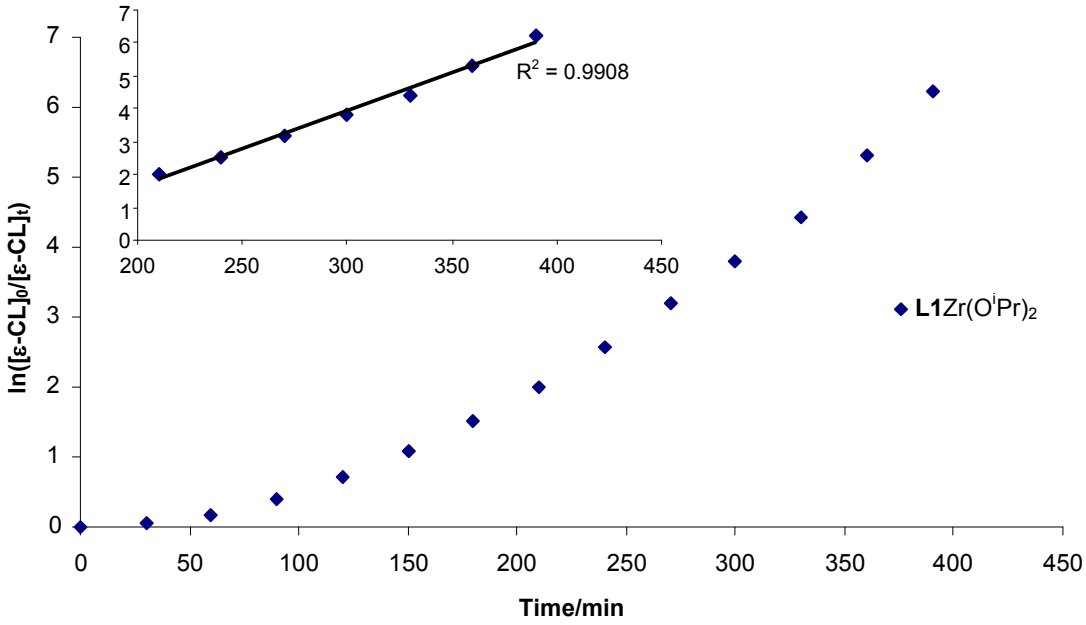

Figure 3.17 Plot of $\ln([\varepsilon\text{-CL}]_0/[\varepsilon\text{-CL}]_t)$ versus time for the ROP of ε-CL initiated by **L1**Zr(O^{i}Pr)$_2$. Inset shows the linear portion of the graph.

Similar induction periods have been observed with other initiator systems, and in the ROP of many different cyclic esters. When aluminium(III) isopropoxide was used as an initiator for the ROP of L-LA, an induction period attributed to aggregation effects was observed.[25] Such an induction period may also be attributed to the coordination step of the coordination-insertion mechanism. However, in some polymerisations initiated by calcium(II)[26] and lanthanide(III)[27] complexes, no induction period is observed.

The plot of $\ln([\varepsilon\text{-CL}]_0/[\varepsilon\text{-CL}]_t)$ versus time for the polymerisation initiated by **L1**Hf(O^{i}Pr)$_2$ was somewhat different (Figure 3.18). Again, an induction period was apparent, after which time a linear increase in $\ln([\varepsilon\text{-CL}]_0/[\varepsilon\text{-CL}]_t)$ with time was observed (r^2 = 0.9985). However, after 510 minutes (97% conversion), the rate of conversion appears to decrease.

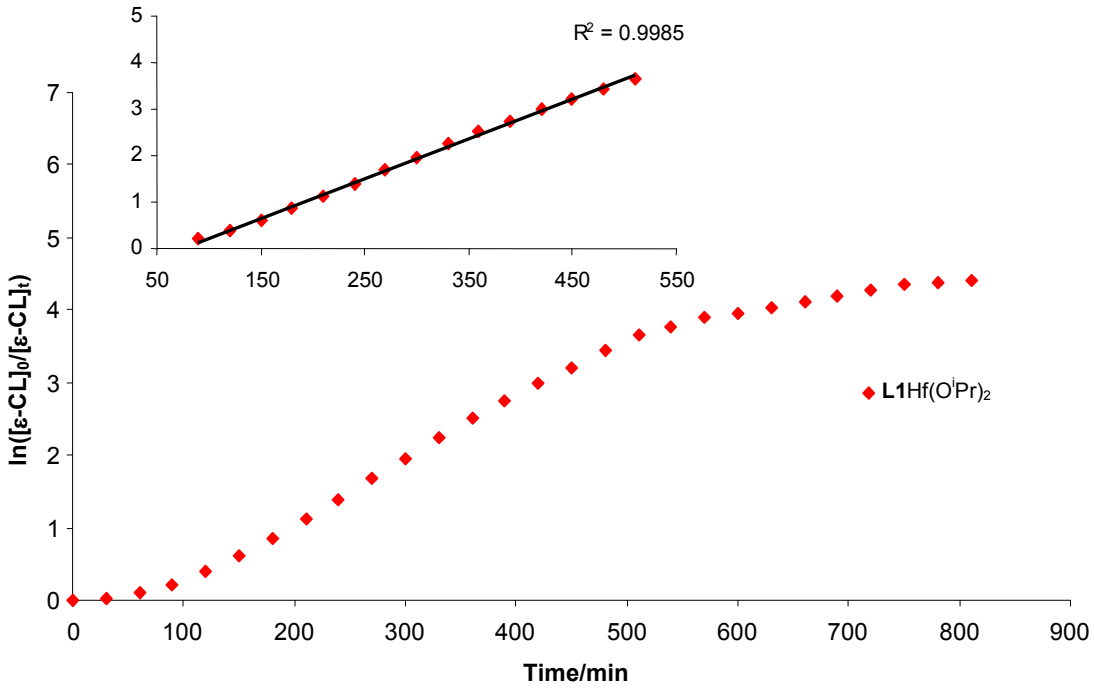

Figure 3.18 Plot of $\ln([\varepsilon\text{-CL}]_0/[\varepsilon\text{-CL}]_t)$ versus time for the ROP of ε-CL initiated by **L1**Hf(OiPr)$_2$. Inset shows the linear portion of the graph.

Analysis of the plots of $\ln([\varepsilon\text{-CL}]_0/[\varepsilon\text{-CL}]_t)$ versus time for the five-coordinate titanium(IV) complexes **L6**Ti(O^{i}Pr)$_2$, **L7**Ti(O^{i}Pr)$_2$ and **L10**Ti(O^{i}Pr)$_2$ were more straightforward. Again, an induction period was observed (Figure 3.19), after which time a first order dependence on monomer concentration is observed up to the highest conversion values reached (>99%, >99% and 97% respectively). The linear natures of the plots for all five initiators indicate that the ROP proceeds in a controlled manner.

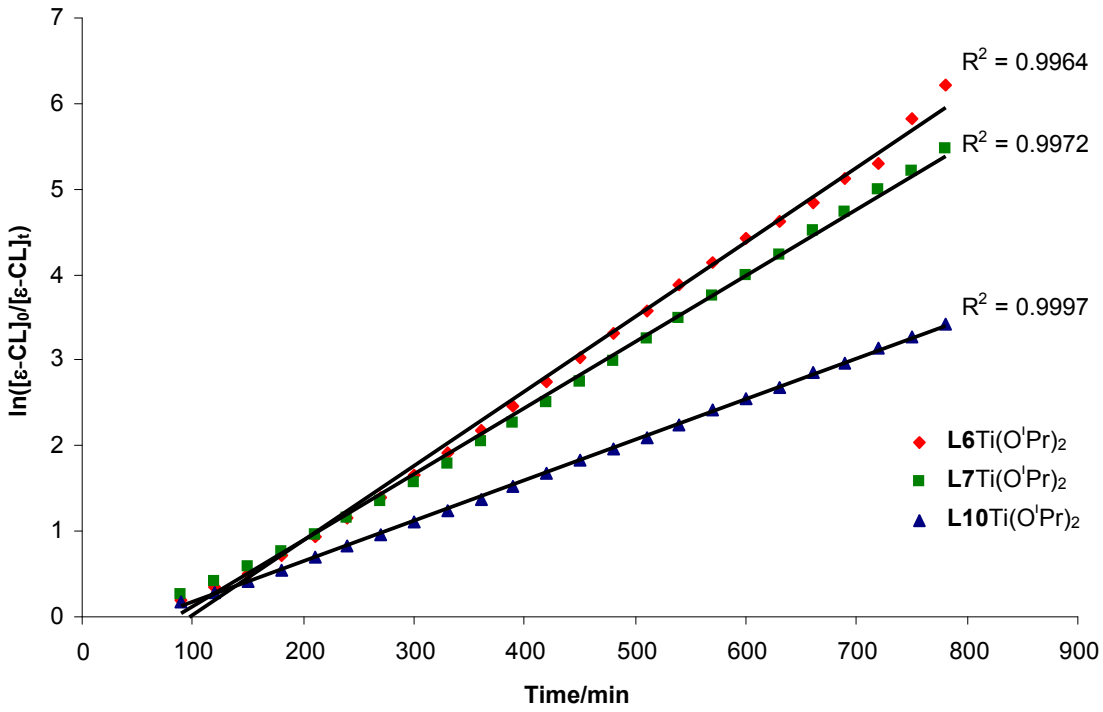

Figure 3.19 Plot of $\ln([\varepsilon\text{-CL}]_0/[\varepsilon\text{-CL}]_t)$ versus time for the ROP of ε-CL initiated by **L6**Ti(O^{i}Pr)$_2$, **L7**Ti(O^{i}Pr)$_2$ and **L10**Ti(O^{i}Pr)$_2$.

The ROP of ε-CL initiated by **L1**Zr(O^{i}Pr)$_2$, **L1**Hf(O^{i}Pr)$_2$, **L6**Ti(O^{i}Pr)$_2$, **L7**Ti(O^{i}Pr)$_2$ and **L10**Ti(O^{i}Pr)$_2$ was also monitored using GPC analysis. This allowed determination of the molecular weight increase with time, along with the ability to monitor the polydispersity index in a similar manner. In each case, the polymerisation reaction was carried out in dry toluene in an argon filled glove box. A monomer to initiator ratio of 100:1 was used and the reaction was carried out for a time exceeding the known time needed to reach full conversion as determined by ^{1}H NMR spectroscopic measurements. For the polymerisation reaction employing **L1**Zr(O^{i}Pr)$_2$, aliquots were removed from the reaction vessel at 1, 2, 4 and 6 hours. This procedure was repeated for the polymerisation reactions employing the other initiators, with additional aliquots being taken at 8 and 14 hours. These were removed from the glove box, quenched, the polymers precipitated with hexanes, washed (hexanes) and dried under reduced pressure. GPC measurements of these polymer samples indicated that in each case the M_n of the polymer increased fairly linearly with time while the PDI values remained relatively constant. The results for polymerisations initiated by **L1**Zr(O^{i}Pr)$_2$, **L6**Ti(O^{i}Pr)$_2$ and **L7**Ti(O^{i}Pr)$_2$ are shown in Figures 3.20, 3.21 and 3.22, respectively.

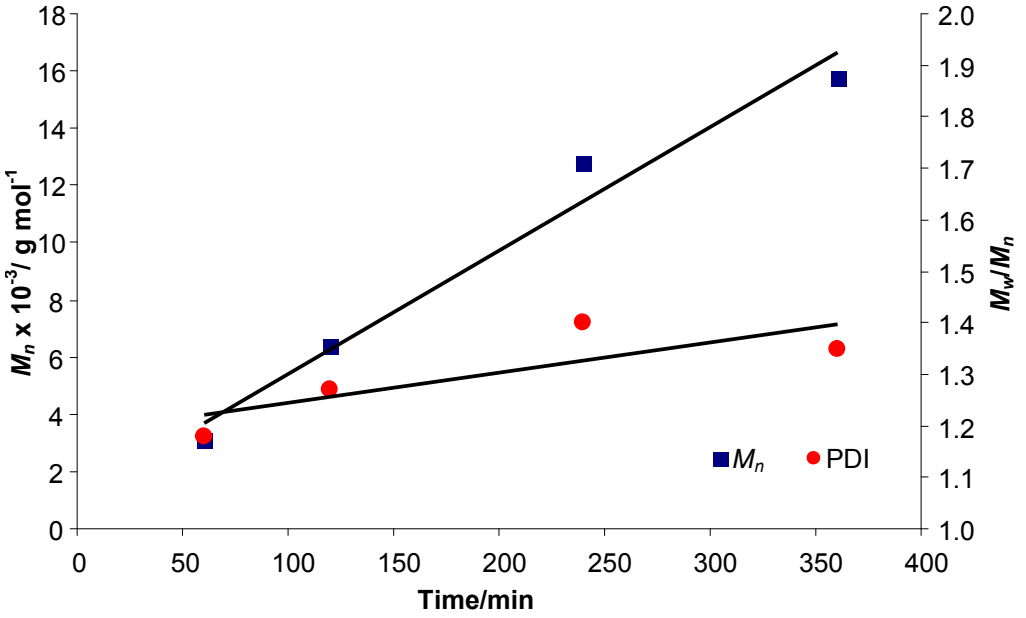

Figure 3.20 ROP of ε-CL initiated by **L1**Zr(O^{i}Pr)$_2$. M_n and PDI versus Time (GPC).

The observed relatively linear increase in M_n with time along with the relatively constant values for the polydispersity index indicates that the polymerisation initiated by **L1**Zr(O^{i}Pr)$_2$ is well controlled.

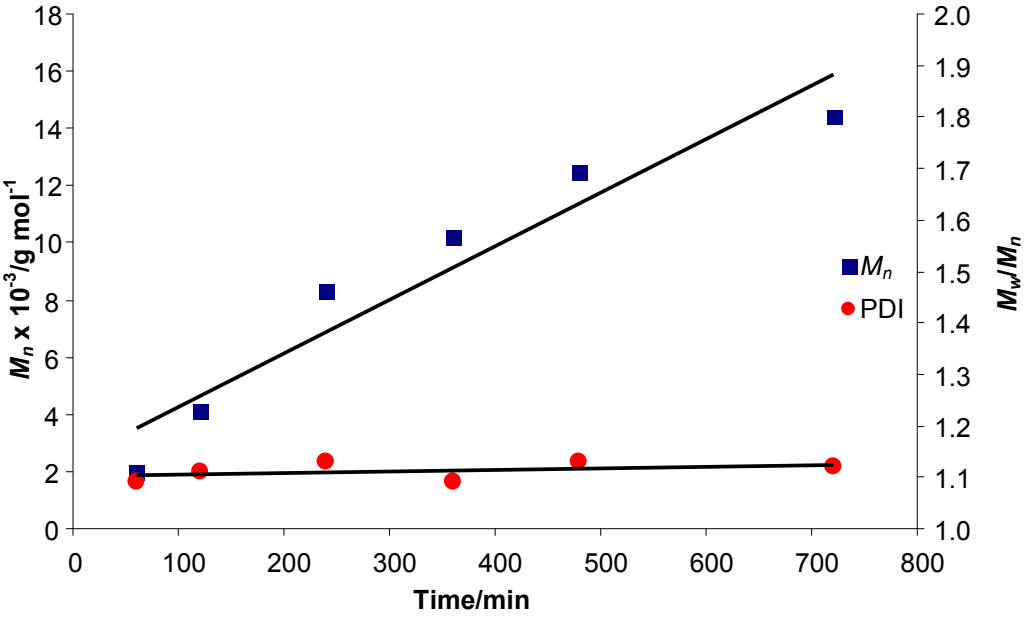

Figure 3.21 ROP of ε-CL initiated by **L6**Ti(O^{i}Pr)$_2$. M_n and PDI versus Time (GPC).

Similar plots of M_n and PDI versus time for the polymerisations initiated by **L6**Ti(O^{i}Pr)$_2$ and **L7**Ti(O^{i}Pr)$_2$ indicate that the ROP of ε-CL is again well controlled when these initiators are used.

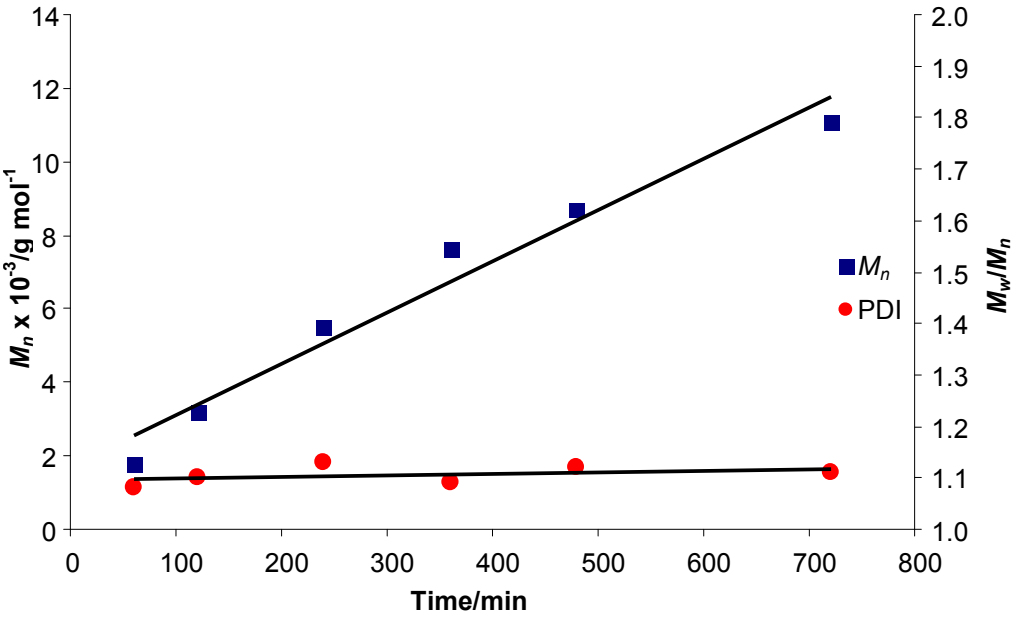

Figure 3.22 ROP of ε-CL initiated by **L7**Ti(O^{i}Pr)$_2$. M_n and PDI versus Time (GPC).

As noted in chapter 1, ROP of cyclic esters such as ε-CL initiated by metal complexes is often described as living, i.e. there is an absence of termination and chain transfer reactions; the rate of initiation is faster than the rate of propagation and polymer chain growth occurs in a controlled fashion, resulting in polymers with narrow PDI values. These linear increases in molecular weight and conversion with time and the PDI values of <1.4 observed for the polymers produced using **L1**Zr(O^{i}Pr)$_2$, **L1**Hf(O^{i}Pr)$_2$, **L6**Ti(O^{i}Pr)$_2$, **L7**Ti(O^{i}Pr)$_2$ and **L10**Ti(O^{i}Pr)$_2$ indicates well-controlled, living polymerisation processes.

Table 3.4 Results for the ROP of ε-caprolactone. Conditions [ε-CL]:[I] = 100:1, 10 mL toluene, 20 °C. [a]determined from GPC using polystyrene as the reference. Results given after the first addition of 100 molar equivalents of ε-CL, and after the second addition of a further 100 equivalents.

	After 1st Addition		After 2nd Addition	
Initiator	M_n[a]/g mol^{-1}	PDI[a]	M_n[a]/g mol^{-1}	PDI[a]
L1Zr(O^{i}Pr)$_2$	13800	1.35	22000	1.48
L1Hf(O^{i}Pr)$_2$	12400	1.17	21300	1.17
L6Ti(O^{i}Pr)$_2$	14300	1.10	21800	1.12
L7Ti(O^{i}Pr)$_2$	11400	1.08	20200	1.12
L10 Ti(O^{i}Pr)$_2$	12100	1.09	21100	1.13

In order to further test the *livingness* of the ROP process (i.e. if the propagating site remained active after all monomer had been consumed) the reactions were carried out stepwise. Monomer and polymer were combined in toluene and the reaction continued for 24 hours at room temperature. After this time a second portion of 100 molar equivalents monomer was added to the reaction mixture and stirred at room temperature for 16 hours. Subsequent GPC analysis of the PCL polymers produced showed that the

M_n had increased substantially in each case (Table 3.4). The growth in the value of M_n indicates that the active initiator complex was still present and further monomer could be inserted, increasing the chain length and thus M_n. Figure 3.23 illustratess the GPC traces for polymers produced using **L1**Zr(O^{i}Pr)$_2$ as the initiator, after the first (blue line) and second (red line) addition of 100 molar equivalents of monomer.

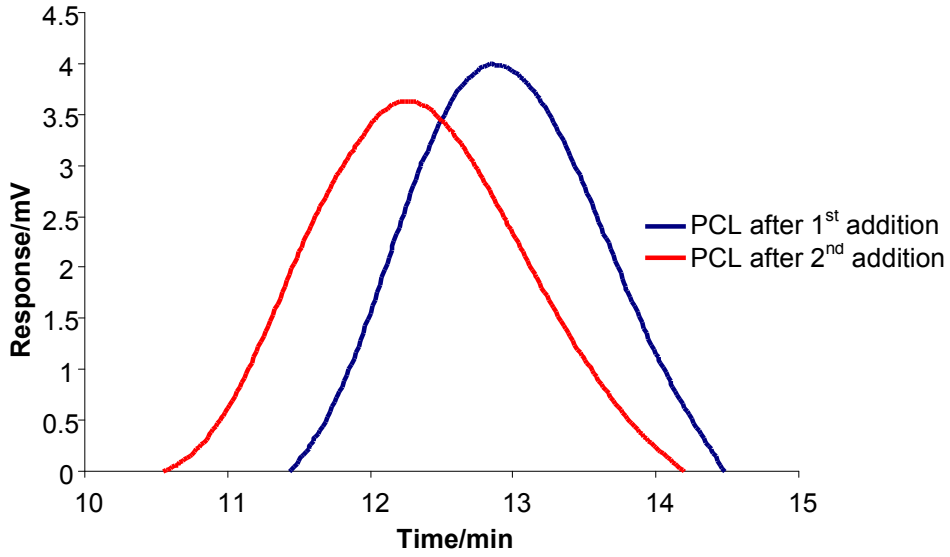

Figure 3.23 GPC traces of PCL produced using L1Zr(O^{i}Pr)$_2$ as the initiator after the first addition of 100 molar equivalents monomer (blue line) and after the second addition of the same (red line).

ROP of L-LA

Polymerisation Reactions

Polymerisations of L-LA were carried out in an inert atmosphere glove box. In all cases L-LA was dissolved in toluene in a thick-walled Young's ampoule and the initiator was added directly to this solution. The ampoule was sealed and removed from the glove box, placed in an oil bath at a temperature of 110 ºC and the reaction mixture stirred for two hours. The ampoule was subsequently removed from the oil bath, its contents exposed to air and methanol added to quench the polymerisation. The volatiles were removed and the resulting polymer was washed with methanol and dried under reduced pressure.

Analysis of Polymerisation Reaction Products

Although both monomer and polymer exist as white solids at room temperature, ^{1}H NMR spectroscopy may be used as a straightforward method for analysis of ROP reaction products. Due to the symmetry of the monomer and its structure, the ^{1}H NMR spectrum of L-LA is much simpler than that of ε-CL. With regard to L-LA, on proceeding from the monomer to a polymeric form, the methine, C*H*, proton shifts of the order of > 1 ppm downfield whilst the methyl, C*H*$_3$, protons shift of the order of ~0.2 ppm downfield

(Figure 3.24). In addition to ^{1}H NMR spectroscopy GPC can also be used to analyse PLLA.

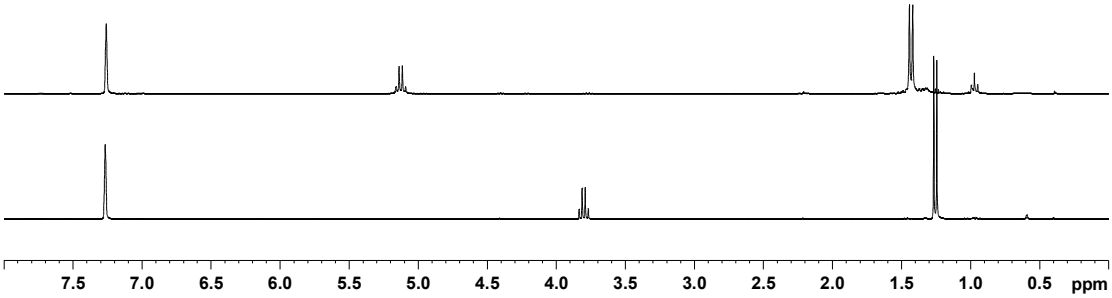

Figure 3.24 ^{1}H NMR spectra of L-LA monomer (below) and poly(L-lactide) (above).

ROP of L-LA using Five- and Six-Coordinate Group 4 Complexes

Polymerisation of L-LA was attempted with the six-coordinate Group 4 complexes **L1**Ti(O^{i}Pr)$_2$, **L2**Ti(O^{i}Pr)$_2$, **L3**Ti(O^{i}Pr)$_2$, **L1**Zr(O^{i}Pr)$_2$, **L2**Zr(O^{i}Pr)$_2$, **L1**Hf(O^{i}Pr)$_2$ and **L2**Hf(O^{i}Pr)$_2$. In addition, the three five-coordinate titanium(IV) complexes, **L6**Ti(O^{i}Pr)$_2$, **L7**Ti(O^{i}Pr)$_2$ and **L10**Ti(O^{i}Pr)$_2$ were tested for activity towards polymerisation of L-LA. The positive results are summarised in Table 3.5.

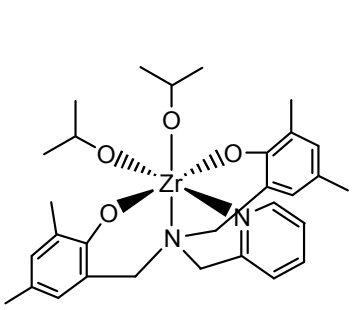

L1Zr(O^{i}Pr)$_2$

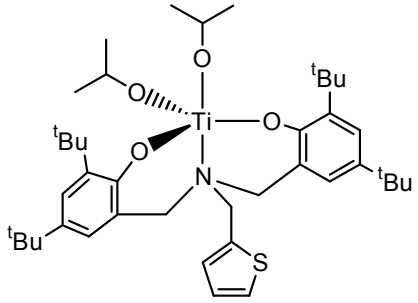

L10 Ti(O^{i}Pr)$_2$

Figure 3.25 Active initiators for the ROP of L-LA in toluene solution at 110 ºC.

Table 3.5 Results for the ROP of L-LA. Conditions [L-LA]:[I] = 100:1, 10 mL toluene, time 24 hours, 20 °C. [a]isolated yield, [b]determined from GPC using poly(styrene) standards as the reference.

Initiator	Yield[a] /%	M_w[b]/g mol^{-1}	M_n[b]/g mol^{-1}	PDI[b]
L1Zr(O^{i}Pr)$_2$	98	12200	10800	1.13
L10 Ti(O^{i}Pr)$_2$	97	13400	11600	1.15

The only six-coordinate Group 4 metal complex which initiated the ROP of L-LA under the reaction conditions was the zirconium(IV) complex **L1**Zr(O^{i}Pr)$_2$ (Figure 3.25), which gave a 98% yield of PLLA. As the lactide monomer has a molecular weight of 144.13 g mol^{-1} and a monomer to initiator ratio of 100:1 was used for these polymerisation reactions, a theoretical M_n value of ~14,400 g mol^{-1} is expected, although as noted previously, the limitations of the GPC system used make accurate molecular weight detection impossible. The PDI value of 1.13 for the PLLA produced with **L1**Zr(O^{i}Pr)$_2$ indicates a polymer with a narrow molecular weight distribution, indicative of a

controlled polymerisation process. The high activity of **L1**Zr(O^iPr)$_2$ relative to similar titanium(IV) complexes **L1**Ti(O^iPr)$_2$, **L2**Ti(O^iPr)$_2$, and **L3**Ti(O^iPr)$_2$ and the zirconium(IV) complex **L2**Zr(O^iPr)$_2$ with bulkier *tert*-butyl groups in the *ortho* and *para* positions on the phenolate rings is consistent with the activity trends for the ROP of ε-CL and may be attributed to the steric factors discussed in the previous section. However, the dramatic difference in reactivity between **L1**Zr(O^iPr)$_2$ and **L1**Hf(O^iPr)$_2$ is somewhat surprising, given their similar activity towards the ROP of ε-CL. The polymerisation reaction using **L1**Hf(O^iPr)$_2$ as the initiator yielded no polymer, only a small amount of low molecular weight oligomer with a repeat unit of ~3 estimated from ^{1}H NMR spectroscopy. As described in chapter 2, the solid-state structure of **L1**Hf(O^iPr)$_2$ was not determined, due to the lack of suitable single crystals, so the structural parameters cannot be compared with those of **L1**Zr(O^iPr)$_2$ in an attempt to shed light on the reactivity difference. However, a comparison of the structural parameters of the zirconium(IV) and hafnium(IV) complexes of **L2** was possible and revealed that all of the bond lengths in the metal-ligand coordination sphere were slightly shorter for the hafnium(IV) complex. In addition, the ^{1}H NMR spectra for both complexes were very similar, suggesting very similar solution-state structures.

Of the five-coordinate titanium(IV) complexes reported herein, only **L10**Ti(O^iPr)$_2$, with a thiophene moiety on the pendant arm of the ligand, was an active initiator for the ROP of L-LA under the stated conditions. The polymer produced using this initiator had an M_n value of 11600 g mol^{-1} (by GPC) and a PDI value of 1.15. In contrast, all three of the five-coordinate titanium(IV) complexes were active initiators for the ROP of ε-CL, affording polymers in high yields and with narrow PDI values. This difference of reactivity for the hydrocarbon aryl substituted complexes is unexpected. In the ROP of ε-CL, conversion versus time measurements showed that **L10**Ti(O^iPr)$_2$ reached maximum conversion slowest, compared to all other Group 4 complexes tested.

The generally lower activity of the complexes towards the ROP of L-LA is perhaps unsurprising. Lactide is a more challenging monomer to ring-open than ε-caprolactone, because as a six-membered ring it has less ring strain than the seven-membered ring of caprolactone (Figure 3.26). Relief of this ring strain is the major thermodynamic driving force for the ROP reaction as the ring-opening polymerisation results in a decrease in entropy as the monomer is incorporated into a polymer chain.[28] The presence of the methyl substituents on the LA monomer hinder the approach of the monomer to the initiator, further decreasing its polymerisability relative to ε-CL.

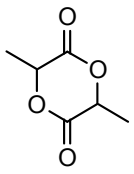

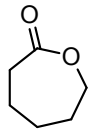

	LA	ε-CL
ΔH/kJ mol^{-1}	-22.9	-28.8
ΔS/J mol^{-1} K^{-1}	-25.0	-53.9

Figure 3.26 Enthalpies and entropies of ROP for L-LA and ε-CL at 298K.[28]

In context, Kol and co-workers recently prepared titanium(IV) and zirconium(IV) complexes of similar amine bis(phenolate) ligands, with a tertiary amine as the pendant arm donor (Figure 3.27).[29] Of those tested, the zirconium(IV) complex (iv) was found to be the most active initiator for the ROP of L-LA at 130 ºC in the absence of solvent, producing PLLA to 75% conversion in one hour, with a PDI value of 1.56. Complex (iii) was less active, producing a 21% yield of polymer after more than five hours. The titanium(IV) complexes (i) and (ii) were less active still, giving low polymer yields (31% and 6%, respectively) after long reaction times (53 h and 28 h, respectively). Although these bulk ROP reactions were carried out at higher temperatures, these differences in activities mirror the results seen for the six-coordinate titanium(IV) and zirconium(IV) complexes reported herein.

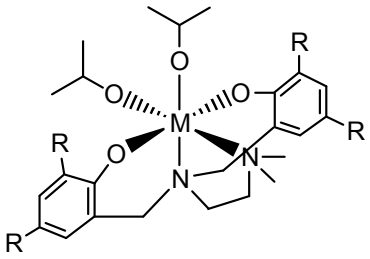

(i) M = Ti, R = ^{t}Bu
(ii) M = Ti, R = Cl
(iii) M = Zr, R = ^{t}Bu
(iv) M = Zr, R = Cl

Figure 3.27 Titanium(IV) and zirconium(IV) complexes prepared by Kol *et al*.[29]

Block Co-Polymerisation of ε-CL and L-LA

Having identified that both **L1**Zr(O^{i}Pr)$_2$ and **L10**Ti(O^{i}Pr)$_2$ were active initiators for the ROP of ε-CL and L-LA which produced polymer in a well-controlled manner, we considered these complexes to be ideal candidates as initiators for the block co-polymerisation of the two monomers.

PCL/PLLA co-polymers can have widely varying mechanical properties ranging from elastomeric to rigid, depending on the microstructures of the polymers. The *in vitro* rate of degradation of these co-polymers has been shown to be dependent on the degree of L-LA content and on ε-CL crystallinity,[30] and their relatively slow degradation rate makes them ideal for applications in long-term drug delivery.[31]

Co-Polymerisation Reaction

The co-polymerisation of ε-CL and L-LA was attempted by first dissolving 0.1 mmol of initiator in toluene in a Young's ampoule, and then adding 10 mmol of ε-caprolactone. The reaction mixture was stirred for seven hours (when **L1**Zr(OiPr)$_2$ was used as the initiator) or fourteen hours (when **L10**Ti(OiPr)$_2$ was used as the initiator) at room temperature. 10 mmol of L-lactide dissolved in toluene was then added to the ampoule which was sealed and removed from the glove box. The ampoule was placed in an oil bath at a temperature of 110 ºC and stirred for two hours, removed from the oil bath and methanol was added to quench the polymerisation. The volatiles were removed and the resulting polymer was washed with methanol and dried under reduced pressure.

Co-polymerisation Results

The co-polymerisation of ε-CL and L-LA with **L1**Zr(O^{i}Pr)$_2$ was attempted by combining the experimental methods used to produce the respective homopolymers in two steps (Figure 3.28). However, instead of isolating the PCL polymer after the first step, the active initiator species was allowed to remain in solution and to initiate ROP of L-LA.

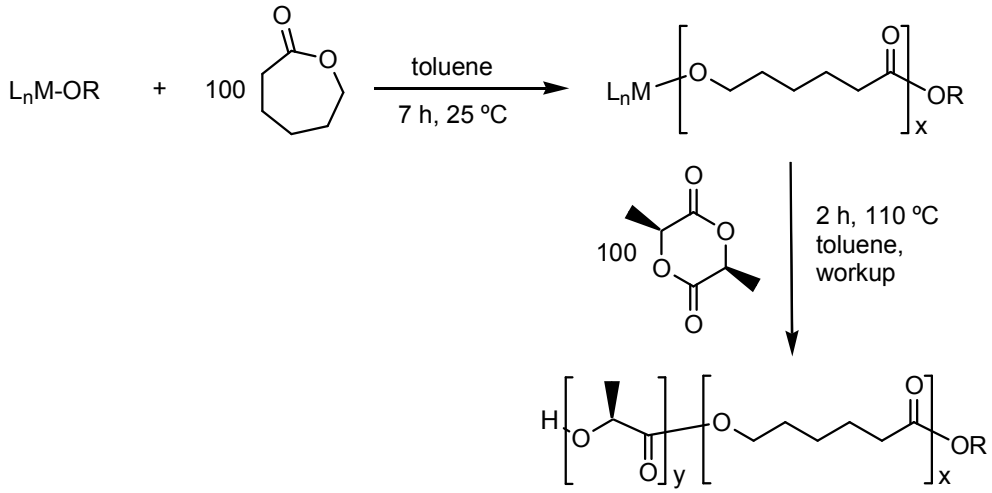

Figure 3.28 Reaction scheme for the block co-polymerisation of ε-CL and L-LA.

The polymeric material obtained from this experiment was analysed by ^{1}H and ^{13}C{^{1}H} NMR spectroscopy and by GPC. The ^{1}H NMR spectrum of the co-polymerisation reaction product showed peaks due to both PCL and PLLA blocks. In addition, the ^{13}C{^{1}H} NMR spectrum, although complicated, clearly showed two peaks in the carbonyl region, signals due to the PCL and PLLA blocks, respectively (Figure 3.29).

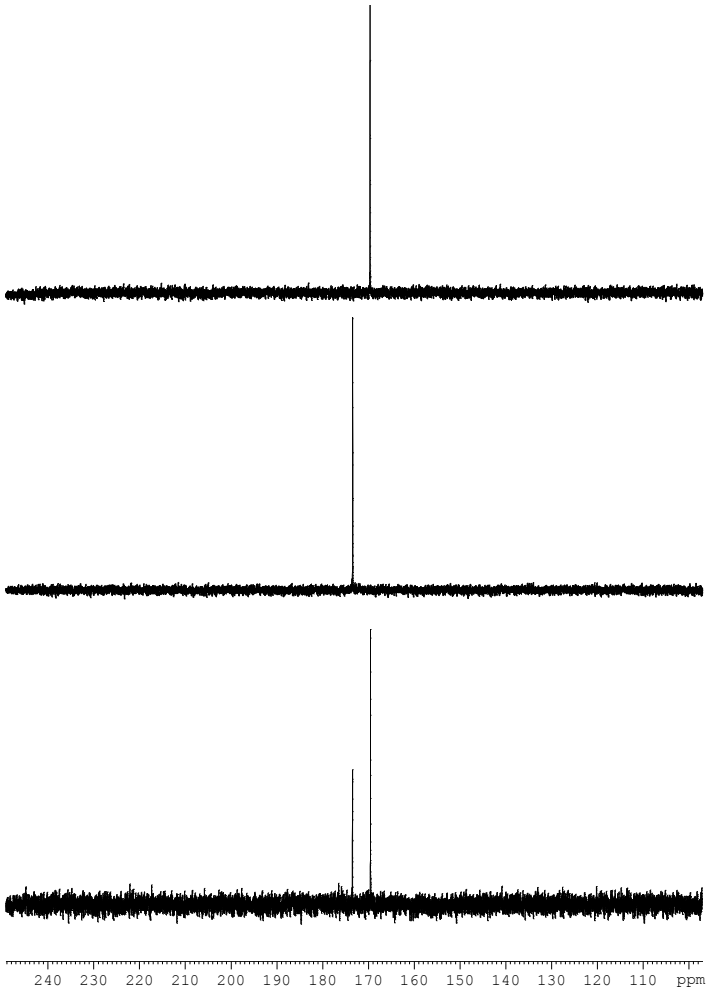

Figure 3.29 Carbonyl regions of the $^{13}C\{^{1}H\}$ NMR spectra of PLLA (top), PCL (middle) and PCL-*b*-PLLA (bottom).

Despite evidence from ^{1}H and $^{13}C\{^{1}H\}$ NMR spectroscopy, confirmation of the formation of the block co-polymer could not be absolute, as a blend of PCL and PLLA homopolymers would produce very similar spectra to the block co-polymer. However, the ^{1}H and $^{13}C\{^{1}H\}$ NMR spectroscopic experiments did confirm that a random copolymer had not formed, as many more peaks would be expected for this type of polymer. GPC analysis was necessary to provide further evidence for the formation of the block co-polymer. If the copolymerisation reaction product was a blend of the two homopolymers, the GPC elution curve would be expected to be bimodal and the molecular weight values for the polymer product would be similar to those obtained from homopolymerisations. M_n values obtained by GPC for the PCL and PLLA homopolymers using **L1**Zr($O^{i}Pr$)$_2$ were 13800 g mol^{-1} and 10800 g mol^{-1}, respectively.

Table 3.6 Results of the block co-polymerisation of ε-CL and L-LA initiated by **L1**Zr(O^iPr)$_2$ and **L10**Ti(O^iPr)$_2$. Conditions as described previously. [a]determined from GPC using poly(styrene) standards as the reference.

Initiator	Polymer	M_w[a]/g mol^{-1}	M_n[a]/g mol^{-1}	PDI[a]
L1Zr(O^iPr)$_2$	PCL	18600	13800	1.35
	PLLA	12200	10800	1.13
	PCL-PLLA	34500	28300	1.22
L10 Ti(O^iPr)$_2$	PCL	13200	12100	1.09
	PLLA	13400	11600	1.15
	PCL-PLLA	27900	24500	1.14

GPC analysis of the polymerisation reaction product revealed a polymer with an M_n value of 28,300 g mol^{-1}, implying that addition of the 100 equivalents of L-LA monomer had occurred, forming the desired PCL-PLLA block co-polymer (Table 3.6). In addition, a unimodal GPC elution curve was observed for the polymer, further supporting the conclusion that the reaction product was indeed the block co-polymer (Figure 3.30).

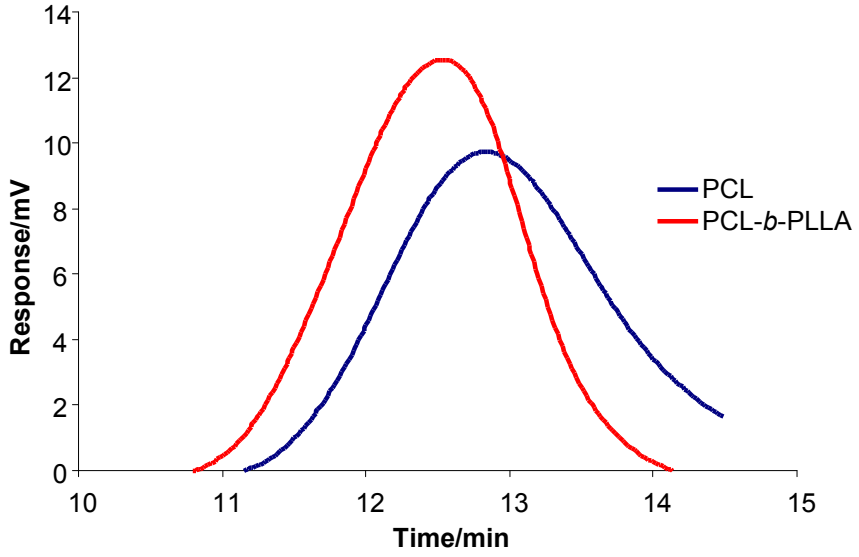

Figure 3.30 GPC trace of PCL and PCL-PLLA formed using **L1**Zr(O^iPr)$_2$.

The order of addition was crucial for the formation of the AB block copolymer. The copolymerisation reaction was also attempted by polymerising 100 molar equivalents of L-LA (relative to initiator) followed by addition of 100 molar equivalents of ε-CL. In this case, no further reaction occurred and the reaction product was PLLA homopolymer. In addition, attempts to form the triblock PCL-*b*-PLLA-*b*-PCL copolymer were also unsuccessful. This phenomenon has been observed before and attributed to slower rates of polymerisation when the initiator is a metal-PLA complex as compared to a metal-PCL initiator although Duda, Penczek and co-workers[32] have recently demonstrated the formation of triblock PCL-*b*-PLLA-*b*-PCL copolymers using the aluminium(III) salbinap complex introduced by Spassky and co-workers[33] as described in chapter 1. The authors

attribute the activity (or lack thereof) towards ABA block copolymerisation to the nature of the metal initiator.

3.3 Summary

Several of the complexes described in chapter 2 were tested for activity towards the ring-opening polymerisation of ε-CL and L-LA. Of the six-coordinate Group 4 metal complexes tested, only the zirconium(IV) and hafnium(IV) complexes employing an amine bis(phenolate) ligand with *ortho*, *para*-methyl substitution on the phenolate arms, **L1**Zr(O^iPr)$_2$ and **L1**Hf(O^iPr)$_2$, were active for the ROP of ε-CL in toluene solution at room temperature. The zirconium(IV) and hafnium(IV) complexes of **L2**, a ligand with bulkier *tert*-butyl groups in the phenol *ortho* and *para* positions, were found to be inactive as were both six-coordinate titanium(IV) complexes. The three five-coordinate titanium(IV) complexes, **L6**Ti(O^iPr)$_2$, **L7**Ti(O^iPr)$_2$ and **L10**Ti(O^iPr)$_2$ were found to be active for the ROP of ε-CL under the same reaction conditions. In each case where polymerisation did occur, PCL polymers were obtained in high yield and with narrow molecular weight distributions. Subsequent ^{1}H NMR spectroscopic experiments in which the polymerisation reactions were monitored, and GPC measurements showed the ROP reactions to be well-controlled in each case. Further ^{1}H NMR spectroscopic analysis revealed that the polymerisations proceeded via a coordination-insertion mechanism.

These same complexes were tested for the ROP of L-LA in toluene solution at 100 ºC, but only **L1**Zr(O^iPr)$_2$ and **L10**Ti(O^iPr)$_2$ were found to be active for the polymerisation, producing PLLA polymers with narrow molecular weight distributions and in high yields. The activity of **L1**Zr(O^iPr)$_2$ was shown to be comparable to similar complexes recently reported in the literature. **L1**Zr(O^iPr)$_2$ showed activity towards the ROP of both ε-CL and L-LA, and so the AB block copolymerisation of these monomers was attempted with these species. PCL-*b*-PLLA was readily formed using **L1**Zr(O^iPr)$_2$ under the same conditions used for the respective homopolymerisations. Attempts to prepare the PLLA-*b*-PCL diblock or PCL-*b*-PLLA-*b*-PCL triblock copolymers were unsuccessful.

In all, these results would seem to support the conclusions made in chapter 1 with regard to the varied factors which contribute to the polymerisation activity of a particular initiator.

References

[1] M. H. Chisholm and Z. P. Zhou, *J. Mater. Chem.* **2004,** 14, (21), 3081-3092.
[2] A. C. Albertsson and I. K. Varma, *Biomacromolecules* **2003,** 4, (6), 1466-1486.
[3] A. R. Simioni, C. Vaccari, M. I. Re and A. C. Tedesco, *J. Mater. Sci.* **2008,** 43, (2), 580-584.

[4] J. Cayuela, V. Bounor-Legare, P. Cassagnau and A. Michel, *Macromolecules* **2006,** 39, (4), 1338-1346.
[5] D. Takeuchi, T. Nakamura and T. Aida, *Macromolecules* **2000,** 33, (3), 725-729.
[6] C. Miola-Delaite, T. Hamaide and R. Spitz, *Macromol. Chem. Phys.* **1999,** 200, (7), 1771-1778.
[7] D. Thomas, P. Arndt, N. Peulecke, A. Spannenberg, R. Kempe and U. Rosenthal, *Eur. J. Inorg. Chem.* **1998**, (9), 1351-1357.
[8] M. Bero, P. Dobrzynski and J. Kasperczyk, *Polymer Bulletin* **1999,** 42, (2), 131-139.
[9] Y. Perez, I. del Hierro, I. Sierra, P. Gomez-Sal, M. Fajardo and A. Otero, *J. Organomet. Chem.* **2006,** 691, (13), 3053-3059.
[10] Y. J. Kim and J. G. Verkade, *Macromol. Rapid Commun.* **2002,** 23, (15), 917-921.
[11] Y. Kim, G. K. Jnaneshwara and J. G. Verkade, *Inorg. Chem.* **2003,** 42, (5), 1437-1447.
[12] Y. Kim and J. G. Verkade, *Organometallics* **2002,** 21, (12), 2395-2399.
[13] H. R. Kricheldorf, M. Berl and N. Scharnagl, *Macromolecules* **1988,** 21, (2), 286-293.
[14] P. Dobrzynski, J. Kasperczyk, H. Janeczek and M. Bero, *Macromolecules* **2001,** 34, (15), 5090-5098.
[15] P. Dobrzynski, *J. Polym. Sci., Part A: Polym. Chem.* **2004,** 42, (8), 1886-1900.
[16] M. L. Guo, H. Z. Sun, S. Bihari, J. A. Parkinson, R. O. Gould, S. Parsons and P. J. Sadler, *Inorg. Chem.* **2000,** 39, (2), 206-215.
[17] J. P. Fackler, F. J. Kristine, A. M. Mazany, T. J. Moyer and R. E. Shepherd, *Inorg. Chem.* **1985,** 24, (12), 1857-1860.
[18] Y. Sarazin, R. H. Howard, D. L. Hughes, S. M. Humphrey and M. Bochmann, *Dalton Trans.* **2006**, (2), 340-350.
[19] K. C. Hsieh, W. Y. Lee, L. F. Hsueh, H. M. Lee and J. H. Huang, *Eur. J. Inorg. Chem.* **2006**, (11), 2306-2312.
[20] O. Dechy-Cabaret, B. Martin-Vaca and D. Bourissou, *Chem. Rev.* **2004,** 104, (12), 6147-6176.
[21] Y. Takashima, Y. Nakayama, T. Hirao, H. Yasuda and A. Harada, *J. Organomet. Chem.* **2004,** 689, (3), 612-619.
[22] Y. Takashima, Y. Nakayama, K. Watanabe, T. Itono, N. Ueyama, A. Nakamura, H. Yasuda, A. Harada and J. Okuda, *Macromolecules* **2002,** 35, (20), 7538-7544.
[23] C. Marschner, *Angew. Chem., Int. Ed. Engl.* **2007,** 46, (36), 6770-6771.
[24] A. L. Mogstad and R. M. Waymouth, *Macromolecules* **1994,** 27, (8), 2313-2315.
[25] A. Kowalski, A. Duda and S. Penczek, *Macromolecules* **1998,** 31, (7), 2114-2122.
[26] Z. Y. Zhong, P. J. Dijkstra, C. Birg, M. Westerhausen and J. Feijen, *Macromolecules* **2001,** 34, (12), 3863-3868.
[27] W. M. Stevels, M. J. K. Ankone, P. J. Dijkstra and J. Feijen, *Macromolecules* **1996,** 29, (19), 6132-6138.
[28] C. K. Williams, *Chem. Soc. Rev.* **2007,** 36, 1573-1580.
[29] S. Gendler, S. Segal, I. Goldberg, Z. Goldschmidt and M. Kol, *Inorg. Chem.* **2006,** 45, (12), 4783-4790.
[30] B. Buntner, M. Nowak, J. Kasperczyk, M. Ryba, P. Grieb, M. Walski, P. Dobrzynski and M. Bero, *J. Controlled Release* **1998,** 56, (1-3), 159-167.
[31] M. R. Lostocco, C. A. Murphy, J. A. Cameron and S. J. Huang, *Polym. Degrad. Stab.* **1998,** 59, (1-3), 303-307.
[32] M. Florczak, J. Libiszowski, J. Mosnacek, A. Duda and S. Penczek, *Macromol. Rapid Commun.* **2007,** 28, (13), 1385-1391.
[33] N. Spassky, M. Wisniewski, C. Pluta and A. LeBorgne, *Macromol. Chem. Phys.* **1996,** 197, (9), 2627-2637.

Chapter 4

Stereoselective Ring-Opening Polymerisation of D,L-Lactide

4 Stereoselective Ring-Opening Polymerisation of D,L-Lactide

4.1 Introduction

As noted in Chapter 1, the presence of two chiral carbon centres in the lactide molecule may result in several possible stereochemical polymer architectures which can be accessed and controlled by the addition order of monomer in living ROP processes. When the monomer is a 1:1 mixture of D- and L-LA (D,L-LA), three limiting cases exist for possible polymer architectures, as shown in Figure 4.1. These are (i) atactic PDLLA, where the stereocentres are distributed in a random fashion (although, if epimerisation at the chiral carbon atom is negligible adjacent paired stereocentres will still exist); (ii) stereoblock isotactic PDLLA, in which the ROP of one enantiomer of monomer is highly favoured in comparison with ROP of the other enantiomer, resulting in a block co-polymer of D-LA and L-LA; (iii) heterotactic PDLLA may be formed when one enantiomer of LA is ring-opened, followed by the other enantiomer, in sequence.

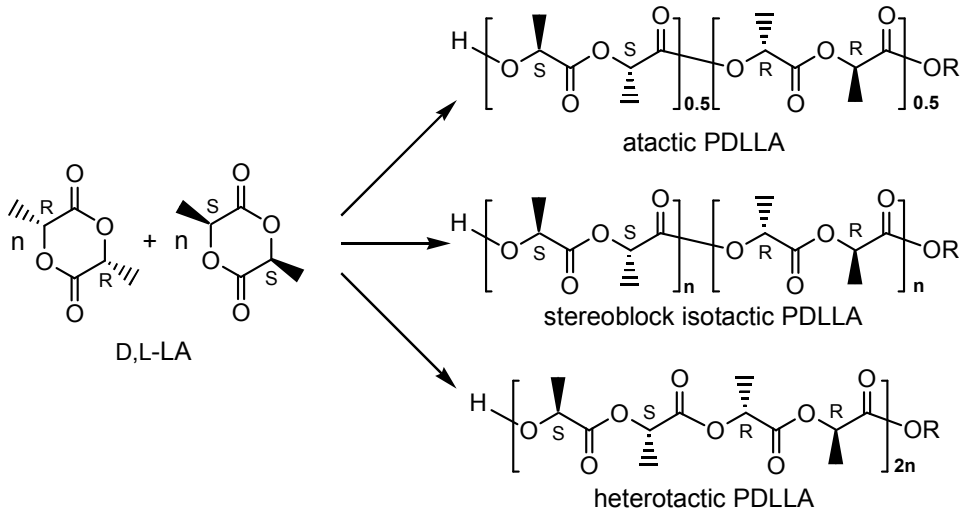

Figure 4.1 Stereopolymers available from ROP of D,L-LA via the coordination-insertion mechanism.

The initiator may also selectively polymerise a single enantiomer of LA resulting in truly isotactic PDLA or PLLA. However, although differences in the rates of ROP of enantiopure D-LA or L-LA and D,L-LA are known, there are no known examples of initiators being active for the ROP of a single enantiomer of LA. Even an initiator with a very high preference for producing isotactic PDLA or PLLA from D,L-LAhas been shown to produce a gradient stereoblock isotactic polymer, inserting the 'wrong' monomer as its concentration increases.[1]

Producing PDLLA polymers with these varying microstructures has been the subject of intensive investigation in recent years, not only because of the precise chemical control needed to produce them but also because the physical properties of PDLLA polymers

vary significantly with microstructure. As noted in chapter 1, properties such as crystallinity and melting temperature are dependent on the sequence of stereocentres along the backbone of the polymer chain. It was also noted that several groups have had success in stereoselective ROP of cyclic esters both prior to and during our work, utilising a wide variety of initiators, such as zinc(II) complexes of β-diketonate ligands (Coates)[1, 2], lanthanide(III) complexes of amine bis(phenolate) ligands (Carpentier)[3] and aluminium(III) complexes of salen ligands (Spassky,[4] Gibson,[5] Nomura[6]). Although in some of these cases a remarkable degree of stereocontrol over the polymerisation process has been achieved (e.g. $P_r > 0.90$, see chapter 1 for definition of terms), most studies have been carried out in solution.

The polymerisation reactions reported herein begin with those carried out at room temperature in toluene solution. The ring-opening polymerisation of D,L-LA in solution has been attempted with a wide variety of initiators, as discussed in chapter 1.[7, 8] Particularly with regard to stereoselective ROP of D,L-LA, in some cases solution polymerisation studies can give useful information about the origin of stereocontrol in the polymerisation process.[7] Solution ROP carried out at lower temperatures can enhance control both in terms of stereoselectivity and activity of the polymerisation, affording PDLLA with high degrees of stereoregularity and narrow molecular weight distributions.[7, 9] In contrast a solvent-free, melt ROP process carried out at temperatures in excess of 130 ºC is the favoured process for industrial production of PLLA but very few studies have presented a high degree of stereocontrol over the polymerisation under solvent-free conditions.[6, 10] Clearly, any initiator which could be considered for commercial use in the ROP of D,L-LA would need to retain both stability and stereocontrol over the polymerisation at elevated temperatures. When results, in terms of stereochemical enrichment of the polymer, are consistent between solution phase and melt polymerisation reactions, the results of the ROP carried out in solution may act as a model for the solvent-free melt reaction.

4.2 Polymerisation Results and Discussion

ROP of D,L-LA using complexes of di-anionic amine bis(phenolate) ligands

Solution Polymerisations

For solution polymerisations, D,L-LA monomer was dissolved in dry toluene in a thick-walled Young's ampoule within an argon filled glove box. The initiator was added to the ampoule, which was then sealed and removed from the glove box and stirred for a fixed time period. The polymerisation was carried out either at room temperature or at an elevated temperature obtained using an oil bath. The polymerisation was quenched by

addition of methanol to the reaction mixture, the volatiles were then removed and the polymer was washed with methanol and dried under reduced pressure.

Of the initiators which were tested for the ROP of L-LA under solution conditions (chapter 3), only those that were found to be active, **L1**Zr(O^{i}Pr)$_2$ and **L10**Ti(O^{i}Pr)$_2$, were tested in solution for the ROP of D,L-LA. In addition, **L8**Zr(O^{i}Pr)$_2$, which was not screened for the ROP of L-LA, was tested (Figure 4.2).

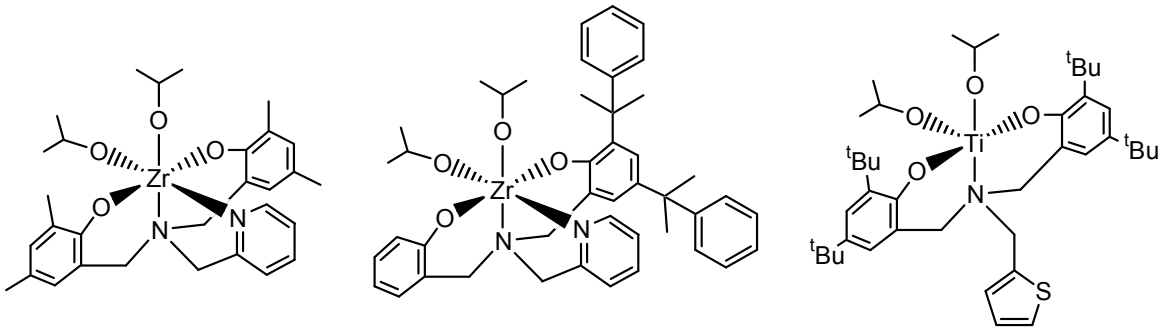

L1Zr(O^{i}Pr)$_2$ **L8**Zr(O^{i}Pr)$_2$ **L10**Ti(O^{i}Pr)$_2$

Figure 4.2 Group 4 complexes of di-anionic amine bis(phenolate) ligands tested for ROP of D,L-LA.

When **L1**Zr(O^{i}Pr)$_2$ was initially tested at room temperature in toluene solution (Table 4.1, entry 1), it was found to be inactive for the ROP of D,L-LA. When the same reaction was carried out at 100 ºC (entry 3), PDLLA polymer was produced in >99% yield. This result is consistent with those obtained using **L1**Zr(O^{i}Pr)$_2$ as an initiator for the ROP of L-LA described in chapter 3 in that a high reaction temperature is needed to achieve ROP under solution conditions when using these initiators. Similar results were observed when **L10**Ti(O^{i}Pr)$_2$ was used as the initiator; no polymer formed after 48 hours, but a high yield of atactic PDLLA was obtained after 3 hours in toluene solution at 110 ºC (entries 2 and 5).

Table 4.1 Results for the ROP of D,L-LA in toluene solution with [M]:[I]=100. [a]Isolated yield; [b]determined by GPC; [c]determined from analysis of the methine region of the ^{1}H homonuclear decoupled NMR spectrum.

Entry	Initiator	Temp/ºC	Time/h	% Yield[a]	M_n[b]	PDI[b]	P_r[c]
1	**L1**Zr(O^{i}Pr)$_2$	25	48	0	-	-	-
2	**L10**Ti(O^{i}Pr)$_2$	25	48	0	-	-	-
3	**L8**Zr(O^{i}Pr)$_2$	25	48	0	-	-	-
4	**L1**Zr(O^{i}Pr)$_2$	110	2	>99	7100	1.11	0.40
5	**L10**Ti(O^{i}Pr)$_2$	110	2	92	8100	1.13	0.52
6	**L8**Zr(O^{i}Pr)$_2$	110	2	75	8700	1.10	0.35

The polymer produced using **L1**Zr(O^{i}Pr)$_2$ was analysed using ^{1}H homonuclear decoupled NMR spectroscopy, revealing that the initiator was able to exert a degree of stereocontrol over the polymerisation producing PDLLA with a slight isotactic enrichment (P_r = 0.40). With an aim of enhancing this modest isotactic enrichment, ligand **L8** and complex

L8Zr(O^iPr)$_2$ were prepared. While **L1**Zr(O^iPr)$_2$ is *pseudo* C_s symmetric, with identical phenolate groups **L8**Zr(O^iPr)$_2$ has only C_i symmetry, with one very bulky dimethylphenyl-substituted phenolate group and one unsubstituted phenolate group. This ligand and its corresponding zirconium(IV) complex were prepared in order to determine if the reduced symmetry would have a significant effect on the microstructure of PDLLA polymer produced by enhancing the degree of stereocontrol over the polymerisation.

In accord with the result obtained for **L1**Zr(O^iPr)$_2$, when the ROP of D,L-LA was attempted at room temperature in toluene solution using **L8**Zr(O^iPr)$_2$ as the initiator (entry 3), no polymer was produced, whereas at a reaction temperature of 110 ºC PDLLA polymer was obtained in high yield (entry 6). When this polymer was analysed using ^{1}H homonuclear decoupled NMR spectroscopy, it was found to have only a slightly higher isotactic enrichment than the PDLLA produced using the C_s symmetric initiator **L1**Zr(O^iPr)$_2$. The methine region of the ^{1}H homonuclear decoupled NMR spectrum for the PDLLA polymer described in Table 4.1 entrie 4 is shown in Figure 4.3, where the intensity of the *iii* tetrad is clearly enhanced relative to the spectrum shown in chapter 1 for an atactic PDLLA polymer.

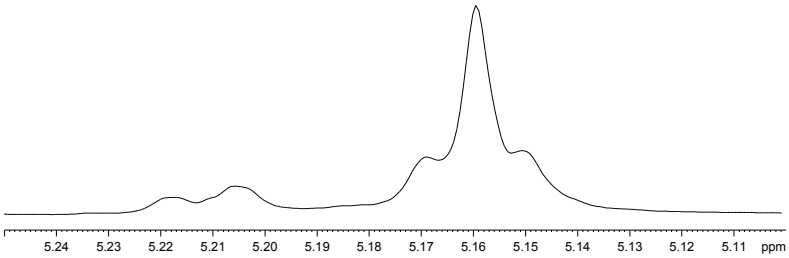

Figure 4.3 Methine region of the ^{1}H homonuclear decoupled NMR spectrum of PDLLA formed using **L1**Zr(O^iPr)$_2$ as the initiator.

Although the increase in the degree of isotactic enrichment is quite small when **L8**Zr(O^iPr)$_2$ is used as the initiator (over **L1**Zr(O^iPr)$_2$) it is not insignificant. The asymmetry of the initiator complex, with bulky phenolate substituents on one arm of the ligand may still hinder the approach of the unfavoured monomer somewhat, leading to a preference for the monomer with the stereochemistry which causes the least steric repulsions during approach and subsequent ring-opening.

These polymerisation results show for the first time that amine bis(phenolate) ligands are applicable to group 4 metal initiated ROP of D,L-LA. In 2005, Mountford and co-workers reported dimeric neodymium(III), samarium(III) and yttrium(III) complexes of **L2**, bridged by BH_4 groups (Figure 4.4).[11] When the neodymium(III) complex was used

as an initiator for the ROP of D,L-LA in THF solution, PDLLA with a slight heterotactic bias (P_r = 0.67) was formed.

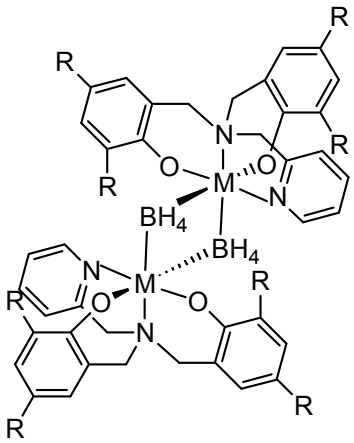

Figure 4.4 Lanthanide(III) complexes prepared by Mountford *et al*.[11] M=Nd, Sm, Y. When M=Nd, Y, each metal centre carries an additional THF molecule bound through the oxygen atom.

As noted in chapter 1, Carpentier and co-workers prepared a series of lanthanide(III) initiators bearing amine bis(phenolate) ligands, which were active for the ROP of D,L-LA in tetrahydrofuran solution. Some of these initiators produced polymers with a high degree of heterotactic enrichment, manifested in P_r values of between 0.80 and 0.90.[3]

For melt polymerisations, D,L-LA monomer and the initiator were combined in a thick-walled Young's ampoule in an argon filled glove box. The ampoule was removed from the glove box and placed in an oil bath at 130 ºC and stirred for a fixed time period. The polymerisation was terminated by adding methanol to the reaction mixture. Dichloromethane was then added to dissolve the glassy product. The volatiles were removed and the resulting polymer was washed with methanol and dried under reduced pressure.

Although several of the group 4 metal complexes reported herein were not tested for activity towards the ROP of D,L-LA under solution conditions, all reported complexes (chapter 2) were tested under solvent-free, melt reaction conditions. Group 4 complexes of di-anionic amine bis(phenolate) ligands bound in a tetradentate fashion (Figure 4.6) will be considered first.

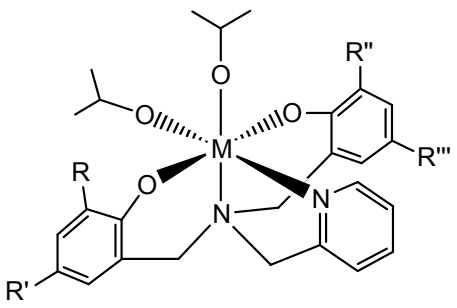

L1Ti(O^iPr)$_2$ R = R' = Me, R'' = R''' = Me;
L2Ti(O^iPr)$_2$ R = R' = ^{t}Bu, R'' = R''' = ^{t}Bu;
L3Ti(O^iPr)$_2$ R = R'' = H, R' = R''' = NO_2;

L1Zr(O^iPr)$_2$ R = R' = Me, R'' = R''' = Me;
L2Zr(O^iPr)$_2$ R = R' = ^{t}Bu, R'' = R''' = ^{t}Bu;
L8Zr(O^iPr)$_2$ R = R' = H, R'' = R''' = $C(CH_3)_2Ph$;

L1Hf(O^iPr)$_2$ R = R' = Me, R'' = R''' = Me;
L2Hf(O^iPr)$_2$ R = R' = ^{t}Bu, R'' = R''' = ^{t}Bu

Figure 4.5 Group 4 complexes of di-anionic tetradentate amine bis(phenolate) ligands tested for ROP of D,L-LA under solvent-free conditions.

With the exception of **L2**Ti(O^iPr)$_2$, all complexes were active for the ROP of D,L-LA under solvent-free, melt conditions (Table 4.2, entries 1-8). The titanium(IV) complexes **L1**Ti(O^iPr)$_2$, and **L3**Ti(O^iPr)$_2$ each produced PDLLA in 75% and 52% yield, respectively, after a 2 hour reaction time with PDI values of 1.37 and 1.38, respectively. In each case the PDLLA polymer produced was atactic (entries 1 and 3). The zirconium(IV) complexes **L1**Zr(O^iPr)$_2$, **L2**Zr(O^iPr)$_2$ and **L8**Zr(O^iPr)$_2$ also produced polymer under the above reaction conditions (entries 4-6), although the yields obtained were considerably lower than those obtained using the aforementioned titanium(IV) complexes. Indeed for **L2**Zr(O^iPr)$_2$ a 24 hour reaction time was needed to generate a 13% yield of atactic PDLLA. In the case of **L1**Zr(O^iPr)$_2$ and **L8**Zr(O^iPr)$_2$, yields were also low, but the PDLLA polymers produced showed a small degree of isotactic enrichment (P_r = 0.45 and 0.40, respectively). These results are consistent with those obtained under solution reaction conditions (Table 4.1). The activities of the hafnium(IV) complexes **L1**Hf(O^iPr)$_2$ and **L2**Hf(O^iPr)$_2$ mirrors that of their zirconium(IV) analogues (entries 7 and 8). Again a 24 hour reaction time was needed to afford a 30% yield of atactic PDLLA when **L2**Hf(O^iPr)$_2$ was used and PDLLA produced using **L1**Hf(O^iPr)$_2$ as the initiator had a small degree of isotactic enrichment (P_r = 0.43).

Table 4.2 Results for the ROP of D,L-LA under solvent-free conditions with [M]:[I]=300. [a]Isolated yield; [b]determined by GPC; [c]determined from analysis of the methine region of the ^{1}H homonuclear decoupled NMR spectrum.

Entry	Initiator	Time/h	% Yield[a]	M_n[b]	PDI[b]	P_r[c]
1	**L1**Ti(O^iPr)$_2$	2	75	32700	1.38	0.50
2	**L2**Ti(O^iPr)$_2$	2	0	-	-	-
3	**L3**Ti(O^iPr)$_2$	2	52	31300	1.37	0.51
4	**L1**Zr(O^iPr)$_2$	2	45	4400	1.27	0.45
5	**L2**Zr(O^iPr)$_2$	24	13	10300	1.14	0.50
6	**L8**Zr(O^iPr)$_2$	2	10	1700	1.42	0.40
7	**L1**Hf(O^iPr)$_2$	2	80	33800	1.28	0.43
8	**L2**Hf(O^iPr)$_2$	24	30	7800	1.29	0.50

These results are in some respects surprising, particularly the enhanced activity of the titanium(IV) complexes (as compared to the solution studies of the ROP of L-LA detailed in chapter 3) and the relatively low yields produced by the zirconium(IV) and hafnium(IV) initiators. In terms of polymer stereochemistry, these results contrast with those obtained by Davidson *et al*.[12] using group 4 complexes of similar amine bis(phenolate) ligands linked through an ethylene diamine group (Figure 4.7).

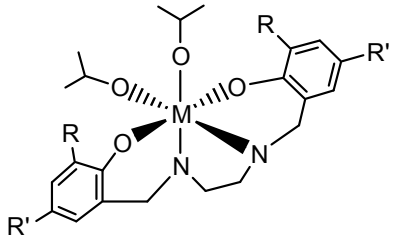

Figure 4.6 Group 4 initiators prepared by Davidson and co-workers.[12]

Zirconium(IV) and hafnium(IV) complexes of this type, where R = R' = Me, produced PDLLA with a higher degree of isotactic enrichment, in each case the P_r value obtained for the polymer was 0.30 (molecular weight and polydispersity index values were in the expected range. Although these complexes initially appear quite similar to those reported herein, a possible explanation for the enhancement in stereocontrol of the complexes bearing 'linked' amine bis(phenolate) ligands may be traced back to structural differences in the metal complexes. The coordination mode of ligands **L1**, **L2** and **L8** around octahedral zirconium(IV) and hafnium(IV) centres leads to complexes with *pseudo* C_s symmetry which are non-chiral. However, the coordination mode of the ligands reported by Davidson *et al* around octahedral zirconium(IV) and hafnium(IV) centres affords *pseudo* C_2 symmetric chiral complexes (Δ or Λ forms). This difference between the two ligand systems may account for the difference in selectivity via a chain end controlled mechanism. In such a process the stereocentre of the last inserted monomer affects the insertion of the next monomer, governing the microstructure of the resulting polymer.[13]

Davidson and co-workers also prepared titanium(IV) complexes of 'linked' amine bis(phenolate) ligands and found that these complexes produced atactic PDLLA under melt conditions. These results are consistent with those obtained with the complexes described in this thesis. The general lack of stereocontrol over the polymerisation when titanium(IV) complexes are used as initiators may also be due to the coordination environment around the metal centre. Rzepa and co-workers have recently reported work utilising DFT calculations to ascertain the origin of stereocontrol in ROP of D,L-LA initiated by magnesium alkoxide complexes.[14, 15] The study showed that chelation of lactate units of the growing polymer chain is a significant factor in determining the

stereoselectivity of the next monomer insertion. Considering that zirconium(IV) and hafnium(IV) metal centers can more easily accommodate higher coordination numbers than titanium(IV),[16] chelation of the growing polymer chain is likely to occur to a greater extent in zirconium(IV) and hafnium(IV) complexes which in turn enhances stereoselectivity of the next addition (relative to titanium(IV) which is too small to allow extensive chelation). Consequently, if chelation within titanium(IV) complexes is less favoured, stereoselectivity of subsequent monomer insertions will be reduced.

Next, the effect of having a complex where the third arm of the amine bis(phenolate) ligand is non-coordinating on the ROP of D,L-LA (Figure 4.8) was investigated. The five-coordinate titanium(IV) complexes **L6**Ti(O^{i}Pr)$_2$ and **L7**Ti(O^{i}Pr)$_2$ failed to produce PDLLA after thirty minutes in the melt reaction (Table 4.3, entries 1 and 2). **L6**Ti(O^{i}Pr)$_2$ did, however, give a product in 21% yield which was detectable by ^{1}H NMR spectroscopy and not isolated. The was determined to be an oligomer with a repeat unit of roughly four, by examination of the ^{1}H NMR spectrum of the polymerisation product with a molecular weight of ~ 577 g mol^{-1}.

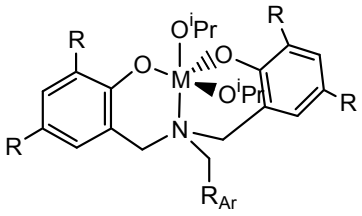

L6Ti(O^{i}Pr)$_2$ R = ^{t}Bu, R$_{Ar}$ = phenyl
L7Ti(O^{i}Pr)$_2$ R = ^{t}Bu, R$_{Ar}$ = 1-naphthalene
L10 Ti(O^{i}Pr)$_2$ R = ^{t}Bu, R$_{Ar}$ = 2-thiophene

Figure 4.7 Group 4 complexes of di-anionic amine bis(phenolate) ligands bound in a tridentate fashion tested for ROP of D,L-LA.

It is somewhat surprising that **L6**Ti(O^{i}Pr)$_2$ and **L7**Ti(O^{i}Pr)$_2$ are not active for the ROP of D,L-LA under melt conditions, as the six-coordinate titanium(IV) complexes **L1**Ti(O^{i}Pr)$_2$ and **L3**Ti(O^{i}Pr)$_2$ both produced polymer under the same conditions. However, as noted in previous chapters, the balance between a complex being active or inactive towards the ROP of cyclic esters is very fine.

Table 4.3 Results for the ROP of D,L-LA under solvent-free conditions with [M]:[I]=300. [a]Isolated yield; [b]determined by GPC; [c]determined from analysis of the methine region of the ^{1}H homonuclear decoupled NMR spectrum.

Entry	Initiator	% Yield[a]	M_n[b]/g mol^{-1}	PDI[b]	P_r[c]
1	**L6**Ti(O^{i}Pr)$_2$	0	-	-	-
2	**L7**Ti(O^{i}Pr)$_2$	0	-	-	-
3	**L10**Ti(O^{i}Pr)$_2$	89	30400	1.32	0.53

In contrast, the five-coordinate titanium(IV) complex **L10**Ti(O^iPr)$_2$ was active for the ROP of D,L-LA and produced polymer in high yield (entry 3). Analysis of the methine region of the ^{1}H homonuclear decoupled NMR spectrum of the polymer product revealed that the polymer produced was atactic, with a P_r value of 0.53. The activity pattern for the three five-coordinate titanium(IV) complexes towards D,L-LA under melt conditions mirrors that of the complexes under solution conditions for the ROP of L-LA described in the previous chapter.

ROP of D,L-LA using complexes of tri-anionic amine bis(phenolate) ligands

As noted in chapter 2, the coordination chemistry of the C_3 symmetric ligand **L11**H$_3$ is rich and varied.[17-19] It was considered that Group 4 metal complexes of this ligand (Figure 4.9) would be attractive candidates as initiators for the ROP of D,L-LA. The inherent chirality of the complexes, conferred by the C_3 symmetry of the ligand, was considered to raise some interesting possibilities about stereoselective ROP and consequently, these complexes were tested for activity towards ROP of D,L-LA and specifically for stereoselective polymerisation.

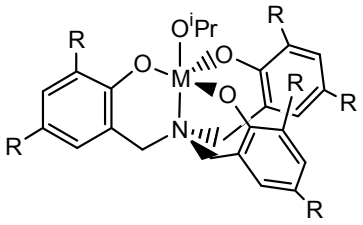

L11 Ti(O^iPr), M = Ti, R = ^{t}Bu
L11 Zr(O^iPr), M = Zr, R = ^{t}Bu
L11 Hf(O^iPr), M = Hf, R = ^{t}Bu

Figure 4.8 Group 4 complexes of **L11** tested for ROP of D,L-LA.

In toluene solution at room temperature, **L11**Ti(O^iPr) was found to be inactive for the ROP reaction, producing no polymer after stirring for 48 hours. However, under the same conditions both **L11**Zr(O^iPr) and **L11**Hf(O^iPr)$_2$ were found to be active for the polymerisation, producing polymer in 50% and 30% yields, respectively (Table 4.4). The molecular weights of these polymers were in the expected range, and the PDI values were 1.09 and 1.08, respectively, indicating a very narrow molecular weight distribution in each sample. Analysis of the polymer microstructure using ^{1}H homonuclear decoupled NMR spectroscopy revealed that in both cases, PDLLA with a very high degree of heterotactic enrichment had been produced.

Table 4.4 Results for the ROP of D,L-LA under solution conditions for 48 hours with [M]:[I]=100. [a]Isolated yield; [b]determined by GPC; [c]determined from analysis of the methine region of the ^{1}H homonuclear decoupled NMR spectrum.

Entry	Initiator	Temp/ºC	% Yield[a]	M_n[b]/g mol^{-1}	PDI[b]	P_r[c]
1	**L11**Ti(O^{i}Pr)	25	0	-	-	-
2	**L11**Zr(O^{i}Pr)	25	50	11700	1.09	0.98
3	**L11**Hf(O^{i}Pr)	25	30	8900	1.08	0.97

The inactivity of the titanium(IV) complex, **L11**Ti(O^{i}Pr), is not surprising; in both chapter 3 and the previous section of this chapter, it was noted that solution polymerisation experiments employing both six- and five-coordinate titanium(IV) complexes did not yield polymer. Previously, no zirconium(IV) or hafnium(IV) complexes were known to affect the ROP of D,L-LA at room temperature in solution, however, subsequent work in our laboratory has produced zirconium(IV) and hafnium(IV) complexes of chiral Schiff base ligands which are active initiators for the ROP, yielding PDLLA with a slight heterotactic bias.[20]

Perhaps more surprising is the high degree of stereocontrol over the polymerisation which **L11**Zr(O^{i}Pr) and **L11**Hf(O^{i}Pr) achieve. The ^{1}H homonuclear decoupled NMR spectrum of PDLLA produced using **L12**Zr(O^{i}Pr) as the initiator (Figure 4.10) shows enhanced *sis* and *isi* peaks with respect to the peaks due to the *sii*, *iis*, and *iii* tetrads, indicating a high proportion of syndiotactic linkages (i.e. major portions of the polymer backbone containing $(RRSS)_n$ stereocentres). The ^{1}H homonuclear decoupled NMR spectrum for PDLLA produced using **L11**Hf(O^{i}Pr) was qualitatively and quantitatively very similar.

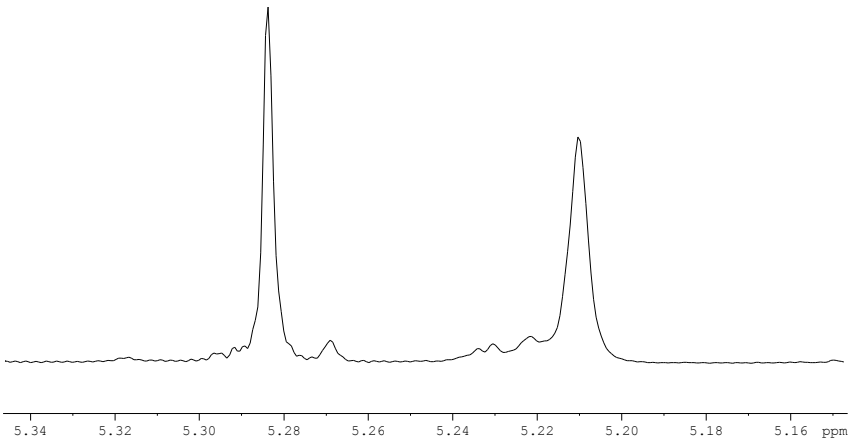

Figure 4.9 Methine region of the ^{1}H homonuclear decoupled spectrum for PDLLA produced using **L11**Zr(O^{i}Pr) as the initiator in toluene solution, entry 2, Table 4.4.

Although in toluene solution only the zirconium(IV) and hafnium(IV) complexes bearing the **L11** ligand were active for the ROP of D,L-LA, under melt conditions all three complexes of ligand **L11**, including the titanium(IV) analogue, were active initiators (Table 4.5). The polymerisation initiated by **L11**Ti(O^{i}Pr) at 130 ºC under solvent-free

conditions produced PDLLA polymer in 50% yield after 30 minutes (entry 1). Analysis of the polymer microstructure using ^{1}H homonuclear decoupled NMR spectroscopy revealed the stereosequence distribution along the polymer backbone to be random, atactic, PDLLA with a P_r value of 0.50.

Table 4.5 Results for the ROP of D,L-LA under solvent-free conditions for 30 minutes with [M]:[I]=300. [a]Isolated yield; [b]determined by GPC; [c]determined from analysis of the methine region of the ^{1}H homonuclear decoupled NMR spectrum.

Entry	Initiator	% Yield[a]	M_n[b]/g mol^{-1}	PDI[b]	P_r[c]
1	**L11**Ti(O^{i}Pr)	50	37100	1.38	0.50
2	**L11**Zr(O^{i}Pr)	78	32300	1.22	0.96
3	**L11**Hf(O^{i}Pr)	95	71200	1.19	0.88

When **L11**Zr(O^{i}Pr) or **L11**Hf(O^{i}Pr) were used as initiators, the ROP of D,L-LA under melt conditions proceeded to give polymer in 78% and 95% yield, respectively, within 30 minutes. PDI values for these polymers were slightly higher than those for the PDLLA polymers produced by these initiators under solution conditions, although the molecular weight distributions for the polymer produced in the melt were still relatively narrow. Strikingly, the P_r values obtained by ^{1}H homonuclear decoupled NMR spectroscopic analysis (Figure 4.10) of the polymers showed that, even at high temperatures and in the absence of solvent, polymer with a very high degree of heterotactic enrichment was formed (P_r = 0.96, 0.88, respectively).

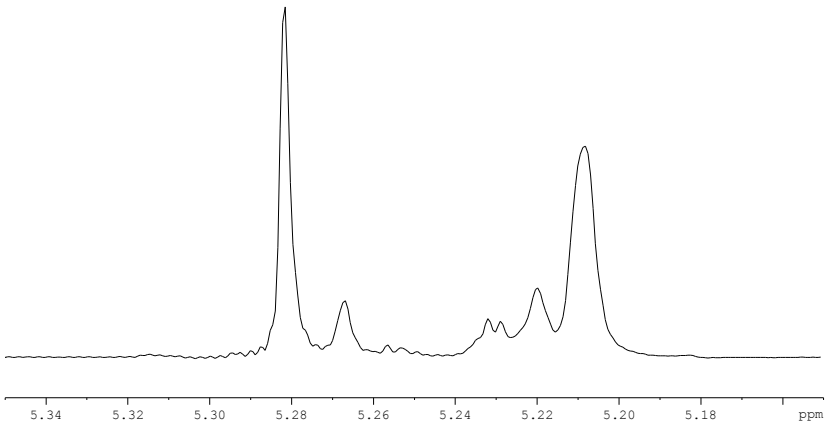

Figure 4.10 Methine region of the ^{1}H homonuclear decoupled spectrum for PDLLA produced using **L11**Zr(O^{i}Pr) as the initiator under solvent-free conditions, entry 2, Table 4.5.

Although the activity of **L11**Ti(O^{i}Pr) towards the ROP of D,L-LA under solvent-free conditions contrasts with the inactivity under solution conditions, this is not surprising. As **L1**Zr(O^{i}Pr)$_2$ and **L8**Ti(O^{i}Pr)$_2$ were observed to be inactive for the ROP of D,L-LA at room temperature in toluene solution, but produced polymer under melt conditions.

In addition, Verkade and co-workers found that similar titanium(IV) phenoxide complexes (Figure 4.11) were active for the ROP of both L- and D,L-LA under solvent-

free conditions at 130 ºC, producing PLLA and PDLLA with molecular weight and PDI values similar to those reported herein for **L11**Ti(O^{i}Pr).[21, 22] When the polymerisation reactions were carried out in toluene solution, even at temperatures of 130 ºC, no polymer formed. Similar to the polymer produced using **L11**Ti(O^{i}Pr), PDLLA produced in polymerisation reactions initiated by the complexes prepared by Verkade and co-workers was atactic.

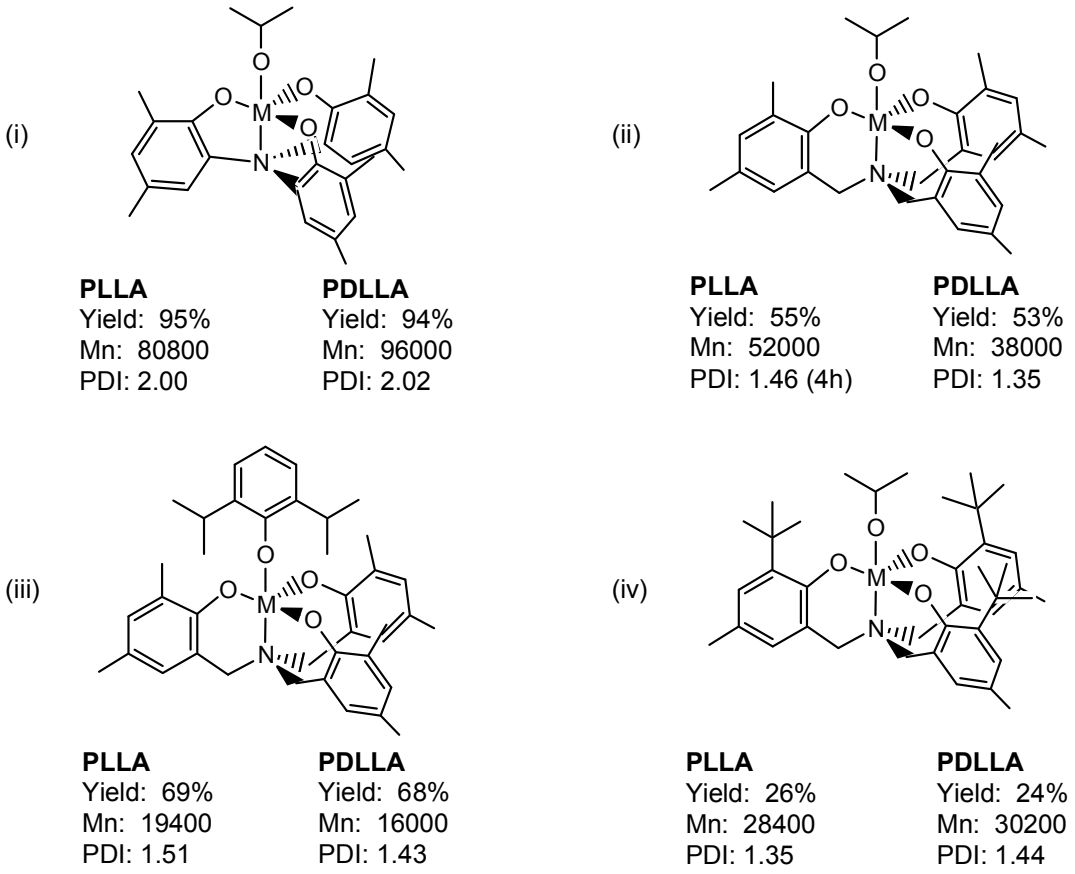

Figure 4.11 Titanium(IV) alkoxide and aryloxide complexes of C_3-symmetric ligands prepared by Verkade and co-workers.[21, 22] Melt polymerisation results, [M]:[I] = 300:1.

Interestingly, the authors noted that of the complexes bearing an isopropoxide group, that (ii) and (iv) were considerably poorer initiators than (i) in terms of yield of polymer. In (i), the phenol groups of the ligand are connected to the apical nitrogen atom through one bond and the authors reasoned that the lack of steric protection in the equatorial plane for (i) as compared to (ii) and (iv) accounts for the observed differences in activity. This observation may in some respects account for the differences in activity between **L11**Ti(O^{i}Pr) and its zirconium(IV) and hafnium(IV) analogues. Analysis of the solid-state structures of **L11**M(O^{i}Pr) (M = Ti, Zr, Hf) revealed that the bond lengths between the metal centre and the principle atoms in the metal coordination sphere were in general longer for the zirconium(IV) and hafnium(IV) complexes, locating the steric bulk of the ligands further away from the active metal centre. Thus, the ligand occupies and enshrouds a smaller percentage of the surface area of the metal centre in the

zirconium(IV) and hafnium(IV) complexes of **L11**. This could in part account for the observed activity towards the ROP of D,L-LA at room temperature in solution of **L11**Zr(O^{i}Pr) and **L11**Hf(O^{i}Pr) compared to the inactivity of **L11**Ti(O^{i}Pr).

As in the solution polymerisation reaction carried out with these initiators, under melt conditions a marked difference is observed in both the activity and selectivity of the titanium(IV) complex versus the zirconium(IV) and hafnium(IV) complexes. The high degree of heterotactic enrichment is notable in itself, but particularly in the context of other reports in this area. Previous to the results obtained herein using **L11**Zr(O^{i}Pr) and **L11**Hf(O^{i}Pr), only two initiators which produced highly stereoenriched PDLLA under melt conditions had been reported. The aluminium(III) salen complexes prepared by Feijen and co-workers[23] (Figure 4.12(a)) and Nomura and co-workers[24] (Figure 4.12(b)), introduced in chapter 1, produced PDLLA with P_i and P_r values of 0.12 and 0.09, respectively, indicating the presence of a high proportion of isotactic linkages along the polymer backbone.

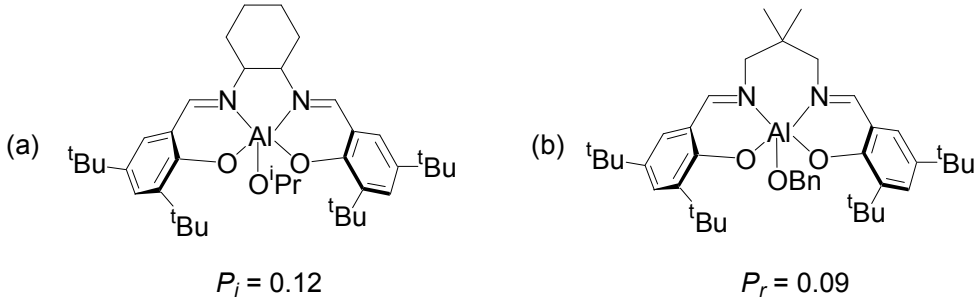

Figure 4.12 Aluminium(III) complexes prepared by (a) Feijen and co-workers[23] and (b) Nomura and co-workers[24] which produce PDLLA with a high degree of isotactic enrichment under melt conditions.

Investigations into the origin of stereocontrol

The high degree of heterotactic enrichment achieved when **L11**Zr(O^{i}Pr) or **L11**Hf(O^{i}Pr) were used as initiators for the ROP of D,L-LA, both in solution and under solvent-free conditions is intriguing. This particularly contrasts to the complexes of amine bis(phenolate) ligands **L1**Zr(O^{i}Pr)$_2$, **L8**Zr(O^{i}Pr)$_2$ and **L10**Ti(O^{i}Pr)$_2$ discussed earlier. Although the ligand frameworks of **L1**Zr(O^{i}Pr)$_2$, **L8**Zr(O^{i}Pr)$_2$ and **L10**Ti(O^{i}Pr)$_2$ are similar to those of **L11**Zr(O^{i}Pr) or **L11**Hf(O^{i}Pr), the former produced polymer with little or no stereoenrichment. One of the main differences between these ligands is that **L11** is a *trianionic*, tetradentate ligand while **L1, L8** and **L10** are *dianionic*, tetradentate ligands; in addition, the possibility that the C_3 symmetric nature of **L11** could be responsible in some way for the surprising stereoselectivity observed in ROP of D,L-LA was considered.

In order to investigate these topics further we prepared ligand **L12**H$_3$ and its titanium(IV) and zirconium(IV) isopropoxide complexes (Figure 4.14). Here, one of the phenolate

arms of the C_3 symmetric ligand is replaced with an ethanolate group, thereby reducing the symmetry of the ligand and of any metal complexes.

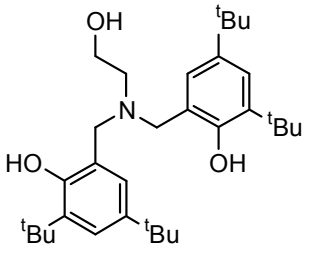

L12H_3

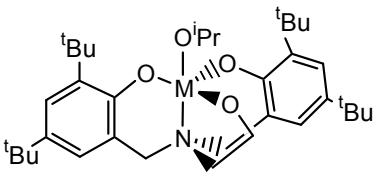

L12 Ti(O^{i}Pr)
L12 Zr(O^{i}Pr)

Figure 4.13 Ligand **L12**H_2 and its corresponding titanium(IV) and zirconium(IV) complexes. The synthesis of these compounds is described in chapter 2.

Complexes **L12**Ti(O^{i}Pr) and **L12**Zr(O^{i}Pr) were tested for activity towards ROP of D,L-LA under both solution and solvent-free conditions; the results are summarised in Table 4.6. After 48 hours at room temperature in toluene solution, **L12**Ti(O^{i}Pr) failed to produce polymer (entry 1), which is as expected as no other titanium(IV) complex reported herein had proven to be active under these conditions. The zirconium(IV) analogue **L12**Zr(O^{i}Pr) was also inactive under the same reaction conditions (entry 2). However, this contrasts markedly to the results obtained for **L11**Zr(O^{i}Pr), which proceeded to give a 50% yield of PDLLA with a high degree of heterotactic enrichment after the same 48 hour reaction time. Under solvent-free conditions at a temperature of 130 ºC, both complexes were active initiators for the ROP of D,L-LA (entries 3 and 4).

Table 4.6 Results for the ROP of D,L-LA under solution and solvent-free conditions. [a]Isolated yield; [b]determined by GPC; [c]determined from analysis of the methine region of the ^{1}H homonuclear decoupled NMR spectrum.

Entry	Initiator	T/ºC	[M]:[I]	Time/h	% Yield[a]	M_n[b]/g mol^{-1}	PDI[b]	P_r[c]
1	**L12**Ti(O^{i}Pr)	25	100	48	0	-	-	-
2	**L12**Zr(O^{i}Pr)	25	100	48	0	-	-	-
3	**L12**Ti(O^{i}Pr)	130	300	0.5	16	30100	1.21	0.51
4	**L12**Zr(O^{i}Pr)	130	300	0.5	87	33000	1.18	0.54

Under melt conditions, the polymerisation initiated by the zirconium(IV) complex gave a higher yield of polymer after the 30 minute reaction time than the polymerisation initiated by the titanium(IV) congener (87% versus 16%, respectively), mirroring the results obtained with **L11**Ti(O^{i}Pr) and **L11**Zr(O^{i}Pr) under melt conditions. However, although the PDLLA produced by **L12**Ti(O^{i}Pr) was atactic, the PDLLA produced using **L12**Zr(O^{i}Pr) as the initiator was also atactic, with a P_r value of 0.54. This result sharply contrasts with that obtained using **L11**Zr(O^{i}Pr) as the initiator, when PDLLA with a high degree of heterotactic enrichment (P_r = 0.96) was produced in the melt. Thus, the activity of titanium(IV) and zirconium(IV) complexes of **L12** is similar to those complexes of

L11, but the stereoselectivity for the production of PDLLA with a high degree of heterotactic enrichment is greatly reduced.

As discussed in chapter 1, stereoselective ROP of D,L-LA is considered possible through two mechanisms: *chain end control* or *enantiomorphic site control*. As the lactide monomer is chiral, it is possible that a chain end control mechanism could be operating to produce highly stereoregular polymer in this case. Under the chain end control mechanism, the chirality of the last inserted monomer and its relationship to the steric environment of the initiator determines the preferred stereochemistry of the next monomer insertion (Figure 4.14 using **L11**Zr(O^{i}Pr) as the example) which could result in isotactic or heterotactic propagation. If a chain end control mechanism was operating during the ROP of D,L-LA by **L11**Zr(O^{i}Pr) or **L11**Hf(O^{i}Pr), the chirality of the initiator would not contribute to the mechanism of stereocontrol.

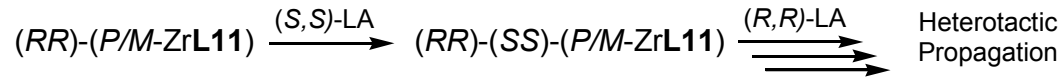

Figure 4.14 ROP of D,L-LA initiated by **L11**Zr(O^{i}Pr) (or **L11**Hf(O^{i}Pr)) under a chain end control mechanism, leading to heterotactic propagation.

However, in general chain end control mechanisms operate when the initiator complex is *achiral*.[8] In the case of **L11**Zr(O^{i}Pr) and **L11**Hf(O^{i}Pr), the initiator complexes are racemic, raising the question as to whether the chirality at the metal centre is involved in the observed stereocontrol. In addition, the inconsistency in the stereoenrichment of PDLLA polymers produced using **L11**Ti(O^{i}Pr) (atactic) versus **L11**Zr(O^{i}Pr) and **L11**Hf(O^{i}Pr) (highly heterotactic), suggests chain end control, if in operation, may not be operating in isolation.

In chapter 2, it was observed that due to the C_3 symmetry of the ligand, group 4 metal complexes of **L11**, in which the ligand is bound in a tetradentate fashion with the three phenolate arms in equatorial positions will exist as a pair of enantiomers, labelled *P* and *M* (Figure 4.15).

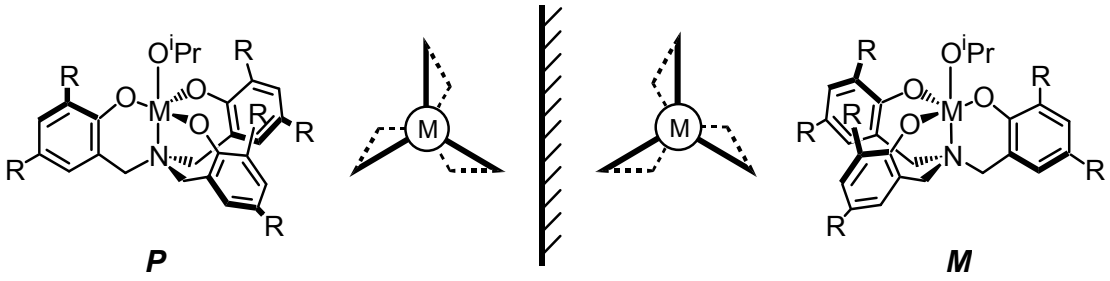

Figure 4.15 *P* and *M* enantiomers of **L11**M(O^{i}Pr), M = Ti, Zr, Hf, R = ^{t}Bu.

On the timescale of ^{1}H NMR spectroscopy such complexes can interchange between the two enantiomers. Kol and co-workers[25] and Verkade and co-workers[21] have observed

sharp resonances for the ligand methylene protons in the ^{1}H NMR spectrum of titanium(IV) complexes of such ligands (with a variety of R groups). In contrast, when Davidson and co-workers initially reported characterisation data for **L11**Zr(O^{i}Pr), broad resonances were observed for these protons which sharpened on cooling to lower temperatures, indicating relatively facile 'switching' between the two enantomeric forms on the ^{1}H NMR spectroscopic timescale.[26] Finally, chapter 2 detailed the synthesis and characterisation of the hafnium(IV) congener, which also showed broad resonances for the ligand methylene protons in the ^{1}H NMR spectrum at room temperature. These were resolved to a pair of sharp 3H doublets at 233 K.

With the ^{1}H NMR spectral data for the complexes and the results for their activity and selectivity towards the ROP of D,L-LA in mind, we considered whether the facile interconversion between the *P* and *M* enantiomeric forms of **L11**Zr(O^{i}Pr) and **L11**Hf(O^{i}Pr) could be responsible for the high degree of heterotactic enrichment observed in polymers produced using these initiators. If this were the case and the chirality of the metal complex dominated the 'selection' of a particular enantiomer of the monomer, the origin of stereocontrol in the ROP would be enantiomorphic site control. In this particular case, due to the nature of the metal complex and the noted facile interconverison between the two enantiomers, the process could be called *dynamic* enantiomorphic site control. If we assume (for the sake of argument) that the *P* enantiomer of the metal complex 'prefers' to insert an L-LA (*S,S*-LA) monomer we can envisage a situation in which a single diastereomer is present on the timescale of the next monomer insertion (Figure 4.16).

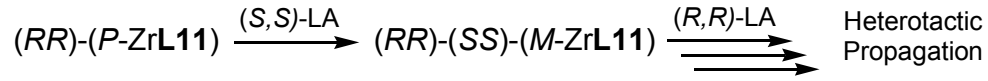

Figure 4.16 ROP of D,L-LA initiated by **L11**Zr(O^{i}Pr) (or **L11**Hf(O^{i}Pr)) under a dynamic enantiomorphic site control mechanism.

The chirality of the initiator complex dominates the next monomer insertion such that an L-LA monomer is inserted and this in turn forces an inversion in stereochemistry at the metal centre, leading to the *M* enantiomer of the complex, which preferentially inserts a D-LA (*R,R*-LA) monomer. This insertion drives the stereochemistry of the complex back to the opposite enantiomer and the process continues, generating alternating ring-opened D-LA and L-LA units: a heterotactic PDLLA polymer.

This postulated mechanism completely relies on the ability of the metal initiator complex to interchange between the *P* and *M* enantiomers. If this facile interconversion could be stopped – if, effectively, the initiator could be 'locked in' to a single enantiomeric form,

this hypothesis could be tested. We were provided with a modified version of **L11**H_3, **L11**$^{R\text{-Me}}H_3$, with a methyl group on one arm of the ligand, at a methylene carbon atom (Figure 4.17).

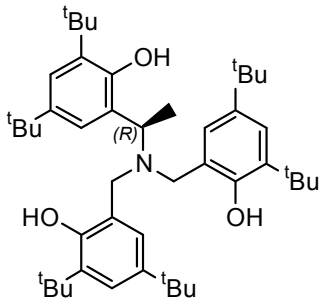

L11$^{R\text{-Me}}H_3$

Figure 4.17 Ligand **L11**$^{R\text{-Me}}H_3$, prepared by Axe and Bull.[27]

This ligand was provided through the synthetic efforts of Mr Philip Axe and Dr Steven Bull.[27] Zirconium(IV) and hafnium(IV) complexes of this ligand were prepared by reacting a dichloromethane solution of the ligand with the appropriate metal tetra-isopropoxide starting material, stirring at room temperature and subsequent removal of volatiles. In each case, the resulting white solid was recrystallized from toluene solution. ^{1}H and $^{13}C\{^{1}H\}$ NMR spectroscopic analysis of each reaction product indicated that the desired product, with one equivalent of the chiral ligand bound to the metal centre in a tetradentate fashion, had formed in each case (Figure 4.18), although the ^{1}H NMR spectrum of the hafnium(IV) complex indicated that an equivalent of isopropanol remained bound to the metal centre.

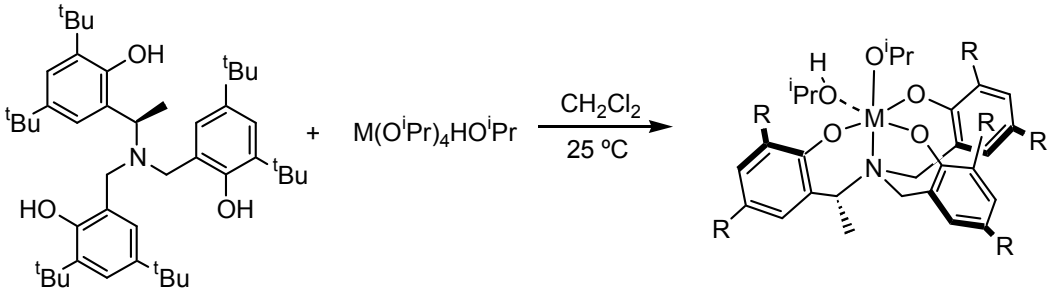

L11$^{R\text{-Me}}H_3$ M = Zr, Hf **L11**$^{R\text{-Me}}$Zr(O^{i}Pr)
L11$^{R\text{-Me}}$Hf(O^{i}Pr)HO^{i}Pr

Figure 4.18 Synthetic route to complexes **L11**$^{R\text{-Me}}$M(O^{i}Pr), M = Ti, Zr.

The solid-state structures of both complexes were determined using X-ray diffraction techniques. These analyses confirmed the structures to be those which was predicted by NMR spectroscopic analysis. (Figures 4.19 and 4.20).

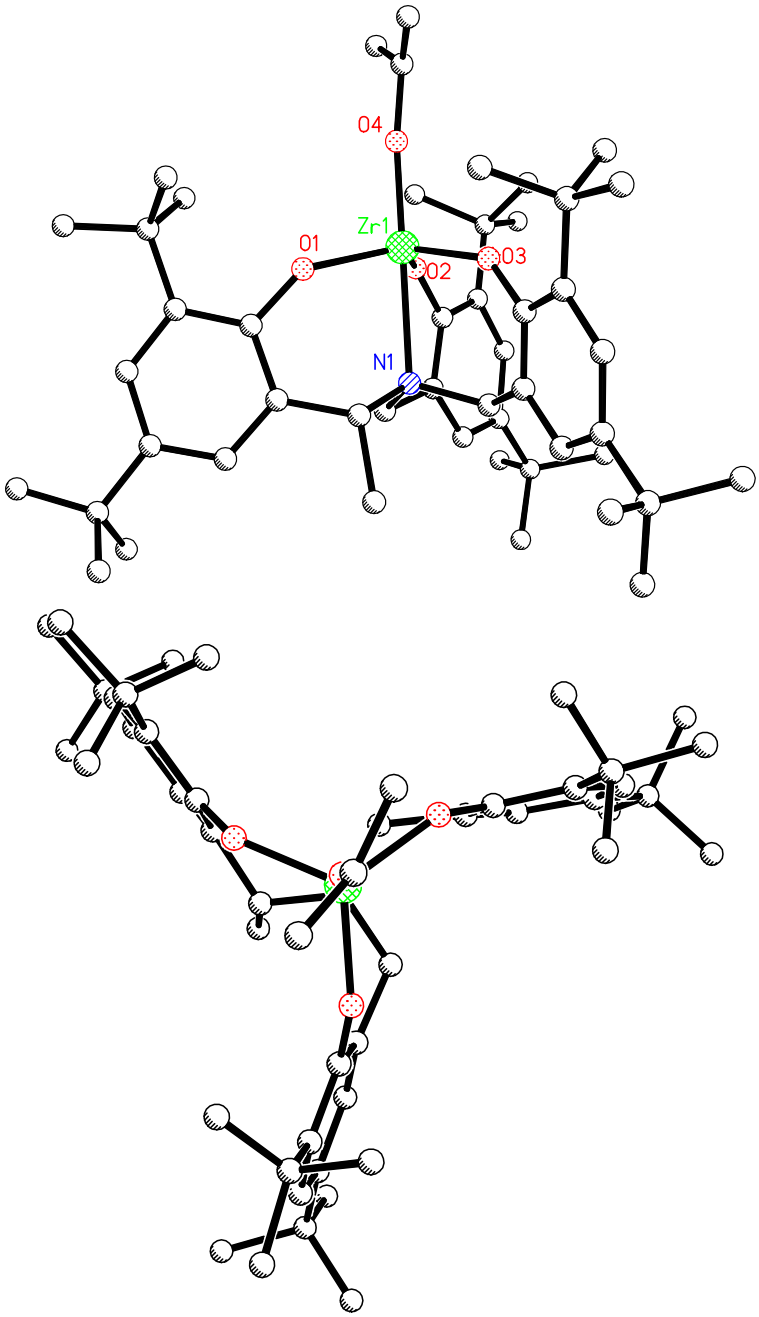

Figure 4.19 Molecular structure of **L11**$^{R\text{-Me}}$Zr(O^{i}Pr) as determined by X-ray crystallography. Hydrogen atoms omitted for clarity.

The determined solid-state structure of **L11**$^{R\text{-Me}}$Zr(O^{i}Pr) comprises a *pseudo* trigonal bipyramidal zirconium(IV) centre with the tris(phenolate) ligand arranged with the phenolate oxygen atoms in *cis* equatorial positions. The isopropoxide ligand is *trans* to the apical nitrogen atom and the solitary methyl group forces the ligand to adopt a conformation akin to that of the *M* enantiomer in the racemic complex **L11**Zr(O^{i}Pr).

The solid-state structure of **L11**$^{R\text{-Me}}$Hf(O^{i}Pr) also agrees with the prediction made from analysis of the ^{1}H NMR spectrum on the complex, namely that an equivalent of isopropanol remains bound to the metal centre (Figure 4.18).

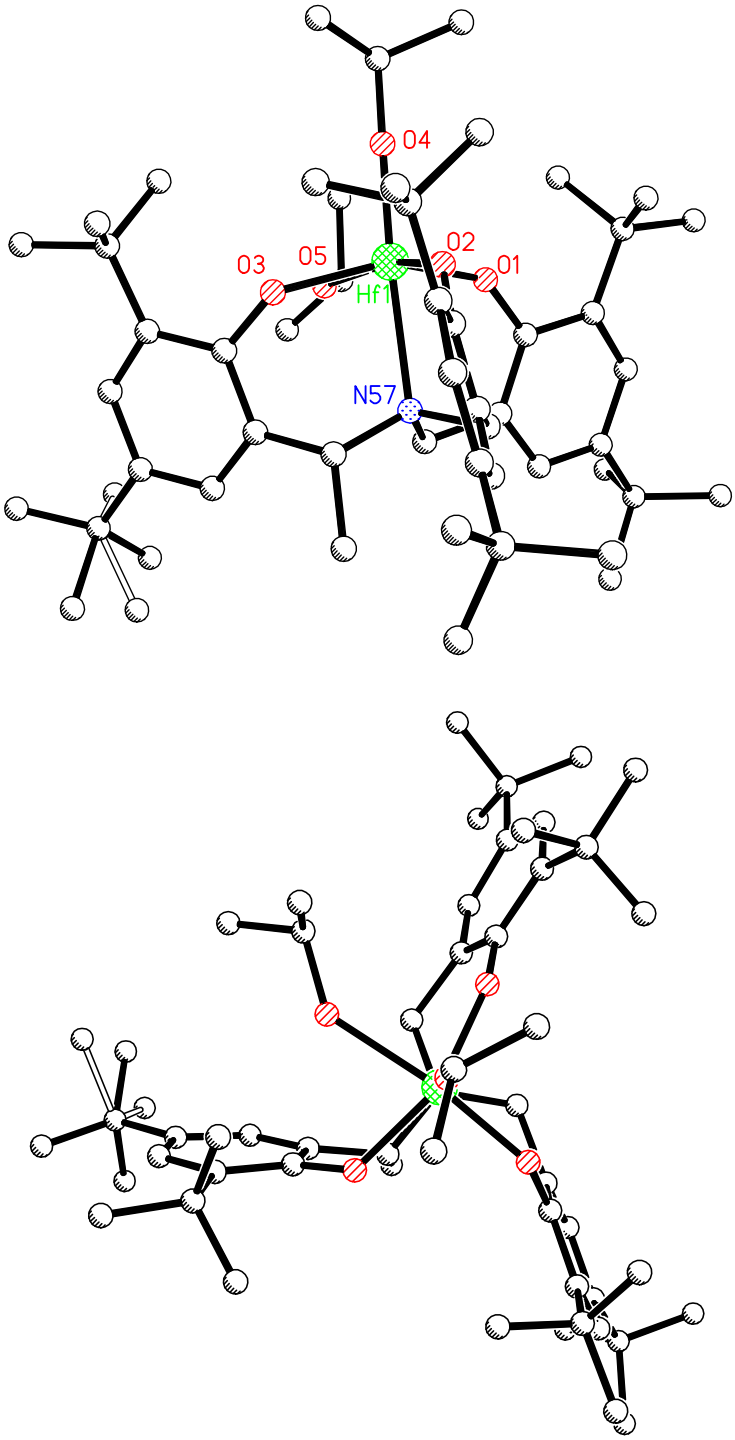

Figure 4.20 Molecular structure of **L11**$^{R\text{-}Me}$Hf(O^{i}Pr) as determined by X-ray crystallography. Hydrogen atoms omitted for clarity. A minor component of disorder in one *tert*-butyl group is shown with open bonds.

The structure comprises a *pseudo* octahedral hafnium(IV) centre, again with the three oxygen atoms of the tris(phenolate) ligand bound in a *meridional* fashion and the isopropoxide oxygen atom and apical nitrogen atom in mutually *trans* positions. Although the alcohol hydrogen atom could not be unambiguously located in the X-ray structure, it is clear from the M-O and O-C bond lengths (Hf1-O4 = 1.926 Å, Hf1-O5 = 2.277 Å; O4-C50 = 1.396 Å, O5-C47 = 1.464 Å) that the bound isopropanol oxygen atom is in a position mutually *cis* to the arm of the tris(phenolate) ligand which contains the substituted methylene carbon. Although the coordinated isopropanol is present, the

ligand can still be considered to be bound in a helical fashion, and as such it is again present in a conformation similar to the *M* enantiomer of **L11**Hf(O^{i}Pr). Although there are differences in the coordination environments of these complexes, but the differences in bond lengths between the central metal atom and the nitrogen and isopropoxide oxygen atoms in each complex can be compared (Table 4.7).

Table 4.7 Bond distances in Å between the central metal atom and the tripodal nitrogen atom, and between the central metal atom and the isopropoxide oxygen atom in zirconium(IV) and hafnium(IV) complexes of **L11**$^{R\text{-Me}}$.

	L11$^{R\text{-Me}}$Zr(O^{i}Pr)	**L11**$^{R\text{-Me}}$Hf(O^{i}Pr)
M-O4	1.919(2)	1.925(3)
M-N	2.453(3)	2.429(3)

The ^{1}H NMR spectra of **L11**$^{R\text{-Me}}$Zr(O^{i}Pr) and **L11**$^{R\text{-Me}}$Hf(O^{i}Pr) show that the solid-state structures described previously appear to persist in $CDCl_3$ solution. In contrast to the room temperature ^{1}H NMR spectra of **L11**Zr(O^{i}Pr) and **L11**Hf(O^{i}Pr), in which the amine tris(phenolate) ligand methylene proton signals appeared as broad resonances, the methylene regions of the ^{1}H NMR spectra for **L11**$^{R\text{-Me}}$Zr(O^{i}Pr) and **L11**$^{R\text{-Me}}$Hf(O^{i}Pr) both have a set of five sharp resonances. Due to the presence of the methyl groups on one phenolate arm of the ligand, the five methylene protons of the **L11**$^{R\text{-Me}}$ ligand are rendered inequivalent. The sharp nature of the peaks suggests that in each metal complex the ligand remains in a single conformation in solution. This rigidity in solution is unsurprising, as a change in conformation of the amine tris(phenolate) ligand to one resembling that of the *P* enantiomer of **L11**Zr(O^{i}Pr) (or **L11**Hf(O^{i}Pr)) would force the methyl group into a position which would result in unfavourable steric repulsions with the adjacent phenol ring (Figure 4.21).

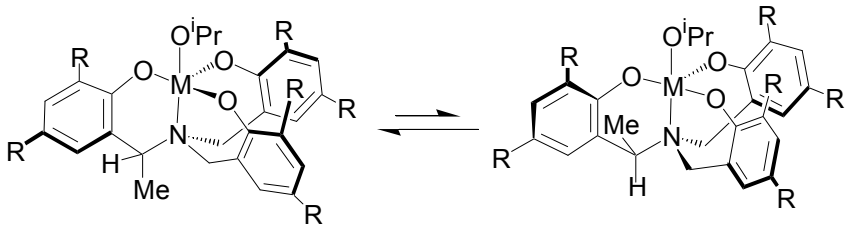

Figure 4.21 Possible diastereomers of **L11**$^{R\text{-Me}}$M(O^{i}Pr), M = Zr, Hf, R = ^{t}Bu.

When **L11**$^{R\text{-Me}}$Zr(O^{i}Pr) and **L11**$^{R\text{-Me}}$Hf(O^{i}Pr) were tested for activity towards the ROP of D,L-LA at room temperature in toluene solution, after 48 hours a small amount of polymer was produced in each case (Table 4.8). Surprisingly, the PDLLA which formed again had a high degree of heterotactic enrichment (P_r = 0.92, 0.91, respectively), although the molecular weight of the polymers was very low, suggesting lower activity than for complexes of the C_3 symmetric ligands **L11**Zr(O^{i}Pr) and **L11**Hf(O^{i}Pr).

Table 4.8 Results for the ROP of D,L-LA under solution and solvent-free conditions. [a]Isolated yield; [b]determined by GPC; [c]determined from analysis of the methine region of the ^{1}H homonuclear decoupled NMR spectrum.

Initiator	T/°C	[M]:[I]	Time/h	% Yield[a]	M_n[b]/g mol^{-1}	PDI[b]	P_r[c]
L11$^{R\text{-Me}}$Zr(O^{i}Pr)	25	100	48	12	1600	1.09	0.92
L11$^{R\text{-Me}}$Hf(O^{i}Pr)	25	100	48	7	1100	1.10	0.91
L11$^{R\text{-Me}}$Zr(O^{i}Pr)	130	300	0.5	75	35300	1.19	0.89
L11$^{R\text{-Me}}$Hf(O^{i}Pr)	130	300	0.5	72	39200	1.20	0.83

The polymerisation reactions carried out under melt conditions also yielded polymer with high values for P_r, again indicating a polymer with a significant degree of heterotactic enrichment. These results would seem to be unsupportive to the dynamic enantiomorphic site control mechanism postulated as the origin of the stereocontrol in the polymerisation. If such a mechanism were in operation, the results of polymerisation experiments utilising enantiopure complexes **L11**$^{R\text{-Me}}$Zr(O^{i}Pr) and **L11**$^{R\text{-Me}}$Hf(O^{i}Pr) would be expected to yield PDLLA with a lower degree of heterotactic enrichment (or even a switch to *isotactic* enrichment) as the complex conformation is effectively 'locked' due to the presence of the extra methyl group.

At present, neither a chain end control mechanism nor an enantiomorphic site control mechanism can completely account for the observation of the high degree of stereocontrol over the ROP of D,L-LA conferred by **L11**Zr(O^{i}Pr), **L11**Hf(O^{i}Pr), **L11**$^{R\text{-Me}}$Zr(O^{i}Pr) and **L11**$^{R\text{-Me}}$Hf(O^{i}Pr). As such, we are compelled to suggest a mechanism which lies somewhere in between these limiting cases and is dependent on *both* the chirality of the metal complex *and* the chirality of the last inserted monomer unit (Figure 4.22): an *enhanced chain end control* mechanism.

Figure 4.22 ROP of D,L-LA initiated by **L11**Zr(O^{i}Pr) (or **L11**Hf(O^{i}Pr)) under an enhanced chain end control mechanism.

In such a case we can envisage that one diastereomer of the monomer-initiator complex 'prefers' to insert a monomer of a particular stereochemistry (for example an (*R,R*)-(*P*-Zr) monomer-initiator complex prefers to insert an *S,S*-LA monomer). Conversely, the selectivity for the monomer of the opposite stereochemistry (here the selectivity of the (*R,R*)-(*M*-Zr) monomer-initiator complex for the *S,S*-LA monomer) is very low. Thus, the monomer of the preferred stereochemistry is inserted. This new monomer-initiator complex (*R,R*)-(*S,S*)-(*P*-Zr) may then switch between diastereomers to one which prefers

to insert an *R,R*-LA monomer (here *R,R*)-(*S,S*)-(*M*-Zr)). In this way both the chirality of the last inserted monomer and the ability of the metal amine tris(phenolate) complex to shuttle between enantiomeric forms (or diastereomeric forms when the polymer chain is growing) are involved in achieving the exceptional degree of selectivity for heterotactic enchainment observed when these initiators are used.

The enhanced chain end control mechanism explains the high degree of heterotactic enrichment in PDLLA produced using **L11**Zr(O^{i}Pr) or **L11**Hf(O^{i}Pr) as the initiator and relies in some part on the facile interconversion between the *P* and *M* forms of the initiator complex. We have already seen that the enantiopure complexes **L11**$^{R\text{-Me}}$Zr(O^{i}Pr) and **L11**$^{R\text{-Me}}$Hf(O^{i}Pr) are 'locked' into a conformation resembling that of the *M* enantiomer of **L11**Zr(O^{i}Pr) or **L11**Hf(O^{i}Pr) by the additional methyl group present on one arm of the **L11**$^{R\text{-Me}}$ ligand. Yet, ROP of D,L-LA initiated by zirconium(IV) and hafnium(IV) complexes of **L11**$^{R\text{-Me}}$ produces PDLLA with a high degree of heterotactic enrichment under both solution and melt conditions.

Figure 4.23 ROP of D,L-LA initiated by **L11**$^{R\text{-Me}}$Zr(O^{i}Pr) (or **L11**$^{R\text{-Me}}$Hf(O^{i}Pr)) under an enhanced chain end control mechanism.

These observations lead us to suggest that a similar enhanced chain end control mechanism is operating in these cases, though the conversion between the *pseudo P* and *M* forms of the initiators favour the *M* conformation (Figure 4.23). The observed reduction in the rate of polymerisation and the retention of stereocontrol at room temperature when **L11**$^{R\text{-Me}}$Zr(O^{i}Pr) or **L11**$^{R\text{-Me}}$Hf(O^{i}Pr) were used as initiators supports this proposed scenario.

4.3 Summary and Perspective

All group 4 metal complexes reported in chapter 2 were tested for activity towards the ROP of D,L-LA, under solution and/or melt conditions with the particular goal of determining both the extent of any stereocontrol achieved over the polymerisation and its origin.

L1Zr(O^{i}Pr)$_2$ and **L10**Ti(O^{i}Pr)$_2$, both of which were active for the ROP of L-LA at 110 ºC in toluene solution (chapter 3), were tested under solution conditions at 25 ºC and 110 ºC. At room temperature, no polymer was produced after 48 hours whereas at 110 ºC PDLLA

was produced in each case in moderate to high yield with molecular weights in the expected range and relatively narrow molecular weight distributions. Examination of the polymer microstructure using ^{1}H homonuclear decoupled NMR spectroscopy revealed **L10**Ti(O^{i}Pr)$_2$ produced atactic PDLLA and **L1**Zr(O^{i}Pr)$_2$ produced PDLLA with a small degree of isotactic enrichment. **L8**Zr(O^{i}Pr)$_2$ was prepared in order to gauge whether a decrease in symmetry of the initiator would have an effect on its ability to exert stereocontrol over the polymerisation. ROP of D,L-LA initiated by **L8**Zr(O^{i}Pr)$_2$ produced PDLLA with a slightly higher degree of isotactic enrichment than that produced using **L1**Zr(O^{i}Pr)$_2$.

With the exception of **L2**Ti(O^{i}Pr)$_2$, all complexes bearing di-anionic amine bis(phenolate) ligands bound in a tetradentate fashion were active for the ROP of D,L-LA under solvent-free conditions at 130 ºC. The titanium(IV) complexes **L1**Ti(O^{i}Pr)$_2$ and **L3**Ti(O^{i}Pr)$_2$ produced atactic PDLLA and in general produced polymer in higher yields than did the zirconium(IV) and hafnium(IV) complexes **L1**Zr(O^{i}Pr)$_2$, **L2**Zr(O^{i}Pr)$_2$, **L8**Zr(O^{i}Pr)$_2$, **L1**Hf(O^{i}Pr)$_2$ and **L2**Hf(O^{i}Pr)$_2$, which all produced PDLLA with a slight enrichment in isotactic linkages. Of the three titanium(IV) complexes bearing di-anionic amine bis(phenolate) ligands bound in a tridentate fashion only **L10**Ti(O^{i}Pr)$_2$ was an active initiator for the ROP of D,L-LA, producing atactic PDLLA under solvent-free, melt conditions.

Zirconium(IV) and hafnium(IV) complexes of the C_3 symmetric amine tris(phenolate) ligand **L11** are active initiators for the ROP at room temperature in toluene solution, producing PDLLA with an exceptionally high degree of heterotactic enrichment, the titanium(IV) analogue was inactive under the same reaction conditions. At 130 ºC under solvent-free conditions **L11**Ti(O^{i}Pr) was active for the ROP of D,L-LA, producing atactic PDLLA, whereas **L11**Zr(O^{i}Pr) and **L11**Hf(O^{i}Pr) again produced PDLLA with a high degree of heterotactic enrichment, a rare achievement under such conditions.

In order to gain some insight into the origin of the remarkable stereocontrol achieved when **L11**Zr(O^{i}Pr) and **L11**Hf(O^{i}Pr) were used as initiators, **L12**Ti(O^{i}Pr) and **L12**Zr(O^{i}Pr) were prepared in which one phenoxy arm of the tri-anionic ligand was replaced with an ethoxy arm, reducing the symmetry of the initiator. These complexes both produced atactic PDLLA under melt reaction conditions and were inactive initiators under room temperature, solution conditions. In addition, zirconium(IV) and hafnium(IV) complexes of the enantiopure ligand **L11**$^{\boldsymbol{R}\text{-Me}}$ were prepared and tested for activity towards the ROP of D,L-LA, again yielding PDLLA with a very high degree of heterotactic enrichment, both at room temperature in solution and under melt conditions.

These results in conjunction with the observation that the room temperature, solution ROP of D,L-LA initiated by **L11**$^{R\text{-}Me}$Zr(O^{i}Pr) or **L11**$^{R\text{-}Me}$Hf(O^{i}Pr) appeared to proceed at a reduced rate as compared to **L11**Zr(O^{i}Pr) or **L11**Hf(O^{i}Pr), led to the conclusion that the origin of stereocontrol in these cases was an enhanced chain end control mechanism. Under this regime, *both* the chirality of the last inserted monomer unit and the chirality at the metal centre influence the stereosequence distribution along the PDLLA backbone.

These results demonstrate that group 4 metal complexes of amine bis(phenolate) and tris(phenolate) ligand are active initiators for the ROP of D,L-LA and exert varying degrees of stereocontrol over the polymerisation. Importantly, several of the complexes were shown to be active under the industrially favoured solvent-free, melt conditions. The exceptionally high degree of heterotactic enrichment observed when **L11**Zr(O^{i}Pr) or **L11**Hf(O^{i}Pr) were used as the initiator reinforces and extends the conclusions drawn from chapters 1 and 3 that subtle variations in ligand structure have a dramatic influence not only on the activity of the initiator, but also on the degree of stereocontrol which it exerts over the polymerisation. The overarching aim of this work was to make a contribution to the search for new initiator systems, which may eventually bring degradable polymers derived from annually renewable resources out of the specialty market and into the mainstream.

References

[1] B. M. Chamberlain, M. Cheng, D. R. Moore, T. M. Ovitt, E. B. Lobkovsky and G. W. Coates, *J. Am. Chem. Soc.* **2001,** 123, (14), 3229-3238.

[2] L. R. Rieth, D. R. Moore, E. B. Lobkovsky and G. W. Coates, *J. Am. Chem. Soc.* **2002,** 124, (51), 15239-15248.

[3] A. Amgoune, C. M. Thomas, T. Roisnel and J. F. Carpentier, *Chem. Eur. J.* **2005,** 12, (1), 169-179.

[4] N. Spassky, M. Wisniewski, C. Pluta and A. LeBorgne, *Macromol. Chem. Phys.* **1996,** 197, (9), 2627-2637.

[5] P. Hormnirun, E. L. Marshall, V. C. Gibson, A. J. P. White and D. J. Williams, *J. Am. Chem. Soc.* **2004,** 126, (9), 2688-2689.

[6] R. Ishii, N. Nomura and T. Kondo, *Polymer Journal* **2004,** 36, (3), 261-264.

[7] O. Dechy-Cabaret, B. Martin-Vaca and D. Bourissou, *Chem. Rev.* **2004,** 104, (12), 6147-6176.

[8] B. J. O'Keefe, M. A. Hillmyer and W. B. Tolman, *J. Chem. Soc.-Dalton Trans.* **2001**, (15), 2215-2224.

[9] A. C. Albertsson and I. K. Varma, *Biomacromolecules* **2003,** 4, (6), 1466-1486.

[10] E. T. H. Vink, K. R. Rabago, D. A. Glassner and P. R. Gruber, *Polym. Degrad. Stab.* **2003,** 80, (3), 403-419.

[11] F. Bonnet, A. R. Cowley and P. Mountford, *Inorg. Chem.* **2005,** 44, (24), 9046-9055.

[12] A. J. Chmura, M. G. Davidson, M. D. Jones, M. D. Lunn, M. F. Mahon, A. F. Johnson, P. Khunkamchoo, S. L. Roberts and S. S. F. Wong, *Macromolecules* **2006,** 39, (21), 7250-7257.

[13] S. K. Russell, C. L. Gamble, K. J. Gibbins, K. C. S. Juhl, W. S. Mitchell, A. J. Tumas and G. E. Hofmeister, *Macromolecules* **2005,** 38, (24), 10336-10340.

[14] A. P. Dove, V. C. Gibson, E. L. Marshall, H. S. Rzepa, A. J. P. White and D. J. Williams, *J. Am. Chem. Soc.* **2006,** 128, (30), 9834-9843.
[15] E. L. Marshall, V. C. Gibson and H. S. Rzepa, *J. Am. Chem. Soc.* **2005,** 127, (16), 6048-6051.
[16] C. E. Housecroft and A. G. Sharpe, *Inorganic Chemistry*, 2nd ed., Pearson Education Ltd, Harlow, Essex, **2005**.
[17] L. E. Turner, M. G. Davidson, M. D. Jones, H. Ott, V. S. Schulz and P. J. Wilson, *Inorg. Chem.* **2006,** 45, (16), 6123-6125.
[18] S. Groysman, I. Goldberg, Z. Goldschmidt and M. Kol, *Inorg. Chem.* **2005,** 44, (14), 5073-5080.
[19] S. Groysman, I. Goldberg, M. Kol, E. Genizi and Z. Goldschmidt, *Adv. Synth. Catal.* **2005,** 347, (2-3), 409-415.
[20] A. J. Chmura, D. M. Cousins, M. G. Davidson, M. D. Jones, M. D. Lunn and M. F. Mahon, *Dalton Trans.* **2008**, (11), 1437-1443.
[21] Y. Kim, G. K. Jnaneshwara and J. G. Verkade, *Inorg. Chem.* **2003,** 42, (5), 1437-1447.
[22] Y. Kim and J. G. Verkade, *Organometallics* **2002,** 21, (12), 2395-2399.
[23] Z. Y. Zhong, P. J. Dijkstra and J. Feijen, *Angew. Chem., Int. Ed. Engl.* **2002,** 41, (23), 4510-+.
[24] N. Nomura, R. Ishii, Y. Yamamoto and T. Kondo, *Chem. Eur. J.* **2007,** 13, (16), 4433-4451.
[25] M. Kol, M. Shamis, I. Goldberg, Z. Goldschmidt, S. Alfi and E. Hayut-Salant, *Inorg. Chem. Commun.* **2001,** 4, (4), 177-179.
[26] M. G. Davidson, C. L. Doherty, A. L. Johnson and M. F. Mahon, *Chem. Commun.* **2003**, (15), 1832-1833.
[27] P. Axe, S. D. Bull, M. G. Davidson, C. J. Gilfillan, M. D. Jones, D. Robinson, L. E. Turner and W. L. Mitchell, *Org. Lett.* **2007,** 9, (2), 223-226.

Chapter 5
Experimental

5 Experimental

5.1 General

All manipulations involving metal complexes were carried out under an atmosphere of dry argon using standard Schlenk and glove-box techniques. Solvents were dried using an MBraun SPS solvent system. $Ti(O^iPr)_4$ was purchased from Aldrich and vacuum distilled prior to use. $Zr(O^iPr)_4(HO^iPr)$ and $Hf(O^iPr)_4(HO^iPr)$ were purchased from Strem and used without further purification. **L1**H_2, **L2**H_2,[1] **L3**H_2[2] and **L11**H_3[3] were prepared using standard literature procedures. Solution ^1H and $^{13}C\{^1H\}$ NMR spectroscopic experiments were performed at ambient temperature unless otherwise stated using a Bruker Advance-300 or 400 MHz FT-NMR spectrometer. $^1H/^{13}C$ NMR chemical shifts are referenced to residual protio solvent resonances. CD_2Cl_2 was vacuum distilled over calcium hydride. Mass Spectra were recorded at the EPSRC National Mass Spectrometry Service Centre, Swansea, UK. Elemental analysis was performed in-house at the Department of Chemistry, University of Bath.

5.2 Ligand Synthesis

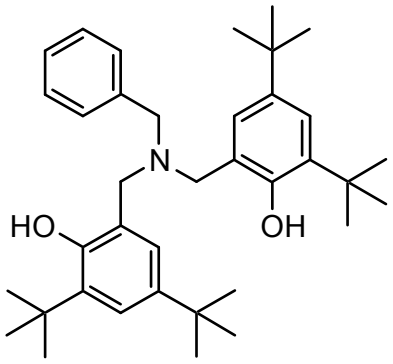

L6H_2

Paraformaldehyde (0.601 g, 20.0 mmol) was suspended in methanol (20 mL) and potassium hydroxide (0.004 g, 0.072 mmol) was added with stirring. Benzylamine (1.09 mL, 1.07 g, 10.0 mmol) was added. A solution of 2,4-di-*tert*-butylphenol (2.06 g, 10.0 mmol) in methanol (20 mL) was then added. The resulting mixture was refluxed for 16 h, after which time the solvent was removed under reduced pressure to afford an yellow oil. The residue was purified by column chromatography on silica with 1:1 CH_2Cl_2:hexane as eluent. The first eluted fraction was collected and the volatiles were removed under reduced pressure, yielding a yellow oil, identified as the *N*-benzyl benzoxazine (**L4,** 2.0 g). Benzoxazine (2.0 g, 5.9 mmol) and 2,4-di-*tert*-butylphenol (1.2 g, 5.9 mmol) were combined in a round bottom flask fitted with a water cooled condenser. The mixture was heated to 155 ºC for 3 h, then allowed to cool. The residue was purified by column chromatography on silica with 1:1 CH_2Cl_2:hexane as eluent. The first eluted fraction was

collected and the volatiles removed under reduced pressure affording **L6**H_2 as a white powder. Yield 1.9 g, 59%. HRMS (ESI): *calcd.* for ($C_{37}H_{53}NO_2$+H): 544.4149, *found* 544.4151 (M+H). Anal: Calc for $C_{37}H_{53}NO_2$, 81.72%; H, 9.82%; N, 2.58%;. Found C, 81.6%; H, 9.71%; N, 2.61%.

^{1}H NMR (400 13 MHz, $CDCl_3$)
7.35-7.37 (m, 5H, Ar*H*)
7.21 (d, 2H, Ar*H*), ^{4}J(H-H) 2.4 Hz
6.93 (m, 2H, Ar*H*), ^{4}J(H-H) 2.4 Hz
3.65 (s, 4H, CH_2)
3.59 (s, 2H, CH_2)
1.40 (s, 18H, C(CH_3)$_3$)
1.27 (s, 18H, C(CH_3)$_3$)

^{13}C{^{1}H} NMR (100.62 MHz, $CDCl_3$)
152.5 (*C*)
141.8 (*C*)
137.8 (*C*)
136.3 (*C*)
130.0 (*C*H)
129.3 (*C*H)
128.2 (*C*H)
125.5 (*C*H)
124.0 (*C*H)
121.8 (*C*)
58.8 (*C*H_2)
57.2 (*C*H_2)
35.2 (*C*(CH_3)$_3$)
34.5 (*C*(CH_3)$_3$)
32.0 (C(*C*H_3)$_3$)
30.0 (C(*C*H_3)$_3$)

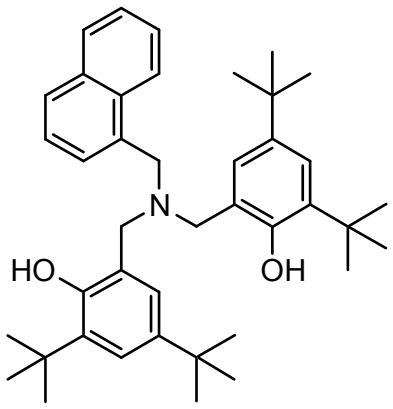

L7H_2
Paraformaldehyde (0.465 g, 15.5 mmol) was suspended in methanol (20 mL) and potassium hydroxide (0.004 g, 0.072 mmol) was added with stirring. The resulting colourless solution was cooled to 0 ºC and 1-naphthalenemethylamine (1.0 g, 6.3 mmol) was added. A solution of 2,4-di-*tert*-butylphenol (1.3 g, 6.5 mmol) in methanol (25 mL) was then added and the mixture allowed to warm to room temperature. The resulting mixture was refluxed for 16 h, after which time the solvent was removed under reduced pressure to afford an orange-brown oil. The residue was purified by column chromatography on silica with 1:1 CH_2Cl_2:hexane as eluent. The first eluted fraction was collected and the volatiles were removed under reduced pressure, yielding a yellow oil, identified as the naphthyl-substituted benzoxazine (**L5,** 1.3 g). Benzoxazine (1.3 g, 3.4 mmol) and 2,4-di-*tert*-butylphenol (0.70 g, 3.4 mmol) were combined in a round bottom flask fitted with a water cooled condenser. The mixture was heated to 155 ºC for 3.5 h,

then allowed to cool. The residue was purified by column chromatography on silica with 2:1 hexane:CH_2Cl_2 as eluent, the first eluted fraction was collected and the volatiles were removed under reduced pressure to give a yellow oil which solidified on standing overnight. Dissolution of the solid in a minimum amount of hexane with gentle heating followed by cooling to room temperature produced **L7**H_2 as pale yellow needles. Yield 1.6 g, 43%. HRMS (ESI): *calcd.* for ($C_{41}H_{55}NO_2$+H): 594.4306, *found* 594.4309 (M+H). Anal: Calc for $C_{41}H_{55}NO_2$, 82.92%; H, 9.33%; N, 2.36%. Found C, 82.7%; H, 9.57%; N, 2.25%.

^{1}H NMR (400.13 MHz, $CDCl_3$)

7.82 (m, 3H, Ar*H*)	4.04 (s, 4H, CH_2)
7.49 (m, 4H, Ar*H*)	3.69 (s, 4H, CH_2)
7.23 (d, 2H, Ar*H*), ^{4}J(H-H) 2.4 Hz	1.40 (s, 18H, C(CH_3)$_3$)
6.99 (d, 2H, Ar*H*), ^{4}J(H-H) 2.4 Hz	1.28 (s, 18H. C(CH_3)$_3$)

^{13}C{^{1}H} NMR (100.62 MHz, $CDCl_3$)

151.8 (*C*)	125.5 (*C*H)
141.6 (*C*)	125.1 (*C*H)
136.2 (*C*)	123.7 (*C*H)
134.0 (*C*)	123.6 (*C*H)
133.0 (*C*)	121.5 (*C*)
132.1 (*C*)	57.5 (*C*H$_2$)
129.2 (*C*H)	56.9 (*C*H$_2$)
128.9 (*C*H)	34.9 (*C*(CH$_3$)$_3$)
128.7 (*C*H)	34.1 (*C*(CH$_3$)$_3$)
126.7 (*C*H)	31.5 (C(*C*H$_3$)$_3$)
126.0 (*C*H)	29.7 (C(*C*H$_3$)$_3$)

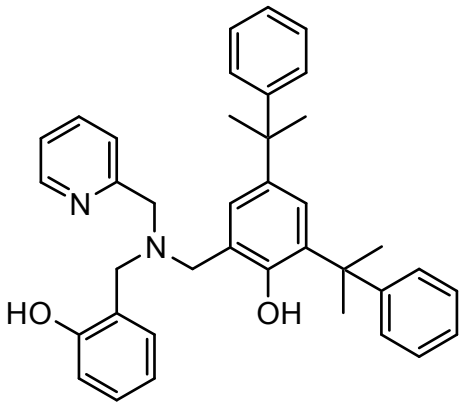

L8H_2

2-(2-hydroxybenzylaminomethyl)pyridine[2] (1.0 g, 4.7 mmol), paraformaldehyde (0.14 g, 4.67 mmol) and 2,4-Bis(*α,α*-dimethylbenzyl)phenol (1.5 g, 4.7 mmol) were combined in a round bottomed flask and heated together at 110 ºC with stirring for 2 hours, after which time TLC (CH_2Cl_2) showed that all starting material had been consumed. The reaction mixture was allowed to cool and the resulting light orange glassy solid was dissolved in dichloromethane. The volatiles were removed under reduced pressure and the resulting

light orange oil triturated with methanol. The white solid **L8**H_2 was filtered and washed with methanol. 1.8 g, 69%. HRMS (ESI): *calcd.* for ($C_{38}H_{40}N_2O_2$+H): 557.3163, *found* 557.3161 (M+H). Anal: Calc for $C_{38}H_{40}N_2O_2$ C, 81.98%; H, 7.24%; N, 5.03%. Found: C, 81.7%; H, 7.27%; N 5.07%.

^{1}H NMR (400.13MHz, $CDCl_3$)

8.47 (m, 1H, Ar*H*)
7.62 (m, 1H, Ar*H*)
7.15-7.30 (m, 13 H, Ar*H*)
6.89 (m, 3H, Ar*H*)
6.71 (m, 2H, Ar*H*)
3.70 (s, 2H, CH_2)
3.63 (s, 2H, CH_2)
3.62 (s, 2H, CH_2)
1.69 (s, 6H CPh(CH_3)$_2$)
1.68 (s, 6H CPh(CH_3)$_2$)

^{13}C{^{1}H} NMR (100.62 MHz, $CDCl_3$)

157.2 (*C*)
155.2 (*C*)
153.4 (*C*)
151.4 (*C*)
147.6 (*C*H)
140.1 (*C*)
137.8 (*C*H)
135.7 (*C*)
131.8 (*C*H)
129.3 (*C*H)
127.9 (*C*H)
127.6 (*C*H)
126.7 (*C*H)
125.7 (*C*H)
125.4 (*C*H)
125.1 (*C*H)
124.8 (*C*H)
124.6 (*C*H)
122.8 (*C*H)
121.5 (*C*)
121.2 (*C*)
119.5 (*C*H)
117.6 (*C*H)
57.5 (*C*H_2)
54.4 (*C*H_2)
52.8 (*C*H_2)
42.4 (*C*Ph(CH$_3$)$_2$)
42.1 (*C*Ph(CH$_3$)$_2$)
31.1 (CPh(*C*H$_3$)$_2$)
29.4 (CPh(*C*H$_3$)$_2$)

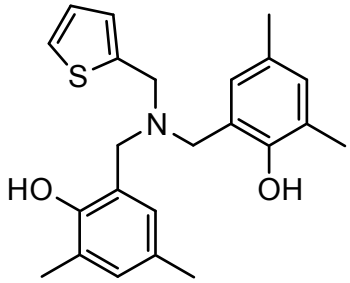

L9H_2

2,4-dimethylphenol (2.10 mL, 2.16 g, 17.7 mmol), paraformaldehyde (0.584 g, 19.4 mmol) and 2-(aminomethyl)thiophene (0.91 mL, 1.00 g, 8.8 mmol) were combined in a round bottomed flask and heated together with stirring to 100 ºC for 2 hours, until TLC (CH_2Cl_2) showed no 2-(aminomethyl)thiophene starting material remained. The resulting dark yellow oil was purified by column chromatography (silica, CH_2Cl_2 as eluent), **L9**H_2 as a yellow oil. Yield 1.01 g, 30%. HRMS (ESI): *calcd.* for ($C_{23}H_{27}NO_2S$+H): 382.1835,

found 382.1836 (M+H). Anal: Calc for $C_{23}H_{27}NO_2S$, C, 72.40%; H, 7.13%, N, 3.67%. Found C, 73.8%; H, 7.01%; N, 3.60%.

^{1}H NMR (400.13 MHz, $CDCl_3$)

7.26 (m, 1H, SAr*H*)	3.84 (s, 2H, CH_2)
6.99 (m, 2H, SAr*H*)	3.69 (s, 4H, CH_2)
6.87 (s, 2H, Ar*H*)	2.22 (s, 12H, CH_3)
6.75 (s, 2H, Ar*H*)	

^{13}C{^{1}H} NMR (100.62 MHz, $CDCl_3$)

151.8 (*C*)	126.1 (*C*H)
138.8 (*C*)	124.5 (*C*)
131.1 (*C*H)	121.2 (*C*)
128.7 (*C*H)	55.3 (*C*H$_2$)
128.6 (*C*)	51.0 (*C*H$_2$)
127.9 (*C*H)	20.4 (*C*H$_3$)
127.0 (*C*H)	15.9 (*C*H$_3$)

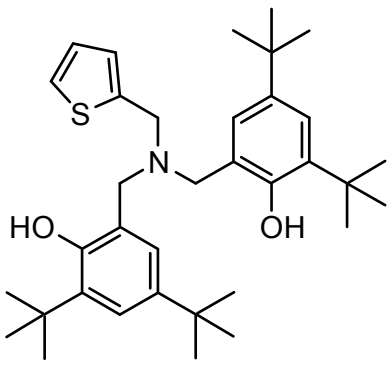

L10H_2

2,4-di-*tert*-butylphenol (1.8 g, 8.8 mmol), paraformaldehyde (0.30 g, 10 mmol) and 2-(aminomethyl)thiophene (0.45 mL, 0.50 g, 4.4 mmol) were combined in a round bottomed flask and heated together with stirring to 100 ºC for 5 hours, until TLC (CH_2Cl_2) showed no 2-(aminomethyl)thiophene starting material remained. The resulting yellow oil solidified on standing and was washed with methanol yielding **L10**H_2 as a white powder. Yield 0.20 g, 8.3%. HRMS (ESI): *calcd.* for ($C_{35}H_{51}NO_2S$+H): 550.3713, *found* 550.3714 (M+H). Anal: Calc for $C_{35}H_{51}NO_2S$, C, 76.45%; H, 9.35%, N, 2.55%. Found C, 77.8%; H, 9.29%; N, 2.50%.

^{1}H NMR (400.13 MHz, $CDCl_3$)

7.26 (m, 1H, SAr*H*)	3.85 (s, 2H, CH_2)
7.22 (d, 2H, Ar*H*), ^{4}J(H-H) 2.4 Hz	3.69 (s, 4H, CH_2)
7.01 (m, 2H, SAr*H*)	1.41 (s, 18H, CH_3)
6.94 (d, 2H, Ar*H*), ^{4}J(H-H) 2.4 Hz	1.28 (s, 18H, CH_3)

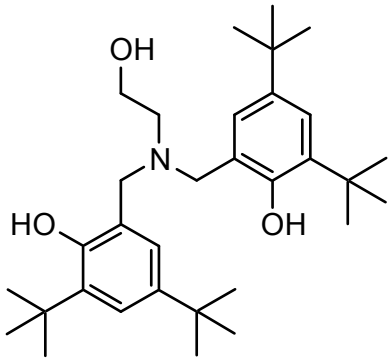

L12H_3

2,4-di-*tert*-butylphenol (10.1 g, 49.1 mmol) was dissolved in methanol and paraformaldehyde (1.80 g, 60.0 mmol) was added with stirring. Ethanolamine (1.48 mL, 1.50 g, 24.6 mmol) was added and the reaction mixture brought to reflux overnight. After this time, the volatiles were removed under reduced pressure yielding a yellow oil which, on standing, afforded the desired product as a white microcrystalline solid. The solid was washed with pentane and dried in air. Yield 1.63 g, 13%. HRMS (ESI): *calcd.* for ($C_{32}H_{51}NO_3H$): 498.3948, *found* 498.3934 (M+H). Anal: Calc for $C_{32}H_{51}NO_3$, C, 77.22%; H, 10.33%, N, 2.81%. Found C, 77.2%; H, 10.3%; N, 2.77%.

^{1}H NMR (400.13 MHz, $CDCl_3$)

7.23 (d, 1H, Ar*H*), ^{4}J(H-H) 2.5 Hz
6.91 (d, 1H, Ar*H*), ^{4}J(H-H) 2.5 Hz
3.88 (t, 2H, CH_2), ^{3}J(H-H) 5.3 Hz
3.77 (s, 4H, CH_2)
2.74 (t, 2H, CH_2, ^{3}J(H-H) 5.3 Hz)
1.41 (s, 18H, CH_3)
1.28 (s, 18H, CH_3)

^{13}C{^{1}H} NMR (100.62 MHz, $CDCl_3$)

152.6 (*C*)
141.1 (*C*)
136.0 (*C*)
125.0 (*C*H)
123.5 (*C*H)
121.6 (*C*)
61.0 (*C*H_2)
57.7 (*C*H_2)
53.5 (*C*H_2)
34.9 (*C*)
34.1 (*C*)
31.6 (*C*H_3)
29.6 (*C*H_3)

5.3 Complex Synthesis

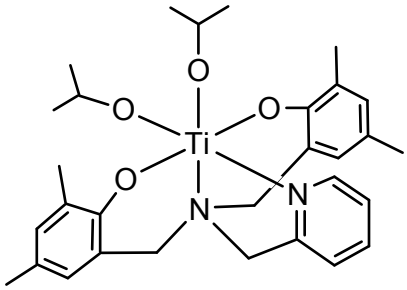

L1Ti(O^iPr)$_2$

L1H_2 (1.0 g, 2.7 mmol) was dissolved in CH_2Cl_2 (10 mL) in a Schlenk tube. Ti(O^iPr)$_4$ (0.78 mL, 2.7 mmol) was added, and the previously clear, pale pink solution turned bright yellow. Stirring continued for 2h, after which time the volatiles were removed under reduced pressure to leave a yellow solid. Crystallisation from hexane solution afforded **L1**Ti(O^iPr)$_2$ as yellow blocks. Yield 1.4 g, 97%. Anal: Calc for $C_{30}H_{40}N_2O_4Ti$, C, 66.66%; H, 7.46%; N, 5.18%. Found C, 66.3%; H, 7.36%; N, 5.28%.

^{1}H NMR (400.13 MHz, $CDCl_3$)

8.76 (d, 1H, NAr*H*), ^{3}J(H-H) 4.8 Hz
7.28 (td, 1H, NAr*H*), ^{3}J(H-H) 7.6 Hz, ^{3}J(H-H) 1.8 Hz
6.93 (t, 1H, NAr*H*), ^{3}J(H-H) 5.7 Hz
6.65 (s, 4H, Ar*H*)
6.43 (d, 1H, NAr*H*), ^{3}J(H-H) 8.0 Hz
5.31 (sept, 1H, C*H*(CH_3)$_2$), ^{3}J(H-H) 6.1 Hz
4.82 (sept, 1H, C*H*(CH_3)$_2$), ^{3}J(H-H) 6.1 Hz
4.64 (d, 2H, CH_2), ^{3}J(H-H) 12.3 Hz
3.67 (s, 2H, CH_2)
3.29 (d, 2H, CH_2), ^{3}J(H-H) 12.6 Hz
2.15 (s, 6H, CH_3)
2.00 (s, 6H, CH_3)
1.46 (d, CH(CH_3)$_2$), ^{3}J(H-H) 6.1 Hz
1.18 (d, CH(CH_3)$_2$), ^{3}J(H-H) 6.1 Hz

^{13}C{^{1}H} NMR (100.62 MHz, $CDCl_3$)

160.6 (*C*)
156.6 (*C*)
148.8 (*C*H)
137.5 (*C*H)
130.7 (*C*H)
127.3 (*C*H)
125.6 (*C*)
124.9 (*C*)
123.0 (*C*)
121.7 (*C*H)
120.1 (*C*H)
76.8 (*C*H(CH_3)$_2$)
63.6 (*C*H_2)
58.6 (*C*H_2)
26.2 (CH_3)
26.1 (CH_3)
20.4 (CH(*C*H_3)$_2$)
16.4 (CH(*C*H_3)$_2$)

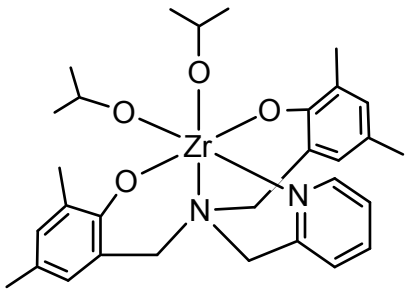

L1Zr(O^iPr)$_2$

L1H_2 (0.50 g, 1.3 mmol) was dissolved in CH_2Cl_2 (10 mL) in a Schlenk tube. A solution of Zr(O^iPr)$_4$(HO^iPr) (0.52 g, 1.3 mmol) in CH_2Cl_2 was added, and the previously colourless solution remained unchanged. Stirring continued for 2h, after which time the volatiles were removed under reduced pressure to leave a white solid. Crystallisation from hexane solution yielded **L1**Zr(TiO^iPr)$_2$ as colourless blocks. Yield 0.75 g, 96%. Anal: Calc for $C_{30}H_{40}N_2O_4Zr$, C, 61.71%; H, 6.91%; N, 4.80%. Found C, 61.3%; H, 6.83%; N, 4.78%.

^{1}H NMR (400.13 MHz, $CDCl_3$)

8.76 (d, 1H, NAr*H*), ^{3}J(H-H) 5.1 Hz
7.29 (td, 1H, NAr*H*), ^{3}J(H-H) 7.7 Hz, ^{3}J(H-H) 1.6 Hz
6.94 (t, 1H, NAr*H*), ^{3}J(H-H) 6.1 Hz
6.65 (s, 4H, Ar*H*)
6.41 (d, 1H, NAr*H*), ^{3}J(H-H) 7.9 Hz
5.71 (d, 2H, CH_2), ^{3}J(H-H) 12.3 Hz
4.62 (sept, 1H, CH(CH_3)$_2$), ^{3}J(H-H) 6.1 Hz
4.40 (sept, 1H, CH(CH_3)$_2$), ^{3}J(H-H) 6.1 Hz
3.62 (s, 2H, CH_2)
3.28 (d, 2H, CH_2), ^{3}J(H-H) 12.6 Hz
2.15 (s, 6H, CH_3)
1.96 (s, 6H, CH_3)
1.43 (d, 6H, CH(CH_3)$_2$), ^{3}J(H-H) 6.1 Hz
1.18 (d, 6H, CH(CH_3)$_2$), ^{3}J(H-H) 6.1 Hz

^{13}C{^{1}H} NMR (100.62 MHz, $CDCl_3$)

160.0 (*C*)
156.4 (*C*)
148.4 (*C*H)
137.8 (*C*H)
131.1 (*C*H)
127.7 (*C*H)
125.9 (*C*)
124.9 (*C*)
122.5 (*C*)
121.7 (*C*H)
120.7 (*C*H)
71.1 (*C*H(CH_3)$_2$)
71.2 (*C*H(CH_3)$_2$)
63.3 (*C*H_2)
27.3 (*C*H_3)
27.1 (*C*H_3)
20.4 (CH(*C*H_3)$_2$)
16.1 (CH(*C*H_3)$_2$)

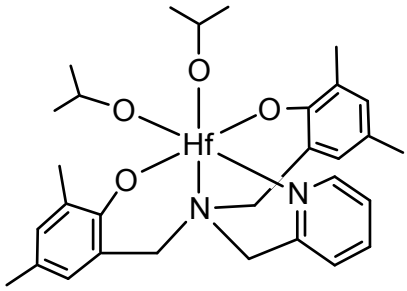

L1Hf(O^iPr)$_2$

L1H_2 (0.57 g, 1.2 mmol) was dissolved in CH_2Cl_2 (20mL) in a Schlenk tube. A solution of Hf(O^iPr)$_4$(HO^iPr) (0.45 g, 1.2 mmol) in CH_2Cl_2 was added, and the previously clear, colourless solution remained unchanged. Stirring continued for 2 h, after which time the volatiles were removed under reduced pressure to leave an oily, white solid. Crystallisation from a hexane/toluene solution yielded **L1**Hf(O^iPr)$_2$ as a white, microcrystalline solid. Yield 0.67 g, 82%. Anal: Calc for $C_{31}H_{44}N_2O_4Hf$, C, 53.18%; H, 6.45%, N, 4.08%. Found C, 56.0%; H, 6.37%; N, 4.16%.

^{1}H NMR (400.13 MHz, $CDCl_3$)

8.70 (d, 1H, NAr*H*), ^{3}J(H-H) 5.1 Hz
7.32 (dt, 1H, NAr*H*), ^{3}J(H-H) 7.7 Hz, ^{4}J(H-H) 1.9 Hz
7.96 (m, 1H, NAr*H*)
6.68 (s, 1H, Ar*H*)
6.64 (s, 1H, Ar*H*)
6.44 (d, 1H, NAr*H*), ^{3}J(H-H) 7.9 Hz
4.77 (d, 2H, CH_2), ^{3}J(H-H) 12.5 Hz
4.73 (sept, 1H, CH(CH_3)$_2$), ^{3}J(H-H) 6.1 Hz
4.50 (sept, 1H, CH(CH_3)$_2$), ^{3}J(H-H) 6.0 Hz
3.67 (s, 2H, CH_2)
3.28 (d, 2H, CH_2), ^{3}J(H-H) 12.5 Hz
2.16 (s, 6H, CH_3)
1.97 (s, 6H, CH_3)
1.44 (d, 6H, CH(CH_3)$_2$), ^{3}J(H-H) 6.0 Hz
1.19 (d, 6H, CH(CH_3)$_2$), ^{3}J(H-H) 6.1 Hz

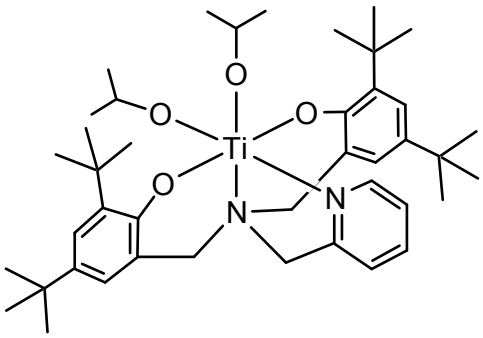

L2Ti(O^iPr)$_2$

L2H_2 (1.0 g, 1.8 mmol) was dissolved in CH_2Cl_2 (10 mL) in a Schlenk tube. Ti(O^iPr)$_4$ (0.54 mL, 1.8 mmol) was added, and the previously clear, colourless solution turned bright yellow. Stirring continued for 2h, after which time the volatiles were removed under reduced pressure to leave a yellow solid. Crystallisation from hexane solution

yielded **L2**Ti(O^iPr)$_2$ as yellow plates. Yield 1.3 g, 97%. Anal: Calc for $C_{42}H_{66}N_2O_4Ti$, C, 70.96%; H, 9.36%; N, 3.94%. Found C, 68.8%; H, 8.81%; N, 3.53%.

^{1}H NMR (400.13 MHz, $CDCl_3$)

8.72 (d, 1H, NAr*H*), ^{3}J(H-H) 4.6 Hz
7.23 (td, 1H, NAr*H*), ^{3}J(H-H) 7.6 Hz, ^{3}J(H-H) 1.8 Hz
7.03 (d, 2H, Ar*H*), ^{4}J(H-H) 2.5 Hz
6.89 (d, 2H, Ar*H*), ^{4}J(H-H) 2.5 Hz
6.82 (m, 1H, NAr*H*)
6.39 (d, 1H, NAr*H*), ^{3}J(H-H) 7.8 Hz
5.26 (sept, 1H, C*H*(CH_3)$_2$), ^{3}J(H-H) 6.1 Hz
5.03 (sept, 1H, C*H*(CH_3)$_2$), ^{3}J(H-H) 6.1 Hz
4.76 (d, 2H, CH_2), ^{3}J(H-H) 12.1 Hz
3.76 (s, 2H, CH_2)
3.34 (d, 2H, CH_2), ^{3}J(H-H) 12.1 Hz
1.47 (d, 6H, CH(CH_3)$_2$), ^{3}J(H-H) 6.1 Hz
1.29 (s, 18H, C(CH_3)$_3$)
1.24 (s, 18H, C(CH_3)$_3$)
1.22 (d, 6H, CH(CH_3)$_2$), ^{3}J(H-H) 6.1 Hz

^{13}C{^{1}H} NMR (100.62 MHz, $CDCl_3$)

160.9 (*C*)
156.7 (*C*)
150.2 (*C*H)
138.5 (*C*)
137.4 (*C*H)
135.4 (*C*)
124.3 (*C*H)
123.8 (*C*)
123.2 (*C*H)
121.2 (*C*H)
119.6 (*C*H)
77.2 (*C*H(CH_3)$_2$)
77.1 (*C*H(CH_3)$_2$)
64.4 (*C*H)
57.8 (*C*H_2)
34.9 (*C*(CH_3)$_3$)
34.0 (*C*(CH_3)$_3$)
31.8 (C(*C*H_3)$_3$)
30.0 (C(*C*H_3)$_3$)
26.9 (CH(*C*H_3)$_2$)
26.3 (CH(*C*H_3)$_2$)

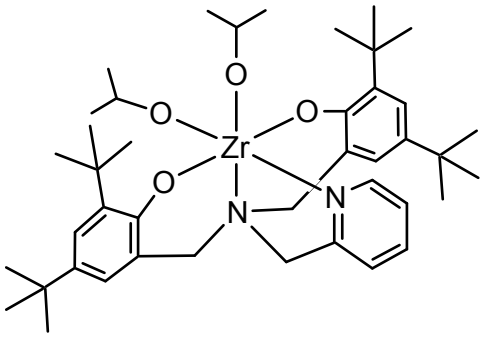

L2Zr(O^iPr)$_2$

L2H_2 (0.50 g, 0.91 mmol) was dissolved in CH_2Cl_2 (10mL) in a Schlenk tube. A solution of Zr(O^iPr)$_4$(HO^iPr) (0.35 g, 0.91 mmol) in CH_2Cl_2 was added, and the previously clear, colourless solution remained unchanged. Stirring continued for 2 h, after which time the volatiles were removed under reduced pressure to leave a white solid. Recrystallisation from hexane solution yielded **L2**Zr(O^iPr)$_2$ as colourless blocks. Yield 0.64 g, 94%. Anal: Calc for $C_{42}H_{66}N_2O_4Zr$, C, 66.89%; H, 8.82%; N, 3.71%. Found C, 66.5%; H, 8.46%; N, 3.84%.

^{1}H NMR (400.13 MHz, $CDCl_3$)

8.62 (d, 1H, NAr*H*), ^{3}J(H-H) 4.6 Hz
7.26 (td, 1H, NAr*H*), ^{3}J(H-H) 7.6 Hz, ^{3}J(H-H) 1.8 Hz
7.04 (d, 2H, Ar*H*), ^{4}J(H-H) 2.5 Hz
6.93 (m, 1H, NAr*H*)
6.90 (d, 2H, Ar*H*), ^{4}J(H-H) 2.5 Hz
6.41 (d, 1H, NAr*H*), ^{3}J(H-H) 7.9 Hz
4.79 (d, 2H, CH_2), ^{3}J(H-H) 12.3 Hz
4.64 (sept, 1H, CH(CH_3)$_2$), ^{3}J(H-H) 6.0 Hz
4.40 (sept, 1H, CH(CH_3)$_2$), ^{3}J(H-H) 6.0 Hz
3.73 (s, 2H, CH_2)
3.36 (d, 2H, CH_2), ^{3}J(H-H) 12.4 Hz
1.42 (d, 6H, CH(CH_3)$_2$), ^{3}J(H-H) 6.0 Hz
1.28 (s, 18H, C(CH_3)$_3$)
1.25 (s, 18H, C(CH_3)$_3$)
1.21 (d, 6H, CH(CH_3)$_2$), ^{3}J(H-H) 6.0 Hz

^{13}C{^{1}H} NMR (100.62 MHz, $CDCl_3$)

159.5 (*C*)
157.6 (*C*)
149.8 (*C*H)
137.9 (*C*)
137.7 (*C*H)
136.2 (*C*)
124.7 (*C*H)
123.4 (*C*H)
123.4 (*C*)
121.5 (*C*H)
120.3 (*C*H)
71.1 (*C*H(CH_3)$_2$)
70.9 (*C*H(CH_3)$_2$)
63.9 (*C*H$_2$)
57.1 (*C*H$_2$)
34.9 (*C*(CH_3)$_3$)
34.0 (*C*(CH_3)$_3$)
31.8 (C(*C*H$_3$)$_3$)
29.6 (C(*C*H$_3$)$_3$)
27.7 (CH(*C*H$_3$)$_2$)
27.2 (CH(*C*H$_3$)$_2$)

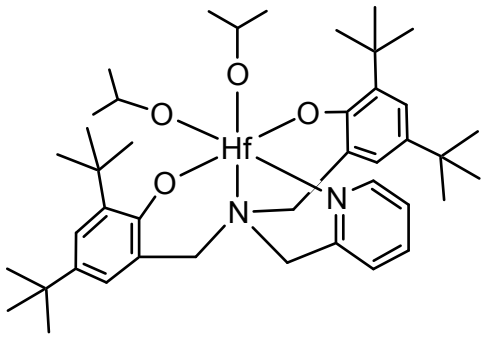

L2Hf(O^{i}Pr)$_2$

L2H_2 (0.40 g, 0.73 mmol) was dissolved in CH_2Cl_2 (10mL) in a Schlenk tube. A solution of Hf(O^{i}Pr)$_4$(HO^{i}Pr) (0.35 g, 0.73 mmol) in CH_2Cl_2 was added, and the previously clear, colourless solution remained unchanged. Stirring continued for 2 h, after which time the volatiles were removed under reduced pressure to leave a white solid. Crystallisation from hexane solution yielded **L1**Hf(O^{i}Pr)$_2$ as colourless blocks. Yield 0.58 g, 94%. Anal: Calc for $C_{42}H_{66}N_2O_4Hf$, C, 59.95%; H, 7.91%, N, 3.33%. Found C, 59.6%; H, 7.59%; N, 3.23%.

^{1}H NMR (400.13 MHz, $CDCl_3$)

8.66 (d, 1H, NAr*H*), ^{3}J(H-H) 4.6 Hz
7.29 (dt, 1H, NAr*H*), ^{3}J(H-H) 7.7 Hz, ^{3}J(H-H) 1.7 Hz
7.07 (d, 2H, Ar*H*), ^{4}J(H-H) 2.5 Hz
6.95 (t, 1H, NAr*H*), ^{3}J(H-H) 6.6 Hz
6.89 (d, 2H, Ar*H*), ^{4}J(H-H) 2.5 Hz
6.44 (d, 1H, NAr*H*), ^{3}J(H-H) 7.9 Hz
4.84 (d, 2H, CH_2), ^{3}J(H-H) 12.3 Hz
4.84 (d, 2H, CH_2), ^{3}J(H-H) 12.4 Hz
4.73 (sept, 1H, CH(CH_3)$_2$), ^{3}J(H-H) 6.0 Hz
4.50 (sept, 1H, CH(CH_3)$_2$), ^{3}J(H-H) 6.0 Hz
3.79 (s, 2H, CH_2)
3.36 (d, 2H CH_2), ^{3}J(H-H) 12.4
1.42 (d, 6H, CH(CH_3)$_2$), ^{3}J(H-H) 6.0 Hz
1.27 (s, 18H, C(CH_3)$_3$)
1.24 (s, 18H, C(CH_3)$_3$)
1.22 (d, 6H, CH(CH_3)$_2$), ^{3}J(H-H) 6.0 Hz

^{13}C{^{1}H} NMR (100.62 MHz, $CDCl_3$)

159.6 (*C*)
150.1 (*C*H)
138.0 (*C*)
137.9 (*C*H)
136.8 (*C*)
124.6 (*C*H)
123.7 (*C*H)
123.2 (*C*)
121.6 (*C*H)
120.4 (*C*H)
70.9 (*C*H(CH$_3$)$_2$)
70.5 (*C*H(CH$_3$)$_2$)
63.9 (*C*H$_2$)
57.3 (*C*H$_2$)
34.9 (*C*(CH$_3$)$_3$)
34.0 (*C*(CH$_3$)$_3$)
31.8 (C(*C*H$_3$)$_3$)
29.7 (C(*C*H$_3$)$_3$)
27.9 (CH(C*H*$_3$)$_2$)
27.5 (CH(C*H*$_3$)$_2$)

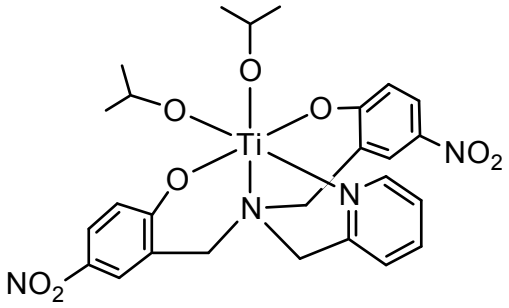

L3Ti(O^{i}Pr)$_2$

L3H_2 (0.50 g, 1.2 mmol) was dissolved in CH_2Cl_2 (20mL) in a Schlenk tube. Ti(O^{i}Pr)$_4$ (0.35 g, 0.36 mL, 1.2 mmol) was added, and the previously clear, pale yellow solution turned bright yellow and remained clear. Stirring continued for 2 h, after which time the volatiles were removed under reduced pressure to leave a yellow solid. Crystallisation from toluene yielded **L1**Hf(O^{i}Pr)$_2$ as yellow plates. Yield 0.65 g, 93%. Anal: Calc for $C_{26}H_{36}N_4O_8Ti$, C, 54.37%; H, 5.26%, N, 9.75%. Found C, 55.4.9%; H, 5.31%; N, 9.67%.

^{1}H NMR (400.13 MHz, $CDCl_3$)

8.71 (d, 1H, NAr*H*), ^{3}J(H-H) 4.9 Hz
8.01 (m, 2H, Ar*H*)
7.93 (m, 2H, Ar*H*)
7.46 (t, 1H, NAr*H*), ^{3}J(H-H) 7.7 Hz
7.17 (t, 1H, NAr*H*), ^{3}J(H-H) 5.9 Hz
6.70 (d, 1H, NAr*H*), ^{3}J(H-H) 7.7 Hz
6.47 (d, 2H, Ar*H*), ^{3}J(H-H) 9.0 Hz
5.18 (sept, 1H, CH(CH$_3$)$_2$), ^{3}J(H-H) 6.1 Hz
4.80 (sept, 1H, CH(CH$_3$)$_2$), ^{3}J(H-H) 6.1 Hz
4.62 (d, 2H, CH_2), ^{3}J(H-H) 13.2 Hz
3.86 (s, 2H, CH_2)
3.58 (d, 2H CH_2), ^{3}J(H-H) 13.2

1.51 (d, 6H, CH(CH_3)$_2$), ^{3}J(H-H) 6.1 Hz
1.16 (d, 6H, CH(CH_3)$_2$), ^{3}J(H-H) 6.0 Hz

^{13}C{^{1}H} NMR (100.62 MHz, $CDCl_3$)
170.6 (*C*)
155.4 (*C*)
149.1 (*C*H)
139.1 (*C*H)
138.1 (*C*)
126.2 (*C*H)
125.8 (*C*H)
123.4 (*C*H)
123.0 (*C*)
121.4 (*C*H)
117.6 (*C*H)
80.1 (*C*H(CH$_3$)$_2$)
79.9 (*C*H(CH$_3$)$_2$)
62.7 (*C*H$_2$)
58.9 (*C*H$_2$)
25.9 (CH(CH_3)$_2$)
25.7 (CH(CH_3)$_2$)

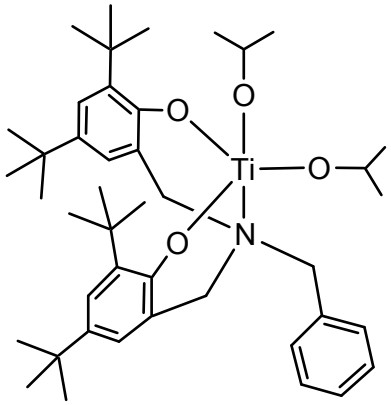

L6Ti(O^{i}Pr)$_2$

L6H$_2$ (1.0 g, 1.8 mmol) was dissolved in CH_2Cl_2 (10 mL) in a Schlenk tube. Ti(O^{i}Pr)$_4$ (0.54 mL, 1.8 mmol) was added, and the previously clear, colourless solution turned bright yellow. Stirring continued for 2 h, after which time the volatiles were removed under reduced pressure to leave a yellow solid. Crystallisation from hexane solution yielded **L6**Ti(O^{i}Pr)$_2$ as yellow plates. Yield 0.32 g, 91%. Anal: Calc for $C_{43}H_{65}NO_4Ti$, C, 72.96%; H, 9.26%; N, 1.98%. Found C, 72.2%; H, 9.48%; N, 1.60%.

^{1}H NMR (400.13 MHz, $CDCl_3$)
7.22 (m, 3H, Ar*H*)
7.15 (d, 2H, Ar*H*), ^{4}J(H-H) 2.5 Hz
6.94 (m, 2H, Ar*H*)
6.72 (d, 2H, Ar*H*), ^{4}J(H-H) 2.5 Hz
5.01 (sept, 1H, C*H*(CH$_3$)$_2$), ^{3}J(H-H) 6.1 Hz
4.91 (sept, 1H, C*H*(CH$_3$)$_2$), ^{3}J(H-H) 6.1 Hz
3.94 (br s, 2H, CH_2)
3.82 (br m, 2H, CH_2)
3.79 (br s, 2H, CH_2)
1.41 (s, 18H, C(CH_3)$_3$)
1.26 (d, 6H, CH(CH_3)$_2$), ^{3}J(H-H) 6.1 Hz
1.22 (s, 18H, C(CH_3)$_3$)
1.20 (d, 6H, CH(CH_3)$_2$), ^{3}J(H-H) 6.1 Hz

^{13}C{^{1}H} NMR (100.62 MHz, $CDCl_3$)
159.0 (*C*)
140.7 (*C*)
135.5 (*C*)
79.1 (*C*H(CH$_3$)$_2$)
78.6 (*C*H(CH$_3$)$_2$)
54.8 (*C*H$_2$)

132.6 (*C*H)
132.5 (*C*)
127.8 (*C*H)
127.7 (*C*H)
125.1 (*C*H)
123.6 (*C*)
122.8 (*C*H)
53.7 (*C*H_2)
35.0 (*C*$(CH_3)_3$)
34.2 (*C*$(CH_3)_3$)
31.6 (C(*C*$H_3)_3$)
29.6 (C(*C*$H_3)_3$)
26.5 (CH(*C*$H_3)_2$)
26.4 (CH(*C*$H_3)_2$)

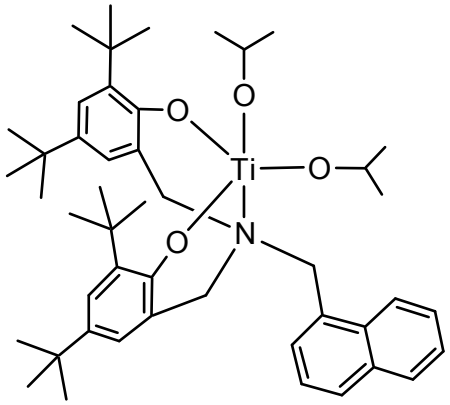

L7Ti(O^{i}Pr)$_2$

L7H_2 (0.20 g, 0.34 mmol) was dissolved in CH_2Cl_2 (10 mL) in a Schlenk tube. Ti(O^{i}Pr)$_4$ (0.10 mL, 0.34 mmol) was added, and the previously clear, pale yellow solution turned bright yellow. Stirring continued for 1.5 h, after which time the volatiles were removed under reduced pressure to leave a yellow solid. Crystallisation from hexane solution yielded **L7**Ti(O^{i}Pr)$_2$ as yellow blocks. Yield 0.24 g, 91%. Anal: Calc for $C_{47}H_{67}NO_4Ti$, C, 74.48%; H, 8.91%; N, 1.85%. Found C, 72.2%; H, 8.73%; N, 2.07%.

^{1}H NMR (400.13 MHz, $CDCl_3$)
8.25 (m, 1H, Ar*H*)
7.86 – 7.93 (m, 2H, Ar*H*)
7.49 – 7.51 (m, 2H, Ar*H*)
7.37 – 7.43 (m, 2H, Ar*H*)
7.21 (m, 2H, Ar*H*)
6.75 (br s, 2H, Ar*H*)
5.24 (sept, 1H, C*H*), ^{3}J(H-H) 6.1Hz
5.12 (sept, 1H, C*H*), ^{3}J(H-H) 6.1Hz
4.73 (br s, 2H, CH_2)
3.97 (br s, 2H, CH_2)
3.49 (br m, 2H, CH_2)
1.49 (s, 18H, CH_3)
1.44 (d, 6H, CH_3), ^{3}J(H-H) 6.1Hz
1.42 (d, 6H, CH_3), ^{3}J(H-H) 6.1Hz
1.26 (s, 18H, CH_3)

^{13}C{^{1}H} NMR (100.62 MHz, $CDCl_3$)
159.3 (*C*)
141.1 (*C*)
135.4 (*C*)
134.8 (*C*)
133.9 (*C*)
130.9 (*C*H)
129.8 (*C*)
128.9 (*C*H)
128.8 (*C*H)
124.5 (*C*H)
124.1 (*C*)
122.9 (*C*H)
79.7 (*C*H$(CH_3)_2$)
78.6 (*C*H$(CH_3)_2$)
50.0 (CH_2)
35.0 (*C*$(CH_3)_3$)
34.3 (*C*$(CH_3)_3$)
31.7 (C(*C*$H_3)_3$)

126.2 (*C*H)
125.5 (*C*H)
125.0 (*C*H)
124.8 (*C*H)
29.7 (C(*C*H$_3$)$_3$)
26.7 (CH(*C*H$_3$)$_2$)
26.6 (CH(*C*H$_3$)$_2$)

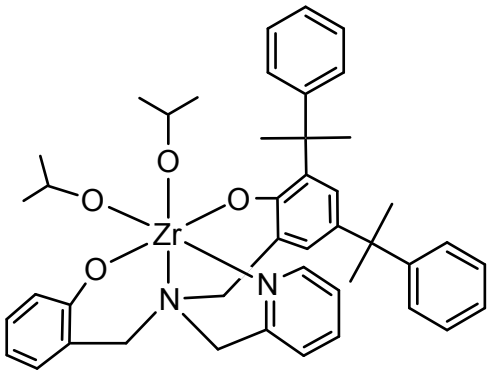

L8Zr(O^{i}Pr)$_2$

L8H$_2$ (0.10 g, 0.18 mmol) was dissolved in CH_2Cl_2 (10mL) in a Schlenk tube. A solution of Zr(O^{i}Pr)$_4$(HO^{i}Pr) (0.07 g, 0.18 mmol) in CH_2Cl_2 was added, and the previously clear, slightly yellow solution remained unchanged. Stirring continued for 2 h, after which time the volatiles were removed under reduced pressure to leave a white solid. Crystallisation from hexane solution yielded **L8**Zr(O^{i}Pr)$_2$ as a microcrystalline solid. Yield 0.12 g, 90%. Anal: Calc for $C_{44}H_{52}N_2O_4Zr$, C, 69.19%; H, 6.86%; N, 3.67%. Found C, 70.0%; H, 6.79%; N, 3.60%.

^{1}H NMR (400.13 MHz, $CDCl_3$)
8.22 (d, 1H, NAr*H*), ^{3}J(H-H) 4.4 Hz
6.69-6.86 (m, 16H, Ar*H*)
6.40 (m, 1H, NAr*H*)
6.31 (d, 2H, NAr*H*), ^{3}J(H-H) 7.6 Hz
6.09 (d, 1H, NAr*H*), ^{3}J(H-H) 8.2 Hz
4.75 (d, 1H, CH_2) ^{3}J(H-H) 12.4 Hz
4.56 (sept, 1H, C*H*(CH$_3$)$_2$) ^{3}J(H-H) 6.0 Hz
4.54 (d, 1H, CH_2), ^{3}J(H-H) 12.4 Hz
4.24 (sept, 1H, C*H*(CH$_3$)$_2$), ^{3}J(H-H) 6.0 Hz
3.72 (d, 1H, CH_2), ^{3}J(H-H) 12.6 Hz
3.28 (d, 1H, CH_2), ^{3}J(H-H) 12.5 Hz
3.24 (d, 1H, CH_2), ^{3}J(H-H) 12.4 Hz
3.17 (d, 1H, CH_2), ^{3}J(H-H) 12.6 Hz
1.79 (s, 3H, CH_3)
1.66 (s, 3H, CH_3)
1.64 (s, 3H, CH_3)
1.61 (s, 3H, CH_3)
1.38 (d, 3H,C(CH_3)$_2$), ^{3}J(H-H) 6.0 Hz
1.20 (d, 3H, C(CH_3)$_2$), ^{3}J(H-H) 6.0 Hz
1.08 (d, 3H, C(CH_3)$_2$), ^{3}J(H-H) 6.0 Hz
1.05 (d, 3H, C(CH_3)$_2$), ^{3}J(H-H) 6.0 Hz,

^{13}C{^{1}H} NMR (100.62 MHz, $CDCl_3$)
149.2 (*C*H)
144.8 (*C*)
142.1 (*C*)
137.6 (*C*H)
135.4 (*C*)
129.6 (*C*H)
129.5 (*C*)
129.3 (*C*H)
124.4 (*C*H)
121.6 (*C*H)
121.1 (*C*)
120.6 (*C*H)
117.7 (*C*H)
116.1 (*C*H)
71.0 (*C*H)
63.4 (*C*H$_2$)

127.7 (*C*H)
127.2 (*C*)
126.8 (*C*H)
126.8 (*C*H)
126.7 (*C*H)
126.3 (*C*)
126.1 (*C*)
125.8 (*C*H)
125.6 (*C*)
125.3 (*C*H)

63.4 (*C*H_2)
57.5 (*C*H_2)
32.4 (*C*$(CH_3)_3$)
31.2 (*C*H_3)
31.1 (*C*H_3)
29.2 (*C*$(CH_3)_3$)
28.1 (*C*H_3)
27.2 (*C*H_3)
27.0 (*C*H_3)
26.1 (*C*H_3)

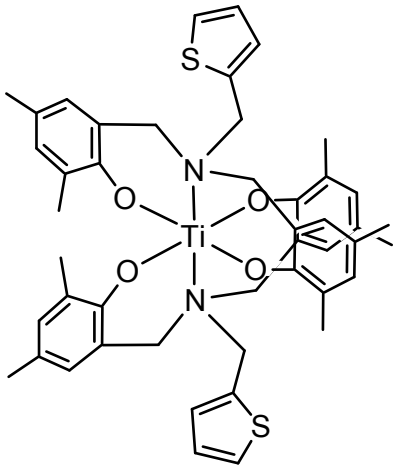

L9$_2$Ti

L9H_2 (0.50 g, 1.3 mmol) was dissolved in CH_2Cl_2 (20 mL) in a Schlenk tube. Ti(O^iPr)$_4$ (0.39 mL, 1.3 mmol) was added, and the previously clear, pale yellow solution turned bright red. Stirring continued for 1.5 h, after which time the volatiles were removed under reduced pressure to leave a bright red solid. Crystallisation from a hexane/CH_2Cl_2 layer yielded **L9**$_2$Ti as red needles. Yield 0.40 g, 38%. Anal: Calc for $C_{46}H_{50}N_2O_4S_2Ti$, C, 68.47%; H, 6.25%; N, 3.47%. Found C, 69.2%; H, 6.32%; N, 3.36%.

^{1}H NMR (400.13 MHz, $CDCl_3$)
7.37 (d, 1H, SAr*H*), ^{3}J(H-H) 5.1 Hz
7.00 (t, 2H, SAr*H*), ^{3}J(H-H) 3.8 Hz
6.97 (s, 1H, Ar*H*)
6.88 (s, 1H, Ar*H*)
6.82 (s, 1H, Ar*H*)
6.75 (s, 1H, Ar*H*)
6.71 (d, 1H, SAr*H*), ^{3}J(H-H) 2.8 Hz
4.72 (d, 1H, CH_2), ^{3}J(H-H) 13.6 Hz
4.48 (d, 1H, CH_2), ^{3}J(H-H) 13.2 Hz
4.42 (d, 1H, CH_2), ^{3}J(H-H) 13.4 Hz
4.34 (d, 1H, CH_2), ^{3}J(H-H) 13.2 Hz
3.80 (d, 1H, CH_2), ^{3}J(H-H) 13.0 Hz
3.68 (d, 1H, CH_2), ^{3}J(H-H) 13.5 Hz
2.30 (s, 3H, CH_3)
2.23 (s, 3H, CH_3)
2.04 (s, 3H, CH_3)
1.60 (s, 3H, CH_3)

$^{13}C\{^1H\}$ NMR (100.62 MHz, $CDCl_3$)

160.4 (*C*)
159.3 (*C*)
133.1 (*C*)
131.9 (*C*H)
131.5 (*C*H)
130.8 (*C*H)
128.7 (*C*H)
128.5 (*C*H)
127.0 (*C*)
126.9 (*C*)
126.9 (*C*H)
126.3 (*C*H)
123.2 (*C*)
123.0 (*C*)
121.0 (*C*)
121.8 (*C*)
59.2 (CH_2)
58.4 (CH_2)
57.5 (CH_2)
55.0 (CH_2)
54.8 (CH_2)
48.2 (CH_2)
20.7 (CH_3)
20.6 (CH_3)
17.0 (CH_3)
16.6 (CH_3)

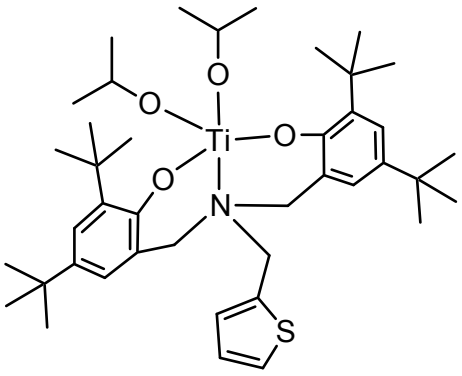

L10 Ti(O^iPr)$_2$

L10H_2 (0.10 g, 0.02 mmol) was dissolved in CH_2Cl_2 (10 mL) in a Schlenk tube. Ti(O^iPr)$_4$ (0.05 mL, 0.02 mmol) was added, and the previously clear, colourless solution turned bright yellow. Stirring continued for 2 h, after which time the volatiles were removed under reduced pressure to leave a sticky, bright yellow oil. Crystallisation from hexane solution yielded **L10**Ti(O^iPr)$_2$ as yellow blocks. Yield 0.10 g, 81%. Anal: Calc for $C_{41}H_{63}NO_4STi$, C, 68.98%; H, 8.90%; N, 1.96%. Found C, 69.7%; H, 8.10%; N, 2.24%.

^1H NMR (400.13MHz, $CDCl_3$)

7.31 (d, 1H, SAr*H*), ^{3}J(H-H) 4.9 Hz
7.24 (d, 2H, Ar*H*), ^{4}J(H-H) 2.4 Hz
6.94 (t, 1H, SAr*H*), ^{3}J(H-H) 3.6 Hz
6.92 (d, 2H, Ar*H*), ^{4}J(H-H) 2.4 Hz
6.68 (d, 1H, SAr*H*), ^{3}J(H-H) 2.9 Hz
5.04 (sept, 1H, C*H*(CH_3)$_2$), ^{3}J(H-H) 6.0 Hz
4.98 (sept, 1H, C*H*(CH_3)$_2$), ^{3}J(H-H) 6.0 Hz
4.15 (br s, 2H, CH_2)
3.86 (br m, 2H, CH_2)
3.72 (br s, 2H, CH_2)
1.35 (d, 6H, CH(CH_3)$_2$), ^{3}J(H-H) 6.0 Hz
1.23 (s, 18H, C(CH_3)$_3$)
1.22 (d, 6H, CH(CH_3)$_2$), ^{3}J(H-H) 6.0 Hz)
1.21 (s, 18H, C(CH_3)$_3$

$^{13}C\{^{1}H\}$ NMR (100.62 MHz, $CDCl_3$)

158.1 (*C*)
140.4 (*C*)
134.9 (*C*)
133.9 (*C*)
131.1 (*C*H)
127.5 (*C*H)
127.3 (*C*H)
125.0 (*C*H)
123.8 (*C*)
122.5 (*C*H)
78.8 (*C*H$(CH_3)_2$)
76.4 (*C*H$(CH_3)_2$)
56.0 (*C*H_2)
49.8 (*C*H_2)
35.1 (*C*$(CH_3)_3$)
34.5 (*C*$(CH_3)_3$)
33.0 (C(*C*$H_3)_3$)
29.9 (C(*C*$H_3)_3$)
26.7 (CH(*C*$H_3)_2$)
26.6 (CH(*C*$H_3)_2$)

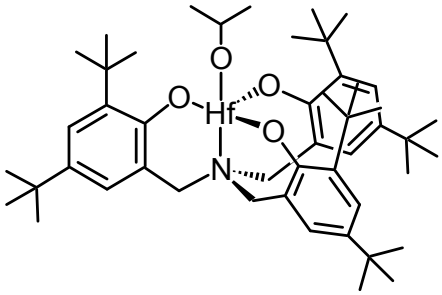

L11 Hf(O^iPr)

L11H_3 (1.0 g, 1.5 mmol) was dissolved in toluene (20 mL) in a Schlenk tube and a solution of Hf(O^iPr)$_4$HO^iPr (0.71 g, 1.5 mmol) in toluene and the previously clear, colourless solution remained unchanged. Stirred continued for 2 h, after which time the volatiles were removed under reduced pressure leaving a white solid. Crystallisation from hexane at -20 °C yielded **L11**Hf(O^iPr) as colourless blocks. Yield 1.2 g, 88%. Anal: Calc for $C_{48}H_{73}NO_4Hf$, C, 63.6%; H, 8.12%; N, 1.54%. Found: C, 64.9%; H, 8.79%; N 1.18%.

^{1}H NMR (400.13 MHz, $CDCl_3$)

7.27 (d, 3H, Ar*H*), ^{4}J(H-H) 2.3 Hz
6.98 (d, 3H, Ar*H*), ^{4}J(H-H) 2.3 Hz
4.73 (sept, 1H, C*H*$(CH_3)_2$), ^{3}J(H-H) 6.0 Hz
4.01 (br s, 3H, CH_2)
2.96 (br s, 3H, CH_2)
1.45 (s, 27H, C(C$H_3)_3$)
1.40 (d, 6H, CH(C$H_3)_2$), ^{3}J(H-H) 6.0 Hz

$^{13}C\{^1H\}$ NMR (100.62 MHz, $CDCl_3$)

157.2 (*C*)
141.5 (*C*)
136.7 (*C*)
124.6 (*C*H)
123.7 (*C*H)
123.6 (*C*)
72.3 (*C*H(CH_3)$_2$)
59.5 (*C*H$_2$)
34.9 (*C*(CH_3)$_3$)
34.2 (*C*(CH_3)$_3$)
31.6 (C(*C*H_3)$_3$)
27.7 (C(*C*H_3)$_3$)
27.4 (CH(*C*H_3)$_2$)

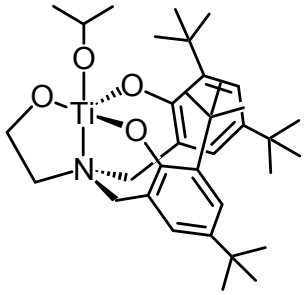

L12 Ti(O^{i}Pr)

L12H_3 (0.50 g, 1.0 mmol) was dissolved in CH_2Cl_2 (10 mL) in a Schlenk tube. Ti(O^{i}Pr)$_4$ (0.30 mL, 1.0 mmol) was added, and the previously clear, colourless solution turned yellow. Stirring continued for 16 h, after which time the volatiles were removed under reduced pressure to leave a yellow solid. Crystallisation from hexane yielded **L12**Ti(O^{i}Pr) as a microcrystalline powder. Yield 0.51 g, 85%. Anal: Calc for $C_{35}H_{55}NO_4Ti$, C, 69.87%; H, 9.21%; N, 2.33%. Found C, 70.2%; H, 9.02%; N, 2.56%.

^1H NMR (400.13 MHz, $CDCl_3$)

7.23 (d, 3H, Ar*H*), ^{4}J(H-H) 2.4 Hz
6.88 (d, 3H, Ar*H*), ^{4}J(H-H) 2.4 Hz
4.91 (sept, 1H, C*H*(CH_3)$_2$), ^{3}J(H-H) 6.1 Hz
4.29 (br m, 2H, CH_2) (ethanolate arm)
3.75 (br d, 2H, CH_2)
3.42 (br d, 2H, CH_2)
2.89 (br m, 2H, CH_2) (ethanolate arm)
1.33 (s, 18H, C(CH_3)$_3$)
1.18 (s, 18H, C(CH_3)$_3$)
1.11 (d, 6H, CH(CH_3)$_2$), ^{3}J(H-H) 6.1 Hz

$^{13}C\{^1H\}$ NMR (100.62 MHz, $CDCl_3$)

149.6 (*C*)
143.8 (*C*)
132.9 (*C*H)
123.0 (*C*)
122.7 (*C*)
122.3 (*C*H)
75.2 (*C*H(CH_3)$_2$)
57.3 (*C*H$_2$)
56.6 (*C*H$_2$)
45.3 (*C*H$_2$)
35.1 (*C*(CH_3)$_3$)
34.7 (*C*(CH_3)$_3$)
33.9 (C(*C*H_3)$_3$)
30.2 (C(*C*H_3)$_3$)
26.9 (CH(*C*H_3)$_2$)

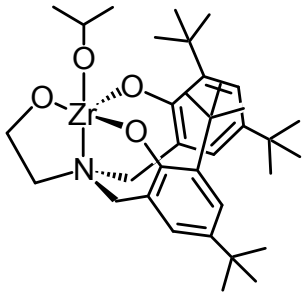

L12 Zr(O^iPr)

L12H_3 (0.50 g, 1.0 mmol) was dissolved in CH_2Cl_2 (10 mL) in a Schlenk tube. A solution of Zr(O^iPr)$_4$HO^iPr (0.39 g, 1.0 mmol) in CH_2Cl_2 under argon was added, and the previously clear, colourless solution remained unchanged. Stirring continued for 16 h, after which time the volatiles were removed under reduced pressure to leave an off-white solid. Crystallisation from hexane/toluene yielded **L12**Zr(O^iPr) as a microcrystalline powder. Yield 0.54 g, 83%. Anal: Calc for $C_{35}H_{55}NO_4Zr$, C, 65.17%; H, 8.59%; N, 2.17%. Found C, 66.5%; H, 8.42%; N, 2.25%.

^{1}H NMR (400.13 MHz, $CDCl_3$)

7.39 (d, 3H, Ar*H*), ^{4}J(H-H) 2.3 Hz
6.97 (d, 3H, Ar*H*), ^{4}J(H-H) 2.3 Hz
4.51 (sept, 1H, C*H*(CH_3)$_2$), ^{3}J(H-H) 6.0 Hz
4.21 (br m, 2H, CH_2) (ethanolate arm)
3.75 (br d, 2H, CH_2)
3.62 (br d, 2H, CH_2)
2.92 (br m, 2H, CH_2) (ethanolate arm)
1.62 (s, 18H, C(CH_3)$_3$)
1.37 (s, 18H, C(CH_3)$_3$)
1.12 (d, 6H, CH(CH_3)$_2$), ^{3}J(H-H) 6.0 Hz

5.4 Polymer Characterisation – Gel Permeation Chromatography

Gel permeation chromatography (GPC) is a form of size exclusion chromatography (SEC) which relies on the principle that particles pass through a stationary phase at different rates, depending on their size. The stationary phase in the GPC setup used to analyse many polymer samples is made from small porous beads, with a controlled pore size distribution. The solution phase contains the polymer sample dissolved in a suitable solvent. For the analysis of PCL and PLA polymers, tetrahydrofuran is commonly used. As the solution phase moves through the stationary phase, polymer molecules move into and out of the pores in the stationary phase. The largest polymer molecules cannot fit into the pores and so move through the stationary phase and elute most quickly. The smallest polymer molecules can access the pores and may become trapped, meaning they take the longest time to elute. Polymer molecules with sizes between these two extremes can access some of the pores but not others and so elute at an intermediate time. In this way,

the polymer particles can be separated based on size and a Gaussian distribution is seen for the GPC elution curve.

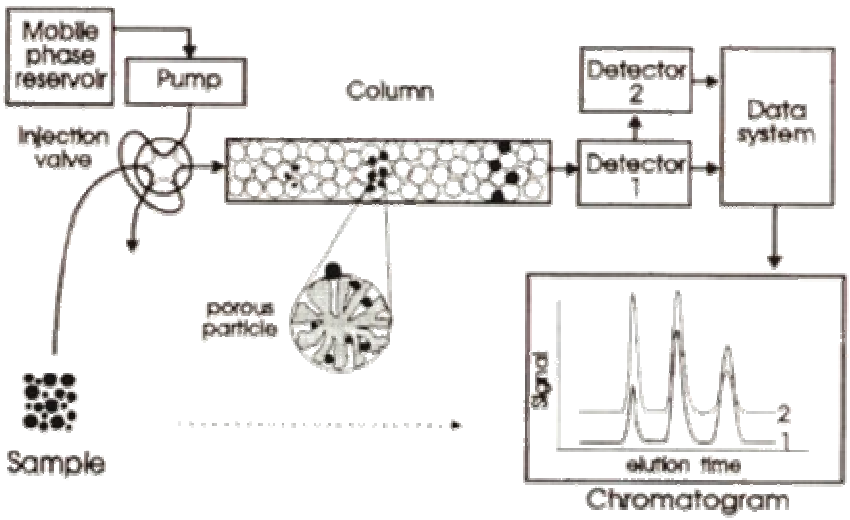

Figure 5.1 Schematic representation of a Gel Permeation Chromatography system.

A typical GPC setup is shown in Figure 5.1. A mobile phase reservoir holds the solvent which has also been used to dissolve the polymer sample and this mobile or solution phase is continually pumped through the system. The solution of polymer sample at a specific concentration is introduced to the system via an injection valve and proceeds onto the column, which is encased in an oven. A refractive index (RI) detector and data processing system give the gel permeation chromatogram and information about the relative molecular weights.

RI detectors are the most commonly used detection systems with GPC. The system is calibrated with narrow standards of known molecular weight at the same concentration used when preparing the samples. The refractive index of the polymer sample is then compared against the calibration curve and the relative molecular weight is calculated. The limitations in using this type of system are two-fold. Firstly, because the determined molecular weights are not absolute, a true measure of the polymer sample molecular weight is not obtained. Secondly, the standards used for calibration are poly(styrene) samples with narrow molecular weight distributions. This polymer is significantly different in structure than the poly(ester) systems under study and so their refractive indices cannot be directly compared. Absolute determination of polymer molecular weights can be achieved by using light scattering or viscometry detectors, and systems

offering triple detection, i.e. refractive index, viscometry and light scattering, are now available.

Although there are limitations with the GPC system, it provides extremely useful information about the molecular weights of the polymer sample. Of particular interest are the number average molecular weight (M_n) and weight average molecular weight (M_w). With these two numbers M_n and M_w, the molecular weight distribution in the polymer sample can also be obtained. This distribution, or polydispersity index (PDI) is determined by dividing the number average molecular weight by the weight average molecular weight.

GPC analyses were performed on a Polymer Laboratories PL-GPC 50 integrated system using a PLgel 5μm MIXED-D 300 x 75 mm column at 35 ºC and GPC grade THF flowing at 1.0 mL/min as the mobile phase.

References

[1] E. Y. Tshuva, I. Goldberg, M. Kol and Z. Goldschmidt, *Organometallics* **2001,** 20, (14), 3017-3028.
[2] Y. L. Tong, Y. Yan, E. S. H. Chan, Q. C. Yang, T. C. W. Mak and D. K. P. Ng, *J. Chem. Soc., Dalton Trans.* **1998**, (18), 3057-3064.
[3] M. Kol, M. Shamis, I. Goldberg, Z. Goldschmidt, S. Alfi and E. Hayut-Salant, *Inorg. Chem. Commun.* **2001,** 4, (4), 177-179.

Appendix A – X-ray Crystal Structure Data

L1Ti($O^{i}Pr$)$_2$

Identification code	h05mgd05
Empirical formula	C30 H40 N2 O4 Ti
Formula weight	540.54
Temperature	150(2) K
Wavelength	0.71073 A
Crystal system, space group	Tetragonal, $I4_1/a$
Unit cell dimensions	a = 25.54800(10) A alpha = 90 deg. b = 25.54800(10) A beta = 90 deg. c = 18.31900(10) A gamma = 90 deg.
Volume	11956.82(9) A^3
Z, Calculated density	16, 1.188 Mg/m^3
Absorption coefficient	0.321 mm^-1
F(000)	4512
Crystal size	0.30 x 0.25 x 0.25 mm
Theta range for data collection	5.20 to 27.47 deg.
Limiting indices	-33<=h<=33, -33<=k<=33, -22<=l<=23
Reflections collected / unique	83022 / 6798 [R(int) = 0.0487]
Completeness to theta = 27.47	99.1 %
Absorption correction	None
Max. and min. transmission	0.9242 and 0.9100
Refinement method	Full-matrix least-squares on F^2
Data / restraints / parameters	6798 / 0 / 347
Goodness-of-fit on F^2	1.041
Final R indices [I>2sigma(I)]	R1 = 0.0502, wR2 = 0.1429
R indices (all data)	R1 = 0.0638, wR2 = 0.1648
Largest diff. peak and hole	0.689 and -0.418 e.A^-3

L1$Zr(O^iPr)_2$

Identification code	k05mgd16
Empirical formula	C30 H40 N2 O4 Zr
Formula weight	583.86
Temperature	150(2) K
Wavelength	0.71073 A
Crystal system, space group	monoclinic, $P2_1/c$
Unit cell dimensions	a = 14.5850(2) A alpha = 90.0000(10) deg. b = 14.2930(2) A beta = 109.7070(10) deg. c = 15.6680(2) A gamma = 90.0000(10) deg.
Volume	3074.90(7) A^3
Z, Calculated density	4, 1.261 Mg/m^3
Absorption coefficient	0.391 mm^-1
F(000)	1224
Crystal size	0.20 x 0.10 0.05 mm
Theta range for data collection	3.60 to 29.00 deg.
Limiting indices	-19<=h<=19, -19<=k<=19, -21<=l<=21
Reflections collected / unique	34306 / 8071 [R(int) = 0.1370]
Completeness to theta = 29.00	98.8 %
Absorption correction	None
Refinement method	Full-matrix least-squares on F^2
Data / restraints / parameters	8071 / 0 / 343
Goodness-of-fit on F^2	1.155
Final R indices [I>2sigma(I)]	R1 = 0.0745, wR2 = 0.2173
R indices (all data)	R1 = 0.0918, wR2 = 0.2364
Largest diff. peak and hole	0.716 and -1.331 e.A^-3

L2Ti($O^{i}Pr$)$_2$

Identification code	k05mgd14
Empirical formula	C43.50 H67.50 N2 O4 Ti
Formula weight	730.40
Temperature	150(2) K
Wavelength	0.71073 A
Crystal system, space group	triclinic, P-1
Unit cell dimensions	a = 13.3300(3) A alpha = 102.4090(10)deg b = 18.8090(4) A beta = 101.8250(10) deg c = 18.9470(4) A gamma = 105.2970(10)deg
Volume	4299.08(16) A^3
Z, Calculated density	4, 1.128 Mg/m^3
Absorption coefficient	0.239 mm^-1
F(000)	1586
Crystal size	0.20 x 0.16 x 0.10 mm
Theta range for data collection	3.57 to 27.61 deg.
Limiting indices	-17<=h<=17, -24<=k<=24, -24<=l<=23
Reflections collected / unique	68617 / 19543 [R(int) = 0.1020]
Completeness to theta = 27.61	97.8 %
Absorption correction	None
Refinement method	Full-matrix least-squares on F^2
Data / restraints / parameters	19543 / 0 / 943
Goodness-of-fit on F^2	1.148
Final R indices [I>2sigma(I)]	R1 = 0.0998, wR2 = 0.1865
R indices (all data)	R1 = 0.1448, wR2 = 0.2039
Largest diff. peak and hole	0.717 and -0.513 e.A^-3

L2$Zr(O^iPr)_2$

Identification code	k05mgd23
Empirical formula	C42 H64 N2 O4 Zr
Formula weight	752.17
Temperature	150(2) K
Wavelength	0.71073 A
Crystal system, space group	monoclinic, $P2_1/c$
Unit cell dimensions	a = 11.07900(10) A alpha = 90 deg. b = 20.2810(2) A beta = 97.3830(10) deg. c = 18.9470(2) A gamma = 90 deg.
Volume	4221.97(7) A^3
Z, Calculated density	4, 1.183 Mg/m^3
Absorption coefficient	0.300 mm^-1
F(000)	1608
Crystal size	0.50 x 0.15 x 0.10 mm
Theta range for data collection	3.54 to 24.00 deg.
Limiting indices	-12<=h<=12, -23<=k<=23, -21<=l<=21
Reflections collected / unique	62147 / 6614 [R(int) = 0.1176]
Completeness to theta = 24.00	99.6 %
Absorption correction	None
Max. and min. transmission	0.9707 and 0.8646
Refinement method	Full-matrix least-squares on F^2
Data / restraints / parameters	6614 / 0 / 458
Goodness-of-fit on F^2	1.047
Final R indices [I>2sigma(I)]	R1 = 0.0501, wR2 = 0.0905
R indices (all data)	R1 = 0.0728, wR2 = 0.0976
Largest diff. peak and hole	0.365 and -0.481 e.A^-3

L2$Hf(O^iPr)_2$

Identification code	h05mgd17
Empirical formula	C42 H64 Hf N2 O4
Formula weight	839.44
Temperature	150(2) K
Wavelength	0.71073 A
Crystal system, space group	monoclinic, $P2_1/c$
Unit cell dimensions	a = 11.1038(2) A alpha = 90 deg. b = 20.2199(3) A beta = 97.3430(10) deg. c = 18.9272(3) A gamma = 90 deg.
Volume	4214.64(12) A^3
Z, Calculated density	4, 1.323 Mg/m^3
Absorption coefficient	2.514 mm^-1
F(000)	1736
Crystal size	0.25 x 0.25 x 0.15 mm
Theta range for data collection	3.64 to 30.03 deg.
Limiting indices	-15<=h<=15, -28<=k<=28, -26<=l<=26
Reflections collected / unique	97741 / 12300 [R(int) = 0.0748]
Completeness to theta = 30.03	99.8 %
Absorption correction	None
Max. and min. transmission	0.7042 and 0.5721
Refinement method	Full-matrix least-squares on F^2
Data / restraints / parameters	12300 / 0 / 458
Goodness-of-fit on F^2	1.012
Final R indices [I>2sigma(I)]	R1 = 0.0323, wR2 = 0.0618
R indices (all data)	R1 = 0.0649, wR2 = 0.0693
Largest diff. peak and hole	1.542 and -1.781 e.A^-3

L3$Ti(O^iPr)_2$

Identification code	k05mgd34
Empirical formula	C26 H30 N4 O8 Ti
Formula weight	574.44
Temperature	173(2) K
Wavelength	0.71073 A
Crystal system, space group	Orthorhombic, P21nb
Unit cell dimensions	a = 12.3870(2) A alpha = 90 deg. b = 13.7820(2) A beta = 90 deg. c = 16.5820(3) A gamma = 90 deg.
Volume	2830.84(8) A^3
Z, Calculated density	4, 1.348 Mg/m^3
Absorption coefficient	0.356 mm^-1
F(000)	1200
Crystal size	0.25 x 0.25 x 0.15 mm
Theta range for data collection	3.60 to 24.00 deg.
Limiting indices	-14<=h<=14, -15<=k<=15, -18<=l<=18
Reflections collected / unique	33290 / 4432 [R(int) = 0.1242]
Completeness to theta = 24.00	99.6 %
Absorption correction	None
Refinement method	Full-matrix least-squares on F^2
Data / restraints / parameters	4432 / 1 / 356
Goodness-of-fit on F^2	1.077
Final R indices [I>2sigma(I)]	R1 = 0.0571, wR2 = 0.1014
R indices (all data)	R1 = 0.0797, wR2 = 0.1078
Absolute structure parameter	0.02(3)
Largest diff. peak and hole	0.337 and -0.408 e.A^-3

L6$Ti(O^iPr)_2$

Identification code	k05mgd12
Empirical formula	C46 H72 N O4 Ti
Formula weight	750.95
Temperature	150(2) K
Wavelength	0.71073 A
Crystal system, space group	triclinic, P-1
Unit cell dimensions	a = 9.33900(10) A alpha = 86.77 deg. b = 9.63900(10) A beta = 81.4570(10) deg. c = 27.3100(3) A gamma = 68.4520(10) deg.
Volume	2261.22(4) A^3
Z, Calculated density	2, 1.103 Mg/m^3
Absorption coefficient	0.229 mm^-1
F(000)	818
Crystal size	0.20 x 0.20 x 0.10 mm
Theta range for data collection	3.57 to 27.59 deg.
Limiting indices	-12<=h<=12, -12<=k<=12, -35<=l<=34
Reflections collected / unique	35306 / 10208 [R(int) = 0.0387]
Completeness to theta = 27.59	97.3 %
Absorption correction	None
Max. and min. transmission	0.9775 and 0.9557
Refinement method	Full-matrix least-squares on F^2
Data / restraints / parameters	10208 / 0 / 516
Goodness-of-fit on F^2	1.034
Final R indices [I>2sigma(I)]	R1 = 0.0471, wR2 = 0.1255
R indices (all data)	R1 = 0.0550, wR2 = 0.1312
Largest diff. peak and hole	0.448 and -0.559 e.A^-3

L7$Ti(O^iPr)_2$

Identification code	k05mgd28
Empirical formula	C47 H67 N O4 Ti
Formula weight	757.92
Temperature	150(2) K
Wavelength	0.71073 A
Crystal system, space group	monoclinic, $P2_1/n$
Unit cell dimensions	a = 11.1670(2) A alpha = 90.0000(10) deg. b = 22.1960(3) A beta = 98.7180(10) deg. c = 18.0800(4) A gamma = 90.0000(10) deg.
Volume	4429.58(14) A^3
Z, Calculated density	4, 1.136 Mg/m^3
Absorption coefficient	0.234 mm^-1
F(000)	1640
Crystal size	0.20 x 0.10 x 0.10 mm
Theta range for data collection	3.54 to 27.46 deg.
Limiting indices	-14<=h<=14, -28<=k<=26, -23<=l<=18
Reflections collected / unique	37110 / 9971 [R(int) = 0.0678]
Completeness to theta = 27.46	98.4 %
Absorption correction	None
Max. and min. transmission	0.9770 and 0.9547
Refinement method	Full-matrix least-squares on F^2
Data / restraints / parameters	9971 / 0 / 506
Goodness-of-fit on F^2	1.027
Final R indices [I>2sigma(I)]	R1 = 0.0565, wR2 = 0.1050
R indices (all data)	R1 = 0.0949, wR2 = 0.1176
Largest diff. peak and hole	0.288 and -0.534 e.A^-3

L9$_2$Ti

Identification code	h06mgd21
Empirical formula	C46 H50 N2 O4 S2 Ti
Formula weight	806.90
Temperature	150(2) K
Wavelength	0.71073 A
Crystal system, space group	Triclinic, P-1
Unit cell dimensions	a = 11.566(4) A alpha = 80.113(1) deg. b = 12.604(4) A beta = 89.664(1) deg. c = 14.014(5) A gamma = 88.693(2) deg.
Volume	2012.06(12) A^3
Z, Calculated density	2, 1.332 Mg/m^3
Absorption coefficient	0.363 mm^-1
F(000)	852
Crystal size	0.15 x 0.13 x 0.13 mm
Theta range for data collection	3.82 to 25.42 deg.
Limiting indices	-13<=h<=13, -15<=k<=15, -16<=l<=16
Reflections collected / unique	22153 / 7276 [R(int) = 0.0713]
Completeness to theta = 25.42	98.2 %
Absorption correction	None
Max. and min. transmission	0.9543 and 0.9475
Refinement method	Full-matrix least-squares on F^2
Data / restraints / parameters	7276 / 1 / 531
Goodness-of-fit on F^2	1.069
Final R indices [I>2sigma(I)]	R1 = 0.0491, wR2 = 0.1152
R indices (all data)	R1 = 0.0779, wR2 = 0.1333
Largest diff. peak and hole	0.352 and -0.441 e.A^-3

L10 Ti(O^iPr)$_2$

Identification code	k06mgd20
Empirical formula	C41 H63 N O4 S Ti
Formula weight	713.88
Temperature	150(2) K
Wavelength	0.71073 A
Crystal system	tetragonal
Space group	I 41 c d (no.110)
Unit cell dimensions	a = 38.3000(6) A alpha = 90 deg. b = 38.3000(6) A beta = 90 deg. c = 11.6610(2) A gamma = 90 deg.
Volume	17105.4(5) A^3
Z, Calculated density	16, 1.109 Mg/m^3
Absorption coefficient	0.286 mm^-1
F(000)	6176
Crystal size	0.25 x 0.25 x 0.23 mm
Theta range for data collection	3.57 to 24.09 deg.
Limiting indices	-43<=h<=43, -43<=k<=43, -13<=l<=13
Reflections collected / unique	53132 / 6730 [R(int) = 0.0913]
Completeness to theta = 24.09	99.2 %
Max. and min. transmission	0.9372 and 0.9320
Refinement method	Full-matrix least-squares on F^2
Data / restraints / parameters	6730 / 1 / 475
Goodness-of-fit on F^2	1.181
Final R indices [I>2sigma(I)]	R1 = 0.0733, wR2 = 0.1586
R indices (all data)	R1 = 0.0778, wR2 = 0.1606
Absolute structure parameter	0.07(5)
Largest diff. peak and hole	0.317 and -0.393 e.A^-3

L11$Hf(O^iPr)_2$

Identification code	k06mgd17
Empirical formula	C54 H88 N O4 Hf
Formula weight	992.74
Temperature	150(2) K
Wavelength	0.71073 A
Crystal system	tetragonal
Space group	$P4_3$
Unit cell dimensions	a = 14.57000(10) A alpha = 90 deg. b = 14.57000(10) A beta = 90 deg. c = 25.4100(2) A gamma = 90 deg.
Volume	5394.16(7) A^3
Z, Calculated density	4, 1.222 Mg/m^3
Absorption coefficient	1.974 mm^-1
F(000)	2088
Crystal size	0.50 x 0.40 x 0.35 mm
Theta range for data collection	3.51 to 27.48 deg.
Limiting indices	-18<=h<=18, -18<=k<=18, -32<=l<=32
Reflections collected / unique	81147 / 12310 [R(int) = 0.0362]
Completeness to theta = 27.48	99.2 %
Max. and min. transmission	0.438 and 0.545
Refinement method	Full-matrix least-squares on F^2
Data / restraints / parameters	11451 / 1 / 721
Goodness-of-fit on F^2	0.986
Final R indices [I>2sigma(I)]	R1 = 0.0231, wR2 = 0.0595
R indices (all data)	R1 = 0.0231, wR2 = 0.0620
Absolute structure parameter	0.431(6)
Largest diff. peak and hole	0.506 and -1.502 e.A^-3

L11$^{R\text{-}Me}$Zr(O^{i}Pr)

Identification code	k06mgd16
Empirical formula	C55 H89 N O4 Zr
Formula weight	919.49
Temperature	150(2) K
Wavelength	0.71073 A
Crystal system, space group	tetragonal, P43
Unit cell dimensions	a = 14.64100(10) A alpha = 90 deg. b = 14.64100(10) A beta = 90 deg. c = 25.5410(3) A gamma = 90 deg.
Volume	5474.94(8) A^3
Z, Calculated density	4, 1.116 Mg/m^3
Absorption coefficient	0.242 mm^-1
F(000)	1992
Crystal size	0.25 x 0.20 x 0.20 mm
Theta range for data collection	3.67 to 25.03 deg.
Limiting indices	-17<=h<=17, -17<=k<=17, -30<=l<=30
Reflections collected / unique	78683 / 9601 [R(int) = 0.0660]
Completeness to theta = 25.03	99.4 %
Absorption correction	None
Max. and min. transmission	0.9533 and 0.9421
Refinement method	Full-matrix least-squares on F^2
Data / restraints / parameters	9601 / 1 / 603
Goodness-of-fit on F^2	1.057
Final R indices [I>2sigma(I)]	R1 = 0.0407, wR2 = 0.1012
R indices (all data)	R1 = 0.0473, wR2 = 0.1063
Absolute structure parameter	-0.02(3)
Largest diff. peak and hole	0.498 and -0.388 e.A^-3

L11$^{R\text{-}Me}$Hf(O^{i}Pr)

Identification code	k06mgd15
Empirical formula	C55 H88 Hf N O5
Formula weight	1021.75
Temperature	150(2) K
Wavelength	0.71073 A
Crystal system, space group	monoclinic, $P2_1$
Unit cell dimensions	a = 14.3780(1) A alpha = 90 deg. b = 26.3410(2) A beta = 97.69 deg. c = 14.8380(1) A gamma = 90 deg.
Volume	5569.11(7) A^3
Z, Calculated density	4, 1.219 Mg/m^3
Absorption coefficient	1.916 mm^-1
F(000)	2148
Crystal size	0.25 x 0.23 x 0.23 mm
Theta range for data collection	3.61 to 27.50 deg.
Limiting indices	-18<=h<=18, -34<=k<=34, -19<=l<=19
Reflections collected / unique	66777 / 24947 [R(int) = 0.0401]
Completeness to theta = 27.50	99.3 %
Absorption correction	None
Max. and min. transmission	0.6670 and 0.6460
Refinement method	Full-matrix least-squares on F^2
Data / restraints / parameters	24947 / 1 / 1182
Goodness-of-fit on F^2	1.028
Final R indices [I>2sigma(I)]	R1 = 0.0307, wR2 = 0.0652
R indices (all data)	R1 = 0.0367, wR2 = 0.0680
Absolute structure parameter	-0.014(4)
Largest diff. peak and hole	0.846 and -0.819 e.A^-3

Appendix B – Publications arising from this work

1. A. J. Chmura, M. G. Davidson, M. D. Jones, M. D. Lunn and M. F. Mahon, *Dalton Transactions*, **2006**, 7, 887.

2. A. J. Chmura, M. G. Davidson, M. D. Jones, M. D. Lunn, M. F. Mahon, A. F. Johnson, P. Khunkamchoo, S. L. Roberts, and S. S. F. Wong, *Macromolecules*, **2006**, 39, 7250.

3. A. J. Chmura, M. G. Davidson, C. J. Frankis, M. D. Jones and M. D. Lunn, *Chemical Communications*, **2008**, 11, 1239.